Turn-signal lamps 760
Twin suspension links 623
Twin-flow turbine housings, ATL 443
Twin-tube shock-absorbers 617
Two-bed three-way catalytic converters 449
Two-component adhesives 322
Two-line braking systems 646, 674
Two-stage carburetors 460
Two-stage turbocharger systems 445
Two-step control (exhaust emissions) 525
Two-stroke process 388
Two-way radio networks 801

U

U-engines 394
UIS, see Unit Injector Systems 548
Ultrasonic passenger-compartment protection 768
Ultrasonic remote control 815
Ultrasonic sensors 791
Ultrasonic transit-time processes 101
Ultrasound 50
Underbody preservation 724
Understeer 352, 355
Uniform distribution (A/F mixture) 519
Uninhibited corrosion 256
Unit Injector Systems (UIS) 535, 548
Unit Pump Systems (UPS) 535, 549
Unitized all-steel bodies 722
Units (conversion) 19
Units of angle (conversion) 21
Units of area (conversion) 20
Units of length (conversion) 19
Units of mass (conversion) 22
Units of power (conversion) 25
Units of stress (conversion) 24
Units of temperature (conversion) 26
Units of volume (conversion) 20
Units, statutory 13
Universal (drive) shafts 602
Universal joints 602
Universal test adapters 510
Unleaded gasoline 238
Uplighting (lighting) 783
UPS, see Unit Pump Systems 549
Urban bus (definition) 716
USA test (emissions testing) 529, 562
Useful speed range 414
Useful-signal frequency (EMC) 893
Utrasonic flow measurement 115

V

Vacuum advance mechanisms (ignition timing) 489
Vacuum brake boosters 655
Valence (chemical elements) 176
Valence (electrolytic materials) 64
Valve arrangements, springs 408
Valve deactivation 377
Valve gear 408
Valve guides 409
Valve seats, timing 408
Valve timing 520
Valve timing, variable 387
Valve, delivery 537
Valves, canister-purge 506
Valves, dust-unloading 439
Valves, hydraulic 820
Valves, needle (carburetor) 461
Vane-type supply pumps 543
Vapor Lock Index (VLI) 240
Vapor pressure (fuels) 240
Vapour Phase Inhibitors (VPI) 267
Varactor (variable-capacitance diode) 78
Variable-displacement pumps (automotive hydraulics) 825
Variable-geometry intake manifolds 390, 500
VCI, see Volatile Corrosion Inhibitors 267
Vehicle bodies (delivery trucks and vans) 732
Vehicle bodies 713
Vehicle bulbs 763
Vehicle combinations 716
Vehicle control (ESP) 705
Vehicle dynamics (commercial vehicles) 359
Vehicle dynamics (control in pass. cars), see. ESP 701, 704
Vehicle dynamics 338
Vehicle dynamics control system (ESP) 707
Vehicle dynamics, assessment criteria 35
Vehicle handling (ISO) 354, 361
Vehicle Headlamp Aiming Devices (VHAD 749
Vehicle immobilizers 769
Vehicle information system 802
Vehicle lighting 738
Vehicle safety 726
Vehicle speed and engine speed 342
Vehicle surface area, projected 721
Vehicle testing procedures (EMC) 896
Vehicle wheels 624
Vehicle-body calculations 730
Vehicle-body drag coefficient (c_W) 340
Vehicle-body materials 723
Vehicle-body sheet metal 197, 723
Vehicle-body shell 722
Vehicle-speed limiters 611

PETITIONER'S EXHIBIT 1002
US PATENT NO. 6,581,565
Page 1501

Velocity of sound 50
V-engines 394
Venturi chamber (carburetors) 460
Venturi nozzles (mufflers) 451
Venturi tube (carburetors) 461
Vibration absorbers 617
Vibration absorption 32
Vibration and oscillation 29
Vibration corrosion cracking 259
Vibration damping 29, 31, 616
Vibration isolation 31
Vibration period (definition) 29
Vibration reduction, crankshaft 406
Vibration sensors 107
Vibrational stress 612
Viscosity (diesel fuel) 242
Viscosity grades 233
Viscosity units (conversion) 27
Viscous flow behavior, intrinsic (lubricants) 232
Visibility range when passing/overtaking 349
Vision 720
Visual range (lighting) 739
VLI, see Vapor Lock Index 240
Volatile Corrosion Inhibitors (VCI) 267
Volatility of gasoline 239
Voltage drop, permissible 859
Voltage regulators (alternators) 882
Voltage regulators (automotive electrical systems) 882
Voltage ripple (automotive electrical systems) 890
Voltage, magnetic 71
Volume expansion coefficient 181
Volumes of solids 1 49
Volumetric efficiency (gas exchange) 384
Volumetric efficiency (IC engine cylinder) 414, 453, 503
Volumetric efficiency (automotive hydraulics) 816
VPI, see Vapour Phase Inhibitors 267

W

W charging curves (battery charging) 873
Wafer bonding 91
Wankel engines, see Rotary engines 426
Warm-up 470, 505
Warning elements (Park-Pilot) 792
Warning signals (theft-deterrent systems) 767
Washing systems (car windows) 773
Water cooling 430
Water separation (fuel filters) 437
Water vapor (exhaust) 518
Water vapor 191
Watt (unit) 16
Watt linkage (automotive suspension) 622
Wavelengths 50
Wavelength range 137
Waves, vibration and oscillation (definition) 30
Wear 330
Wear inhibition 332
Wear quantities 331
Weber (unit) 18
Wedge shape (body), drag coefficient (c_W) 340
Weibull distribution 161
Weight 13
Weight-to-power ratio (calculation) 418
Weight-to-power ratio (passenger-car specifications) 899
Welding techniques 319
Welding, flash 320
Welding, gas-shielded 321
Welding, laser 328
Weston normal cells 64
Wet boiling point (brake fluids) 247
Wet road surfaces and aquaplaning 343
Wheatstone bridge 63
Wheel and tow-away protection (car alarm) 768
Wheel covers 625
Wheel imbalance and centering 626
Wheel load from crosswind 351
Wheel loading 627
Wheel lockup control system (ABS) 708
Wheel lockup prevention, see ABS 644, 649, 659, 693, 708, 803
Wheel mounting 624
Wheel position 620
Wheel sensors 796
Wheel slip 606, 635, 659
Wheel-arch filters 438
Wheelbase (passenger cars) 900
Wheels, motor vehicle 624
Wheel-slip angle 351, 355
Wheel-speed sensors 103, 670, 659, 695, 712
Wheel-suspension linkage 620
Whitworth pipe threads 318
Width requirement (commercial vehicles) 360
Wind effect (vehicle dynamics) 350
Windingless-rotor alternators 878
Windshield and rear-window cleaning 770
Windshield antennas 788
Windshields 721, 774

PETITIONER'S EXHIBIT 1002
US PATENT NO. 6,581,565
Page 1502

Windshields and window glass, automotive 774
Windshield-wiper mechanism 770
Winter tires (M+S tires) 628
Wiper blades 771
Wiper motors (DC) 772
Wiper potentiometers 96
Wiper systems and accessories 770
Wire-knit mounting (catalytic convertor) 449
Work (energy), electrical 62
Work, braking 345, 648
Worked penetration 234
Worm gears 297

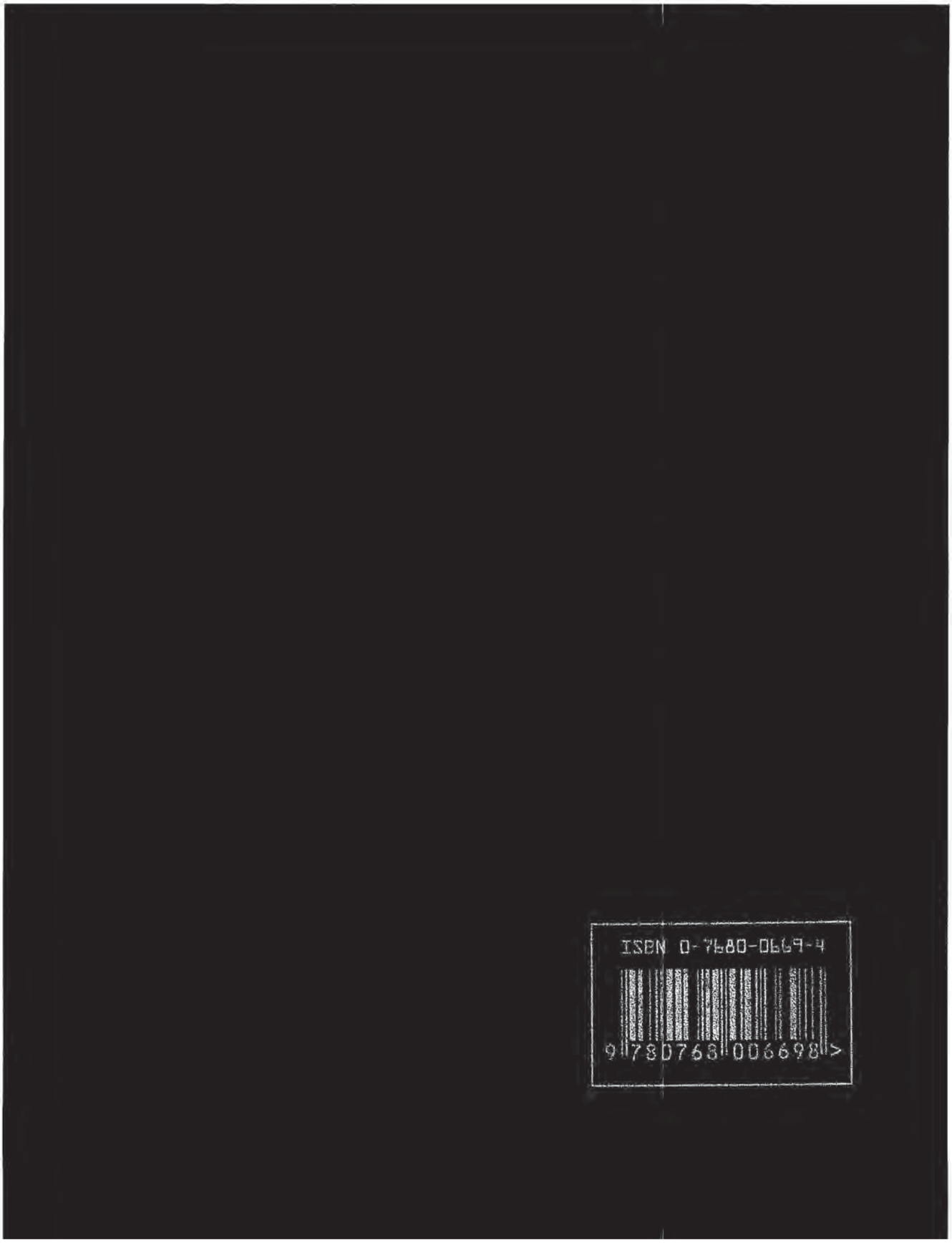
Y

Yard (conversion) 19
Yaw rate 358, 361, 705
Yawing motion 705
Yaw-moment buildup delay (GMA) 662
Yaw-moment coefficients 350
Yaw-rate sensors (gyrometers) 105, 712
Yield point 230
Yield strength (materials) 180

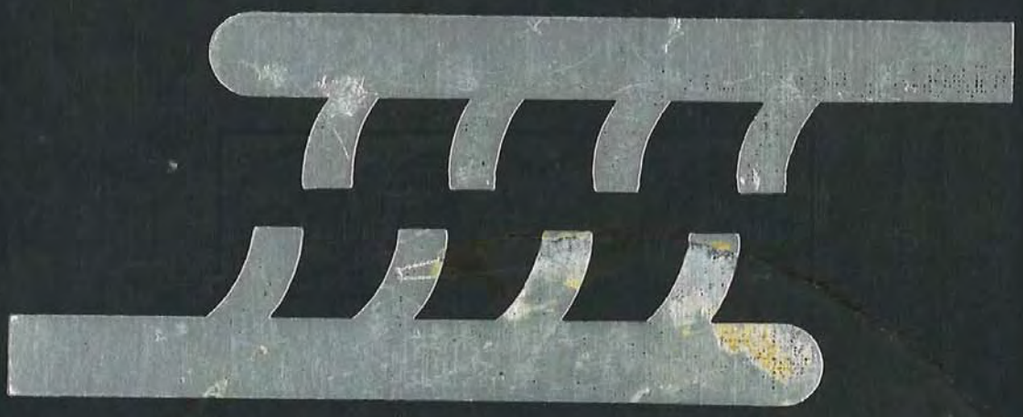
Z

Zener (Z-) diode 78
Zirconium-dioxide oxygen sensor 523

UNIVERSITY OF CALIFORNIA-LOS ANGELES
L 008 290 180 2


ISBN 0-7680-0669-4
9 780768 006698 >

Internal Combustion Engine Fundamentals



John B. Heywood

VW EX1014 (Part 1 of 4)
U.S. Patent No. 6,581,565



INTERNAL COMBUSTION ENGINE FUNDAMENTALS

PETITIONER'S EXHIBIT 1002
US PATENT NO. 6,581,565
Page 1508

McGraw-Hill Series in Mechanical Engineering

Jack P. Holman, *Southern Methodist University*
Consulting Editor

Anderson: *Modern Compressible Flow: With Historical Perspective*
Dieter: *Engineering Design: A Materials and Processing Approach*
Eckert and Drake: *Analysis of Heat and Mass Transfer*
Heywood: *Internal Combustion Engine Fundamentals*
Hinze: *Turbulence, 2/e*
Hutton: *Applied Mechanical Vibrations*
Juvinall: *Engineering Considerations of Stress, Strain, and Strength*
Kane and Levinson: *Dynamics: Theory and Applications*
Kays and Crawford: *Convective Heat and Mass Transfer*
Martin: *Kinematics and Dynamics of Machines*
Phelan: *Dynamics of Machinery*
Phelan: *Fundamentals of Mechanical Design, 3/e*
Pierce: *Acoustics: An Introduction to Its Physical Principles and Applications*
Raven: *Automatic Control Engineering, 4/e*
Rosenberg and Karnopp: *Introduction to Physics*
Schlichting: *Boundary-Layer Theory, 7/e*
Shames: *Mechanics of Fluids, 2/e*
Shigley: *Kinematic Analysis of Mechanisms, 2/e*
Shigley and Mitchell: *Mechanical Engineering Design, 4/e*
Shigley and Uicker: *Theory of Machines and Mechanisms*
Stoecker and Jones: *Refrigeration and Air Conditioning, 2/e*
Vanderplaats: *Numerical Optimization Techniques for Engineering Design: With Applications*

PETITIONER'S EXHIBIT 1002
US PATENT NO. 6,581,565
Page 1509

INTERNAL COMBUSTION ENGINE FUNDAMENTALS

John B. Heywood

Professor of Mechanical Engineering
Director, Sloan Automotive Laboratory
Massachusetts Institute of Technology

McGraw-Hill, Inc.
New York St. Louis San Francisco Auckland Bogotá
Caracas Lisbon London Madrid Mexico City Milan
Montreal New Delhi San Juan Singapore
Sydney Tokyo Toronto

PETITIONER'S EXHIBIT 1002
US PATENT NO. 6,581,565
Page 1510

INTERNAL COMBUSTION ENGINE FUNDAMENTALS

This book was set in Times Roman.
The editors were Anne Duffy and John M. Morriss; the designer
was Joan E. O'Connor; the production supervisor was
Denise L. Puryear. New drawings were done by ANCO.
Project Supervision was done by Santype International Ltd.
R. R. Donnelley & Sons Company was printer and binder.

See acknowledgements on page xxi.

Copyright © 1988 by McGraw-Hill, Inc. All rights reserved.
Printed in the United States of America. Except as permitted under the
United States Copyright Act of 1976, no part of this publication may be
reproduced or distributed in any form or by any means, or stored in a data
base or retrieval system, without the prior written permission
of the publisher.

23 24 25 26 DOC/DOC 0 9

ISBN: 978-0-07-028637-5
MHID: 0-07-028637-X

Library of Congress Cataloging-in-Publication Data

Heywood, John B.
Internal combustion engine fundamentals.
(McGraw-Hill series in mechanical engineering)
Bibliography: p.
Includes index.
1. Internal combustion engines. I. Title. II. Series.
TJ755.H45 1988 621.43 87-15251

This book is printed on acid-free paper.

PETITIONER'S EXHIBIT 1002
US PATENT NO. 6,581,565
Page 1511

ABOUT THE AUTHOR

Dr. John B. Heywood received the Ph.D. degree in mechanical engineering from the Massachusetts Institute of Technology in 1965. Following an additional post-doctoral year of research at MIT, he worked as a research officer at the Central Electricity Generating Board's Research Laboratory in England on magneto-hydrodynamic power generation. In 1968 he joined the faculty at MIT where he is Professor of Mechanical Engineering. At MIT he is Director of the Sloan Automotive Laboratory. He is currently Head of the Fluid and Thermal Science Division of the Mechanical Engineering Department, and the Transportation Energy Program Director in the MIT Energy Laboratory. He is faculty advisor to the MIT Sports Car Club.

Professor Heywood's teaching and research interests lie in the areas of thermodynamics, combustion, energy, power, and propulsion. During the past two decades, his research activities have centered on the operating characteristics and fuels requirements of automotive and aircraft engines. A major emphasis has been on computer models which predict the performance, efficiency, and emissions of spark-ignition, diesel, and gas turbine engines, and in carrying out experiments to develop and validate these models. He is also actively involved in technology assessments and policy studies related to automotive engines, automobile fuel utilization, and the control of air pollution. He consults frequently in the automotive and petroleum industries, and for the U.S. Government.

His extensive research in the field of engines has been supported by the U.S. Army, Department of Energy, Environmental Protection Agency, NASA, National Science Foundation, automobile and diesel engine manufacturers, and petroleum companies. He has presented or published over a hundred papers on

PETITIONER'S EXHIBIT 1002
US PATENT NO. 6,581,565
Page 1512

his research in technical conferences and journals. He has co-authored two previous books: *Open-Cycle MHD Power Generation* published by Pergamon Press in 1969 and *The Automobile and the Regulation of Its Impact on the Environment* published by University of Oklahoma Press in 1975.

He is a member of the American Society of Mechanical Engineers, an associate fellow of the American Institute of Aeronautics and Astronautics, a fellow of the British Institution of Mechanical Engineers, and in 1982 was elected a Fellow of the U.S. Society of Automotive Engineers for his technical contributions to automotive engineering. He is a member of the editorial boards of the journals *Progress in Energy and Combustion Science* and the *International Journal of Vehicle Design.*

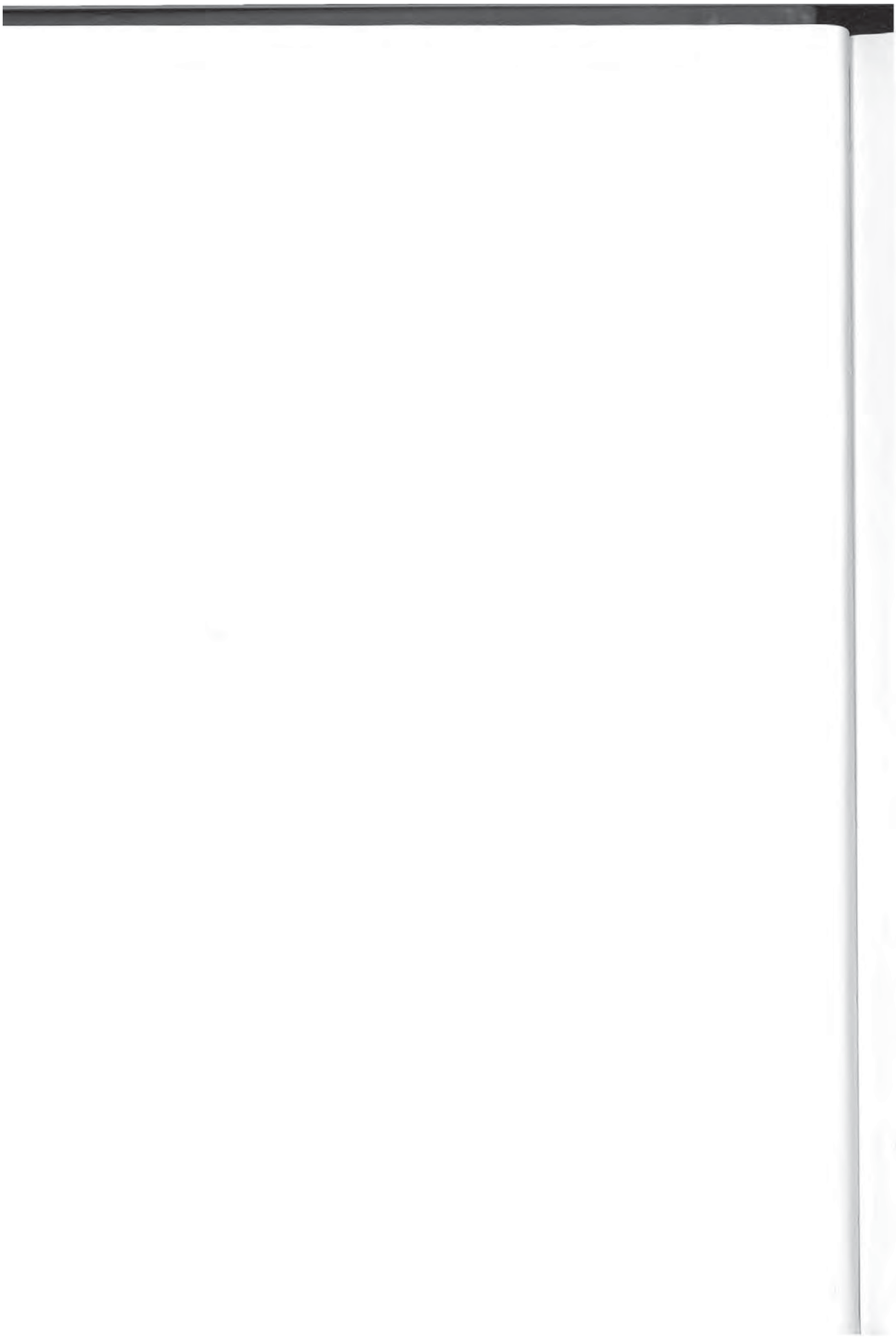
His research publications on internal combustion engines, power generation, and gas turbine combustion have won numerous awards. He was awarded the Ayreton Premium in 1969 by the British Institution of Electrical Engineers. Professor Heywood received a Ralph R. Teetor Award as an outstanding young engineering educator from the Society of Automotive Engineers in 1971. He has twice been the recipient of an SAE Arch T. Colwell Merit Award for an outstanding technical publication (1973 and 1981). He received SAE's Horning Memorial Award for the best paper on engines and fuels in 1984. In 1984 he received the Sc.D. degree from Cambridge University for his published contributions to engineering research. He was selected as the 1986 American Society of Mechanical Engineers Freeman Scholar for a major review of "Fluid Motion within the Cylinder of Internal Combustion Engines."

PETITIONER'S EXHIBIT 1002
US PATENT NO. 6,581,565
Page 1513

THIS BOOK IS DEDICATED TO MY FATHER,
Harold Heywood:

I have followed many of the paths he took.

PETITIONER'S EXHIBIT 1002
US PATENT NO. 6,581,565
Page 1514



CONTENTS

	Preface	xvii
	Commonly Used Symbols, Subscripts, and Abbreviations	xxiii
Chapter 1	**Engine Types and Their Operation**	**1**
1.1	Introduction and Historical Perspective	1
1.2	Engine Classifications	7
1.3	Engine Operating Cycles	9
1.4	Engine Components	12
1.5	Spark-Ignition Engine Operation	15
1.6	Examples of Spark-Ignition Engines	19
1.7	Compression-Ignition Engine Operation	25
1.8	Examples of Diesel Engines	31
1.9	Stratified-Charge Engines	37
Chapter 2	**Engine Design and Operating Parameters**	**42**
2.1	Important Engine Characteristics	42
2.2	Geometrical Properties of Reciprocating Engines	43
2.3	Brake Torque and Power	45
2.4	Indicated Work Per Cycle	46
2.5	Mechanical Efficiency	48
2.6	Road-Load Power	49
2.7	Mean Effective Pressure	50
2.8	Specific Fuel Consumption and Efficiency	51
2.9	Air/Fuel and Fuel/Air Ratios	53

PETITIONER'S EXHIBIT 1002
US PATENT NO. 6,581,565
Page 1516

2.10	Volumetric Efficiency	53
2.11	Engine Specific Weight and Specific Volume	54
2.12	Correction Factors for Power and Volumetric Efficiency	54
2.13	Specific Emissions and Emissions Index	56
2.14	Relationships between Performance Parameters	56
2.15	Engine Design and Performance Data	57
Chapter 3	**Thermochemistry of Fuel-Air Mixtures**	**62**
3.1	Characterization of Flames	62
3.2	Ideal Gas Model	64
3.3	Composition of Air and Fuels	64
3.4	Combustion Stoichiometry	68
3.5	The First Law of Thermodynamics and Combustion	72
3.5.1	Energy and Enthalpy Balances	72
3.5.2	Enthalpies of Formation	76
3.5.3	Heating Values	78
3.5.4	Adiabatic Combustion Processes	80
3.5.5	Combustion Efficiency of an Internal Combustion Engine	81
3.6	The Second Law of Thermodynamics Applied to Combustion	83
3.6.1	Entropy	83
3.6.2	Maximum Work from an Internal Combustion Engine and Efficiency	83
3.7	Chemically Reacting Gas Mixtures	85
3.7.1	Chemical Equilibrium	86
3.7.2	Chemical Reaction Rates	92
Chapter 4	**Properties of Working Fluids**	**100**
4.1	Introduction	100
4.2	Unburned Mixture Composition	102
4.3	Gas Property Relationships	107
4.4	A Simple Analytic Ideal Gas Model	109
4.5	Thermodynamic Charts	112
4.5.1	Unburned Mixture Charts	112
4.5.2	Burned Mixture Charts	116
4.5.3	Relation between Unburned and Burned Mixture Charts	123
4.6	Tables of Properties and Composition	127
4.7	Computer Routines for Property and Composition Calculations	130
4.7.1	Unburned Mixtures	130
4.7.2	Burned Mixtures	135
4.8	Transport Properties	141
4.9	Exhaust Gas Composition	145
4.9.1	Species Concentration Data	145
4.9.2	Equivalence Ratio Determination from Exhaust Gas Constituents	148
4.9.3	Effects of Fuel/Air Ratio Nonuniformity	152
4.9.4	Combustion Inefficiency	154

Chapter 5 Ideal Models of Engine Cycles 161

5.1 Introduction 161
5.2 Ideal Models of Engine Processes 162
5.3 Thermodynamic Relations for Engine Processes 164
5.4 Cycle Analysis with Ideal Gas Working Fluid with c_v and c_p Constant 169
5.4.1 Constant-Volume Cycle 169
5.4.2 Limited- and Constant-Pressure Cycles 172
5.4.3 Cycle Comparison 173
5.5 Fuel–Air Cycle Analysis 177
5.5.1 SI Engine Cycle Simulation 178
5.5.2 CI Engine Cycle Simulation 180
5.5.3 Results of Cycle Calculations 181
5.6 Overexpanded Engine Cycles 183
5.7 Availability Analysis of Engine Processes 186
5.7.1 Availability Relationships 186
5.7.2 Entropy Changes in Ideal Cycles 188
5.7.3 Availability Analysis of Ideal Cycles 189
5.7.4 Effect of Equivalence Ratio 192
5.8 Comparison with Real Engine Cycles 193

Chapter 6 Gas Exchange Processes 205

6.1 Inlet and Exhaust Processes in the Four-Stroke Cycle 206
6.2 Volumetric Efficiency 209
6.2.1 Quasi-Static Effects 209
6.2.2 Combined Quasi-Static and Dynamic Effects 212
6.2.3 Variation with Speed, and Valve Area, Lift, and Timing 216
6.3 Flow Through Valves 220
6.3.1 Poppet Valve Geometry and Timing 220
6.3.2 Flow Rate and Discharge Coefficients 225
6.4 Residual Gas Fraction 230
6.5 Exhaust Gas Flow Rate and Temperature Variation 231
6.6 Scavenging in Two-Stroke Cycle Engines 235
6.6.1 Two-Stroke Engine Configurations 235
6.6.2 Scavenging Parameters and Models 237
6.6.3 Actual Scavenging Processes 240
6.7 Flow Through Ports 245
6.8 Supercharging and Turbocharging 248
6.8.1 Methods of Power Boosting 248
6.8.2 Basic Relationships 249
6.8.3 Compressors 255
6.8.4 Turbines 263
6.8.5 Wave-Compression Devices 270

Chapter 7 SI Engine Fuel Metering and Manifold Phenomena 279

7.1 Spark-Ignition Engine Mixture Requirements 279
7.2 Carburetors 282

PETITIONER'S EXHIBIT 1002
US PATENT NO. 6,581,565
Page 1518

	7.2.1 Carburetor Fundamentals	282
	7.2.2 Modern Carburetor Design	285
7.3	Fuel-Injection Systems	294
	7.3.1 Multipoint Port Injection	294
	7.3.2 Single-Point Throttle-Body Injection	299
7.4	Feedback Systems	301
7.5	Flow Past Throttle Plate	304
7.6	Flow in Intake Manifolds	308
	7.6.1 Design Requirements	308
	7.6.2 Air-Flow Phenomena	309
	7.6.3 Fuel-Flow Phenomena	314
Chapter 8	**Charge Motion within the Cylinder**	**326**
8.1	Intake Jet Flow	326
8.2	Mean Velocity and Turbulence Characteristics	330
	8.2.1 Definitions	330
	8.2.2 Application to Engine Velocity Data	336
8.3	Swirl	342
	8.3.1 Swirl Measurement	343
	8.3.2 Swirl Generation during Induction	345
	8.3.3 Swirl Modification within the Cylinder	349
8.4	Squish	353
8.5	Prechamber Engine Flows	357
8.6	Crevice Flows and Blowby	360
8.7	Flows Generated by Piston–Cylinder Wall Interaction	365
Chapter 9	**Combustion in Spark-Ignition Engines**	**371**
9.1	Essential Features of Process	371
9.2	Thermodynamic Analysis of SI Engine Combustion	376
	9.2.1 Burned and Unburned Mixture States	376
	9.2.2 Analysis of Cylinder Pressure Data	383
	9.2.3 Combustion Process Characterization	389
9.3	Flame Structure and Speed	390
	9.3.1 Experimental Observations	390
	9.3.2 Flame Structure	395
	9.3.3 Laminar Burning Speeds	402
	9.3.4 Flame Propagation Relations	406
9.4	Cyclic Variations in Combustion, Partial Burning, and Misfire	413
	9.4.1 Observations and Definitions	413
	9.4.2 Causes of Cycle-by-Cycle and Cylinder-to-Cylinder Variations	419
	9.4.3 Partial Burning, Misfire, and Engine Stability	424
9.5	Spark Ignition	427
	9.5.1 Ignition Fundamentals	427
	9.5.2 Conventional Ignition Systems	437
	9.5.3 Alternative Ignition Approaches	443
9.6	Abnormal Combustion: Knock and Surface Ignition	450
	9.6.1 Description of Phenomena	450

PETITIONER'S EXHIBIT 1002
US PATENT NO. 6,581,565
Page 1519

9.6.2 Knock Fundamentals 457
9.6.3 Fuel Factors 470

Chapter 10 Combustion in Compression-Ignition Engines 491

10.1 Essential Features of Process 491
10.2 Types of Diesel Combustion Systems 493
10.2.1 Direct-Injection Systems 493
10.2.2 Indirect-Injection Systems 494
10.2.3 Comparison of Different Combustion Systems 495
10.3 Phenomenological Model of Compression-Ignition Engine Combustion 497
10.3.1 Photographic Studies of Engine Combustion 497
10.3.2 Combustion in Direct-Injection, Multispray Systems 503
10.3.3 Application of Model to Other Combustion Systems 506
10.4 Analysis of Cylinder Pressure Data 508
10.4.1 Combustion Efficiency 509
10.4.2 Direct-Injection Engines 509
10.4.3 Indirect-Injection Engines 514
10.5 Fuel Spray Behavior 517
10.5.1 Fuel Injection 517
10.5.2 Overall Spray Structure 522
10.5.3 Atomization 525
10.5.4 Spray Penetration 529
10.5.5 Droplet Size Distribution 532
10.5.6 Spray Evaporation 535
10.6 Ignition Delay 539
10.6.1 Definition and Discussion 539
10.6.2 Fuel Ignition Quality 541
10.6.3 Autoignition Fundamentals 542
10.6.4 Physical Factors Affecting Delay 546
10.6.5 Effect of Fuel Properties 550
10.6.6 Correlations for Ignition Delay in Engines 553
10.7 Mixing-Controlled Combustion 555
10.7.1 Background 555
10.7.2 Spray and Flame Structure 555
10.7.3 Fuel-Air Mixing and Burning Rates 558

Chapter 11 Pollutant Formation and Control 567

11.1 Nature and Extent of Problem 567
11.2 Nitrogen Oxides 572
11.2.1 Kinetics of NO Formation 572
11.2.2 Formation of NO_2 577
11.2.3 NO Formation in Spark-Ignition Engines 578
11.2.4 NO_x Formation in Compression-Ignition Engines 586
11.3 Carbon Monoxide 592
11.4 Unburned Hydrocarbon Emissions 596
11.4.1 Background 596
11.4.2 Flame Quenching and Oxidation Fundamentals 599

PETITIONER'S EXHIBIT 1002
US PATENT NO. 6,581,565
Page 1520

11.4.3	HC Emissions from Spark-Ignition Engines	601
11.4.4	Hydrocarbon Emission Mechanisms in Diesel Engines	620
11.5	Particulate Emissions	626
11.5.1	Spark-Ignition Engine Particulates	626
11.5.2	Characteristics of Diesel Particulates	626
11.5.3	Particulate Distribution within the Cylinder	631
11.5.4	Soot Formation Fundamentals	635
11.5.5	Soot Oxidation	642
11.5.6	Adsorption and Condensation	646
11.6	Exhaust Gas Treatment	648
11.6.1	Available Options	648
11.6.2	Catalytic Converters	649
11.6.3	Thermal Reactors	657
11.6.4	Particulate Traps	659
Chapter 12	**Engine Heat Transfer**	**668**
12.1	Importance of Heat Transfer	668
12.2	Modes of Heat Transfer	670
12.2.1	Conduction	670
12.2.2	Convection	670
12.2.3	Radiation	671
12.2.4	Overall Heat-Transfer Process	671
12.3	Heat Transfer and Engine Energy Balance	673
12.4	Convective Heat Transfer	676
12.4.1	Dimensional Analysis	676
12.4.2	Correlations for Time-Averaged Heat Flux	677
12.4.3	Correlations for Instantaneous Spatial Average Coefficients	678
12.4.4	Correlations for Instantaneous Local Coefficients	681
12.4.5	Intake and Exhaust System Heat Transfer	682
12.5	Radiative Heat Transfer	683
12.5.1	Radiation from Gases	683
12.5.2	Flame Radiation	684
12.5.3	Prediction Formulas	688
12.6	Measurements of Instantaneous Heat-Transfer Rates	689
12.6.1	Measurement Methods	689
12.6.2	Spark-Ignition Engine Measurements	690
12.6.3	Diesel Engine Measurements	692
12.6.4	Evaluation of Heat-Transfer Correlations	694
12.6.5	Boundary-Layer Behavior	697
12.7	Thermal Loading and Component Temperatures	698
12.7.1	Component Temperature Distributions	698
12.7.2	Effect of Engine Variables	701
Chapter 13	**Engine Friction and Lubrication**	**712**
13.1	Background	712
13.2	Definitions	714
13.3	Friction Fundamentals	715

PETITIONER'S EXHIBIT 1002
US PATENT NO. 6,581,565
Page 1521

13.3.1 Lubricated Friction 715
13.3.2 Turbulent Dissipation 719
13.3.3 Total Friction 719
13.4 Measurement Methods 719
13.5 Engine Friction Data 722
13.5.1 SI Engines 722
13.5.2 Diesel Engines 724
13.6 Engine Friction Components 725
13.6.1 Motored Engine Breakdown Tests 725
13.6.2 Pumping Friction 726
13.6.3 Piston Assembly Friction 729
13.6.4 Crankshaft Bearing Friction 734
13.6.5 Valve Train Friction 737
13.7 Accessory Power Requirements 739
13.8 Lubrication 740
13.8.1 Lubrication System 740
13.8.2 Lubricant Requirements 741

Chapter 14 Modeling Real Engine Flow and Combustion Processes 748

14.1 Purpose and Classification of Models 748
14.2 Governing Equations for Open Thermodynamic System 750
14.2.1 Conservation of Mass 750
14.2.2 Conservation of Energy 751
14.3 Intake and Exhaust Flow Models 753
14.3.1 Background 753
14.3.2 Quasi-Steady Flow Models 753
14.3.3 Filling and Emptying Methods 754
14.3.4 Gas Dynamic Models 756
14.4 Thermodynamic-Based In-Cylinder Models 762
14.4.1 Background and Overall Model Structure 762
14.4.2 Spark-Ignition Engine Models 766
14.4.3 Direct-Injection Engine Models 778
14.4.4 Prechamber Engine Models 784
14.4.5 Multicylinder and Complex Engine System Models 789
14.4.6 Second Law Analysis of Engine Processes 792
14.5 Fluid-Mechanic-Based Multidimensional Models 797
14.5.1 Basic Approach and Governing Equations 797
14.5.2 Turbulence Models 800
14.5.3 Numerical Methodology 803
14.5.4 Flow Field Predictions 807
14.5.5 Fuel Spray Modeling 813
14.5.6 Combustion Modeling 816

Chapter 15 Engine Operating Characteristics 823

15.1 Engine Performance Parameters 823
15.2 Indicated and Brake Power and MEP 824

PETITIONER'S EXHIBIT 1002
US PATENT NO. 6,581,565
Page 1522

15.3	Operating Variables That Affect SI Engine Performance, Efficiency, and Emissions	827
	15.3.1 Spark Timing	827
	15.3.2 Mixture Composition	829
	15.3.3 Load and Speed	839
	15.3.4 Compression Ratio	841
15.4	SI Engine Combustion Chamber Design	844
	15.4.1 Design Objectives and Options	844
	15.4.2 Factors That Control Combustion	846
	15.4.3 Factors That Control Performance	850
	15.4.4 Chamber Octane Requirement	852
	15.4.5 Chamber Optimization Strategy	857
15.5	Variables That Affect CI Engine Performance, Efficiency, and Emissions	858
	15.5.1 Load and Speed	858
	15.5.2 Fuel-Injection Parameters	863
	15.5.3 Air Swirl and Bowl-in-Piston Design	866
15.6	Supercharged and Turbocharged Engine Performance	869
	15.6.1 Four-Stroke Cycle SI Engines	869
	15.6.2 Four-Stroke Cycle CI Engines	874
	15.6.3 Two-Stroke Cycle SI Engines	881
	15.6.4 Two-Stroke Cycle CI Engines	883
15.7	Engine Performance Summary	886

Appendixes

A	Unit Conversion Factors	899
B	Ideal Gas Relationships	902
	B.1 Ideal Gas Law	902
	B.2 The Mole	903
	B.3 Thermodynamic Properties	903
	B.4 Mixtures of Ideal Gases	905
C	Equations for Fluid Flow through a Restriction	906
	C.1 Liquid Flow	907
	C.2 Gas Flow	907
D	Data on Working Fluids	911
	Index	917

PETITIONER'S EXHIBIT 1002
US PATENT NO. 6,581,565
Page 1523

PREFACE

Internal combustion engines date back to 1876 when Otto first developed the spark-ignition engine and 1892 when Diesel invented the compression-ignition engine. Since that time these engines have continued to develop as our knowledge of engine processes has increased, as new technologies became available, as demand for new types of engine arose, and as environmental constraints on engine use changed. Internal combustion engines, and the industries that develop and manufacture them and support their use, now play a dominant role in the fields of power, propulsion, and energy. The last twenty-five years or so have seen an explosive growth in engine research and development as the issues of air pollution, fuel cost, and market competitiveness have become increasingly important. An enormous technical literature on engines now exists which has yet to be adequately organized and summarized.

This book has been written as a text and a professional reference in response to that need. It contains a broadly based and extensive review of the fundamental principles which govern internal combustion engine design and operation. It attempts to provide a simplifying framework for the vast and complex mass of technical material that now exists on spark-ignition and compression-ignition engines, and at the same time to include sufficient detail to convey the real world dimensions of this pragmatic engineering field. It is the author's conviction that a sound knowledge of the relevant fundamentals in the many disciplines that contribute to this field, as well as an awareness of the extensive practical knowledge base which has been built up over many decades, are essential tools for engine research, development, and design. Of course, no one text can include everything about engines. The emphasis here is on the thermodynamics, combustion physics and chemistry, fluid flow, heat transfer, friction, and lubrication processes relevant to internal combustion engine design, performance, efficiency, emissions, and fuels requirements.

PETITIONER'S EXHIBIT 1002
US PATENT NO. 6,581,565
Page 1524

From a fundamental point of view, how the fuel-air mixture within an internal combustion engine cylinder is ignited appropriately organizes the field. From the method of ignition—spark-ignition or compression-ignition—follows each type of engine's important features: fuel requirements, method of mixture preparation, combustion chamber design, details of the combustion process, method of load control, emission formation mechanisms, and performance and efficiency characteristics. While many engine processes (such as intake and exhaust flows, convective heat transfer, and friction) are similar in both types of engines, this distinction is fundamental and lies behind the overall organization of the book.

The book is arranged in four major sections. The first (Chapters 1 to 5) provides an introduction to, and overview of, the major characteristics of spark-ignition and compression-ignition engines, defines the parameters used to describe engine operation, and develops the necessary thermodynamics and combustion theory required for a quantitative analysis of engine behavior. It concludes with an integrated treatment of the various methods of analyzing idealized models of internal combustion engine cycles. The second section (Chapters 6 to 8) focuses on engine flow phenomena. The details of the gas exchange process—intake and exhaust processes in four-stroke and scavenging in two-stroke cycles—and the various methods of supercharging engines—are reviewed. Fuel metering methods for spark-ignition engines and air- and fuel-flow phenomena in intake manifolds are described. The essential features of the various types of fluid motion within the engine cylinder are then developed. These flow processes control the amount of air an engine will induct (and therefore its power), and largely govern the rate at which the fuel-air mixture will burn during combustion.

The third section of the book focuses on engine combustion phenomena. These chapters (9, 10, and 11) are especially important. The combustion process releases the fuel's energy within the engine cylinder for eventual conversion to useful work. What fraction of the fuel's energy is converted depends strongly on how combustion takes place. The spark-ignition and compression-ignition engine combustion processes (Chapters 9 and 10, respectively) therefore influence essentially all aspects of engine behavior. Air pollutants are undesirable byproducts of combustion. Our extensive knowledge of how the major pollutants form during these combustion processes and how such emissions can be controlled is reviewed in Chapter 11.

The last section of the book focuses on engine operating characteristics. First, the fundamentals of engine heat transfer and friction, both of which detract from engine performance, are developed in Chapters 12 and 13. Chapter 14 then focuses on the methods available for predicting important aspects of engine behavior based on realistic models of engine flow and combustion processes. Since the various thermodynamic-based and fluid-mechanic-based models which have been developed over the past fifteen years or so are increasingly used in engine research and development, a knowledge of their basic structure and capabilities is most important. Then, Chapter 15 presents a summary of how the operating characteristics—power, efficiency, and emissions—of spark-ignition and compression-ignition engines depend on the major engine design and oper-

PETITIONER'S EXHIBIT 1002
US PATENT NO. 6,581,565
Page 1525

ating variables. These final two chapters effectively integrate the analytical understanding and practical knowledge of individual engine processes together to describe overall spark-ignition and compression-ignition engine behavior. Material on internal combustion engine fuels is distributed appropriately throughout the book. Each chapter is extensively illustrated and referenced, and includes problems for both undergraduate and graduate level courses.

While this book contains much advanced material on engine design and operation intended for the practitioner, each major topic is developed from its beginnings and the more sophisticated chapters have introductory sections to facilitate their use in undergraduate courses. The chapters are extensively cross-referenced and indexed. Thus several arrangements of the material for a course on engines can be followed. For example, an introductory course on internal combustion engines could begin with Chapters 1 and 2, which review the different types of engines and how their performance is characterized, and continue with the parts of Chapters 3 and 5, which introduce the key combustion concepts necessary to understand the effects of fuel/air ratio, and ideal cycle analysis. Selections from the introductory sections of Chapters 6, 9, 10, 11, and 15 could then be used to explain several of the practical and design aspects of spark-ignition and diesel engine intake and exhaust processes, combustion, emissions, and performance. A more advanced course would review this introductory material more rapidly, and then move on to those sections of Chapters 4 and 5, which cover fuel-air cycle analysis, a more extensive discussion of engine breathing using additional sections of Chapter 6, and more in-depth treatment of engine combustion and emissions processes based on the appropriate sections of Chapters 9, 10, and 11. Material on engine heat transfer and friction selected from Chapters 12 and 13 could be included next. While Chapter 14 on modeling the thermodynamics and fluid dynamics of real engine processes is primarily intended for the professional scientist and engineer, material from this chapter along with selections from Chapter 15 could be used to illustrate the performance, efficiency, and emissions characteristics of the different types of internal combustion engines. I have also used much of the more sophisticated material in Chapters 6 through 15 for review seminars on individual engine topics and more extensive courses for professional engineers, an additional important educational and reference opportunity.

Many individuals and organizations have assisted me in various ways as I have worked on this book over the past ten or so years. I am especially indebted to my colleagues in the Sloan Automotive Laboratory at M.I.T., Professors Wai K. Cheng, Ahmed F. Ghoniem, and James C. Keck, and Drs. Jack A. Ekchian, David P. Hoult, Joe M. Rife, and Victor W. Wong, for providing a stimulating environment in which to carry out engine research and for assuming additional burdens as a result of my writing. Many of the Sloan Automotive Laboratory's students have made significant contributions to this text through their research; their names appear in the reference lists. The U.S. Department of Energy provided support during the early stages of the text development and funded the work on engine cycle simulation used extensively in Chapters 14 and 15. I am grateful

PETITIONER'S EXHIBIT 1002
US PATENT NO. 6,581,565
Page 1526

to Churchill College, Cambridge University, for a year spent as a Richard C. Mellon Visiting Fellow, 1977–78, and the Engineering Department, Cambridge University, for acting as my host while I developed the outline and earlier chapters of the book. The M.I.T. sabbatical leave fund supported my full-time writing for eight months in 1983, and the Mechanical Engineering Department at Imperial College graciously acted as host.

I also want to acknowledge several individuals and organizations who have provided major inputs to this book beyond those cited in the references. Members of General Motors Research Laboratories have interacted extensively with the Sloan Automotive Laboratory over many years and provided valuable advice on engine research developments. Engineers from the Engine Research and Fluid Mechanics Departments at General Motors Research Laboratories reviewed and critiqued the final draft manuscript for me. Charles A. Amann, Head of the Engine Research Department, made especially helpful inputs on engine performance. John J. Brogan of the U.S. Department of Energy provided valuable assistance with the initial organization of this effort. My regular interactions over the years with the Advanced Powertrain Engineering Office and Scientific Research Laboratories of the Ford Motor Company have given me a broad exposure to the practical side of engine design and operation. A long-term relationship with Mobil Research and Development Corporation has provided comparable experiences in the area of engine-fuels interactions. Many organizations and individuals supplied specific material and illustrations for the text. I am especially grateful to those who made available the high-quality photographs and line drawings which I have used and acknowledged.

McGraw-Hill and the author would like to express their thanks to the following reviewers for their useful comments and suggestions: Jay A. Bolt, University of Michigan; Gary L. Borman and William L. Brown, University of Wisconsin at Madison; Dwight Bushnell, Oregon State University; Jerald A. Caton, Texas A & M University; David E. Cole, University of Michigan; Lawrence W. Evers, Michigan Technological University; Samuel S. Lestz, Pennsylvania State University; Willard Pulkrabek, University of Wisconsin; Robert F. Sawyer, University of California at Berkeley; Joseph E. Shepherd, Rensselaer Polytechnic Institute; and Spencer C. Sorenson, The Technical University of Denmark.

Special thanks are due to my secretaries for their faithful and thoughtful assistance with the manuscript over these many years, beyond the "call of duty"; Linda Pope typed an earlier draft of the book, and Karla Stryker was responsible for producing and coordinating subsequent drafts and the final manuscript. My wife Peggy, and sons James, Stephen, and Ben have encouraged me throughout this long and time-consuming project which took many hours away from them. Without their continuing support it would never have been finished; for their patience, and faith that it would ultimately come to fruition, I will always be grateful.

John B. Heywood

PETITIONER'S EXHIBIT 1002
US PATENT NO. 6,581,565
Page 1527

ACKNOWLEDGMENTS

The author wishes to acknowledge the following organizations and publishers for permission to reproduce figures and tables from their publications in this text: The American Chemical Society; American Institute of Aeronautics & Astronautics; American Society of Mechanical Engineers; Robert Bosch GmbH, CIMAC, Cambridge University Press; The Combustion Institute; Elsevier Science Publishing Company; G. T. Foulis & Co. Ltd.; General Motors Corporation; Gordon & Breach Science Publishers; The Institution of Mechanical Engineers; The Japan Society of Mechanical Engineers; M.I.T. Press; Macmillan Press Ltd.; McGraw-Hill Book Company; Mir Publishers; Mobil Oil Corporation; Morgan-Grampian Publishers; Pergamon Journals, Inc.; Plenum Press Corporation; The Royal Society of London; Scientific Publications Limited; Society of Automotive Engineers; Society of Automotive Engineers of Japan, Inc.; Society of Tribologists and Lubrications Engineers; Department of Mechanical Engineering, Stanford University.

PETITIONER'S EXHIBIT 1002
US PATENT NO. 6,581,565
Page 1528

COMMONLY USED SYMBOLS, SUBSCRIPTS, AND ABBREVIATIONS†

1. SYMBOLS

a	Crank radius
	Sound speed
	Specific availability
a	Acceleration
A	Area
A_C	Valve curtain area
A_{ch}	Cylinder head area
A_e	Exhaust port area
A_E	Effective area of flow restriction
A_i	Inlet port area
A_p	Piston crown area
B	Cylinder bore
	Steady-flow availability
c	Specific heat
c_p	Specific heat at constant pressure
c_s	Soot concentration (mass/volume)
c_v	Specific heat at constant volume
C	Absolute gas velocity

† Nomenclature specific to a section or chapter is defined in that section or chapter.

PETITIONER'S EXHIBIT 1002
US PATENT NO. 6,581,565
Page 1530

C_s	Swirl coefficient
C_D	Discharge coefficient
	Vehicle drag coefficient
d	Diameter
d_n	Fuel-injection-nozzle orifice diameter
D	Diameter
	Diffusion coefficient
D_d	Droplet diameter
D_{SM}	Sauter mean droplet diameter
D_v	Valve diameter
e	Radiative emissive power
	Specific energy
E_A	Activation energy
f	Coefficient of friction
	Fuel mass fraction
F	Force
g	Gravitational acceleration
	Specific Gibbs free energy
G	Gibbs free energy
h	Clearance height
	Oil film thickness
	Specific enthalpy
h_c	Heat-transfer coefficient
h_p	Port open height
h_s	Sensible specific enthalpy
H	Enthalpy
I	Moment of inertia
J	Flux
k	Thermal conductivity
	Turbulent kinetic energy
k_i^+ , k_i^-	Forward, backward, rate constants for ith reaction
K	Constant
K_c	Equilibrium constant expressed in concentrations
K_p	Equilibrium constant expressed in partial pressures
l	Characteristic length scale
	Connecting rod length
l_T	Characteristic length scale of turbulent flame
L	Piston stroke
L_n	Fuel-injection-nozzle orifice length
L_v	Valve lift
m	Mass
$\dot{m}$	Mass flow rate
m_r	Mass of residual gas
M	Mach number
	Molecular weight

PETITIONER'S EXHIBIT 1002
US PATENT NO. 6,581,565
Page 1531

n	Number of moles
	Polytropic exponent
n_R	Number of crank revolutions per power stroke
N	Crankshaft rotational speed
	Soot particle number density
	Turbocharger shaft speed
p	Cylinder pressure
	Pressure
P	Power
$\dot{q}$	Heat-transfer rate per unit area
	Heat-transfer rate per unit mass of fluid
Q	Heat transfer
$\dot{Q}$	Heat-transfer rate
Q_{ch}	Fuel chemical energy release or gross heat release
Q_{HV}	Fuel heating value
Q_n	Net heat release
r	Radius
r_c	Compression ratio
R	Connecting rod length/crank radius
	Gas constant
	Radius
R^+, R^-	One-way reaction rates
R_s	Swirl ratio
s	Crank axis to piston pin distance
	Specific entropy
S	Entropy
	Spray penetration
S_b	Turbulent burning speed
S_L	Laminar flame speed
S_p	Piston speed
t	Time
T	Temperature
	Torque
u	Specific internal energy
	Velocity
u'	Turbulence intensity
u_s	Sensible specific internal energy
u_T	Characteristic turbulent velocity
U	Compressor/turbine impellor tangential velocity
	Fluid velocity
	Internal energy
v	Specific volume
	Velocity
$\mathbf{v}$	Velocity
v_{ps}	Valve pseudo-flow velocity

PETITIONER'S EXHIBIT 1002
US PATENT NO. 6,581,565
Page 1532

v_{sq}	Squish velocity
V	Cylinder volume
	Volume
V_c	Clearance volume
V_d	Displaced cylinder volume
w	Relative gas velocity
	Soot surface oxidation rate
W	Work transfer
W_c	Work per cycle
W_p	Pumping work
x, y, z	Spatial coordinates
x	Mass fraction
$\tilde{x}$	Mole fraction
x_b	Burned mass fraction
x_r	Residual mass fraction
y	H/C ratio of fuel
	Volume fraction
Y_α	Concentration of species α per unit mass
Z	Inlet Mach index
α	Angle
	Thermal diffusivity $k/(\rho c)$
β	Angle
γ	Specific heat ratio c_p/c_v
Γ_c	Angular momentum of charge
δ	Boundary-layer thickness
δ_L	Laminar flame thickness
$\Delta\tilde{h}^\circ_{f,i}$	Molal enthalpy of formation of species i
$\Delta\theta_b$	Rapid burning angle
$\Delta\theta_d$	Flame development angle
ε	$4/(4 + y)$: y = H/C ratio of fuel
	Turbulent kinetic energy dissipation rate
η_a	Availability conversion efficiency
η_c	Combustion efficiency
η_C	Compressor isentropic efficiency
η_{ch}	Charging efficiency
η_f	Fuel conversion efficiency
η_m	Mechanical efficiency
η_{sc}	Scavenging efficiency
η_t	Thermal conversion efficiency
η_T	Turbine isentropic efficiency
η_{tr}	Trapping efficiency
η_v	Volumetric efficiency
θ	Crank angle
λ	Relative air/fuel ratio
Λ	Delivery ratio

PETITIONER'S EXHIBIT 1002
US PATENT NO. 6,581,565
Page 1533

μ	Dynamic viscosity
μ_i	Chemical potential of species i
ν	Kinematic viscosity μ/ρ
ν_i	Stoichiometric coefficient of species i
ξ	Flow friction coefficient
ρ	Density
$\rho_{a,0}$, $\rho_{a,i}$	Air density at standard, inlet conditions
σ	Normal stress
	Standard deviation
	Stefan-Boltzmann constant
	Surface tension
τ	Characteristic time
	Induction time
	Shear stress
τ_{id}	Ignition delay time
ϕ	Fuel/air equivalence ratio
Φ	Flow compressibility function [Eq. (C.11)]
	Isentropic compression function [Eq. (4.15*b*)]
ψ	Molar N/O ratio
	Throttle plate open angle
Ψ	Isentropic compression function [Eq. (4.15*a*)]
ω	Angular velocity
	Frequency

2. SUBSCRIPTS

a	Air
b	Burned gas
c	Coolant
	Cylinder
C	Compression stroke
	Compressor
cr	Crevice
e	Equilibrium
	Exhaust
E	Expansion stroke
f	Flame
	Friction
	Fuel
g	Gas
i	Indicated
	Intake
	Species i
ig	Gross indicated
in	Net indicated

PETITIONER'S EXHIBIT 1002
US PATENT NO. 6,581,565
Page 1534

l	Liquid
L	Laminar
p	Piston
	Port
P	Prechamber
r, θ, z	r, θ, z components
R	Reference value
s	Isentropic
	Stoichiometric
T	Nozzle or orifice throat
	Turbine
	Turbulent
u	Unburned
v	Valve
w	Wall
x, y, z	x, y, z components
0	Reference value
	Stagnation value

3. NOTATION

Δ	Difference
$\bar{}$	Average or mean value
$\tilde{}$	Value per mole
[ ]	Concentration, moles/vol
{ }	Mass fraction
$\dot{}$	Rate of change with time

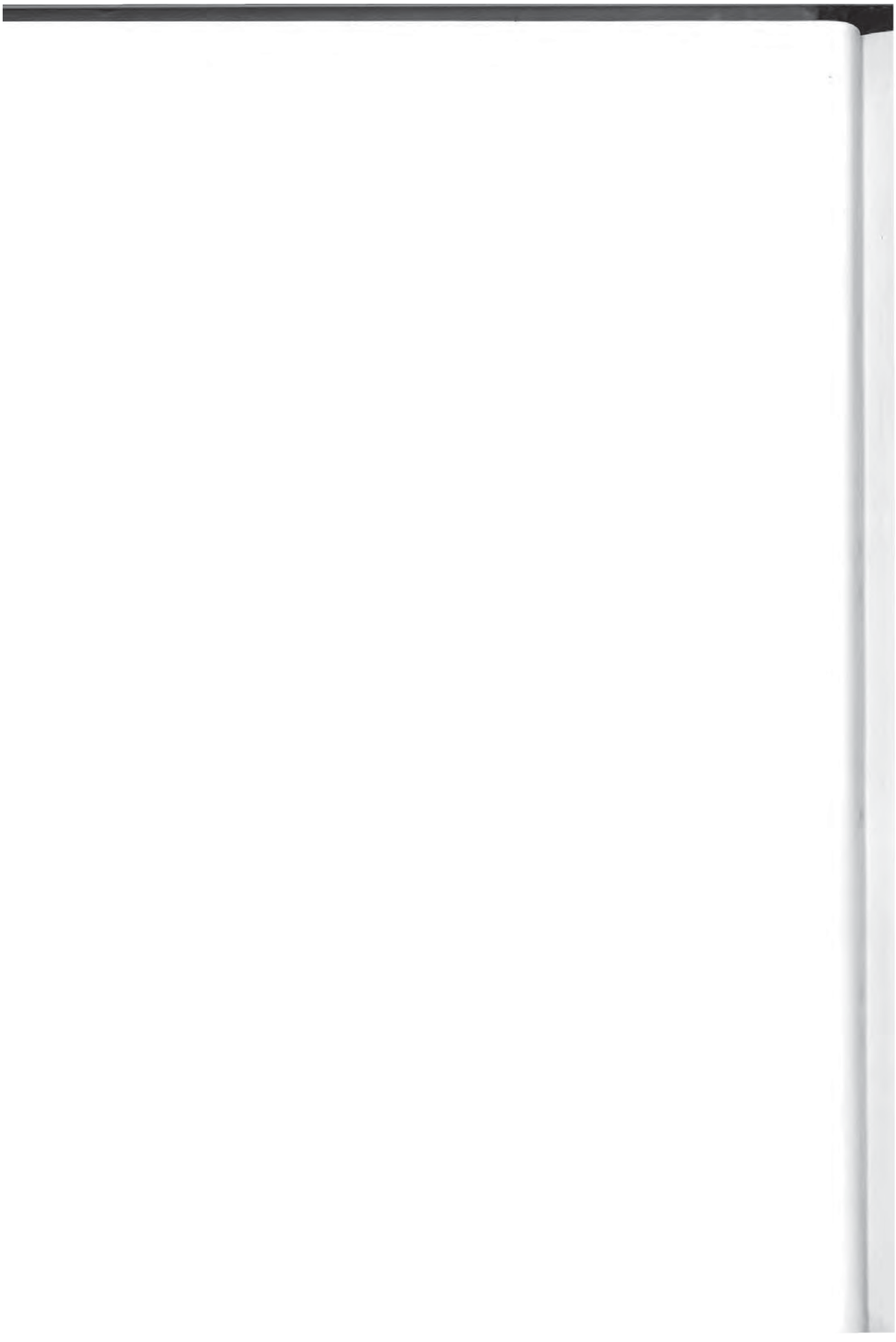
4. ABBREVIATIONS

(A/F)	Air/fuel ratio
BC, ABC, BBC	Bottom-center crank position, after BC, before BC
CN	Fuel cetane number
Da	Damköhler number τ_T/τ_L
EGR	Exhaust gas recycle
EI	Emission index
EPC, EPO	Exhaust port closing, opening
EVC, EVO	Exhaust valve closing, opening
(F/A)	Fuel/air ratio
(G/F)	Gas/fuel ratio
IPC, IPO	Inlet port closing, opening
IVC, IVO	Inlet valve closing, opening
mep	Mean effective pressure
Nu	Nusselt number $h_c\, l/k$

PETITIONER'S EXHIBIT 1002
US PATENT NO. 6,581,565
Page 1535

ON	Fuel octane number
Re	Reynolds number $\rho ul/\mu$
sfc	Specific fuel consumption
TC, ATC, BTC	Top-center crank position, after TC, before TC
We	Weber number $\rho_l u^2 D/\sigma$

PETITIONER'S EXHIBIT 1002
US PATENT NO. 6,581,565
Page 1536



CHAPTER 1

ENGINE TYPES AND THEIR OPERATION

1.1 INTRODUCTION AND HISTORICAL PERSPECTIVE

The purpose of internal combustion engines is the production of mechanical power from the chemical energy contained in the fuel. In *internal* combustion engines, as distinct from *external* combustion engines, this energy is released by burning or oxidizing the fuel *inside* the engine. The fuel-air mixture before combustion and the burned products after combustion are the actual working fluids. The work transfers which provide the desired power output occur directly between these working fluids and the mechanical components of the engine. The internal combustion engines which are the subject of this book are spark-ignition engines (sometimes called Otto engines, or gasoline or petrol engines, though other fuels can be used) and compression-ignition or diesel engines.† Because of their simplicity, ruggedness and high power/weight ratio, these two types of engine have found wide application in transportation (land, sea, and air) and power generation. It is the fact that combustion takes place inside the work-

† The gas turbine is also, by this definition, an "internal combustion engine." Conventionally, however, the term is used for spark-ignition and compression-ignition engines. The operating principles of gas turbines are fundamentally different, and they are not discussed as separate engines in this book.

PETITIONER'S EXHIBIT 1002
US PATENT NO. 6,581,565
Page 1538

producing part of these engines that makes their design and operating characteristics fundamentally different from those of other types of engine.

Practical heat engines have served mankind for over two and a half centuries. For the first 150 years, water, raised to steam, was interposed between the combustion gases produced by burning the fuel and the work-producing piston-in-cylinder expander. It was not until the 1860s that the internal combustion engine became a practical reality.[1, 2] The early engines developed for commercial use burned coal-gas air mixtures at atmospheric pressure—there was no compression before combustion. J. J. E. Lenoir (1822–1900) developed the first marketable engine of this type. Gas and air were drawn into the cylinder during the first half of the piston stroke. The charge was then ignited with a spark, the pressure increased, and the burned gases then delivered power to the piston for the second half of the stroke. The cycle was completed with an exhaust stroke. Some 5000 of these engines were built between 1860 and 1865 in sizes up to six horsepower. Efficiency was at best about 5 percent.

A more successful development—an atmospheric engine introduced in 1867 by Nicolaus A. Otto (1832–1891) and Eugen Langen (1833–1895)—used the pressure rise resulting from combustion of the fuel-air charge early in the outward stroke to accelerate a free piston and rack assembly so its momentum would generate a vacuum in the cylinder. Atmospheric pressure then pushed the piston inward, with the rack engaged through a roller clutch to the output shaft. Production engines, of which about 5000 were built, obtained thermal efficiencies of up to 11 percent. A slide valve controlled intake, ignition by a gas flame, and exhaust.

To overcome this engine's shortcomings of low thermal efficiency and excessive weight, Otto proposed an engine cycle with four piston strokes: an intake stroke, then a compression stroke before ignition, an expansion or power stroke where work was delivered to the crankshaft, and finally an exhaust stroke. He also proposed incorporating a stratified-charge induction system, though this was not achieved in practice. His prototype four-stroke engine first ran in 1876. A comparison between the Otto engine and its atmospheric-type predecessor indicates the reason for its success (see Table 1.1): the enormous reduction in engine weight and volume. This was the breakthrough that effectively founded the internal combustion engine industry. By 1890, almost 50,000 of these engines had been sold in Europe and the United States.

In 1884, an unpublished French patent issued in 1862 to Alphonse Beau de Rochas (1815–1893) was found which described the principles of the four-stroke cycle. This chance discovery cast doubt on the validity of Otto's own patent for this concept, and in Germany it was declared invalid. Beau de Rochas also outlined the conditions under which maximum efficiency in an internal combustion engine could be achieved. These were:

1. The largest possible cylinder volume with the minimum boundary surface
2. The greatest possible working speed

PETITIONER'S EXHIBIT 1002
US PATENT NO. 6,581,565
Page 1539

TABLE 1.1
Comparison of Otto four-stroke cycle and Otto-Langen engines[2]

	Otto and Langen	Otto four-stroke
Brake horsepower	2	2
Weight, lb, approx.	4000	1250
Piston displacement, in^3	4900	310
Power strokes per min	28	80
Shaft speed, rev/min	90	160
Mechanical efficiency, %	68	84
Overall efficiency, %	11	14
Expansion ratio	10	2.5

3. The greatest possible expansion ratio
4. The greatest possible pressure at the beginning of expansion

The first two conditions hold heat losses from the charge to a minimum. The third condition recognizes that the greater the expansion of the postcombustion gases, the greater the work extracted. The fourth condition recognizes that higher initial pressures make greater expansion possible, and give higher pressures throughout the process, both resulting in greater work transfer. Although Beau de Rochas' unpublished writings predate Otto's developments, he never reduced these ideas to practice. Thus Otto, in the broader sense, was the inventor of the modern internal combustion engine as we know it today.

Further developments followed fast once the full impact of what Otto had achieved became apparent. By the 1880s several engineers (e.g., Dugald Clerk, 1854–1913, and James Robson, 1833–1913, in England and Karl Benz, 1844–1929, in Germany) had successfully developed two-stroke internal combustion engines where the exhaust and intake processes occur during the end of the power stroke and the beginning of the compression stroke. James Atkinson (1846–1914) in England made an engine with a longer expansion than compression stroke, which had a high efficiency for the times but mechanical weaknesses. It was recognized that efficiency was a direct function of expansion ratio, yet compression ratios were limited to less than four if serious knock problems were to be avoided with the available fuels. Substantial carburetor and ignition system developments were required, and occurred, before high-speed gasoline engines suitable for automobiles became available in the late 1880s. Stationary engine progress also continued. By the late 1890s, large single-cylinder engines of 1.3-m bore fueled by low-energy blast furnace gas produced 600 bhp at 90 rev/min. In Britain, legal restrictions on volatile fuels turned their engine builders toward kerosene. Low compression ratio "oil" engines with heated external fuel vaporizers and electric ignition were developed with efficiencies comparable to those of gas engines (14 to 18 percent). The Hornsby-Ackroyd engine became the most

PETITIONER'S EXHIBIT 1002
US PATENT NO. 6,581,565
Page 1540

popular oil engine in Britain, and was also built in large numbers in the United States.[2]

In 1892, the German engineer Rudolf Diesel (1858–1913) outlined in his patent a new form of internal combustion engine. His concept of initiating combustion by injecting a liquid fuel into air heated solely by compression permitted a doubling of efficiency over other internal combustion engines. Much greater expansion ratios, without detonation or knock, were now possible. However, even with the efforts of Diesel and the resources of M.A.N. in Ausburg combined, it took five years to develop a practical engine.

Engine developments, perhaps less fundamental but nonetheless important to the steadily widening internal combustion engine markets, have continued ever since.[2–4] One more recent major development has been the rotary internal combustion engine. Although a wide variety of experimental rotary engines have been proposed over the years,[5] the first practical rotary internal combustion engine, the Wankel, was not successfully tested until 1957. That engine, which evolved through many years of research and development, was based on the designs of the German inventor Felix Wankel.[6, 7]

Fuels have also had a major impact on engine development. The earliest engines used for generating mechanical power burned gas. Gasoline, and lighter fractions of crude oil, became available in the late 1800s and various types of carburetors were developed to vaporize the fuel and mix it with air. Before 1905 there were few problems with gasoline; though compression ratios were low (4 or less) to avoid knock, the highly volatile fuel made starting easy and gave good cold weather performance. However, a serious crude oil shortage developed, and to meet the fivefold increase in gasoline demand between 1907 and 1915, the yield from crude had to be raised. Through the work of William Burton (1865–1954) and his associates of Standard Oil of Indiana, a thermal cracking process was developed whereby heavier oils were heated under pressure and decomposed into less complex more volatile compounds. These thermally cracked gasolines satisfied demand, but their higher boiling point range created cold weather starting problems. Fortunately, electrically driven starters, introduced in 1912, came along just in time.

On the farm, kerosene was the logical fuel for internal combustion engines since it was used for heat and light. Many early farm engines had heated carburetors or vaporizers to enable them to operate with such a fuel.

The period following World War I saw a tremendous advance in our understanding of how fuels affect combustion, and especially the problem of knock. The antiknock effect of tetraethyl lead was discovered at General Motors,[4] and it became commercially available as a gasoline additive in the United States in 1923. In the late 1930s, Eugene Houdry found that vaporized oils passed over an activated catalyst at 450 to 480°C were converted to high-quality gasoline in much higher yields than was possible with thermal cracking. These advances, and others, permitted fuels with better and better antiknock properties to be produced in large quantities; thus engine compression ratios steadily increased, improving power and efficiency.

PETITIONER'S EXHIBIT 1002
US PATENT NO. 6,581,565
Page 1541

During the past three decades, new factors for change have become important and now significantly affect engine design and operation. These factors are, first, the need to control the automotive contribution to urban air pollution and, second, the need to achieve significant improvements in automotive fuel consumption.

The automotive air-pollution problem became apparent in the 1940s in the Los Angeles basin. In 1952, it was demonstrated by Prof. A. J. Haagen-Smit that the smog problem there resulted from reactions between oxides of nitrogen and hydrocarbon compounds in the presence of sunlight.[8] In due course it became clear that the automobile was a major contributor to hydrocarbon and oxides of nitrogen emissions, as well as the prime cause of high carbon monoxide levels in urban areas. Diesel engines are a significant source of small soot or smoke particles, as well as hydrocarbons and oxides of nitrogen. Table 1.2 outlines the dimensions of the problem. As a result of these developments, emission standards for automobiles were introduced first in California, then nationwide in the United States, starting in the early 1960s. Emission standards in Japan and Europe, and for other engine applications, have followed. Substantial reductions in emissions from spark-ignition and diesel engines have been achieved. Both the use of catalysts in spark-ignition engine exhaust systems for emissions control and concern over the toxicity of lead antiknock additives have resulted in the reappearance of unleaded gasoline as a major part of the automotive fuels market. Also, the maximum lead content in leaded gasoline has been substantially reduced. The emission-control requirements and these fuel developments have produced significant changes in the way internal combustion engines are designed and operated.

Internal combustion engines are also an important source of noise. There are several sources of engine noise: the exhaust system, the intake system, the fan used for cooling, and the engine block surface. The noise may be generated by aerodynamic effects, may be due to forces that result from the combustion process, or may result from mechanical excitation by rotating or reciprocating engine components. Vehicle noise legislation to reduce emissions to the environment was first introduced in the early 1970s.

During the 1970s the price of crude petroleum rose rapidly to several times its cost (in real terms) in 1970, and concern built up regarding the longer-term availability of petroleum. Pressures for substantial improvements in internal combustion engine efficiency (in all its many applications) have become very substantial indeed. Yet emission-control requirements have made improving engine fuel consumption more difficult, and the removal and reduction of lead in gasoline has forced spark-ignition engine compression ratios to be reduced. Much work is being done on the use of alternative fuels to gasoline and diesel. Of the non-petroleum-based fuels, natural gas, and methanol and ethanol (methyl and ethyl alcohols) are receiving the greatest attention, while synthetic gasoline and diesel made from shale oil or coal, and hydrogen could be longer-term possibilities.

It might be thought that after over a century of development, the internal

PETITIONER'S EXHIBIT 1002
US PATENT NO. 6,581,565
Page 1542

TABLE 1.2
The automotive urban air-pollution problem

Pollutant	Impact	Mobile source emissions as % of total†	Automobile emissions		Truck emissions††	
			Uncontrolled vehicles, g/km‡	Reduction in new vehicles, % ¶	SI engines, g/km	Diesel, g/km
Oxides of nitrogen (NO and NO_2)	Reactant in photochemical smog; NO_2 is toxic	40–60	2.5	75	7	12
Carbon monoxide (CO)	Toxic	90	65	95	150	17
Unburned hydrocarbons (HC, many hydrocarbon compounds)	Reactant in photochemical smog	30–50	10	90	17‡‡	3
Particulates (soot and absorbed hydrocarbon compounds)	Reduces visibility; some of HC compounds mutagenic	50	0.5§	40§	n	0.5

† Depends on type of urban area and source mix.

‡ Average values for pre-1968 automobiles which had no emission controls, determined by U.S. test procedure which simulates typical urban and highway driving. Exhaust emissions, except for HC where 55 percent are exhaust emissions, 20 percent are evaporative emissions from fuel tank and carburetor, and 25 percent are crankcase blowby gases.

§ Diesel engine automobiles only. Particulate emissions from spark-ignition engines are negligible.

¶ Compares emissions from new spark-ignition engine automobiles with uncontrolled automobile levels in previous column. Varies from country to country. The United States, Canada, Western Europe, and Japan have standards with different degrees of severity. The United States, Europe, and Japan have different test procedures. Standards are strictest in the United States and Japan.

†† Representative average emission levels for trucks.

‡‡ With 95 percent exhaust emissions and 5 percent evaporative emissions.

n = negligible.

combustion engine has reached its peak and little potential for further improvement remains. Such is not the case. Conventional spark-ignition and diesel engines continue to show substantial improvements in efficiency, power, and degree of emission control. New materials now becoming available offer the possibilities of reduced engine weight, cost, and heat losses, and of different and more efficient internal combustion engine systems. Alternative types of internal combustion engines, such as the stratified-charge (which combines characteristics normally associated with either the spark-ignition or diesel) with its wider fuel tolerance, may become sufficiently attractive to reach large-scale production. The engine development opportunities of the future are substantial. While they

PETITIONER'S EXHIBIT 1002
US PATENT NO. 6,581,565
Page 1543

present a formidable challenge to automotive engineers, they will be made possible in large part by the enormous expansion of our knowledge of engine processes which the last twenty years has witnessed.

1.2 ENGINE CLASSIFICATIONS

There are many different types of internal combustion engines. They can be classified by:

1. *Application.* Automobile, truck, locomotive, light aircraft, marine, portable power system, power generation
2. *Basic engine design.* Reciprocating engines (in turn subdivided by arrangement of cylinders: e.g., in-line, V, radial, opposed), rotary engines (Wankel and other geometries)
3. *Working cycle.* Four-stroke cycle: naturally aspirated (admitting atmospheric air), supercharged (admitting precompressed fresh mixture), and turbocharged (admitting fresh mixture compressed in a compressor driven by an exhaust turbine), two-stroke cycle: crankcase scavenged, supercharged, and turbocharged
4. *Valve or port design and location.* Overhead (or I-head) valves, underhead (or L-head) valves, rotary valves, cross-scavenged porting (inlet and exhaust ports on opposite sides of cylinder at one end), loop-scavenged porting (inlet and exhaust ports on same side of cylinder at one end), through- or uniflow-scavenged (inlet and exhaust ports or valves at different ends of cylinder)
5. *Fuel.* Gasoline (or petrol), fuel oil (or diesel fuel), natural gas, liquid petroleum gas, alcohols (methanol, ethanol), hydrogen, dual fuel
6. *Method of mixture preparation.* Carburetion, fuel injection into the intake ports or intake manifold, fuel injection into the engine cylinder
7. *Method of ignition.* Spark ignition (in conventional engines where the mixture is uniform and in stratified-charge engines where the mixture is non-uniform), compression ignition (in conventional diesels, as well as ignition in gas engines by pilot injection of fuel oil)
8. *Combustion chamber design.* Open chamber (many designs: e.g., disc, wedge, hemisphere, bowl-in-piston), divided chamber (small and large auxiliary chambers; many designs: e.g., swirl chambers, prechambers)
9. *Method of load control.* Throttling of fuel and air flow together so mixture composition is essentially unchanged, control of fuel flow alone, a combination of these
10. *Method of cooling.* Water cooled, air cooled, uncooled (other than by natural convection and radiation)

All these distinctions are important and they illustrate the breadth of engine designs available. Because this book approaches the operating and emissions

PETITIONER'S EXHIBIT 1002
US PATENT NO. 6,581,565
Page 1544

TABLE 1.3
Classification of reciprocating engines by application

Class	Service	Approximate engine power range, kW	Predominant type		
			D or SI	Cycle	Cooling
Road vehicles	Motorcycles, scooters	0.75–70	SI	2, 4	A
	Small passenger cars	15–75	SI	4	A, W
	Large passenger cars	75–200	SI	4	W
	Light commercial	35–150	SI, D	4	W
	Heavy (long-distance) commercial	120–400	D	4	W
Off-road vehicles	Light vehicles (factory, airport, etc.)	1.5–15	SI	2, 4	A, W
	Agricultural	3–150	SI, D	2, 4	A, W
	Earth moving	40–750	D	2, 4	W
	Military	40–2000	D	2, 4	A, W
Railroad	Rail cars	150–400	D	2, 4	W
	Locomotives	400–3000	D	2, 4	W
Marine	Outboard	0.4–75	SI	2	W
	Inboard motorcrafts	4–750	SI, D	4	W
	Light naval craft	30–2200	D	2, 4	W
	Ships	3500–22,000	D	2, 4	W
	Ships' auxiliaries	75–750	D	4	W
Airborne vehicles	Airplanes	45–2700	SI	4	A
	Helicopters	45–1500	SI	4	A
Home use	Lawn mowers	0.7–3	SI	2, 4	A
	Snow blowers	2–5	SI	2, 4	A
	Light tractors	2–8	SI	4	A
Stationary	Building service	7–400	D	2, 4	W
	Electric power	35–22,000	D	2, 4	W
	Gas pipeline	750–5000	SI	2, 4	W

SI = spark-ignition; D = diesel; A = air cooled; W = water cooled.
Source: Adapted from Taylor.[9]

characteristics of internal combustion engines from a fundamental point of view, the method of ignition has been selected as the primary classifying feature. From the method of ignition—spark-ignition or compression-ignition†—follow the important characteristics of the fuel used, method of mixture preparation, combustion chamber design, method of load control, details of the combustion process, engine emissions, and operating characteristics. Some of the other classifications are used as subcategories within this basic classification. The engine operating cycle—four-stroke or two-stroke—is next in importance; the principles of these two cycles are described in the following section.

Table 1.3 shows the most common applications of internal combustion

† In the remainder of the book, these terms will often be abbreviated by SI and CI, respectively.

PETITIONER'S EXHIBIT 1002
US PATENT NO. 6,581,565
Page 1545

engines, the predominant type of engine used in each classification listed, and the approximate engine power range in each type of service.

1.3 ENGINE OPERATING CYCLES

Most of this book is about reciprocating engines, where the piston moves back and forth in a cylinder and transmits power through a connecting rod and crank mechanism to the drive shaft as shown in Fig. 1-1. The steady rotation of the crank produces a cyclical piston motion. The piston comes to rest at the top-center (TC) crank position and bottom-center (BC) crank position when the cylinder volume is a minimum or maximum, respectively.† The minimum cylinder volume is called the clearance volume V_c. The volume swept out by the

† These crank positions are also referred to as top-dead-center (TDC) and bottom-dead-center (BDC).

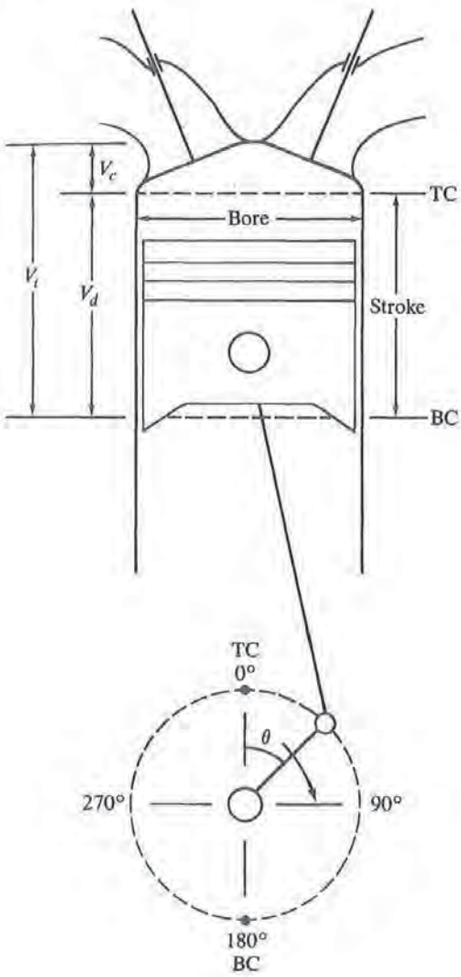


FIGURE 1-1
Basic geometry of the reciprocating internal combustion engine. V_c, V_d and V_t indicate clearance, displaced, and total cylinder volumes.

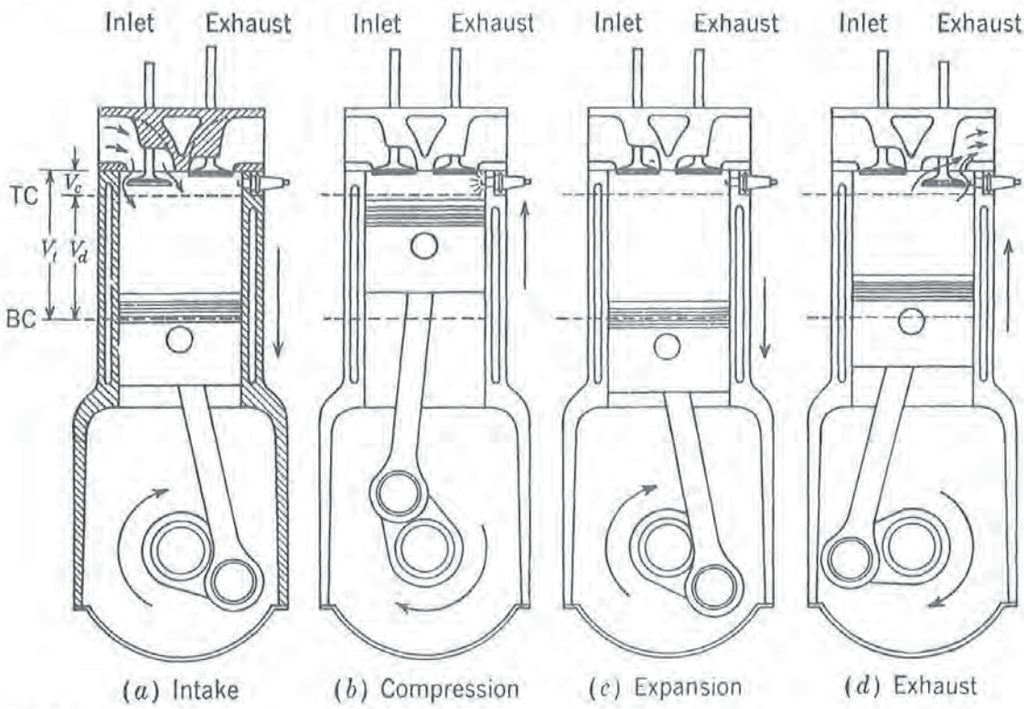


FIGURE 1-2
The four-stroke operating cycle.[10]

piston, the difference between the maximum or total volume V_t and the clearance volume, is called the displaced or swept volume V_d. The ratio of maximum volume to minimum volume is the compression ratio r_c. Typical values of r_c are 8 to 12 for SI engines and 12 to 24 for CI engines.

The majority of reciprocating engines operate on what is known as the *four-stroke cycle*. Each cylinder requires four strokes of its piston—two revolutions of the crankshaft—to complete the sequence of events which produces one power stroke. Both SI and CI engines use this cycle which comprises (see Fig. 1-2):

1. *An intake stroke*, which starts with the piston at TC and ends with the piston at BC, which draws fresh mixture into the cylinder. To increase the mass inducted, the inlet valve opens shortly before the stroke starts and closes after it ends.
2. *A compression stroke*, when both valves are closed and the mixture inside the cylinder is compressed to a small fraction of its initial volume. Toward the end of the compression stroke, combustion is initiated and the cylinder pressure rises more rapidly.
3. *A power stroke*, or expansion stroke, which starts with the piston at TC and ends at BC as the high-temperature, high-pressure, gases push the piston down and force the crank to rotate. About five times as much work is done on the piston during the power stroke as the piston had to do during compression.

PETITIONER'S EXHIBIT 1002
US PATENT NO. 6,581,565
Page 1547

As the piston approaches BC the exhaust valve opens to initiate the exhaust process and drop the cylinder pressure to close to the exhaust pressure.

4. *An exhaust stroke*, where the remaining burned gases exit the cylinder: first, because the cylinder pressure may be substantially higher than the exhaust pressure; then as they are swept out by the piston as it moves toward TC. As the piston approaches TC the inlet valve opens. Just after TC the exhaust valve closes and the cycle starts again.

Though often called the Otto cycle after its inventor, Nicolaus Otto, who built the first engine operating on these principles in 1876, the more descriptive four-stroke nomenclature is preferred.

The four-stroke cycle requires, for each engine cylinder, two crankshaft revolutions for each power stroke. To obtain a higher power output from a given engine size, and a simpler valve design, the *two-stroke* cycle was developed. The two-stroke cycle is applicable to both SI and CI engines.

Figure 1-3 shows one of the simplest types of two-stroke engine designs. Ports in the cylinder liner, opened and closed by the piston motion, control the exhaust and inlet flows while the piston is close to BC. The two strokes are:

1. *A compression stroke*, which starts by closing the inlet and exhaust ports, and then compresses the cylinder contents and draws fresh charge into the crankcase. As the piston approaches TC, combustion is initiated.

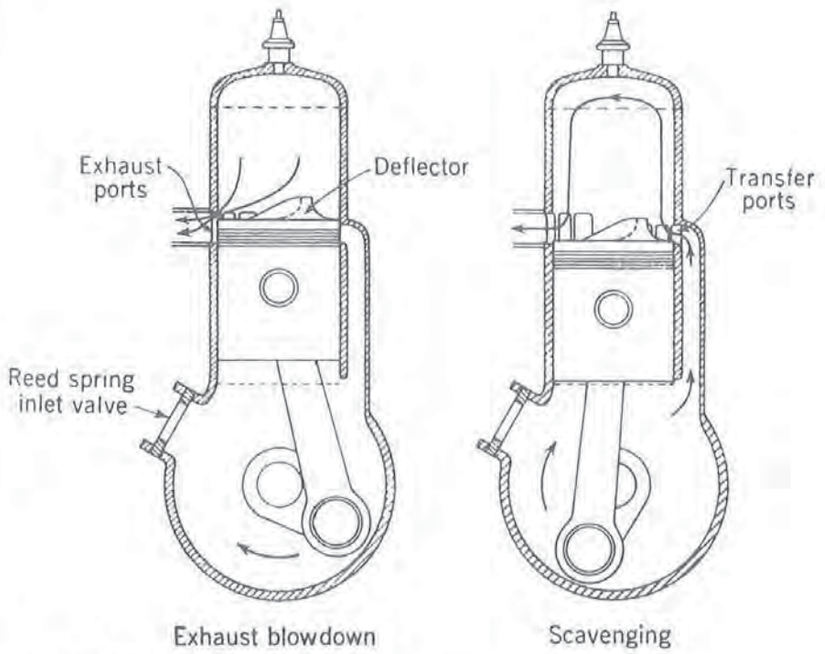


FIGURE 1-3
The two-stroke operating cycle. A crankcase-scavenged engine is shown.[10]

2. *A power or expansion stroke*, similar to that in the four-stroke cycle until the piston approaches BC, when first the exhaust ports and then the intake ports are uncovered (Fig. 1-3). Most of the burnt gases exit the cylinder in an exhaust blowdown process. When the inlet ports are uncovered, the fresh charge which has been compressed in the crankcase flows into the cylinder. The piston and the ports are generally shaped to deflect the incoming charge from flowing directly into the exhaust ports and to achieve effective scavenging of the residual gases.

Each engine cycle with one power stroke is completed in one crankshaft revolution. However, it is difficult to fill completely the displaced volume with fresh charge, and some of the fresh mixture flows directly out of the cylinder during the scavenging process.† The example shown is a *cross-scavenged* design; other approaches use *loop-scavenging* or *uniflow* systems (see Sec. 6.6).

1.4 ENGINE COMPONENTS

Labeled cutaway drawings of a four-stroke SI engine and a two-stroke CI engine are shown in Figs. 1-4 and 1-5, respectively. The spark-ignition engine is a four-cylinder in-line automobile engine. The diesel is a large V eight-cylinder design with a uniflow scavenging process. The function of the major components of these engines and their construction materials will now be reviewed.

The engine cylinders are contained in the engine block. The block has traditionally been made of gray cast iron because of its good wear resistance and low cost. Passages for the cooling water are cast into the block. Heavy-duty and truck engines often use removable cylinder sleeves pressed into the block that can be replaced when worn. These are called *wet liners* or *dry liners* depending on whether the sleeve is in direct contact with the cooling water. Aluminum is being used increasingly in smaller SI engine blocks to reduce engine weight. Iron cylinder liners may be inserted at the casting stage, or later on in the machining and assembly process. The crankcase is often integral with the cylinder block.

The crankshaft has traditionally been a steel forging; nodular cast iron crankshafts are also accepted normal practice in automotive engines. The crankshaft is supported in main bearings. The maximum number of main bearings is one more than the number of cylinders; there may be less. The crank has eccentric portions (crank throws); the connecting rod big-end bearings attach to the crank pin on each throw. Both main and connecting rod bearings use steel-backed precision inserts with bronze, babbit, or aluminum as the bearing materials. The crankcase is sealed at the bottom with a pressed-steel or cast aluminum oil pan which acts as an oil reservoir for the lubricating system.

† It is primarily for this reason that two-stroke SI engines are at a disadvantage because the lost fresh charge contains fuel and air.

PETITIONER'S EXHIBIT 1002
US PATENT NO. 6,581,565
Page 1549

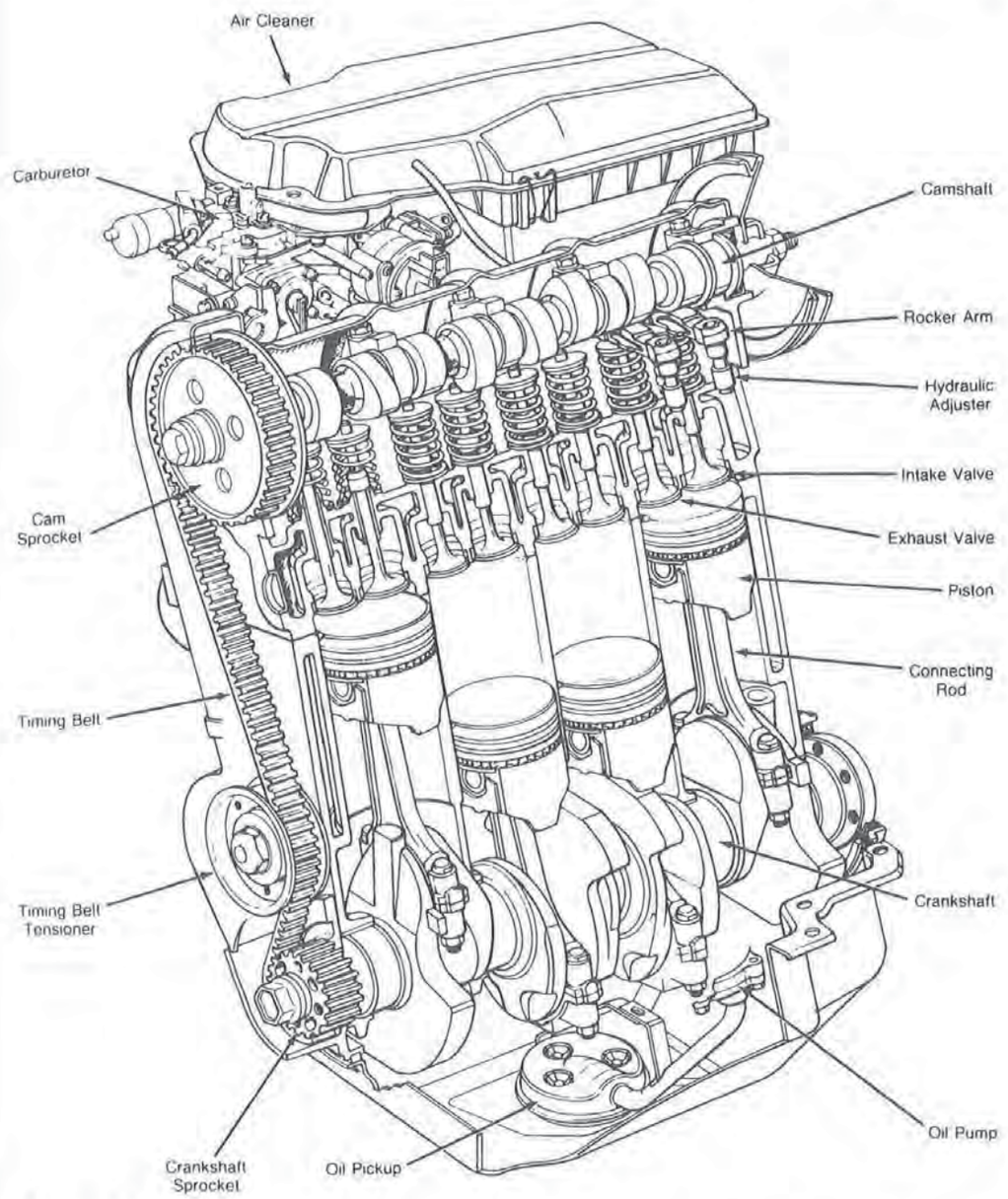


FIGURE 1-4
Cutaway drawing of Chrysler 2.2-liter displacement four-cylinder spark-ignition engine.[11] Bore 87.5 mm, stroke 92 mm, compression ratio 8.9, maximum power 65 kW at 5000 rev/min.

Pistons are made of aluminum in small engines or cast iron in larger slower-speed engines. The piston both seals the cylinder and transmits the combustion-generated gas pressure to the crank pin via the connecting rod. The connecting rod, usually a steel or alloy forging (though sometimes aluminum in small engines), is fastened to the piston by means of a steel piston pin through the rod upper end. The piston pin is usually hollow to reduce its weight.

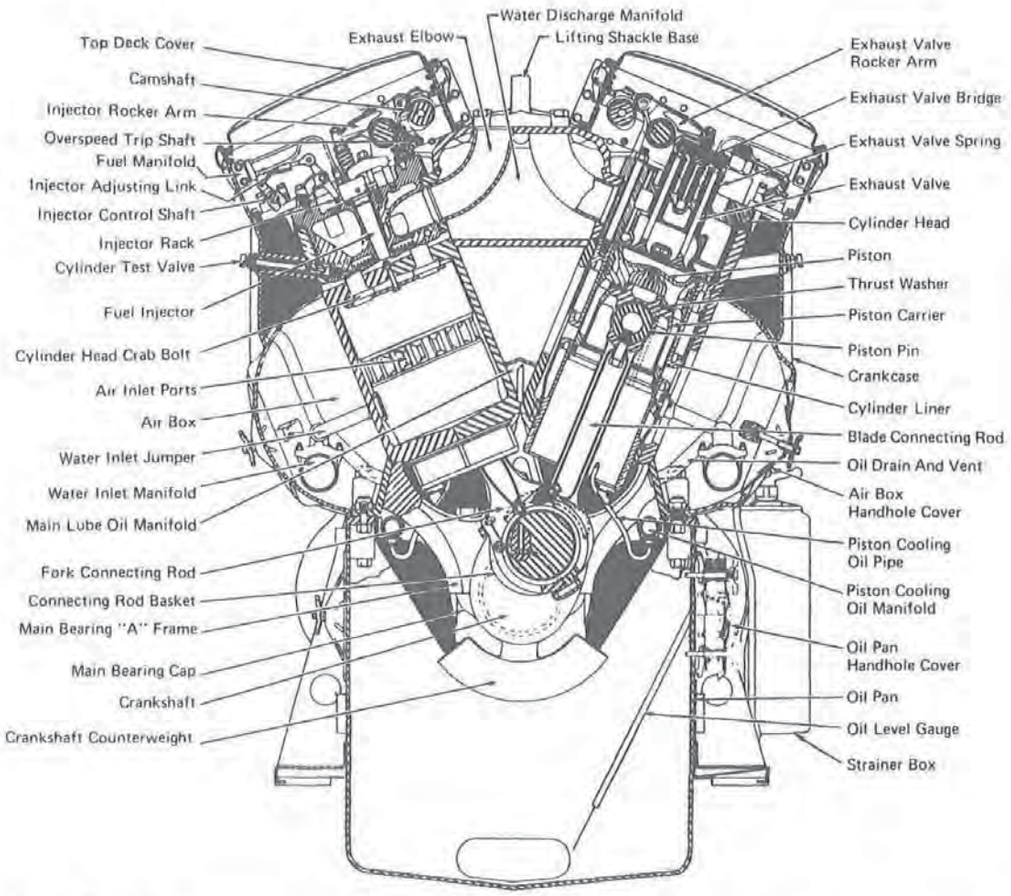


FIGURE 1-5
Cross-section drawing of an Electro-Motive two-stroke cycle diesel engine. This engine uses a uniflow scavenging process with inlet ports in the cylinder liner and four exhaust valves in the cylinder head. Bore 230.2 mm, stroke 254 mm, displaced volume per cylinder 10.57 liters, rated speed 750–900 rev/min. (*Courtesy Electro-Motive Division, General Motors Corporation.*)

The oscillating motion of the connecting rod exerts an oscillating force on the cylinder walls via the piston skirt (the region below the piston rings). The piston skirt is usually shaped to provide appropriate thrust surfaces. The piston is fitted with rings which ride in grooves cut in the piston head to seal against gas leakage and control oil flow. The upper rings are compression rings which are forced outward against the cylinder wall and downward onto the groove face. The lower rings scrape the surplus oil from the cylinder wall and return it to the crankcase. The crankcase must be ventilated to remove gases which blow by the piston rings, to prevent pressure buildup.

The cylinder head (or heads in V engines) seals off the cylinders and is made of cast iron or aluminum. It must be strong and rigid to distribute the gas forces acting on the head as uniformly as possible through the engine block. The cylinder head contains the spark plug (for an SI engine) or fuel injector (for a CI engine), and, in overhead valve engines, parts of the valve mechanism.

PETITIONER'S EXHIBIT 1002
US PATENT NO. 6,581,565
Page 1551

The valves shown in Fig. 1-4 are poppet valves, the valve type normally used in four-stroke engines. Valves are made from forged alloy steel; the cooling of the exhaust valve which operates at about 700°C may be enhanced by using a hollow stem partially filled with sodium which through evaporation and condensation carries heat from the hot valve head to the cooler stem. Most modern spark-ignition engines have overhead valve locations (sometimes called valve-in-head or I-head configurations) as shown in Fig. 1-4. This geometry leads to a compact combustion chamber with minimum heat losses and flame travel time, and improves the breathing capacity. Previous geometries such as the L head where valves are to one side of the cylinder are now only used in small engines.

The valve stem moves in a valve guide, which can be an integral part of the cylinder head (or engine block for L-head engines), or may be a separate unit pressed into the head (or block). The valve seats may be cut in the head or block metal (if cast iron) or hard steel inserts may be pressed into the head or block. A valve spring, attached to the valve stem with a spring washer and split keeper, holds the valve closed. A valve rotator turns the valves a few degrees on opening to wipe the valve seat, avoid local hot spots, and prevent deposits building up in the valve guide.

A camshaft made of cast iron or forged steel with one cam per valve is used to open and close the valves. The cam surfaces are hardened to obtain adequate life. In four-stroke cycle engines, camshafts turn at one-half the crankshaft speed. Mechanical or hydraulic lifters or tappets slide in the block and ride on the cam. Depending on valve and camshaft location, additional members are required to transmit the tappet motion to the valve stem; e.g., in in-head valve engines with the camshaft at the side, a push rod and rocker arm are used. A recent trend in automotive engines is to mount the camshaft over the head with the cams acting either directly or through a pivoted follower on the valve. Camshafts are gear, belt, or chain driven from the crankshaft.

An intake manifold (aluminum or cast iron) and an exhaust manifold (generally of cast iron) complete the SI engine assembly. Other engine components specific to spark-ignition engines—carburetor, fuel injectors, ignition systems—are described more fully in the remaining sections in this chapter.

The two-stroke cycle CI engine shown in Fig. 1-5 is of the uniflow scavenged design. The burned gases exhaust through four valves in the cylinder head. These valves are controlled through cam-driven rocker arms. Fresh air is compressed and fed to the air box by a Roots blower. The air inlet ports at the bottom of each cylinder liner are uncovered by the descending piston, and the scavenging air flows upward along the cylinder axis. The fuel injectors are mounted in the cylinder head and are driven by the camshaft through rocker arms. Diesel fuel-injection systems are discussed in more detail in Sec. 1.7.

1.5 SPARK-IGNITION ENGINE OPERATION

In SI engines the air and fuel are usually mixed together in the intake system prior to entry to the engine cylinder, using a carburetor (Fig. 1-6) or fuel-injection system (Fig. 1-7). In automobile applications, the temperature of the air entering

PETITIONER'S EXHIBIT 1002
US PATENT NO. 6,581,565
Page 1552

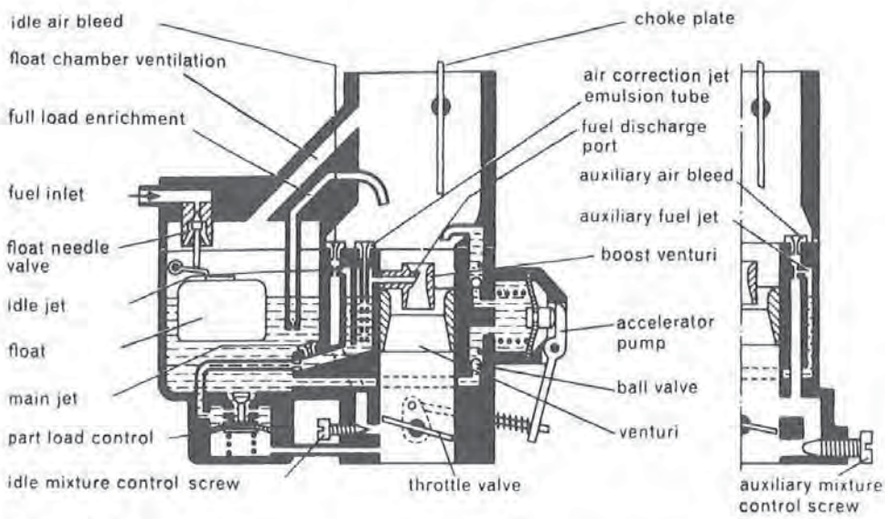


FIGURE 1-6
Cross section of single-barrel downdraft carburetor.[12] (*Courtesy Robert Bosch GmbH and SAE.*)

the intake system is controlled by mixing ambient air with air heated by contact with the exhaust manifold. The ratio of mass flow of air to mass flow of fuel must be held approximately constant at about 15 to ensure reliable combustion. The

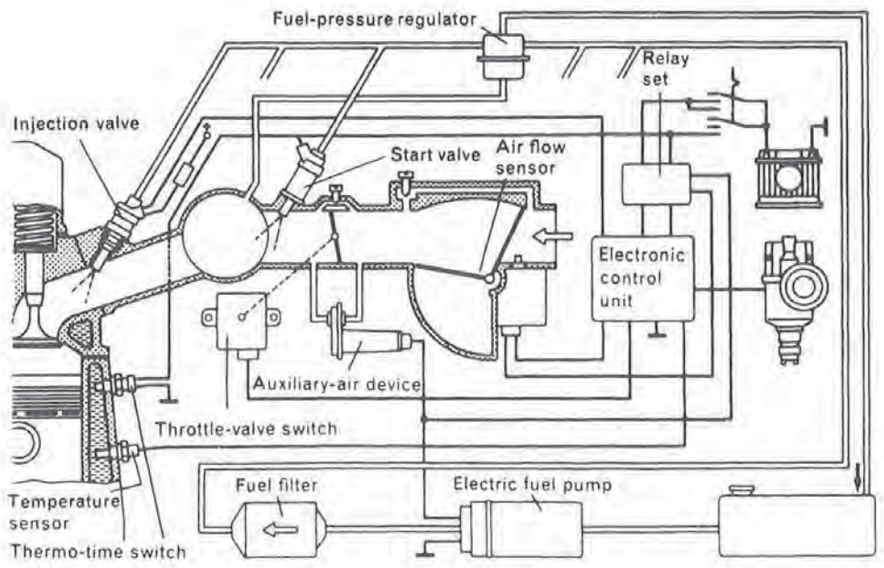


FIGURE 1-7
Schematic drawing of L-Jetronic port electronic fuel-injection system.[12] (*Courtesy Robert Bosch GmbH and SAE.*)

carburetor meters an appropriate fuel flow for the engine air flow in the following manner. The air flow through the venturi (a converging-diverging nozzle) sets up a pressure difference between the venturi inlet and throat which is used to meter an appropriate amount of fuel from the float chamber, through a series of orifices, into the air flow at the venturi throat. Just downstream of the venturi is a throttle valve or plate which controls the combined air and fuel flow, and thus the engine output. The intake flow is throttled to below atmospheric pressure by reducing the flow area when the power required (at any engine speed) is below the maximum which is obtained when the throttle is wide open. The intake manifold is usually heated to promote faster evaporation of the liquid fuel and obtain more uniform fuel distribution between cylinders.

Fuel injection into the intake manifold or inlet port is an increasingly common alternative to a carburetor. With port injection, fuel is injected through individual injectors from a low-pressure fuel supply system into each intake port. There are several different types of systems: mechanical injection using an injection pump driven by the engine; mechanical, driveless, continuous injection; electronically controlled, driveless, injection. Figure 1-7 shows an example of an electronically controlled system. In this system, the air flow rate is measured directly; the injection valves are actuated twice per cam shaft revolution by injection pulses whose duration is determined by the electronic control unit to provide the desired amount of fuel per cylinder per cycle.[12] An alternative approach is to use a single fuel injector located above the throttle plate in the position normally occupied by the carburetor. This approach permits electronic control of the fuel flow at reduced cost.

The sequence of events which take place inside the engine cylinder is illustrated in Fig. 1-8. Several variables are plotted against crank angle through the entire four-stroke cycle. Crank angle is a useful independent variable because engine processes occupy almost constant crank angle intervals over a wide range of engine speeds. The figure shows the valve timing and volume relationship for a typical automotive spark-ignition engine. To maintain high mixture flows at high engine speeds (and hence high power outputs) the inlet valve, which opens before TC, closes substantially after BC. During intake, the inducted fuel and air mix in the cylinder with the *residual* burned gases remaining from the previous cycle. After the intake valve closes, the cylinder contents are compressed to above atmospheric pressure and temperature as the cylinder volume is reduced. Some heat transfer to the piston, cylinder head, and cylinder walls occurs but the effect on unburned gas properties is modest.

Between 10 and 40 crank angle degrees before TC an electrical discharge across the spark plug starts the combustion process. A distributor, a rotating switch driven off the camshaft, interrupts the current from the battery through the primary circuit of the ignition coil. The secondary winding of the ignition coil, connected to the spark plug, produces a high voltage across the plug electrodes as the magnetic field collapses. Traditionally, cam-operated breaker points have been used; in most automotive engines, the switching is now done electronically. A turbulent flame develops from the spark discharge, propagates

PETITIONER'S EXHIBIT 1002
US PATENT NO. 6,581,565
Page 1554

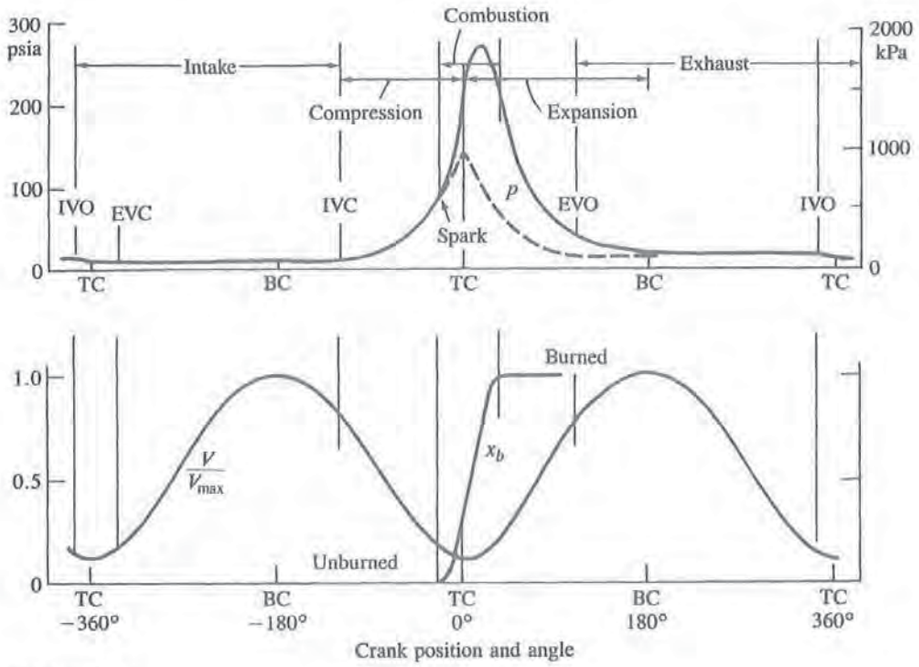


FIGURE 1-8
Sequence of events in four-stroke spark-ignition engine operating cycle. Cylinder pressure p (solid line, firing cycle; dashed line, motored cycle), cylinder volume V/V_{max}, and mass fraction burned x_b are plotted against crank angle.

across the mixture of air, fuel, and residual gas in the cylinder, and extinguishes at the combustion chamber wall. The duration of this burning process varies with engine design and operation, but is typically 40 to 60 crank angle degrees, as shown in Fig. 1-8. As fuel-air mixture burns in the flame, the cylinder pressure in Fig. 1-8 (solid line) rises above the level due to compression alone (dashed line). This latter curve—called the motored cylinder pressure—is the pressure trace obtained from a motored or nonfiring engine.† Note that due to differences in the flow pattern and mixture composition between cylinders, and within each cylinder cycle-by-cycle, the development of each combustion process differs somewhat. As a result, the shape of the pressure versus crank angle curve in each cylinder, and cycle-by-cycle, is not exactly the same.

There is an optimum spark timing which, for a given mass of fuel and air inside the cylinder, gives maximum torque. More advanced (earlier) timing or retarded (later) timing than this optimum gives lower output. Called *maximum*

† In practice, the intake and compression processes of a firing engine and a motored engine are not exactly the same due to the presence of burned gases from the previous cycle under firing conditions.

PETITIONER'S EXHIBIT 1002
US PATENT NO. 6,581,565
Page 1555

brake-torque (MBT) timing,† this optimum timing is an empirical compromise between starting combustion too early in the compression stroke (when the work transfer is *to* the cylinder gases) and completing combustion too late in the expansion stroke (and so lowering peak expansion stroke pressures).

About two-thirds of the way through the expansion stroke, the exhaust valve starts to open. The cylinder pressure is greater than the exhaust manifold pressure and a *blowdown* process occurs. The burned gases flow through the valve into the exhaust port and manifold until the cylinder pressure and exhaust pressure equilibrate. The duration of this process depends on the pressure level in the cylinder. The piston then *displaces* the burned gases from the cylinder into the manifold during the exhaust stroke. The exhaust valve opens before the end of the expansion stroke to ensure that the blowdown process does not last too far into the exhaust stroke. The actual timing is a compromise which balances reduced work transfer to the piston before BC against reduced work transfer to the cylinder contents after BC.

The exhaust valve remains open until just after TC; the intake opens just before TC. The valves are opened and closed slowly to avoid noise and excessive cam wear. To ensure the valves are fully open when piston velocities are at their highest, the valve open periods often overlap. If the intake flow is throttled to below exhaust manifold pressure, then backflow of burned gases into the intake manifold occurs when the intake valve is first opened.

1.6 EXAMPLES OF SPARK-IGNITION ENGINES

This section presents examples of production spark-ignition engines to illustrate the different types of engines in common use.

Small SI engines are used in many applications: in the home (e.g., lawn mowers, chain saws), in portable power generation, as outboard motorboat engines, and in motorcycles. These are often single-cylinder engines. In the above applications, light weight, small bulk, and low cost in relation to the power generated are the most important characteristics; fuel consumption, engine vibration, and engine durability are less important. A single-cylinder engine gives only one power stroke per revolution (two-stroke cycle) or two revolutions (four-stroke cycle). Hence, the torque pulses are widely spaced, and engine vibration and smoothness are significant problems.

Multicylinder engines are invariably used in automotive practice. As rated power increases, the advantages of smaller cylinders in regard to size, weight, and improved engine balance and smoothness point toward increasing the number of

† MBT timing has traditionally been defined as the minimum spark advance for best torque. Since the torque first increases and then decreases as spark timing is advanced, the definition used here is more precise.

PETITIONER'S EXHIBIT 1002
US PATENT NO. 6,581,565
Page 1556

cylinders per engine. An upper limit on cylinder size is dictated by dynamic considerations: the inertial forces that are created by accelerating and decelerating the reciprocating masses of the piston and connecting rod would quickly limit the maximum speed of the engine. Thus, the displaced volume is spread out amongst several smaller cylinders. The increased frequency of power strokes with a multicylinder engine produces much smoother torque characteristics. Multicylinder engines can also achieve a much better state of balance than single-cylinder engines. A force must be applied to the piston to accelerate it during the first half of its travel from bottom-center or top-center. The piston then exerts a force as it decelerates during the second part of the stroke. It is desirable to cancel these inertia forces through the choice of number and arrangement of cylinders to achieve a *primary balance*. Note, however, that the motion of the piston is more rapid during the upper half of its stroke than during the lower half (a consequence of the connecting rod and crank mechanism evident from Fig. 1-1; see also Sec. 2.2). The resulting inequality in piston acceleration and deceleration produces corresponding differences in inertia forces generated. Certain combinations of cylinder number and arrangement will balance out these secondary inertia force effects.

Four-cylinder in-line engines are the most common arrangements for automobile engines up to about 2.5-liter displacement. An example of this in-line arrangement was shown in Fig. 1-4. It is compact—an important consideration for small passenger cars. It provides two torque pulses per revolution of the crankshaft and primary inertia forces (though not secondary forces) are balanced. V engines and opposed-piston engines are occasionally used with this number of cylinders.

The V arrangement, with two banks of cylinders set at 90° or a more acute angle to each other, provides a compact block and is used extensively for larger displacement engines. Figure 1-9 shows a V-6 engine, the six cylinders being arranged in two banks of three with a 60° angle between their axis. Six cylinders are usually used in the 2.5- to 4.5-liter displacement range. Six-cylinder engines provide smoother operation with three torque pulses per revolution. The in-line arrangement results in a long engine, however, giving rise to crankshaft torsional vibration and making even distribution of air and fuel to each cylinder more difficult. The V-6 arrangement is much more compact, and the example shown provides primary balance of the reciprocating components. With the V engine, however, a rocking moment is imposed on the crankshaft due to the secondary inertia forces, which results in the engine being less well balanced than the in-line version. The V-8 and V-12 arrangements are also commonly used to provide compact, smooth, low-vibration, larger-displacement, spark-ignition engines.

Turbochargers are used to increase the maximum power that can be obtained from a given displacement engine. The work transfer to the piston per cycle, in each cylinder, which controls the power the engine can deliver, depends on the amount of fuel burned per cylinder per cycle. This depends on the amount of fresh air that is inducted each cycle. Increasing the air density prior to entry into the engine thus increases the maximum power that an engine of given dis-

PETITIONER'S EXHIBIT 1002
US PATENT NO. 6,581,565
Page 1557

FIGURE 1-9
Cross-section drawings of General Motors 60 degree V-6 spark-ignition engine.[13] Displacement 2.8 liter, bore 89 mm, stroke 76 mm, compression ratio 8.5, maximum power 86 kW at 4800 rev/min.

placement can deliver. Figure 1-10 shows an example of a turbocharged four-cylinder spark-ignition engine. The turbocharger, a compressor-turbine combination, uses the energy available in the engine exhaust stream to achieve compression of the intake flow. The air flow passes through the compressor (2), intercooler (3), carburetor (4), manifold (5), and inlet valve (6) as shown. Engine inlet pressures (or boost) of up to about 100 kPa above atmospheric pressure are typical. The exhaust flow through the valve (7) and manifold (8) drives the turbine (9) which powers the compressor. A wastegate (valve) just upstream of the turbine bypasses some of the exhaust gas flow when necessary to prevent the boost pressure becoming too high. The wastegate linkage (11) is controlled by a boost pressure regulator. While this turbocharged engine configuration has the carburetor downstream of the compressor, some turbocharged spark-ignition engines have the carburetor upstream of the compressor so that it operates at or below atmospheric pressure. Figure 1-11 shows a cutaway drawing of a small automotive turbocharger. The arrangements of the compressor and turbine

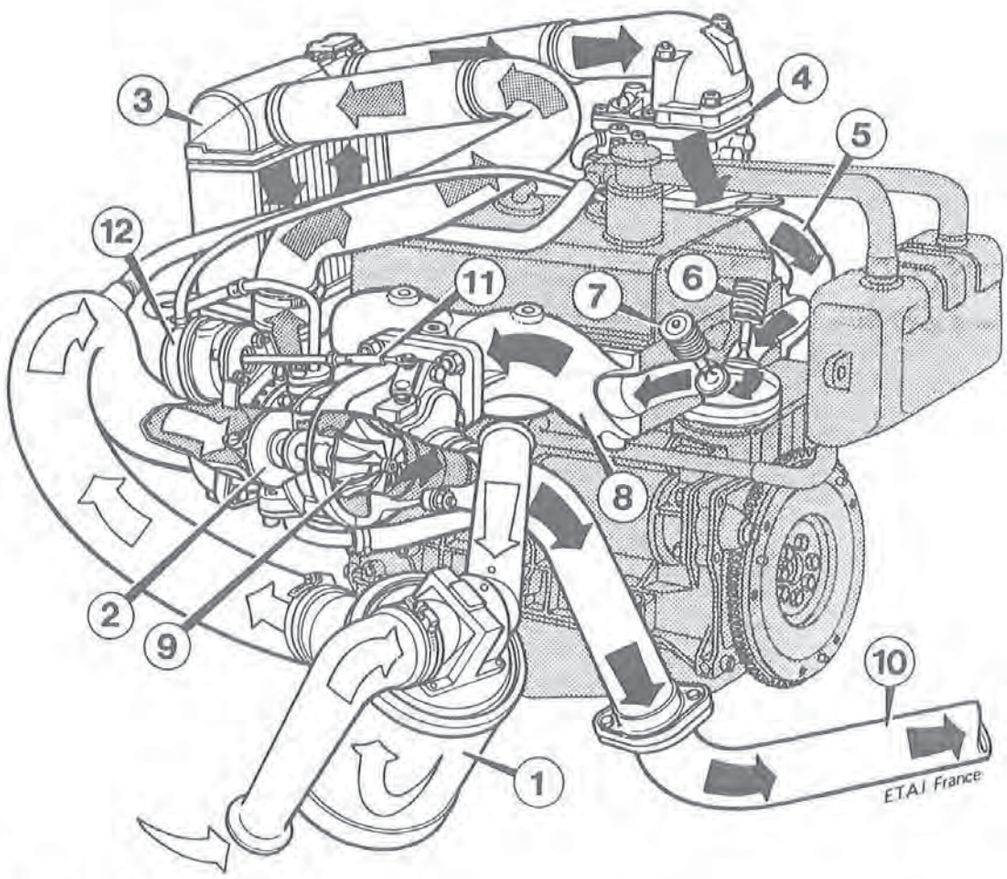


FIGURE 1-10
Turbocharged four-cylinder automotive spark-ignition engine. (*Courtesy Regie Nationale des Usines.*)

PETITIONER'S EXHIBIT 1002
US PATENT NO. 6,581,565
Page 1559

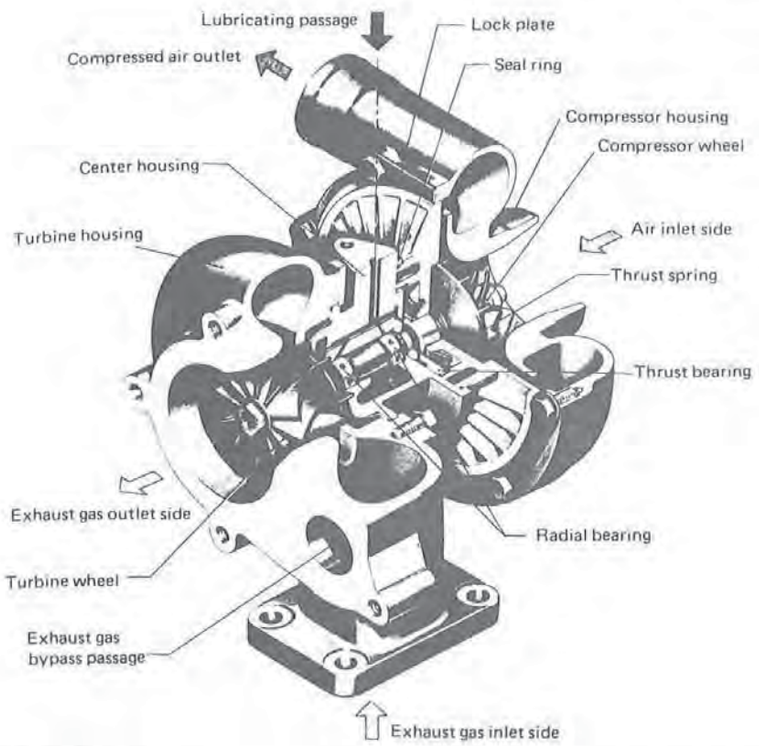


FIGURE 1-11
Cutaway view of small automotive engine turbocharger. (*Courtesy Nissan Motor Co., Ltd.*)

rotors connected via the central shaft and of the turbine and compressor flow passages are evident.

Figure 1-12 shows a two-stroke cycle spark-ignition engine. The two-stroke cycle spark-ignition engine is used for small-engine applications where low cost and weight/power ratio are important and when the use factor is low. Examples of such applications are outboard motorboat engines, motorcycles, and chain saws. All such engines are of the carburetor crankcase-compression type which is one of the simplest prime movers available. It has three moving parts per cylinder: the piston, connecting rod, and the crank. The prime advantage of the two-stroke cycle spark-ignition engine relative to the four-stroke cycle engine is its higher power per unit displaced volume due to twice the number of power strokes per crank revolution. This is offset by the lower fresh charge density achieved by the two-stroke cycle gas-exchange process and the loss of fresh mixture which goes straight through the engine during scavenging. Also, oil consumption is higher in two-stroke cycle engines due to the need to add oil to the fuel to lubricate the piston ring and piston surfaces.

The Wankel rotary engine is an alternative to the reciprocating engine geometry of the engines illustrated above. It is used when its compactness and higher engine speed (which result in high power/weight and power/volume ratios), and inherent balance and smoothness, offset its higher heat transfer, and

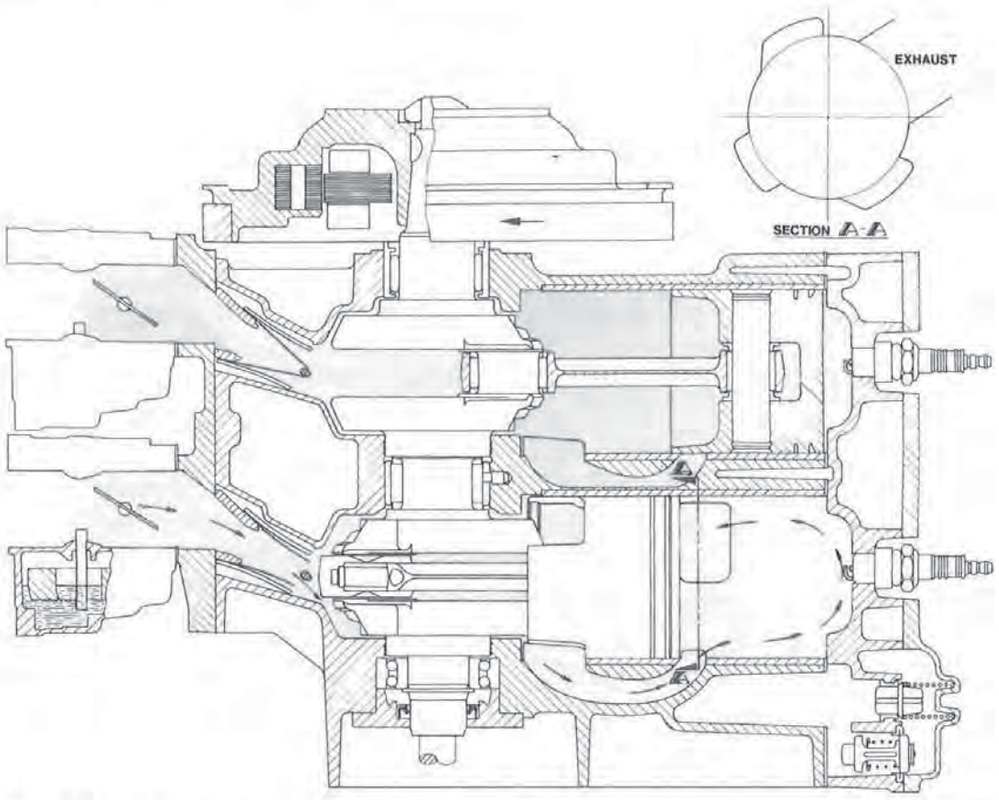


FIGURE 1-12
Cutaway drawing of two-cylinder two-stroke cycle loop-scavenged marine spark-ignition engine. Displaced volume 737 cm^3, maximum power 41 kW at 5500 rev/min. (*Courtesy Outboard Marine Corporation.*)

its sealing and leakage problems. Figure 1-13 shows the major mechanical parts of a simple single-rotor Wankel engine and illustrates its geometry. There are two rotating parts: the triangular-shaped rotor and the output shaft with its integral eccentric. The rotor revolves directly on the eccentric. The rotor has an internal timing gear which meshes with the fixed timing gear on one side housing to maintain the correct phase relationship between the rotor and eccentric shaft rotations. Thus the rotor rotates and orbits around the shaft axis. Breathing is through ports in the center housing (and sometimes the side housings). The combustion chamber lies between the center housing and rotor surface and is sealed by seals at the apex of the rotor and around the perimeters of the rotor sides. Figure 1-13 also shows how the Wankel rotary geometry operates with the four-stroke cycle. The figure shows the induction, compression, power, and exhaust processes of the four-stroke cycle for the chamber defined by rotor surface AB. The remaining two chambers defined by the other rotor surfaces undergo exactly the same sequence. As the rotor makes one complete rotation, during which the eccentric shaft rotates through three revolutions, each chamber produces one power "stroke." Three power pulses occur, therefore, for each rotor revolution;

PETITIONER'S EXHIBIT 1002
US PATENT NO. 6,581,565
Page 1561

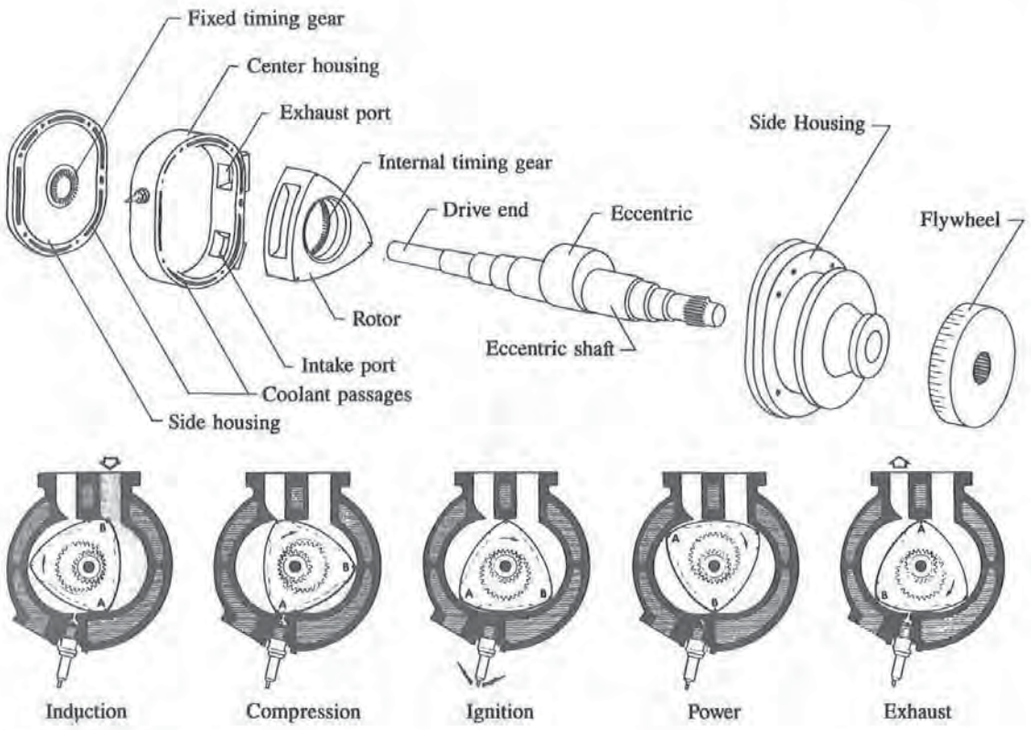


FIGURE 1-13
(*a*) Major components of the Wankel rotary engine; (*b*) induction, compression, power, and exhaust processes of the four-stroke cycle for the chamber defined by rotor surface AB. (*From Mobil Technical Bulletin*, Rotary Engines, © *Mobil Oil Corporation, 1971.*)

thus for each eccentric (output) shaft revolution there is one power pulse. Figure 1-14 shows a cutaway drawing of a two-rotor automobile Wankel engine. The two rotors are out of phase to provide a greater number of torque pulses per shaft revolution. Note the combustion chamber cut out in each rotor face, the rotor apex, and side seals. Two spark plugs per firing chamber are often used to obtain a faster combustion process.

1.7 COMPRESSION-IGNITION ENGINE OPERATION

In compression-ignition engines, air alone is inducted into the cylinder. The fuel (in most applications a light fuel oil, though heated residual fuel is used in marine and power-generation applications) is injected directly into the engine cylinder just before the combustion process is required to start. Load control is achieved by varying the amount of fuel injected each cycle; the air flow at a given engine speed is essentially unchanged. There are a great variety of CI engine designs in use in a wide range of applications—automobile, truck, locomotive, marine, power generation. Naturally aspirated engines where atmospheric air is inducted, turbocharged engines where the inlet air is compressed by an exhaust-driven

PETITIONER'S EXHIBIT 1002
US PATENT NO. 6,581,565
Page 1562

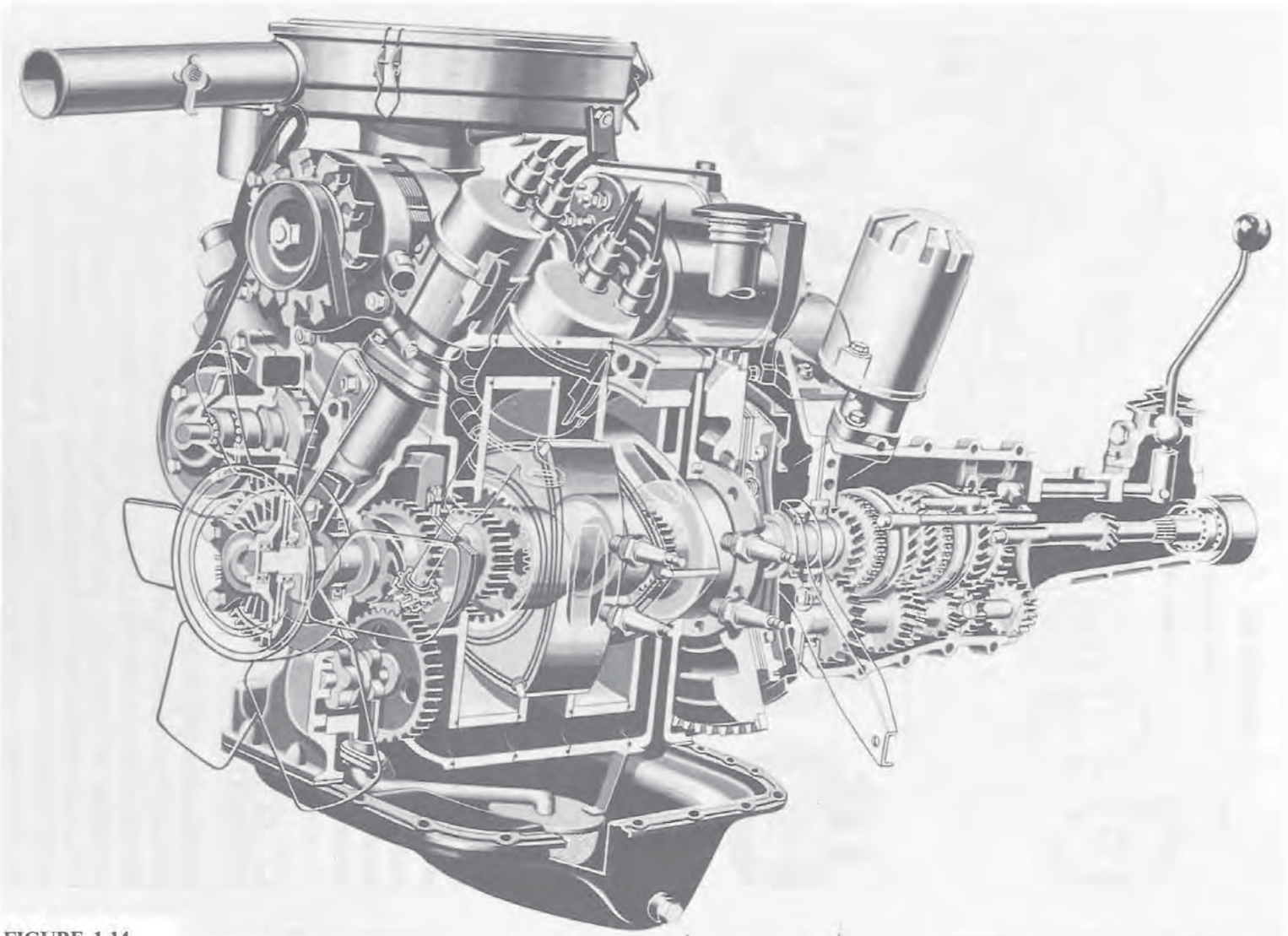


FIGURE 1-14
Cutaway drawing of two-rotor Wankel spark-ignition engine. Displacement of each working chamber 573 cm^3, compression ratio 9.4, maximum

PETITIONER'S EXHIBIT 1002
US PATENT NO. 6,581,565
Page 1563

turbine-compressor combination, and supercharged engines where the air is compressed by a mechanically driven pump or blower are common. Turbocharging and supercharging increase engine output by increasing the air mass flow per unit displaced volume, thereby allowing an increase in fuel flow. These methods are used, usually in larger engines, to reduce engine size and weight for a given power output. Except in smaller engine sizes, the two-stroke cycle is competitive with the four-stroke cycle, in large part because, with the diesel cycle, only air is lost in the cylinder scavenging process.

The operation of a typical four-stroke naturally aspirated CI engine is illustrated in Fig. 1-15. The compression ratio of diesels is much higher than typical SI engine values, and is in the range 12 to 24, depending on the type of diesel engine and whether the engine is naturally aspirated or turbocharged. The valve timings used are similar to those of SI engines. Air at close-to-atmospheric pressure is inducted during the intake stroke and then compressed to a pressure of about 4 MPa (600 lb/in^2) and temperature of about 800 K (1000°F) during the compression stroke. At about 20° before TC, fuel injection into the engine cylinder commences; a typical rate of injection profile is shown in Fig. 1-15*b*. The liquid fuel jet atomizes into drops and entrains air. The liquid fuel evaporates; fuel vapor then mixes with air to within combustible proportions. The air temperature and pressure are above the fuel's ignition point. Therefore after a short *delay period*, spontaneous ignition (autoignition) of parts of the nonuniform fuel-air mixture initiates the combustion process, and the cylinder pressure (solid line in Fig. 1-15*c*) rises above the nonfiring engine level. The flame spreads rapidly through that portion of the injected fuel which has already mixed with sufficient air to burn. As the expansion process proceeds, mixing between fuel, air, and burning gases continues, accompanied by further combustion (see Fig. 1-15*d*). At full load, the mass of fuel injected is about 5 percent of the mass of air in the cylinder. Increasing levels of black smoke in the exhaust limit the amount of fuel that can be burned efficiently. The exhaust process is similar to that of the four-stroke SI engine. At the end of the exhaust stroke, the cycle starts again.

In the two-stroke CI engine cycle, compression, fuel injection, combustion, and expansion processes are similar to the equivalent four-stroke cycle processes; it is the intake and exhaust pressure which are different. The sequence of events in a loop-scavenged two-stroke engine is illustrated in Fig. 1-16. In loop-scavenged engines both exhaust and inlet ports are at the same end of the cylinder and are uncovered as the piston approaches BC (see Fig. 1-16*a*). After the exhaust ports open, the cylinder pressure falls rapidly in a blowdown process (Fig. 1-16*b*). The inlet ports then open, and once the cylinder pressure p falls below the inlet pressure p_i, air flows into the cylinder. The burned gases, displaced by this fresh air, continue to flow out of the exhaust port (along with some of the fresh air). Once the ports close as the piston starts the compression stroke, compression, fuel-injection, fuel-air mixing, combustion and expansion processes proceed as in the four-stroke CI engine cycle.

The diesel fuel-injection system consists of an injection pump, delivery pipes, and fuel injector nozzles. Several different types of injection pumps and

PETITIONER'S EXHIBIT 1002
US PATENT NO. 6,581,565
Page 1564

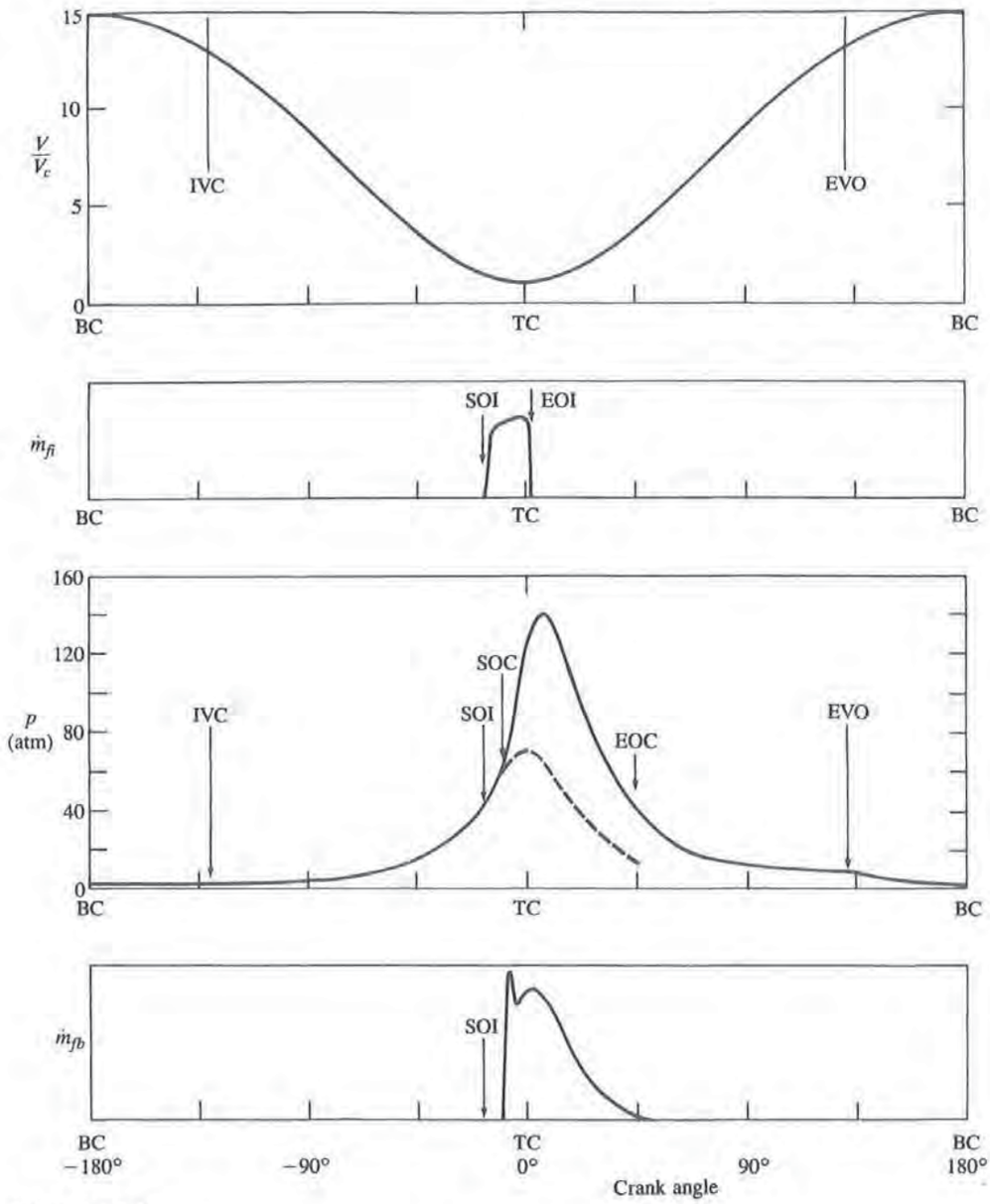


FIGURE 1-15
Sequence of events during compression, combustion, and expansion processes of a naturally aspirated compression-ignition engine operating cycle. Cylinder volume/clearance volume V/V_c, rate of fuel injection $\dot{m}_{fi}$, cylinder pressure p (solid line, firing cycle; dashed line, motored cycle), and rate of fuel burning (or fuel chemical energy release rate) $\dot{m}_{fb}$ are plotted against crank angle.

nozzles are used. In one common fuel pump (an in-line pump design shown in Fig. 1-17) a set of cam-driven plungers (one for each cylinder) operate in closely fitting barrels. Early in the stroke of the plunger, the inlet port is closed and the fuel trapped above the plunger is forced through a check valve into the injection

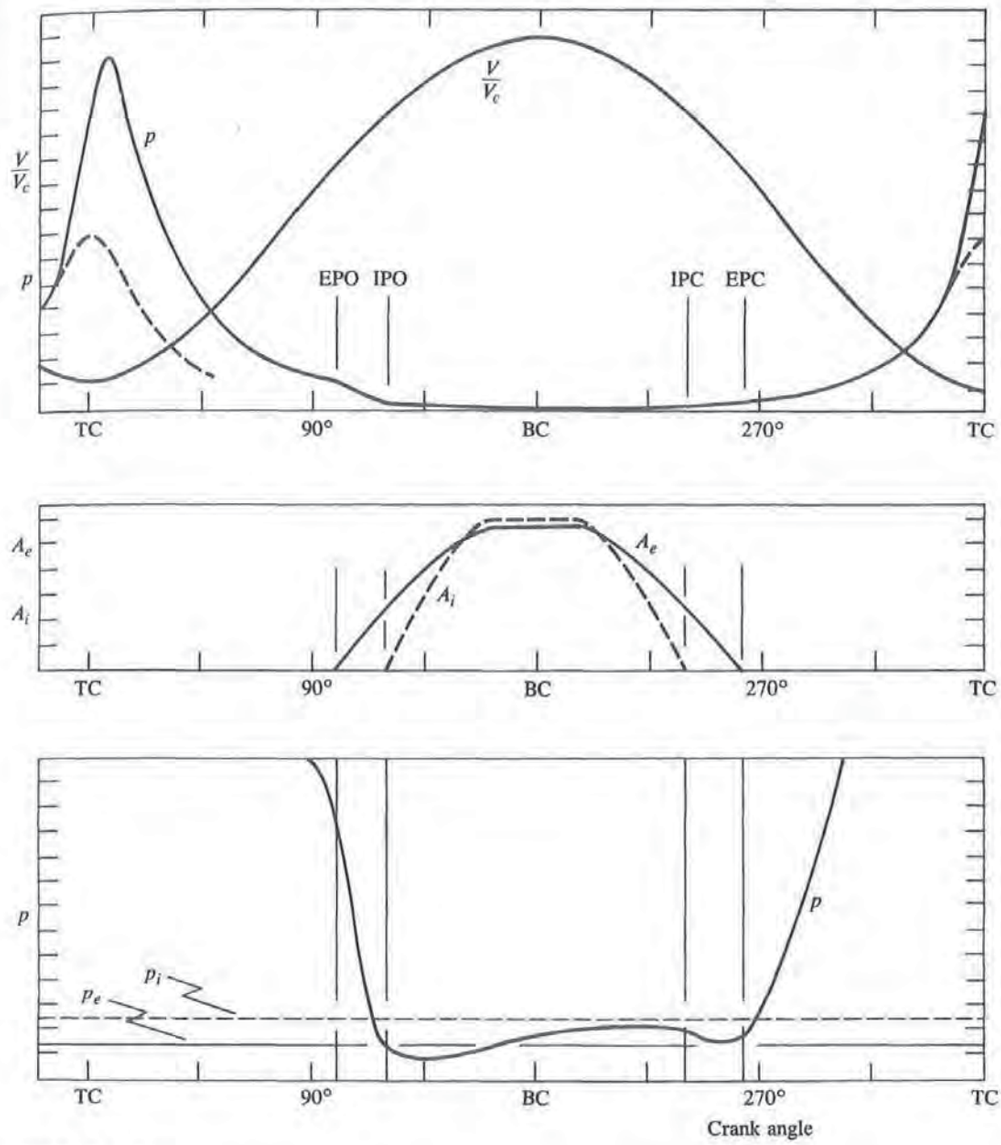


FIGURE 1-16
Sequence of events during expansion, gas exchange, and compression processes in a loop-scavenged two-stroke cycle compression-ignition engine. Cylinder volume/clearance volume V/V_c, cylinder pressure p, exhaust port open area A_e, and intake port open area A_i are plotted against crank angle.

line. The injection nozzle (Fig. 1-18) has one or more holes through which the fuel sprays into the cylinder. A spring-loaded valve closes these holes until the pressure in the injection line, acting on part of the valve surface, overcomes the spring force and opens the valve. Injection starts shortly after the line pressure begins to rise. Thus, the phase of the pump camshaft relative to the engine crankshaft controls the start of injection. Injection is stopped when the inlet port of the pump is uncovered by a helical groove in the pump plunger, because the high

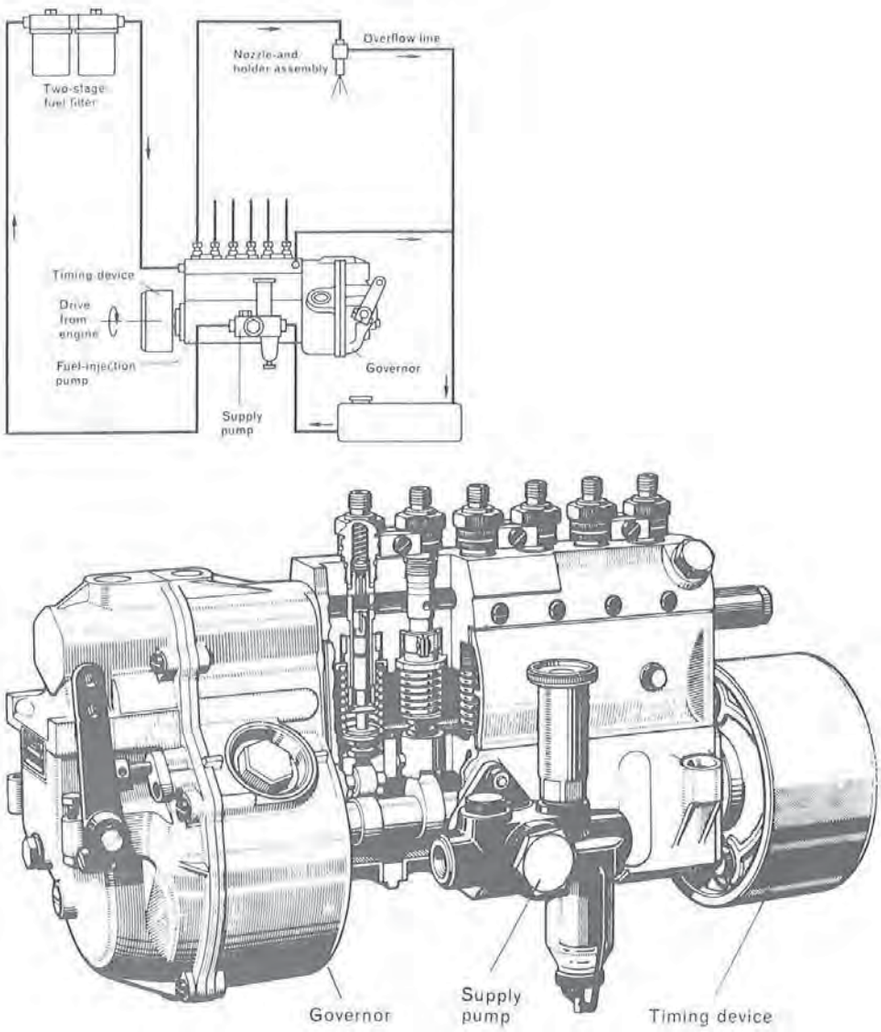
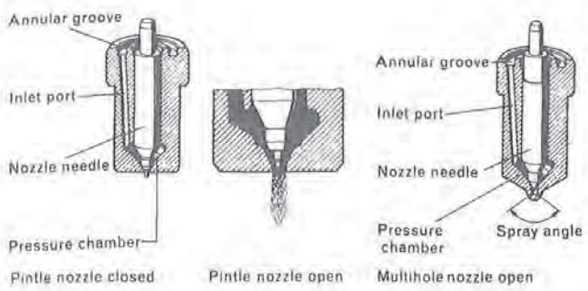


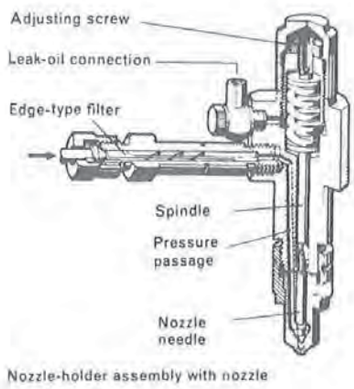
FIGURE 1-17
Diesel fuel system with in-line fuel-injection pump (type PE).[1,2] (*Courtesy Robert Bosch GmbH.*)

pressure above the plunger is then released (Fig. 1-18). The amount of fuel injected (which controls the load) is determined by the injection pump cam design and the position of the helical groove. Thus for a given cam design, rotating the plunger and its helical groove varies the load.

Distributor-type pumps have only one pump plunger and barrel, which meters and distributes the fuel to all the injection nozzles. A schematic of a distributor-type pump is shown in Fig. 1-19. The unit contains a low-pressure fuel pump (on left), a high-pressure injection pump (on right), an overspeed governor, and an injection timer. High pressure is generated by the plunger which is made to describe a combined rotary and stroke movement by the rotating eccentric disc or cam plate; the rotary motion distributes the fuel to the individual injection nozzles.

PETITIONER'S EXHIBIT 1002
US PATENT NO. 6,581,565
Page 1567





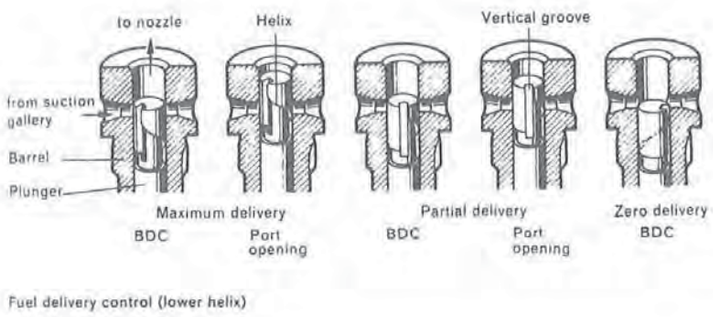


FIGURE 1-18
Details of fuel-injection nozzles, nozzle holder assembly and fuel-delivery control.[12] (*Courtesy Robert Bosch GmbH.*)

Distributor pumps can operate at higher speed and take up less space than in-line pumps. They are normally used on smaller diesel engines. In-line pumps are used in the mid-engine-size range. In the larger diesels, individual single-barrel injection pumps, close mounted to each cylinder with an external drive as shown in Fig. 1-5, are normally used.

1.8 EXAMPLES OF DIESEL ENGINES

A large number of diesel engine configurations and designs are in common use. The very large marine and stationary power-generating diesels are two-stroke

PETITIONER'S EXHIBIT 1002
US PATENT NO. 6,581,565
Page 1568

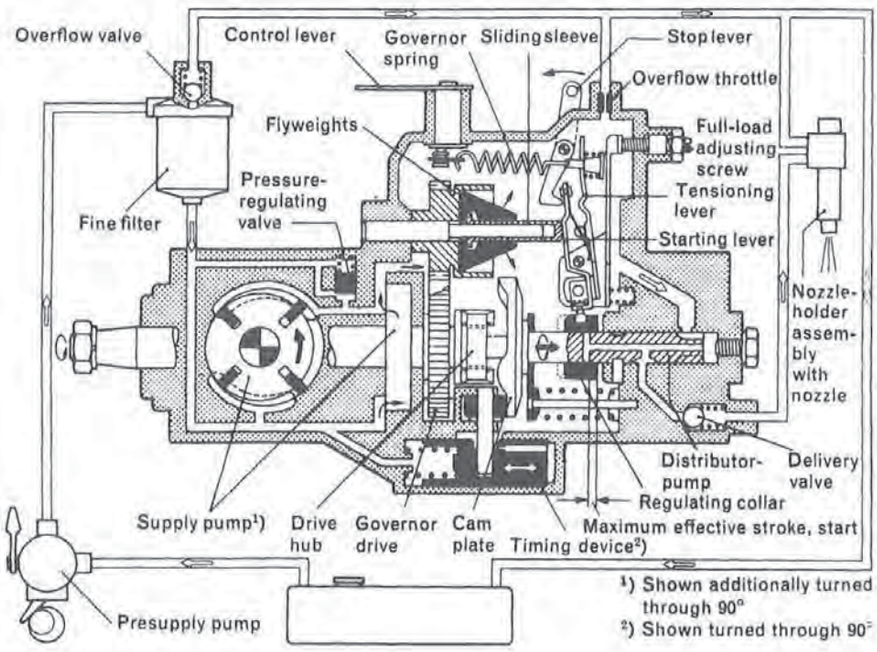


FIGURE 1-19
Diesel fuel system with distributor-type fuel-injection pump with mechanical governor.[1,2] (*Courtesy Robert Bosch GmbH.*)

cycle engines. Small- and medium-size engines use the four-stroke cycle. Because air capacity is an important constraint on the amount of fuel that can be burned in the diesel engine, and therefore on the engine's power, turbocharging is used extensively. All large engines are turbocharged. The majority of smaller diesels are not turbocharged, though they can be turbocharged and many are. The details of the engine design also vary significantly over the diesel size range. In particular, different combustion chamber geometries and fuel-injection characteristics are required to deal effectively with a major diesel engine design problem—achieving sufficiently rapid fuel-air mixing rates to complete the fuel-burning process in the time available. A wide variety of inlet port geometries, cylinder head and piston shapes, and fuel-injection patterns are used to accomplish this over the diesel size range.

Figure 1-20 shows a diesel engine typical of the medium-duty truck application. The design shown is a six-cylinder in-line engine. The drawing indicates that diesel engines are generally substantially heavier than spark-ignition engines because stress levels are higher due to the significantly higher pressure levels of the diesel cycle. The engine shown has a displacement of 10 liters, a compression ratio of 16.3, and is usually turbocharged. The engine has pressed-in cylinder liners to achieve better cylinder wear characteristics. This type of diesel is called a *direct-injection* diesel. The fuel is injected into a combustion chamber directly above the piston crown. The combustion chamber shown is a "bowl-in-piston" design, which puts most of the clearance volume into a compact shape. With this

PETITIONER'S EXHIBIT 1002
US PATENT NO. 6,581,565
Page 1569

size of diesel engine, it is often necessary to use a swirling air flow rotating about the cylinder axis, which is created by suitable design of the inlet port and valve, to achieve adequate fuel-air mixing and fuel burning rates. The fuel injector, shown left-of-center in the drawing, has a multihole nozzle, typically with three to five holes. The fuel jets move out radially from the center of the piston bowl into the (swirling) air flow. The in-line fuel-injection pump is normally used with this type of diesel engine.

Figure 1-21 shows a four-cylinder in-line overhead-valve-cam design automobile diesel engine. The smallest diesels such as this operate at higher engine speed than larger engines; hence the time available for burning the fuel is less and the fuel-injection and combustion system must achieve faster fuel-air mixing rates. This is accomplished by using an *indirect-injection* type of diesel. Fuel is injected into an auxiliary combustion chamber which is separated from the main combustion chamber above the piston by a flow restriction or nozzle. During the latter stages of the compression process, air is forced through this nozzle from the

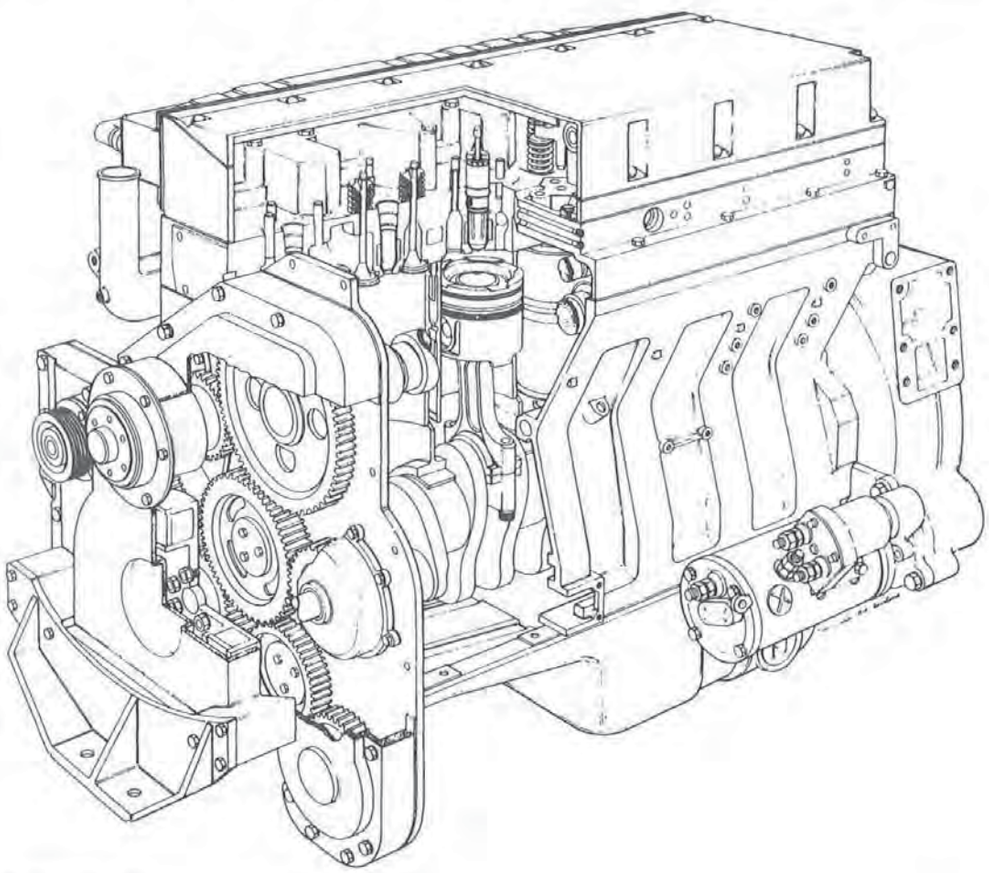


FIGURE 1-20
Direct-injection four-stroke cycle six-cylinder turbocharged Cummins diesel engine. Displaced volume 10 liters, bore 125 mm, stroke 136 mm, compression ratio 16.3, maximum power 168 to 246 kW at rated speed of 2100 rev/min. (*Courtesy Cummins Engine Company, Inc.*)

PETITIONER'S EXHIBIT 1002
US PATENT NO. 6,581,565
Page 1570

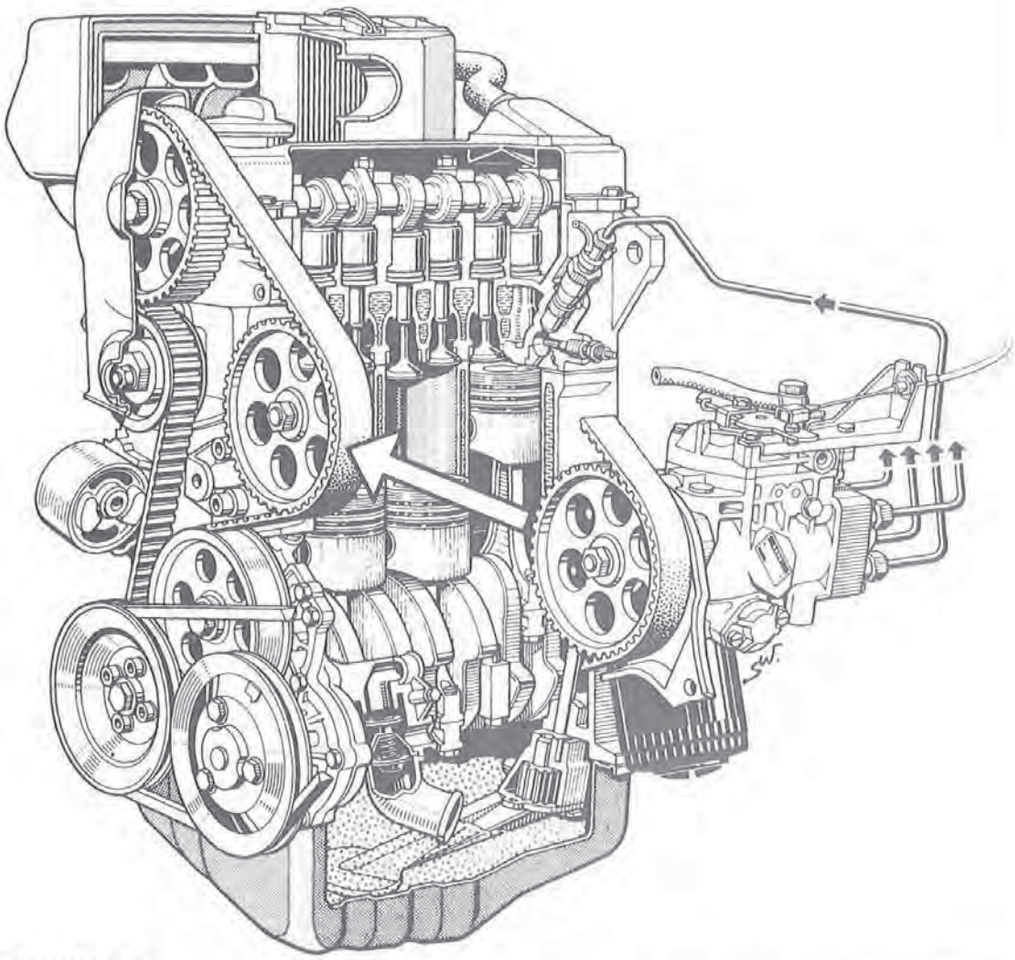


FIGURE 1-21
Four-cylinder naturally aspirated indirect-injection automobile Volkswagen diesel engine.[14] Displaced volume 1.47 liters, bore 76.5 mm, stroke 80 mm, maximum power 37 kW at 5000 rev/min.

cylinder into the prechamber at high velocity. Fuel is injected into this highly turbulent and often rapidly swirling flow in this auxiliary or prechamber, and very high mixing rates are achieved. Combustion starts in the prechamber, and the resulting pressure rise in the prechamber forces burning gases, fuel, and air into the main chamber. Since this outflow is also extremely vigorous, rapid mixing then occurs in the main chamber as the burning jet mixes with the remaining air and combustion is completed. A distributor-type fuel pump, which is normally used in this engine size range, driven off the camshaft at half the crankshaft speed by a toothed belt, is shown on the right of the figure. It supplies high-pressure fuel pulses to the pintle-type injector nozzles in turn. A glow plug is also shown in the auxiliary chamber; this plug is electrically heated prior to and during cold engine start-up to raise the temperature of the air charge and the fuel sufficiently to achieve autoignition. The compression ratio of this engine is 23. Indirect-injection diesel engines require higher compression ratios than direct-injection engines to start adequately when cold.

PETITIONER'S EXHIBIT 1002
US PATENT NO. 6,581,565
Page 1571

Diesel engines are turbocharged to achieve higher power/weight ratios. By increasing the density of the inlet air, a given displaced volume can induct more air. Hence more fuel can be injected and burned, and more power delivered, while avoiding excessive black smoke in the exhaust. All the larger diesels are turbocharged; smaller diesels can be and often are. Figure 1-22 shows how a turbocharger connects to a direct-injection diesel.

All the above diesels are water cooled; some production diesels are air cooled. Figure 1-23 shows a V-8 air-cooled direct-injection naturally aspirated

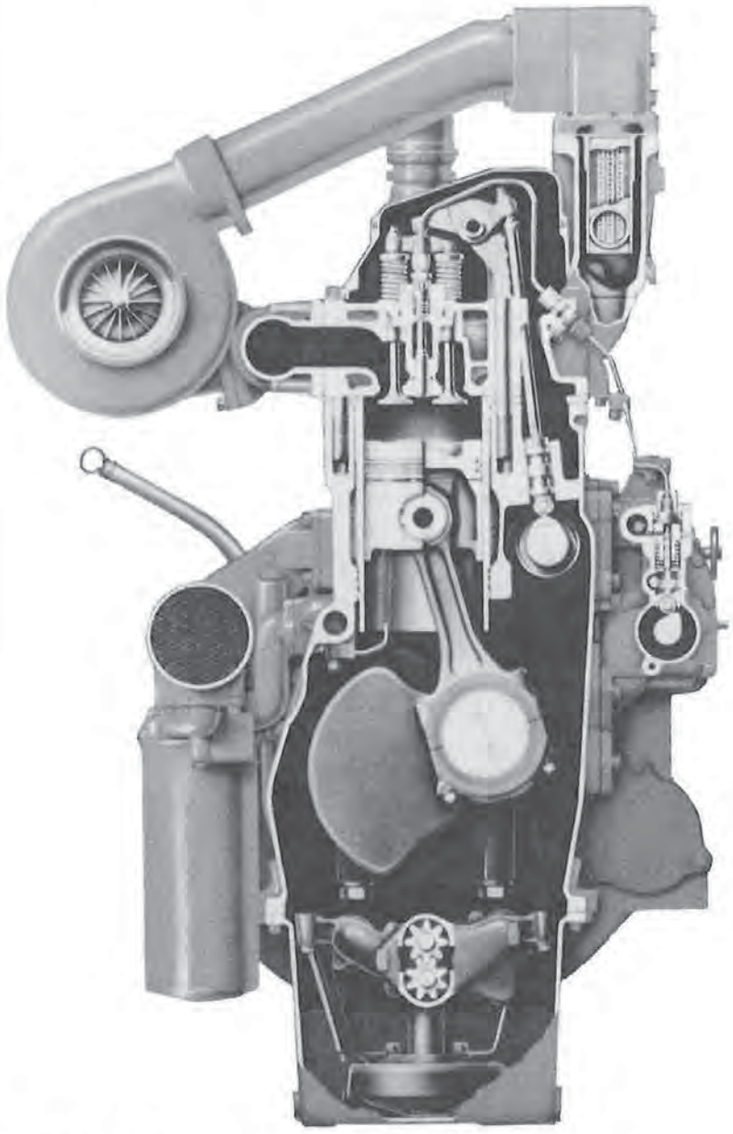


FIGURE 1-22
Turbocharged aftercooled direct-injection four-stroke cycle Caterpillar six-cylinder in-line heavy-duty truck diesel engine. Bore 137.2 mm, stroke 165.1 mm, rated power 200–300 kW and rated speed of 1600–2100 rev/min depending on application. (*Courtesy Caterpillar Tractor Company.*)

PETITIONER'S EXHIBIT 1002
US PATENT NO. 6,581,565
Page 1572

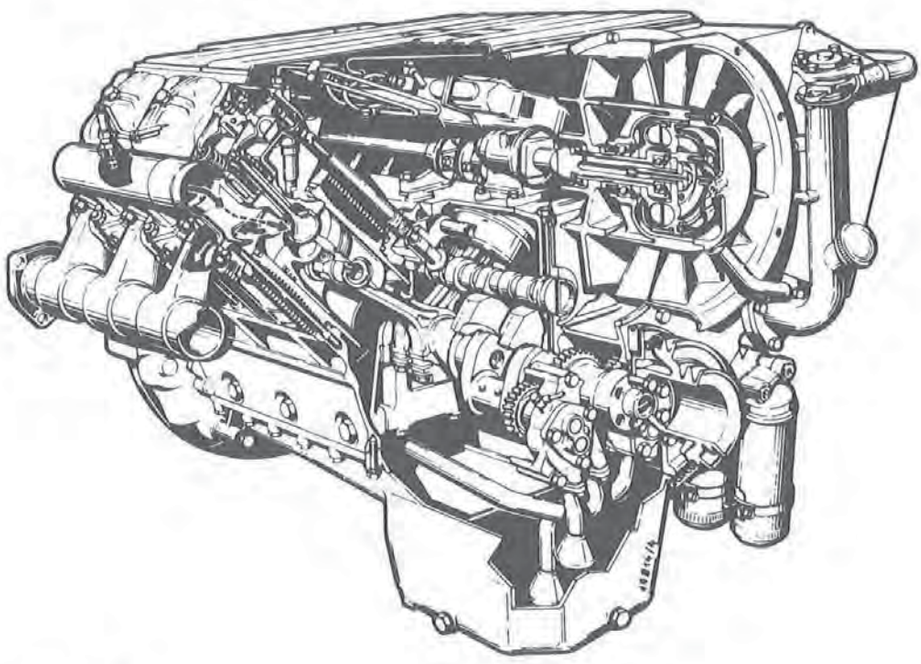


FIGURE 1-23
V-8 air-cooled direct-injection naturally aspirated diesel engine. Displacement 13.4 liter, bore 128 mm, stroke 130 mm, compression ratio 17, maximum rated power 188 kW at rated speed of 2300 rev/min. (*Courtesy Klöcker-Humboldt-Deutz AG.*[15])

diesel. The primary advantage compared to the water-cooled engines is lower engine weight. The fins on the cylinder block and head are necessary to increase the external heat-transfer surface area to achieve the required heat rejection. An air blower, shown on the right of the cutaway drawing, provides forced air convection over the block. The blower is driven off the injection pump shaft, which in turn is driven off the camshaft. The in-line injection pump is placed between the two banks of cylinders. The injection nozzles are located at an angle to the cylinder axis. The combustion chamber and fuel-injection characteristics are similar to those of the engine in Fig. 1-22. The nozzle shown injects four fuel sprays into a reentrant bowl-in-piston combustion chamber.

Diesels are also made in very large engine sizes. These large engines are used for marine propulsion and electrical power generation and operate on the two-stroke cycle in contrast to the small- and medium-size diesels illustrated above. Figure 1-24 shows such a two-stroke cycle marine engine, available with from 4 to 12 cylinders, with a maximum bore of 0.6–0.9 m and stroke of 2–3 m, which operates at speeds of about 100 rev/min. These engines are normally of the crosshead type to reduce side forces on the cylinder. The gas exchange between cycles is controlled by first opening the exhaust valves, and then the piston uncovering inlet ports in the cylinder liner. Expanding exhaust gases leave the cylinder via the exhaust valves and manifold and pass through the turbocharger

PETITIONER'S EXHIBIT 1002
US PATENT NO. 6,581,565
Page 1573

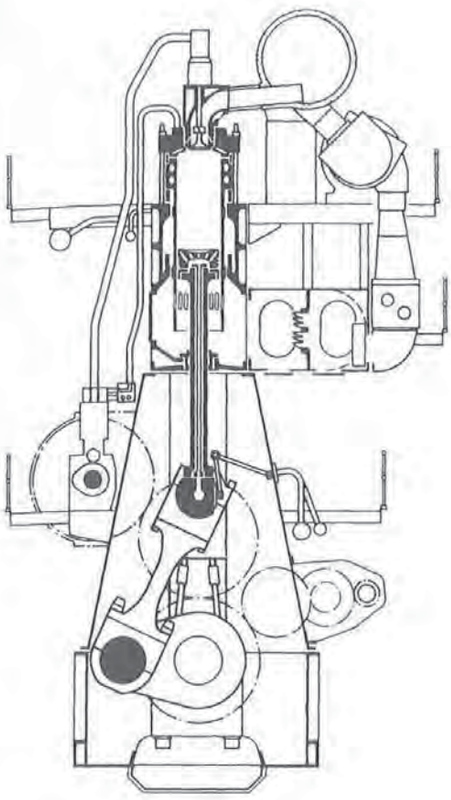


FIGURE 1-24
Large Sulzer two-stroke turbocharged marine diesel engine. Bore 840 mm, stroke 2900 mm, rated power 1.9 MW per cylinder at 78 rev/min, 4 to 12 cylinders. (*Courtesy Sulzer Brothers Ltd.*)

turbine. Compressed air enters via the inlet ports and induces forced scavenging; air is supplied from the turbocharger and cooler. At part load electrically driven blowers cut in to compress the scavenge air. Because these large engines operate at low speed, the motion induced by the centrally injected fuel jets is sufficient to mix the fuel with air and burn it in the time available. A simple open combustion chamber shape can be used, therefore, which achieves efficient combustion even with the low-quality heavy fuels used with these types of engines. The pistons are water cooled in these very large engines. The splash oil piston cooling used in medium- and small-size diesels is not adequate.

1.9 STRATIFIED-CHARGE ENGINES

Since the 1920s, attempts have been made to develop a hybrid internal combustion engine that combines the best features of the spark-ignition engine and the diesel. The goals have been to operate such an engine at close to the optimum compression ratio for efficiency (in the 12 to 15 range) by: (1) injecting the fuel directly into the combustion chamber during the compression process (and thereby avoid the knock or spontaneous ignition problem that limits conventional spark-ignition engines with their premixed charge); (2) igniting the fuel as it mixes with air with a spark plug to provide direct control of the ignition process

PETITIONER'S EXHIBIT 1002
US PATENT NO. 6,581,565
Page 1574

(and thereby avoid the fuel ignition-quality requirement of the diesel); (3) controlling the engine power level by varying the amount of fuel injected per cycle (with the air flow unthrottled to minimize work done pumping the fresh charge into the cylinder). Such engines are often called *stratified-charge engines* from the need to produce in the mixing process between the fuel jet and the air in the cylinder a "stratified" fuel-air mixture, with an easily ignitable composition at the spark plug at the time of ignition. Because such engines avoid the spark-ignition engine requirement for fuels with a high antiknock quality and the diesel requirement for fuels with high ignition quality, they are usually fuel-tolerant and will operate with a wide range of liquid fuels.

Many different types of stratified-charge engine have been proposed, and some have been partially or fully developed. A few have even been used in practice in automotive applications. The operating principles of those that are truly fuel-tolerant or multifuel engines are illustrated in Fig. 1-25. The combustion chamber is usually a bowl-in-piston design, and a high degree of air swirl is created during intake and enhanced in the piston bowl during compression to achieve rapid fuel-air mixing. Fuel is injected into the cylinder, tangentially into the bowl, during the latter stages of compression. A long-duration spark discharge ignites the developing fuel-air jet as it passes the spark plug. The flame spreads downstream, and envelopes and consumes the fuel-air mixture. Mixing continues, and the final stages of combustion are completed during expansion. Most successful designs of this type of engine have used the four-stroke cycle. This concept is usually called a *direct-injection stratified-charge engine*. The engine can be turbocharged to increase its power density.

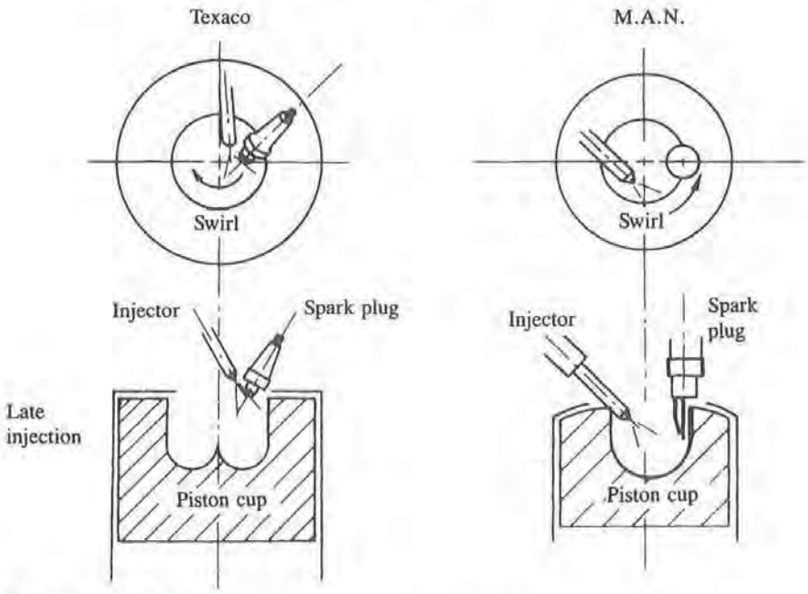


FIGURE 1-25
Two multifuel stratified-charge engines which have been used in commercial practice: the Texaco Controlled Combustion System (TCCS)[16] and the M.A.N.-FM System.[17]

PETITIONER'S EXHIBIT 1002
US PATENT NO. 6,581,565
Page 1575

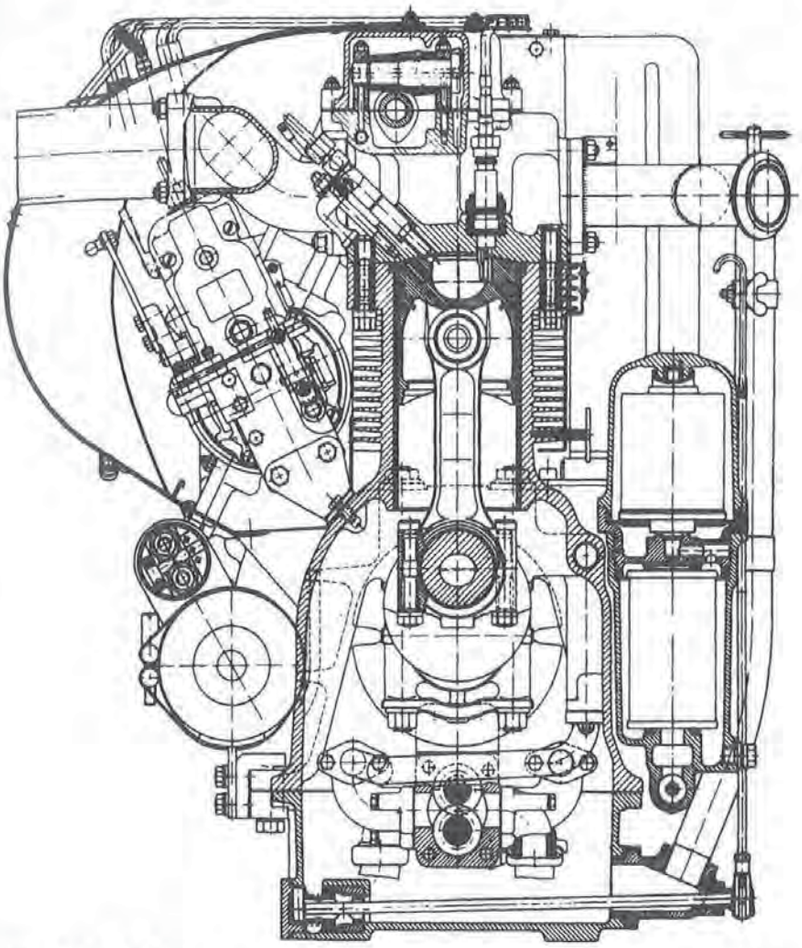


FIGURE 1-26
Sectional drawing of M.A.N. high-speed multifuel four-cylinder direct-injection stratified-charge engine. Bore 94.5 mm, stroke 100 mm, displacement 2.65 liters, compression ratio 16.5, rated power 52 kW at 3800 rev/min.[17]

A commercial multifuel engine is shown in Fig. 1-26. In this particular design, the fuel injector comes diagonally through the cylinder head from the upper left and injects the fuel onto the hot wall of the deep spherical piston bowl. The fuel is carried around the wall of the bowl by the swirling flow, evaporated off the wall, mixed with air, and then ignited by the discharge at the spark plug which enters the chamber vertically on the right. This particular engine is air cooled, so the cylinder block and head are finned to increase surface area.

An alternative stratified-charge engine concept, which has also been mass produced, uses a small *prechamber* fed during intake with an auxiliary fuel system to obtain an easily ignitable mixture around the spark plug. This concept, first proposed by Ricardo in the 1920s and extensively developed in the Soviet Union and Japan, is often called a *jet-ignition* or *torch-ignition* stratified-charge engine. Its operating principles are illustrated in Fig. 1-27 which shows a three-valve

PETITIONER'S EXHIBIT 1002
US PATENT NO. 6,581,565
Page 1576

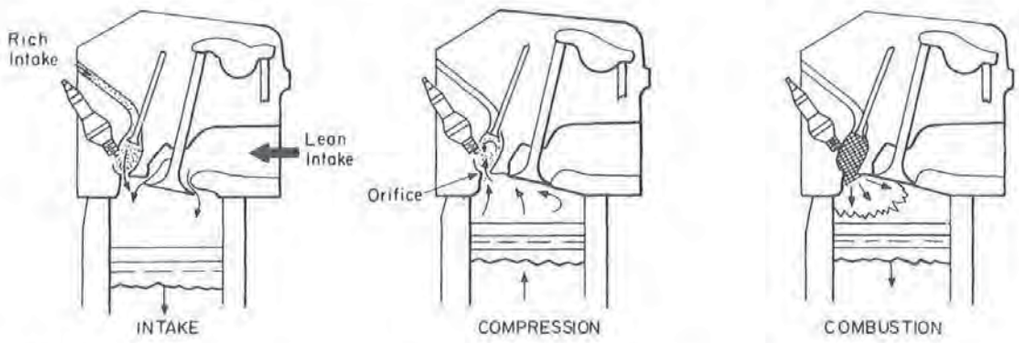


FIGURE 1-27
Schematic of three-valve torch-ignition stratified-charge spark-ignition engine.

carbureted version of the concept.[18] A separate carburetor and intake manifold feeds a fuel-rich mixture (which contains fuel beyond the amount that can be burned with the available air) through a separate small intake valve into the prechamber which contains the spark plug. At the same time, a very lean mixture (which contains excess air beyond that required to burn the fuel completely) is fed to the main combustion chamber through the main carburetor and intake manifold. During intake the rich prechamber flow fully purges the prechamber volume. After intake valve closing, lean mixture from the main chamber is compressed into the prechamber bringing the mixture at the spark plug to an easily ignitable, slightly rich, composition. After combustion starts in the prechamber, rich burning mixture issues as a jet through the orifice into the main chamber, entraining and igniting the lean main chamber charge. Though called a stratified-charge engine, this engine is really a jet-ignition concept whose primary function is to extend the operating limit of conventionally ignited spark-ignition engines to mixtures leaner than could normally be burned.

PROBLEMS

1.1. Describe the major functions of the following reciprocating engine components: piston, connecting rod, crankshaft, cams and camshaft, valves, intake and exhaust manifolds.

1.2. Indicate on an appropriate sketch the different forces that act on the piston, and the direction of these forces, during the engine's expansion stroke with the piston, connecting rod, and crank in the positions shown in Fig. 1-1.

1.3. List five important differences between the design and operating characteristics of spark-ignition and compression-ignition (diesel) engines.

1.4. Indicate the approximate crank angle at which the following events in the four-stroke and two-stroke internal combustion engine cycles occur on a line representing the full cycle (720° for the four-stroke cycle; 360° for the two-stroke cycle): bottom- and top-center crank positions, inlet and exhaust valve or port opening and closing, start of combustion process, end of combustion process, maximum cylinder pressure.

PETITIONER'S EXHIBIT 1002
US PATENT NO. 6,581,565
Page 1577

1.5. The two-stroke cycle has twice as many power strokes per crank revolution as the four-stroke cycle. However, two-stroke cycle engine power outputs per unit displaced volume are less than twice the power output of an equivalent four-stroke cycle engine at the same engine speed. Suggest reasons why this potential advantage of the two-stroke cycle is offset in practice.

1.6. Suggest reasons why multicylinder engines prove more attractive than single-cylinder engines once the total engine displaced volume exceeds a few hundred cubic centimeters.

1.7. The Wankel rotary spark-ignition engine, while lighter and more compact than a reciprocating spark-ignition engine of equal maximum power, typically has worse efficiency due to significantly higher gas leakage from the combustion chamber and higher total heat loss from the hot combustion gases to the chamber walls. Based on the design details in Figs. 1-4, 1-13, and 1-14 suggest reasons for these higher losses.

REFERENCES

1. Cummins, Jr., C. L.: *Internal Fire*, Carnot Press, Lake Oswego, Oreg., 1976.
2. Cummins, Jr., C. L.: "Early IC and Automotive Engines," SAE paper 760604 in *A History of the Automotive Internal Combustion Engine*, SP-409, *SAE Trans.*, vol. 85, 1976.
3. Hempson, J. G. G.: "The Automobile Engine 1920–1950," SAE paper 760605 in *A History of the Automotive Internal Combustion Engine*, SP-409, SAE, 1976.
4. Agnew, W. G.: "Fifty Years of Combustion Research at General Motors," *Progress in Energy and Combustion Science*, vol. 4, pp. 115–156, 1978.
5. Wankel, F.: *Rotary Piston Machines*, Iliffe Books, London, 1965.
6. Ansdale, R. F.: *The Wankel RC Engine Design and Performance*, Iliffe Books, London, 1968.
7. Yamamoto, K.: *Rotary Engine*, Toyo Kogyo Co. Ltd., Hiroshima, 1969.
8. Haagen-Smit, A. J.: "Chemistry and Physiology of Los Angeles Smog," *Ind. Eng. Chem.*, vol. 44, p. 1342, 1952.
9. Taylor, C. F.: *The Internal Combustion Engine in Theory and Practice*, vol. 2, table 10-1, MIT Press, Cambridge, Mass., 1968.
10. Rogowski, A. R.: *Elements of Internal Combustion Engines*, McGraw-Hill, 1953.
11. Weertman, W. L., and Dean, J. W.: "Chrysler Corporation's New 2.2 Liter 4 Cylinder Engine," SAE paper 810007, 1981.
12. Bosch: *Automotive Handbook*, 1st English edition, Robert Bosch GmbH, 1976.
13. Martens, D. A.: "The General Motors 2.8 Liter 60° V-6 Engine Designed by Chevrolet," SAE paper 790697, 1979.
14. Hofbauer, P., and Sator, K.: "Advanced Automotive Power Systems—Part 2: A Diesel for a Subcompact Car," SAE paper 770113, *SAE Trans.*, vol. 86, 1977.
15. Garthe, H.: "The Deutz BF8L 513 Aircooled Diesel Engine for Truck and Bus Application," SAE paper 852321, 1985.
16. Alperstein, M., Schafer, G. H., and Villforth, F. J.: "Texaco's Stratified Charge Engine—Multifuel, Efficient, Clean, and Practical," SAE paper 740563, 1974.
17. Urlaub, A. G., and Chmela, F. G.: "High-Speed, Multifuel Engine: L9204 FMV," SAE paper 740122, 1974.
18. Date, T., and Yagi, S.: "Research and Development of the Honda CVCC Engine," SAE paper 740605, 1974.

PETITIONER'S EXHIBIT 1002
US PATENT NO. 6,581,565
Page 1578

CHAPTER 2

ENGINE DESIGN AND OPERATING PARAMETERS

2.1 IMPORTANT ENGINE CHARACTERISTICS

In this chapter, some basic geometrical relationships and the parameters commonly used to characterize engine operation are developed. The factors important to an engine user are:

1. The engine's performance over its operating range
2. The engine's fuel consumption within this operating range and the cost of the required fuel
3. The engine's noise and air pollutant emissions within this operating range
4. The initial cost of the engine and its installation
5. The reliability and durability of the engine, its maintenance requirements, and how these affect engine availability and operating costs

These factors control total engine operating costs—usually the primary consideration of the user—and whether the engine in operation can satisfy environmental regulations. This book is concerned primarily with the performance, efficiency, and emissions characteristics of engines; the omission of the other factors listed above does not, in any way, reduce their great importance.

PETITIONER'S EXHIBIT 1002
US PATENT NO. 6,581,565
Page 1579

Engine performance is more precisely defined by:

1. The maximum power (or the maximum torque) available at each speed within the useful engine operating range
2. The range of speed and power over which engine operation is satisfactory

The following performance definitions are commonly used:

Maximum rated power. The highest power an engine is allowed to develop for short periods of operation.

Normal rated power. The highest power an engine is allowed to develop in continuous operation.

Rated speed. The crankshaft rotational speed at which rated power is developed.

2.2 GEOMETRICAL PROPERTIES OF RECIPROCATING ENGINES

The following parameters define the basic geometry of a reciprocating engine (see Fig. 2-1):

Compression ratio r_c:

$$r_c = \frac{\text{maximum cylinder volume}}{\text{minimum cylinder volume}} = \frac{V_d + V_c}{V_c} \tag{2.1}$$

where V_d is the displaced or swept volume and V_c is the clearance volume.
Ratio of cylinder bore to piston stroke:

$$R_{bs} = \frac{B}{L} \tag{2.2}$$

Ratio of connecting rod length to crank radius:

$$R = \frac{l}{a} \tag{2.3}$$

In addition, the stroke and crank radius are related by

$$L = 2a$$

Typical values of these parameters are: $r_c = 8$ to 12 for SI engines and $r_c = 12$ to 24 for CI engines; $B/L = 0.8$ to 1.2 for small- and medium-size engines, decreasing to about 0.5 for large slow-speed CI engines; $R = 3$ to 4 for small- and medium-size engines, increasing to 5 to 9 for large slow-speed CI engines.

The cylinder volume V at any crank position θ is

$$V = V_c + \frac{\pi B^2}{4}(l + a - s) \tag{2.4}$$

PETITIONER'S EXHIBIT 1002
US PATENT NO. 6,581,565
Page 1580

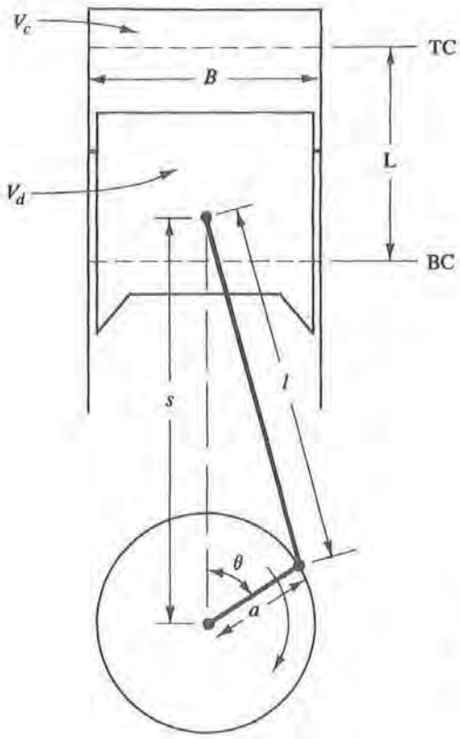


FIGURE 2-1
Geometry of cylinder, piston, connecting rod, and crankshaft where B = bore, L = stroke, l = connecting road length, a = crank radius, θ = crank angle.

where s is the distance between the crank axis and the piston pin axis (Fig. 2-1), and is given by

$$s = a \cos \theta + (l^2 - a^2 \sin^2 \theta)^{1/2} \tag{2.5}$$

The angle θ, defined as shown in Fig. 2-1, is called the *crank angle*. Equation (2.4) with the above definitions can be rearranged:

$$\frac{V}{V_c} = 1 + \tfrac{1}{2}(r_c - 1)[R + 1 - \cos \theta - (R^2 - \sin^2 \theta)^{1/2}] \tag{2.6}$$

The combustion chamber surface area A at any crank position θ is given by

$$A = A_{ch} + A_p + \pi B(l + a - s) \tag{2.7}$$

where A_{ch} is the cylinder head surface area and A_p is the piston crown surface area. For flat-topped pistons, $A_p = \pi B^2/4$. Using Eq. (2.5), Eq. (2-7) can be rearranged:

$$A = A_{ch} + A_p + \frac{\pi BL}{2}[R + 1 - \cos \theta - (R^2 - \sin^2 \theta)^{1/2}] \tag{2.8}$$

An important characteristic speed is the *mean piston speed* $\bar{S}_p$:

$$\bar{S}_p = 2LN \tag{2.9}$$

where N is the rotational speed of the crankshaft. Mean piston speed is often a

PETITIONER'S EXHIBIT 1002
US PATENT NO. 6,581,565
Page 1581

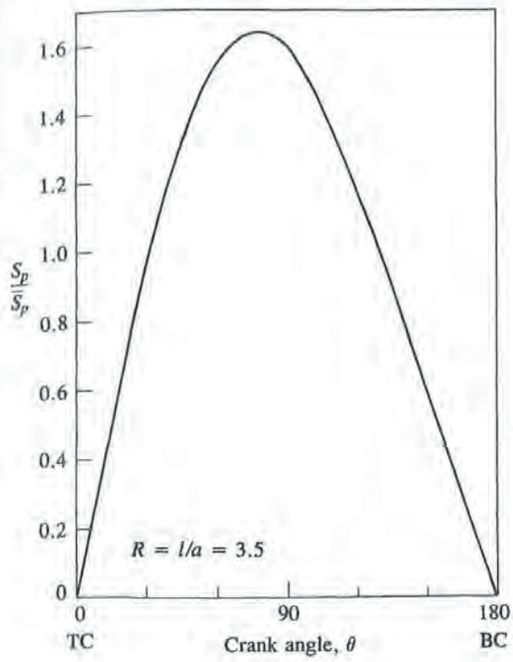


FIGURE 2-2
Instantaneous piston speed/mean piston speed as a function of crank angle for $R = 3.5$.

more appropriate parameter than crank rotational speed for correlating engine behavior as a function of speed. For example, gas-flow velocities in the intake and the cylinder all scale with $\bar{S}_p$. The *instantaneous* piston velocity S_p is obtained from

$$S_p = \frac{ds}{dt} \tag{2.10}$$

The piston velocity is zero at the beginning of the stroke, reaches a maximum near the middle of the stroke, and decreases to zero at the end of the stroke. Differentiation of Eq. (2.5) and substitution gives

$$\frac{S_p}{\bar{S}_p} = \frac{\pi}{2} \sin \theta \left[1 + \frac{\cos \theta}{(R^2 - \sin^2 \theta)^{1/2}} \right] \tag{2.11}$$

Figure 2-2 shows how S_p varies over each stroke for $R = 3.5$.

Resistance to gas flow into the engine or stresses due to the inertia of the moving parts limit the maximum mean piston speed to within the range 8 to 15 m/s (1500 to 3000 ft/min). Automobile engines operate at the higher end of this range; the lower end is typical of large marine diesel engines.

2.3 BRAKE TORQUE AND POWER

Engine torque is normally measured with a dynamometer.[1] The engine is clamped on a test bed and the shaft is connected to the dynamometer rotor. Figure 2-3 illustrates the operating principle of a dynamometer. The rotor is

PETITIONER'S EXHIBIT 1002
US PATENT NO. 6,581,565
Page 1582

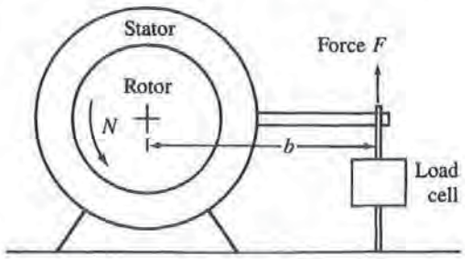


FIGURE 2-3
Schematic of principle of operation of dynamometer.

coupled electromagnetically, hydraulically, or by mechanical friction to a stator, which is supported in low friction bearings. The stator is balanced with the rotor stationary. The torque exerted on the stator with the rotor turning is measured by balancing the stator with weights, springs, or pneumatic means.

Using the notation in Fig. 2-3, if the torque exerted by the engine is T:

$$T = Fb \tag{2.12}$$

The power P delivered by the engine and absorbed by the dynamometer is the product of torque and angular speed:

$$P = 2\pi NT \tag{2.13a}$$

where N is the crankshaft rotational speed. In SI units:

$$P(\text{kW}) = 2\pi N(\text{rev/s})T(\text{N}\cdot\text{m}) \times 10^{-3} \tag{2.13b}$$

or in U.S. units:

$$P(\text{hp}) = \frac{N(\text{rev/min})\ T(\text{lbf}\cdot\text{ft})}{5252} \tag{2.13c}$$

Note that torque is a measure of an engine's ability to do work; power is the rate at which work is done.

The value of engine power measured as described above is called *brake power* P_b. This power is the usable power delivered by the engine to the load—in this case, a "brake."

2.4 INDICATED WORK PER CYCLE

Pressure data for the gas in the cylinder over the operating cycle of the engine can be used to calculate the work transfer from the gas to the piston. The cylinder pressure and corresponding cylinder volume throughout the engine cycle can be plotted on a p-V diagram as shown in Fig. 2-4. The *indicated work per cycle* $W_{c,i}$† (per cylinder) is obtained by integrating around the curve to obtain the

† The term indicated is used because such p-V diagrams used to be generated directly with a device called an engine indicator.

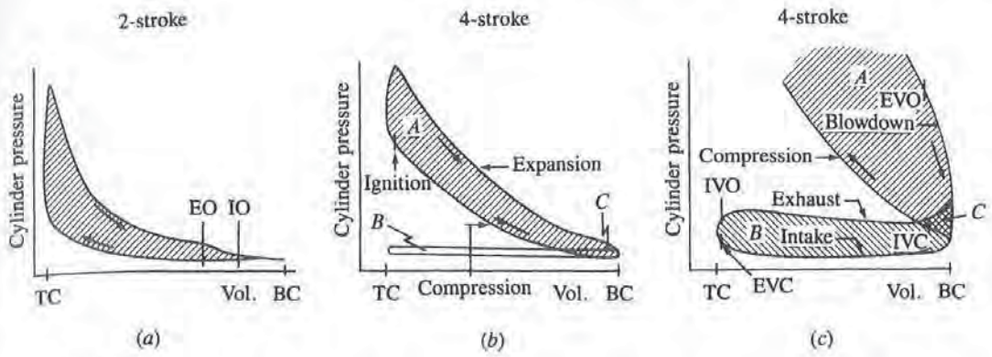


FIGURE 2-4
Examples of p-V diagrams for (*a*) a two-stroke cycle engine, (*b*) a four-stroke cycle engine; (*c*) a four-stroke cycle spark-ignition engine exhaust and intake strokes (pumping loop) at part load.

area enclosed on the diagram:

$$W_{c,i} = \oint p\, dV \tag{2.14}$$

With two-stroke cycles (Fig. 2-4*a*), the application of Eq. (2.14) is straightforward. With the addition of inlet and exhaust strokes for the four-stroke cycle, some ambiguity is introduced as two definitions of indicated output are in common use. These will be defined as:

Gross indicated work per cycle $W_{c,ig}$. Work delivered to the piston over the compression and expansion strokes only.

Net indicated work per cycle $W_{c,in}$. Work delivered to the piston over the entire four-stroke cycle.

In Fig. 2-4*b* and *c*, $W_{c,ig}$ is (area A + area C) and $W_{c,in}$ is (area A + area C) − (area B + area C), which equals (area A − area B), where each of these areas is regarded as a positive quantity. Area B + area C is the work transfer between the piston and the cylinder gases during the inlet and exhaust strokes and is called the *pumping work* W_p (see Chaps. 5 and 13). The pumping work transfer will be *to* the cylinder gases if the pressure during the intake stroke is less than the pressure during the exhaust stroke. This is the situation with naturally aspirated engines. The pumping work transfer will be *from* the cylinder gases to the piston if the exhaust stroke pressure is lower than the intake pressure, which is normally the case with highly loaded turbocharged engines.†

† With some two-stroke engine concepts there is a piston pumping work term associated with compressing the scavenging air in the crankcase.

The power per cylinder is related to the indicated work per cycle by

$$P_i = \frac{W_{c,i} N}{n_R} \tag{2.15}$$

where n_R is the number of crank revolutions for each power stroke per cylinder. For four-stroke cycles, n_R equals 2; for two-stroke cycles, n_R equals 1. This power is the indicated power; i.e., the rate of work transfer from the gas within the cylinder to the piston. It differs from the brake power by the power absorbed in overcoming engine friction, driving engine accessories, and (in the case of gross indicated power) the pumping power.

In discussing indicated quantities of the four-stroke cycle engine, such as work per cycle or power, the definition used for "indicated" (i.e., gross or net) *should always be explicitly stated.* The gross indicated output, the definition most commonly used, will be chosen where possible in this book for the following reasons. Indicated quantities are used primarily to identify the impact of the compression, combustion, and expansion processes on engine performance, etc. The gross indicated output is, therefore, the most appropriate definition. It represents the sum of the useful work available at the shaft and the work required to overcome all the engine losses. Furthermore, the standard engine test codes[2] define procedures for measuring brake power and friction power (the friction power test provides a close approximation to the total lost power in the engine). The sum of brake power and friction power provides an alternative way of estimating indicated power; the value obtained is a close approximation to the gross indicated power.

The terms brake and indicated are used to describe other parameters such as mean effective pressure, specific fuel consumption, and specific emissions (see the following sections) in a manner similar to that used for work per cycle and power.

2.5 MECHANICAL EFFICIENCY

We have seen that part of the gross indicated work per cycle or power is used to expel exhaust gases and induct fresh charge. An additional portion is used to overcome the friction of the bearings, pistons, and other mechanical components of the engine, and to drive the engine accessories. All of these power requirements are grouped together and called *friction power* P_f.† Thus:

$$P_{ig} = P_b + P_f \tag{2.16}$$

Friction power is difficult to determine accurately. One common approach for high-speed engines is to drive or motor the engine with a dynamometer (i.e., operate the engine without firing it) and measure the power which has to be

† The various components of friction power are examined in detail in Chap. 13.

PETITIONER'S EXHIBIT 1002
US PATENT NO. 6,581,565
Page 1585

supplied by the dynamometer to overcome *all* these frictional losses. The engine speed, throttle setting, oil and water temperatures, and ambient conditions are kept the same in the motored test as under firing conditions. The major sources of inaccuracy with this method are that gas pressure forces on the piston and rings are lower in the motored test than when the engine is firing and that the oil temperatures on the cylinder wall are also lower under motoring conditions.

The ratio of the brake (or useful) power delivered by the engine to the indicated power is called the *mechanical efficiency* η_m:

$$\eta_m = \frac{P_b}{P_{ig}} = 1 - \frac{P_f}{P_{ig}} \tag{2.17}$$

Since the friction power includes the power required to pump gas into and out of the engine, mechanical efficiency depends on throttle position as well as engine design and engine speed. Typical values for a modern automotive engine at wide-open or full throttle are 90 percent at speeds below about 30 to 40 rev/s (1800 to 2400 rev/min), decreasing to 75 percent at maximum rated speed. As the engine is throttled, mechanical efficiency decreases, eventually to zero at idle operation.

2.6 ROAD-LOAD POWER

A part-load power level useful as a reference point for testing automobile engines is the power required to drive a vehicle on a level road at a steady speed. Called *road-load power*, this power overcomes the rolling resistance which arises from the friction of the tires and the aerodynamic drag of the vehicle. Rolling resistance and drag coefficients, C_R and C_D, respectively, are determined empirically. An approximate formula for road-load power P_r is

$$P_r = (C_R M_v g + \tfrac{1}{2}\rho_a C_D A_v S_v^2) S_v \tag{2.18a}$$

where C_R = coefficient of rolling resistance ($0.012 < C_R < 0.015$)[3]
M_v = mass of vehicle [for passenger cars: curb mass plus passenger load of 68 kg (150 lbm); in U.S. units W_v = vehicle weight in lbf]
g = acceleration due to gravity
ρ_a = ambient air density
C_D = drag coefficient (for cars: $0.3 < C_D \lesssim 0.5$)[3]
A_v = frontal area of vehicle
S_v = vehicle speed

With the quantities in the units indicated:

$$P_r(\text{kW}) = [2.73 C_R M_v(\text{kg}) + 0.0126 C_D A_v(\text{m}^2) S_v(\text{km/h})^2] S_v(\text{km/h}) \times 10^{-3} \tag{2.18b}$$

or

$$P_r(\text{hp}) = \frac{[C_R W_v(\text{lbf}) + 0.0025 C_D A_v(\text{ft}^2) S_v(\text{mi/h})^2] S_v(\text{mi/h})}{375} \tag{2.18c}$$

PETITIONER'S EXHIBIT 1002
US PATENT NO. 6,581,565
Page 1586

2.7 MEAN EFFECTIVE PRESSURE

While torque is a valuable measure of a particular engine's ability to do work, it depends on engine size. A more useful relative engine performance measure is obtained by dividing the work per cycle by the cylinder volume displaced per cycle. The parameter so obtained has units of force per unit area and is called the *mean effective pressure* (mep). Since, from Eq. (2.15),

$$\text{Work per cycle} = \frac{Pn_R}{N}$$

where n_R is the number of crank revolutions for each power stroke per cylinder (two for four-stroke cycles; one for two-stroke cycles), then

$$\text{mep} = \frac{Pn_R}{V_d N} \tag{2.19a}$$

For SI and U.S. units, respectively,

$$\text{mep(kPa)} = \frac{P(\text{kW})n_R \times 10^3}{V_d(\text{dm}^3)N(\text{rev/s})} \tag{2.19b}$$

$$\text{mep(lb/in}^2) = \frac{P(\text{hp})n_R \times 396{,}000}{V_d(\text{in}^3)N(\text{rev/min})} \tag{2.19c}$$

Mean effective pressure can also be expressed in terms of torque by using Eq. (2.13):

$$\text{mep(kPa)} = \frac{6.28n_R T(\text{N} \cdot \text{m})}{V_d(\text{dm}^3)} \tag{2.20a}$$

or

$$\text{mep(lb/in}^2) = \frac{75.4n_R T(\text{lbf} \cdot \text{ft})}{V_d(\text{in}^3)} \tag{2.20b}$$

The maximum brake mean effective pressure of good engine designs is well established, and is essentially constant over a wide range of engine sizes. Thus, the actual bmep that a particular engine develops can be compared with this norm, and the effectiveness with which the engine designer has used the engine's displaced volume can be assessed. Also, for design calculations, the engine displacement required to provide a given torque or power, at a specified speed, can be estimated by assuming appropriate values for bmep for that particular application.

Typical values for bmep are as follows. For naturally aspirated spark-ignition engines, maximum values are in the range 850 to 1050 kPa ($\sim$ 125 to 150 lb/in^2) at the engine speed where maximum torque is obtained (about 3000 rev/min). At the maximum rated power, bmep values are 10 to 15 percent lower. For turbocharged automotive spark-ignition engines the maximum bmep is in the 1250 to 1700 kPa (180 to 250 lb/in^2) range. At the maximum rated power, bmep is in the 900 to 1400 kPa (130 to 200 lb/in^2) range. For naturally aspirated four-stroke diesels, the maximum bmep is in the 700 to 900 kPa (100 to 130

PETITIONER'S EXHIBIT 1002
US PATENT NO. 6,581,565
Page 1587

lb/in^2) range, with the bmep at the maximum rated power of about 700 kPa (100 lb/in^2). Turbocharged four-stroke diesel maximum bmep values are typically in the range 1000 to 1200 kPa (145 to 175 lb/in^2); for turbocharged aftercooled engines this can rise to 1400 kPa. At maximum rated power, bmep is about 850 to 950 kPa (125 to 140 lb/in^2). Two-stroke cycle diesels have comparable performance to four-stroke cycle engines. Large low-speed two-stroke cycle engines can achieve bmep values of about 1600 kPa.

An example of how the above engine performance parameters can be used to initiate an engine design is given below.

Example. A four-cylinder automotive spark-ignition engine is being designed to provide a maximum brake torque of 150 N·m (110 lbf·ft) in the mid-speed range ($\sim$ 3000 rev/min). Estimate the required engine displacement, bore and stroke, and the maximum brake power the engine will deliver.

Equation (2.20*a*) relates torque and mep. Assume that 925 kPa is an appropriate value for bmep at the maximum engine torque point. Equation (2.20*a*) gives

$$V(\text{dm}^3) = \frac{6.28 n_R T_{\max}(\text{N}\cdot\text{m})}{\text{bmep}_{\max}(\text{kPa})} = \frac{6.28 \times 2 \times 150}{925} = 2 \text{ dm}^3$$

For a four-cylinder engine, the displaced volume, bore, and stroke are related by

$$V_d = 4 \times \frac{\pi}{4} B^2 L$$

Assume $B = L$; this gives $B = L = 86$ mm.

The maximum rated engine speed can be estimated from an appropriate value for the maximum mean piston speed, 15 m/s (see Sec. 2.2):

$$\bar{S}_{\text{pmax}} = 2LN_{\max} \rightarrow N_{\max} = 87 \text{ rev/s (5200 rev/min)}$$

The maximum brake power can be estimated from the typical bmep value at maximum power, 800 kPa (116 lb/in^2), using Eq. (2.19*b*):

$$P_{\text{bmax}}(\text{kW}) = \frac{\text{bmep(kPa)} V(\text{dm}^3) N_{\max}(\text{rev/s})}{n_R \times 10^3} = \frac{800 \times 2 \times 87}{2 \times 10^3} = 70 \text{ kW}$$

2.8 SPECIFIC FUEL CONSUMPTION AND EFFICIENCY

In engine tests, the fuel consumption is measured as a flow rate—mass flow per unit time $\dot{m}_f$. A more useful parameter is the *specific fuel consumption* (sfc)—the fuel flow rate per unit power output. It measures how efficiently an engine is using the fuel supplied to produce work:

$$\text{sfc} = \frac{\dot{m}_f}{P} \tag{2.21}$$

PETITIONER'S EXHIBIT 1002
US PATENT NO. 6,581,565
Page 1588

With units,

$$\text{sfc(mg/J)} = \frac{\dot{m}_f\text{(g/s)}}{P\text{(kW)}} \tag{2.22a}$$

or

$$\text{sfc(g/kW} \cdot \text{h)} = \frac{\dot{m}_f\text{(g/h)}}{P\text{(kW)}} = 608.3\ \text{sfc(lbm/hp} \cdot \text{h)} \tag{2.22b}$$

or

$$\text{sfc(lbm/hp} \cdot \text{h)} = \frac{\dot{m}_f\text{(lbm/h)}}{P\text{(hp)}} = 1.644 \times 10^3\ \text{sfc(g/kW} \cdot \text{h)} \tag{2.22c}$$

Low values of sfc are obviously desirable. For SI engines typical best values of brake specific fuel consumption are about 75 μg/J = 270 g/kW · h = 0.47 lbm/hp · h. For CI engines, best values are lower and in large engines can go below 55 μg/J = 200 g/kW · h = 0.32 lbm/hp · h.

The specific fuel consumption has units. A dimensionless parameter that relates the desired engine output (work per cycle or power) to the necessary input (fuel flow) would have more fundamental value. The ratio of the work produced per cycle to the amount of fuel energy supplied per cycle that can be released in the combustion process is commonly used for this purpose. It is a measure of the engine's efficiency. The fuel energy supplied which can be released by combustion is given by the mass of fuel supplied to the engine per cycle times the heating value of the fuel. The heating value of a fuel, Q_{HV}, defines its energy content. It is determined in a standardized test procedure in which a known mass of fuel is fully burned with air, and the thermal energy released by the combustion process is absorbed by a calorimeter as the combustion products cool down to their original temperature.

This measure of an engine's "efficiency," which will be called the *fuel conversion efficiency* η_f,† is given by

$$\eta_f = \frac{W_c}{m_f Q_{HV}} = \frac{(Pn_R/N)}{(\dot{m}_f n_R/N)Q_{HV}} = \frac{P}{\dot{m}_f Q_{HV}} \tag{2.23}$$

where m_f is the mass of fuel inducted per cycle. Substitution for $P/\dot{m}_f$ from Eq. (2.21) gives

$$\eta_f = \frac{1}{\text{sfc}\ Q_{HV}} \tag{2.24a}$$

† This empirically defined engine efficiency has previously been called thermal efficiency or enthalpy efficiency. The term fuel conversion efficiency is preferred because it describes this quantity more precisely, and distinguishes it clearly from other definitions of engine efficiency which will be developed in Sec. 3.6. Note that there are several different definitions of heating value (see Sec. 3.5). The numerical values do not normally differ by more than a few percent, however. In this text, the lower heating value at constant pressure is used in evaluating the fuel conversion efficiency.

PETITIONER'S EXHIBIT 1002
US PATENT NO. 6,581,565
Page 1589

or with units:

$$\eta_f = \frac{1}{\text{sfc(mg/J)}Q_{\text{HV}}\text{(MJ/kg)}} \tag{2.24b}$$

$$\eta_f = \frac{3600}{\text{sfc(g/kW} \cdot \text{h)}Q_{\text{HV}}\text{(MJ/kg)}} \tag{2.24c}$$

$$\eta_f = \frac{2545}{\text{sfc(lbm/hp} \cdot \text{h)}Q_{\text{HV}}\text{(Btu/lbm)}} \tag{2.24d}$$

Typical heating values for the commercial hydrocarbon fuels used in engines are in the range 42 to 44 MJ/kg (18,000 to 19,000 Btu/lbm). Thus, specific fuel consumption is inversely proportional to fuel conversion efficiency for normal hydrocarbon fuels.

Note that the fuel energy supplied to the engine per cycle is not fully released as thermal energy in the combustion process because the actual combustion process in incomplete. When enough air is present in the cylinder to oxidize the fuel completely, almost all (more than about 96 percent) of this fuel energy supplied is transferred as thermal energy to the working fluid. When insufficient air is present to oxidize the fuel completely, lack of oxygen prevents this fuel energy supplied from being fully released. This topic is discussed in more detail in Secs. 3.5 and 4.9.4.

2.9 AIR/FUEL AND FUEL/AIR RATIOS

In engine testing, both the air mass flow rate $\dot{m}_a$ and the fuel mass flow rate $\dot{m}_f$ are normally measured. The ratio of these flow rates is useful in defining engine operating conditions:

$$\text{Air/fuel ratio } (A/F) = \frac{\dot{m}_a}{\dot{m}_f} \tag{2.25}$$

$$\text{Fuel/air ratio } (F/A) = \frac{\dot{m}_f}{\dot{m}_a} \tag{2.26}$$

The normal operating range for a conventional SI engine using gasoline fuel is $12 \leq A/F \leq 18$ $(0.056 \leq F/A \leq 0.083)$; for CI engines with diesel fuel, it is $18 \leq A/F \leq 70$ $(0.014 \leq F/A \leq 0.056)$.

2.10 VOLUMETRIC EFFICIENCY

The intake system—the air filter, carburetor, and throttle plate (in a spark-ignition engine), intake manifold, intake port, intake valve—restricts the amount of air which an engine of given displacement can induct. The parameter used to measure the effectiveness of an engine's induction process is the *volumetric efficiency* η_v. Volumetric efficiency is only used with four-stroke cycle engines which have a distinct induction process. It is defined as the volume flow rate of air into

PETITIONER'S EXHIBIT 1002
US PATENT NO. 6,581,565
Page 1590

the intake system divided by the rate at which volume is displaced by the piston:

$$\eta_v = \frac{2\dot{m}_a}{\rho_{a,i} V_d N} \tag{2.27a}$$

where $\rho_{a,i}$ is the inlet air density. An alternative equivalent definition for volumetric efficiency is

$$\eta_v = \frac{m_a}{\rho_{a,i} V_d} \tag{2.27b}$$

where m_a is the mass of air inducted into the cylinder per cycle.

The inlet density may either be taken as atmosphere air density (in which case η_v measures the pumping performance of the entire inlet system) or may be taken as the air density in the inlet manifold (in which case η_v measures the pumping performance of the inlet port and valve only). Typical maximum values of η_v for naturally aspirated engines are in the range 80 to 90 percent. The volumetric efficiency for diesels is somewhat higher than for SI engines. Volumetric efficiency is discussed more fully in Sec. 6.2.

2.11 ENGINE SPECIFIC WEIGHT AND SPECIFIC VOLUME

Engine weight and bulk volume for a given rated power are important in many applications. Two parameters useful for comparing these attributes from one engine to another are:

$$\text{Specific weight} = \frac{\text{engine weight}}{\text{rated power}} \tag{2.28}$$

$$\text{Specific volume} = \frac{\text{engine volume}}{\text{rated power}} \tag{2.29}$$

For these parameters to be useful in engine comparisons, a consistent definition of what components and auxiliaries are included in the term "engine" must be adhered to. These parameters indicate the effectiveness with which the engine designer has used the engine materials and packaged the engine components.[4]

2.12 CORRECTION FACTORS FOR POWER AND VOLUMETRIC EFFICIENCY

The pressure, humidity, and temperature of the ambient air inducted into an engine, at a given engine speed, affect the air mass flow rate and the power output. Correction factors are used to adjust measured wide-open-throttle power and volumetric efficiency values to standard atmospheric conditions to provide a more accurate basis for comparisons between engines. Typical standard ambient

PETITIONER'S EXHIBIT 1002
US PATENT NO. 6,581,565
Page 1591

conditions used are:

Dry air pressure	Water vapour pressure	Temperature
736.6 mmHg	9.65 mmHg	29.4°C
29.00 inHg	0.38 inHg	85°F

The basis for the correction factor is the equation for one-dimensional steady compressible flow through an orifice or flow restriction of effective area A_E (see App. C):

$$\dot{m} = \frac{A_E p_0}{\sqrt{RT_0}} \left\{ \frac{2\gamma}{\gamma - 1} \left[\left(\frac{p}{p_0} \right)^{2/\gamma} - \left(\frac{p}{p_0} \right)^{(\gamma+1)/\gamma} \right] \right\}^{1/2} \tag{2.30}$$

In deriving this equation, it has been assumed that the fluid is an ideal gas with gas constant R and that the ratio of specific heats ($c_p/c_v = \gamma$) is a constant; p_0 and T_0 are the total pressure and temperature upstream of the restriction and p is the pressure at the throat of the restriction.

If, in the engine, p/p_0 is assumed constant at wide-open throttle, then for a given intake system and engine, the mass flow rate of dry air $\dot{m}_a$ varies as

$$\dot{m}_a \propto \frac{p_0}{\sqrt{T_0}} \tag{2.31}$$

For mixtures containing the proper amount of fuel to use all the air available (and thus provide maximum power), the indicated power at full throttle P_i will be proportional to $\dot{m}_a$, the *dry* air flow rate. Thus if

$$P_{i,s} = C_F P_{i,m} \tag{2.32}$$

where the subscripts s and m denote values at the standard and measured conditions, respectively, the correction factor C_F is given by

$$C_F = \frac{p_{s,d}}{p_m - p_{v,m}} \left(\frac{T_m}{T_s} \right)^{1/2} \tag{2.33}$$

where $p_{s,d}$ = standard dry-air absolute pressure
p_m = measured ambient-air absolute pressure
$p_{v,m}$ = measured ambient–water vapour partial pressure
T_m = measured ambient temperature, K
T_s = standard ambient temperature, K

The rated *brake* power is corrected by using Eq. (2.33) to correct the *indicated* power and making the assumption that friction power is unchanged. Thus

$$P_{b,s} = C_F P_{i,m} - P_{f,m} \tag{2.34}$$

Volumetric efficiency is proportional to $\dot{m}_a/\rho_a$ [see Eq. (2.27)]. Since ρ_a is proportional to p/T, the correction factor for volumetric efficiency, C'_F, is

$$C'_F = \frac{\eta_{v,s}}{\eta_{v,m}} = \left(\frac{T_s}{T_m} \right)^{1/2} \tag{2.35}$$

PETITIONER'S EXHIBIT 1002
US PATENT NO. 6,581,565
Page 1592

2.13 SPECIFIC EMISSIONS AND EMISSIONS INDEX

Levels of emissions of oxides of nitrogen (nitric oxide, NO, and nitrogen dioxide, NO_2, usually grouped together as NO_x), carbon monoxide (CO), unburned hydrocarbons (HC), and particulates are important engine operating characteristics.

The concentrations of gaseous emissions in the engine exhaust gases are usually measured in parts per million or percent by volume (which corresponds to the mole fraction multiplied by 10^6 or by 10^2, respectively). Normalized indicators of emissions levels are more useful, however, and two of these are in common use. *Specific emissions* are the mass flow rate of pollutant per unit power output:

$$sNO_x = \frac{\dot{m}_{NO_x}}{P} \tag{2.36a}$$

$$sCO = \frac{\dot{m}_{CO}}{P} \tag{2.36b}$$

$$sHC = \frac{\dot{m}_{HC}}{P} \tag{2.36c}$$

$$sPart = \frac{\dot{m}_{part}}{P} \tag{2.36d}$$

Indicated and brake specific emissions can be defined. Units in common use are μg/J, g/kW · h, and g/hp · h.

Alternatively, emission rates can be normalized by the fuel flow rate. An *emission index* (EI) is commonly used: e.g.,

$$EI_{NO_x} = \frac{\dot{m}_{NO_x}(g/s)}{\dot{m}_f(kg/s)} \tag{2.37}$$

with similar expressions for CO, HC, and particulates.

2.14 RELATIONSHIPS BETWEEN PERFORMANCE PARAMETERS

The importance of the parameters defined in Secs. 2.8 to 2.10 to engine performance becomes evident when power, torque, and mean effective pressure are expressed in terms of these parameters. From the definitions of engine power [Eq. (2.13)], mean effective pressure [Eq. (2.19)], fuel conversion efficiency [Eq. (2.23)], fuel/air ratio [Eq. (2.26)], and volumetric efficiency [Eq. (2.27)], the following relationships between engine performance parameters can be developed. For power P:

$$P = \frac{\eta_f m_a N Q_{HV}(F/A)}{n_R} \tag{2.38}$$

PETITIONER'S EXHIBIT 1002
US PATENT NO. 6,581,565
Page 1593

For four-stroke cycle engines, volumetric efficiency can be introduced:

$$P = \frac{\eta_f \eta_v N V_d Q_{HV} \rho_{a,i}(F/A)}{2} \tag{2.39}$$

For torque T:

$$T = \frac{\eta_f \eta_v V_d Q_{HV} \rho_{a,i}(F/A)}{4\pi} \tag{2.40}$$

For mean effective pressure:

$$\text{mep} = \eta_f \eta_v Q_{HV} \rho_{a,i}(F/A) \tag{2.41}$$

The power per unit piston area, often called the *specific power*, is a measure of the engine designer's success in using the available piston area regardless of cylinder size. From Eq. (2.39), the specific power is

$$\frac{P}{A_p} = \frac{\eta_f \eta_v N L Q_{HV} \rho_{a,i}(F/A)}{2} \tag{2.42}$$

Mean piston speed can be introduced with Eq. (2.9) to give

$$\frac{P}{A_p} = \frac{\eta_f \eta_v \bar{S}_p Q_{HV} \rho_{a,i}(F/A)}{4} \tag{2.43}$$

Specific power is thus proportional to the product of mean effective pressure and mean piston speed.

These relationships illustrate the direct importance to engine performance of:

1. High fuel conversion efficiency
2. High volumetric efficiency
3. Increasing the output of a given displacement engine by increasing the inlet air density
4. Maximum fuel/air ratio that can be usefully burned in the engine
5. High mean piston speed

2.15 ENGINE DESIGN AND PERFORMANCE DATA

Engine ratings usually indicate the highest power at which manufacturers expect their products to give satisfactory economy, reliability, and durability under service conditions. Maximum torque, and the speed at which it is achieved, is usually given also. Since both of these quantities depend on displaced volume, for comparative analyses between engines of different displacements in a given engine category normalized performance parameters are more useful. The following measures, at the operating points indicated, have most significance:[4]

PETITIONER'S EXHIBIT 1002
US PATENT NO. 6,581,565
Page 1594

TABLE 2.1
Typical design and operating data for internal combustion engines

	Operating cycle	Compression ratio	Bore, m	Stroke/ bore	Rated maximum: Speed, rev/min	Rated maximum: bmep, atm	Rated maximum: Power per unit volume kW/dm³	Weight/ power ratio, kg/kW	Approx. best bsfc, g/kW·h
Spark-ignition engines:									
Small (e.g., motorcycles)	2S,4S	6–11	0.05–0.085	1.2–0.9	4500–7500	4–10	20–60	5.5–2.5	350
Passenger cars	4S	8–10	0.07–0.1	1.1–0.9	4500–6500	7–10	20–50	4–2	270
Trucks	4S	7–9	0.09–0.13	1.2–0.7	3600–5000	6.5–7	25–30	6.5–2.5	300
Large gas engines	2S,4S	8–12	0.22–0.45	1.1–1.4	300–900	6.8–12	3–7	23–35	200
Wankel engines	4S	≈ 9	0.57 dm³ per chamber		6000–8000	9.5–10.5	35–45	1.6–0.9	300
Diesel engines:									
Passenger cars	4S	17–23	0.075–0.1	1.2–0.9	4000–5000	5–7.5	18–22	5–2.5	250
Trucks (NA)	4S	16–22	0.1–0.15	1.3–0.8	2100–4000	6–9	15–22	7–4	210
Trucks (TC)	4S	14–20	0.1–0.15	1.3–0.8	2100–4000	12–18	18–26	7–3.5	200
Locomotive, industrial, marine	4S,2S	12–18	0.15–0.4	1.1–1.3	425–1800	7–23	5–20	6–18	190
Large engines, marine and stationary	2S	10–12	0.4–1	1.2–3	110–400	9–17	2–8	12–50	180

PETITIONER'S EXHIBIT 1002
US PATENT NO. 6,581,565
Page 1595

1. At maximum or normal rated point:

   Mean piston speed. Measures comparative success in handling loads due to inertia of the parts, resistance to air flow, and/or engine friction.

   Brake mean effective pressure. In naturally aspirated engines bmep is not stress limited. It then reflects the product of volumetric efficiency (ability to induct air), fuel/air ratio (effectiveness of air utilization in combustion), and fuel conversion efficiency. In supercharged engines bmep indicates the degree of success in handling higher gas pressures and thermal loading.

   Power per unit piston area. Measures the effectiveness with which the piston area is used, regardless of cylinder size.

   Specific weight. Indicates relative economy with which materials are used.

   Specific volume. Indicates relative effectiveness with which engine space has been utilized.

2. At all speeds at which the engine will be used with full throttle or with maximum fuel-pump setting:

   Brake mean effective pressure. Measures ability to obtain/provide high air flow and use it effectively over the full range.

3. At all useful regimes of operation and particularly in those regimes where the engine is run for long periods of time:

   Brake specific fuel consumption or *fuel conversion efficiency.*
   Brake specific emissions.

Typical performance data for spark-ignition and diesel engines over the normal production size range are summarized in Table 2.1.[4] The four-stroke cycle dominates except in the smallest and largest engine sizes. The larger engines are turbocharged or supercharged. The maximum rated engine speed decreases as engine size increases, maintaining the maximum mean piston speed in the range of about 8 to 15 m/s. The maximum brake mean effective pressure for turbocharged and supercharged engines is higher than for naturally aspirated engines. Because the maximum fuel/air ratio for spark-ignition engines is higher than for diesels, their naturally aspirated maximum bmep levels are higher. As engine size increases, brake specific fuel consumption decreases and fuel conversion efficiency increases, due to reduced importance of heat losses and friction. For the largest diesel engines, brake fuel conversion efficiencies of about 50 percent and indicated fuel conversion efficiencies of over 55 percent can be obtained.

PROBLEMS

2.1. Explain why the brake mean effective pressure of a naturally aspirated diesel engine is lower than that of a naturally aspirated spark-ignition engine. Explain why the bmep is lower at the maximum rated power for a given engine than the bmep at the maximum torque.

PETITIONER'S EXHIBIT 1002
US PATENT NO. 6,581,565
Page 1596

2.2. Describe the impact on air flow, maximum torque, and maximum power of changing a spark-ignition engine cylinder head from 2 valves per cylinder to 4 valves (2 inlet and 2 exhaust) per cylinder.

2.3. Calculate the mean piston speed, bmep, and specific power of the spark-ignition engines in Figs. 1-4, 1-9, and 1-12 at their maximum rated power.

2.4. Calculate the mean piston speed, bmep, and specific power of the diesel engines in Figs. 1-20, 1-21, 1-22, 1-23, and 1-24 at their maximum rated power. Briefly explain any significant differences.

2.5. Develop an equation for the power required to drive a vehicle at constant speed up a hill of angle α, in terms of vehicle speed, mass, frontal area, drag coefficient, coefficient of rolling resistance, α, and acceleration due to gravity. Calculate this power when the car mass is 1500 kg, the hill angle is 15 degrees, and the vehicle speed is 50 mi/h.

2.6. The spark-ignition engine in Fig. 1-4 is operating at a mean piston speed of 10 m/s. The measured air flow is 60 g/s. Calculate the volumetric efficiency based on atmospheric conditions.

2.7. The diesel engine of Fig. 1-20 is operating with a mean piston speed of 8 m/s. Calculate the air flow if the volumetric efficiency is 0.92. If (F/A) is 0.05 what is the fuel flow rate, and the mass of fuel injected per cylinder per cycle?

2.8. The brake fuel conversion efficiency of a spark-ignition engine is 0.3, and varies little with fuel type. Calculate the brake specific fuel consumption for isooctane, gasoline, methanol, and hydrogen (relevant data are in App. D).

2.9. You are doing a preliminary design study of a turbocharged four-stroke diesel engine. The maximum rated power is limited by stress considerations to a brake mean effective pressure of 1200 kPa and maximum value of the mean piston speed of 12 m/s.

(*a*) Derive an equation relating the engine inlet pressure (pressure in the inlet manifold at the turbocharger compressor exit) to the fuel/air ratio at this maximum rated power operating point. Other reciprocating engine parameters (e.g., volumetric efficiency, fuel conversion efficiency, bmep, etc.) appear in this equation also.

(*b*) The maximum rated brake power requirement for this engine is 400 kW. Estimate sensible values for number of cylinders, cylinder bore, stroke, and determine the maximum rated speed of this preliminary engine design.

(*c*) If the pressure ratio across the compressor is 2, estimate the overall fuel/air and air/fuel ratios at the maximum rated power. Assume appropriate values for any other parameters you may need.

2.10. In the reciprocating engine, during the power or expansion stroke, the gas pressure force acting on the piston is transmitted to the crankshaft via the connecting rod. List the forces acting on the piston during this part of the operating cycle. Show the direction of the forces acting on the piston on a sketch of the piston, cylinder, connecting rod, crank arrangement. Write out the force balance for the piston (*a*) along the cylinder axis and (*b*) transverse to the cylinder axis in the plane containing the connecting rod. (You are not asked to manipulate or solve these equations.)

2.11. You are designing a four-stroke cycle diesel engine to provide a brake power of 300 kW naturally aspirated at its maximum rated speed. Based on typical values for brake mean effective pressure and maximum mean piston speed, estimate the required engine displacement, and the bore and stroke for sensible cylinder geometry and number of engine cylinders. What is the maximum rated engine speed (rev/min)

PETITIONER'S EXHIBIT 1002
US PATENT NO. 6,581,565
Page 1597

for your design? What would be the brake torque (N · m) and the fuel flow rate (g/h) at this maximum speed? Assume a maximum mean piston speed of 12 m/s is typical of good engine designs.

2.12. The power per unit piston area P/A_p (often called the specific power) is a measure of the designer's success in using the available piston area regardless of size.

(*a*) Derive an expression for P/A_p in terms of mean effective pressure and mean piston speed for two-stroke and four-stroke engine cycles.

(*b*) Compute typical maximum values of P/A_p for a spark-ignition engine (e.g., Fig. 1-4), a turbocharged four-stroke cycle diesel engine (e.g., Fig. 1-22), and a large marine diesel (Fig. 1-24). Table 2-1 may be helpful. State your assumptions clearly.

2.13. Several velocities, time, and length scales are useful in understanding what goes on inside engines. Make estimates of the following quantities for a 1.6-liter displacement four-cylinder spark-ignition engine, operating at wide-open throttle at 2500 rev/min.

(*a*) The mean piston speed and the maximum piston speed.

(*b*) The maximum charge velocity in the intake port (the port area is about 20 percent of the piston area).

(*c*) The time occupied by one engine operating cycle, the intake process, the compression process, the combustion process, the expansion process, and the exhaust process. (*Note*: The word *process* is used here not the word *stroke*.)

(*d*) The average velocity with which the flame travels across the combustion chamber.

(*e*) The length of the intake system (the intake port, the manifold runner, etc.) which is filled by one cylinder charge just before the intake valve opens and this charge enters the cylinder (i.e., how far back from the intake valve, in centimeters, one cylinder volume extends in the intake system).

(*f*) The length of exhaust system filled by one cylinder charge after it exits the cylinder (assume an average exhaust gas temperature of 425°C).

You will have to make several appropriate geometric assumptions. The calculations are straightforward, and only approximate answers are required.

2.14. The values of mean effective pressure at rated speed, maximum mean piston speed, and maximum specific power (engine power/total piston area) are essentially independent of cylinder size for naturally aspirated engines of a given type. If we also assume that engine weight per unit displaced volume is essentially constant, how will the *specific weight* of an engine (engine weight/maximum rated power) at fixed total displaced volume vary with the number of cylinders? Assume the bore and stroke are equal.

REFERENCES

1. Obert, E.F.: *Internal Combustion Engines and Air Pollution*, chap. 2, Intext Educational Publishers, New York, 1973.
2. SAE Standard: "Engine Test Code—Spark Ignition and Diesel," SAE J816b, *SAE Handbook*.
3. Bosch: *Automotive Handbook*, 2nd English edition, Robert Bosch GmbH, Stuttgart, 1986.
4. Taylor, C.F.: *The Internal Combustion Engine in Theory and Practice*, vol. II, MIT Press, Cambridge, Mass., 1968.

PETITIONER'S EXHIBIT 1002
US PATENT NO. 6,581,565
Page 1598

CHAPTER 3

THERMOCHEMISTRY OF FUEL-AIR MIXTURES

3.1 CHARACTERIZATION OF FLAMES

Combustion of the fuel-air mixture inside the engine cylinder is one of the processes that controls engine power, efficiency, and emissions. Some background in relevant combustion phenomena is therefore a necessary preliminary to understanding engine operation. These combustion phenomena are different for the two main types of engines—spark-ignition and diesel—which are the subject of this book. In spark-ignition engines, the fuel is normally mixed with air in the engine intake system. Following the compression of this fuel-air mixture, an electrical discharge initiates the combustion process; a flame develops from the "kernal" created by the spark discharge and propagates across the cylinder to the combustion chamber walls. At the walls, the flame is "quenched" or extinguished as heat transfer and destruction of active species at the wall become the dominant processes. An undesirable combustion phenomenon—the "spontaneous" ignition of a substantial mass of fuel-air mixture ahead of the flame, before the flame can propagate through this mixture (which is called the end-gas)—can also occur. This autoignition or self-explosion combustion phenomenon is the cause of spark-ignition engine knock which, due to the high pressures generated, can lead to engine damage.

In the diesel engine, the fuel is injected into the cylinder into air already at high pressure and temperature, near the end of the compression stroke. The autoignition, or self-ignition, of portions of the developing mixture of already

PETITIONER'S EXHIBIT 1002
US PATENT NO. 6,581,565
Page 1599

injected and vaporized fuel with this hot air starts the combustion process, which spreads rapidly. Burning then proceeds as fuel and air mix to the appropriate composition for combustion to take place. Thus, fuel-air mixing plays a controlling role in the diesel combustion process.

Chapters 3 and 4 focus on the thermochemistry of combustion: i.e., the composition and thermodynamic properties of the pre- and postcombustion working fluids in engines and the energy changes associated with the combustion processes that take place inside the engine cylinder. Later chapters (9 and 10) deal with the phenomenological aspects of engine combustion: i.e., the details of the physical and chemical processes by which the fuel-air mixture is converted to burned products. At this point it is useful to review briefly the key combustion phenomena which occur in engines to provide an appropriate background for the material which follows. More detailed information on these combustion phenomena can be found in texts on combustion such as those of Fristrom and Westenberg[1] and Glassman.[2]

The combustion process is a fast exothermic gas-phase reaction (where oxygen is usually one of the reactants). A flame is a combustion reaction which can propagate subsonically through space; motion of the flame relative to the unburned gas is the important feature. Flame structure does not depend on whether the flame moves relative to the observer or remains stationary as the gas moves through it. The existence of flame motion implies that the reaction is confined to a zone which is small in thickness compared to the dimensions of the apparatus—in our case the engine combustion chamber. The reaction zone is usually called the flame front. This flame characteristic of spatial propagation is the result of the strong coupling between chemical reaction, the transport processes of mass diffusion and heat conduction, and fluid flow. The generation of heat and active species accelerate the chemical reaction; the supply of fresh reactants, governed by the convection velocity, limits the reaction. When these processes are in balance, a steady-state flame results.[1]

Flames are usually classified according to the following overall characteristics. The first of these has to do with the composition of the reactants as they enter the reaction zone. If the fuel and oxidizer are essentially uniformly mixed together, the flame is designated as *premixed*. If the reactants are not premixed and must mix together in the same region where reaction takes place, the flame is called a *diffusion* flame because the mixing must be accomplished by a diffusion process. The second means of classification relates to the basic character of the gas flow through the reaction zone: whether it is *laminar* or *turbulent*. In laminar (or streamlined) flow, mixing and transport are done by molecular processes. Laminar flows only occur at low Reynolds number. The Reynolds number (density × velocity × lengthscale/viscosity) is the ratio of inertial to viscous forces. In turbulent flows, mixing and transport are enhanced (usually by a substantial factor) by the macroscopic relative motion of eddies or lumps of fluid which are the characteristic feature of a turbulent (high Reynolds number) flow. A third area of classification is whether the flame is *steady* or *unsteady*. The distinguishing feature here is whether the flame structure and motion change with

PETITIONER'S EXHIBIT 1002
US PATENT NO. 6,581,565
Page 1600

time. The final characterizing feature is the *initial phase* of the reactants—gas, liquid, or solid.

Flames in engines are unsteady, an obvious consequence of the internal combustion engine's operating cycle. Engine flames are turbulent. Only with substantial augmentation of laminar transport processes by the turbulent convection processes can mixing and burning rates and flame-propagation rates be made fast enough to complete the engine combustion process within the time available.

The conventional spark-ignition flame is thus a premixed unsteady turbulent flame, and the fuel-air mixture through which the flame propagates is in the gaseous state. The diesel engine combustion process is predominantly an unsteady turbulent diffusion flame, and the fuel is initially in the liquid phase. Both these flames are extremely complicated because they involve the coupling of the complex chemical mechanism, by which fuel and oxidizer react to form products, with the turbulent convective transport process. The diesel combustion process is even more complicated than the spark-ignition combustion process, because vaporization of liquid fuel and fuel-air mixing processes are involved too. Chapters 9 and 10 contain a more detailed discussion of the spark-ignition engine and diesel combustion processes, respectively. This chapter reviews the basic thermodynamic and chemical composition aspects of engine combustion.

3.2 IDEAL GAS MODEL

The gas species that make up the working fluids in internal combustion engines (e.g., oxygen, nitrogen, fuel vapor, carbon dioxide, water vapor, etc.) can usually be treated as ideal gases. The relationships between the thermodynamic properties of an ideal gas and of ideal gas mixtures are reviewed in App. B. There can be found the various forms of the ideal gas law:

$$pV = mRT = m\frac{\tilde{R}}{M}T = n\tilde{R}T \tag{3.1}$$

where p is the pressure, V the volume, m the mass of gas, R the gas constant for the gas, T the temperature, $\tilde{R}$ the universal gas constant, M the molecular weight, and n the number of moles. Relations for evaluating the specific internal energy u, enthalpy h, and entropy s, specific heats at constant volume c_v and constant pressure c_p, on a per unit mass basis and on a per mole basis (where the notation $\tilde{u}$, $\tilde{h}$, $\tilde{s}$, $\tilde{c}_v$, and $\tilde{c}_p$ is used) of an ideal gas, are developed. Also given are equations for calculating the thermodynamic properties of mixtures of ideal gases.

3.3 COMPOSITION OF AIR AND FUELS

Normally in engines, fuels are burned with air. Dry air is a mixture of gases that has a representative composition by volume of 20.95 percent oxygen, 78.09 percent nitrogen, 0.93 percent argon, and trace amounts of carbon dioxide, neon, helium, methane, and other gases. Table 3.1 shows the relative proportions of the major constituents of dry air.[3]

PETITIONER'S EXHIBIT 1002
US PATENT NO. 6,581,565
Page 1601

TABLE 3.1
Principle constitutents of dry air

Gas	ppm by volume	Molecular weight	Mole fraction	Molar ratio
O_2	209,500	31.998	0.2095	1
N_2	780,900	28.012	0.7905	3.773
Ar	9,300	39.948		
CO_2	300	44.009		
Air	1,000,000	28.962	1.0000	4.773

In combustion, oxygen is the reactive component of air. It is usually sufficiently accurate to regard air as consisting of 21 percent oxygen and 79 percent inert gases taken as nitrogen (often called atmospheric or apparent nitrogen). For each mole of oxygen in air there are

$$\frac{1 - 0.2095}{0.2095} = 3.773$$

moles of atmospheric nitrogen. The molecular weight of air is obtained from Table 3.1 with Eq. (B.17) as 28.962, usually approximated by 29. Because atmospheric nitrogen contains traces of other species, its molecular weight is slightly different from that of pure molecular nitrogen, i.e.,

$$M_{aN_2} = \frac{28.962 - 0.2095 \times 31.998}{1 - 0.2095} = 28.16$$

In the following sections, *nitrogen* will refer to atmospheric nitrogen and a molecular weight of 28.16 will be used. An air composition of 3.773 moles of nitrogen per mole of oxygen will be assumed.

The density of dry air can be obtained from Eq. (3.1) with $R = 8314.3$ J/kmol·K and $M = 28.962$:

$$\rho(\text{kg/m}^3) = \frac{3.483 \times 10^{-3} p(\text{Pa})}{T(\text{K})} \tag{3.2a}$$

or

$$\rho(\text{lbm/ft}^3) = \frac{2.699 p(\text{lbf/in}^2)}{T(^\circ\text{R})} \tag{3.2b}$$

Thus, the value for the density of dry air at 1 atmosphere (1.0133×10^5 Pa, 14.696 lbf/in^2) and 25°C (77°F) is 1.184 kg/m^3 (0.0739 lbm/ft^3).

Actual air normally contains water vapor, the amount depending on temperature and degree of saturation. Typically the proportion by mass is about 1 percent, though it can rise to about 4 percent under extreme conditions. The *relative humidity* compares the water vapor content of air with that required to saturate. It is defined as:

> The ratio of the partial pressure of water vapor actually present to the saturation pressure at the same temperature.

PETITIONER'S EXHIBIT 1002
US PATENT NO. 6,581,565
Page 1602

Water vapor content is measured with a wet- and dry-bulb psychrometer. This consists of two thermometers exposed to a stream of moist air. The dry-bulb temperature is the temperature of the air. The bulb of the other thermometer is wetted by a wick in contact with a water reservoir. The wet-bulb temperature is lower than the dry-bulb temperature due to evaporation of water from the wick. It is a good approximation to assume that the wet-bulb temperature is the adiabatic saturation temperature. Water vapor pressure can be obtained from observed wet- and dry-bulb temperatures and a psychrometric chart such as Fig. 3-1.[4] The effect of humidity on the properties of air is given in Fig. 3-2.[5]

The fuels most commonly used in internal combustion engines (gasoline or petrol, and diesel fuels) are blends of many different hydrocarbon compounds obtained by refining petroleum or crude oil. These fuels are predominantly carbon and hydrogen (typically about 86 percent carbon and 14 percent hydrogen by weight) though diesel fuels can contain up to about 1 percent sulfur. Other fuels of interest are alcohols (which contain oxygen), gaseous fuels (natural gas and liquid petroleum gas), and single hydrocarbon compounds (e.g., methane, propane, isooctane) which are often used in engine research. Properties of the more common internal combustion engine fuels are summarized in App. D.

Some knowledge of the different classes of organic compounds and their

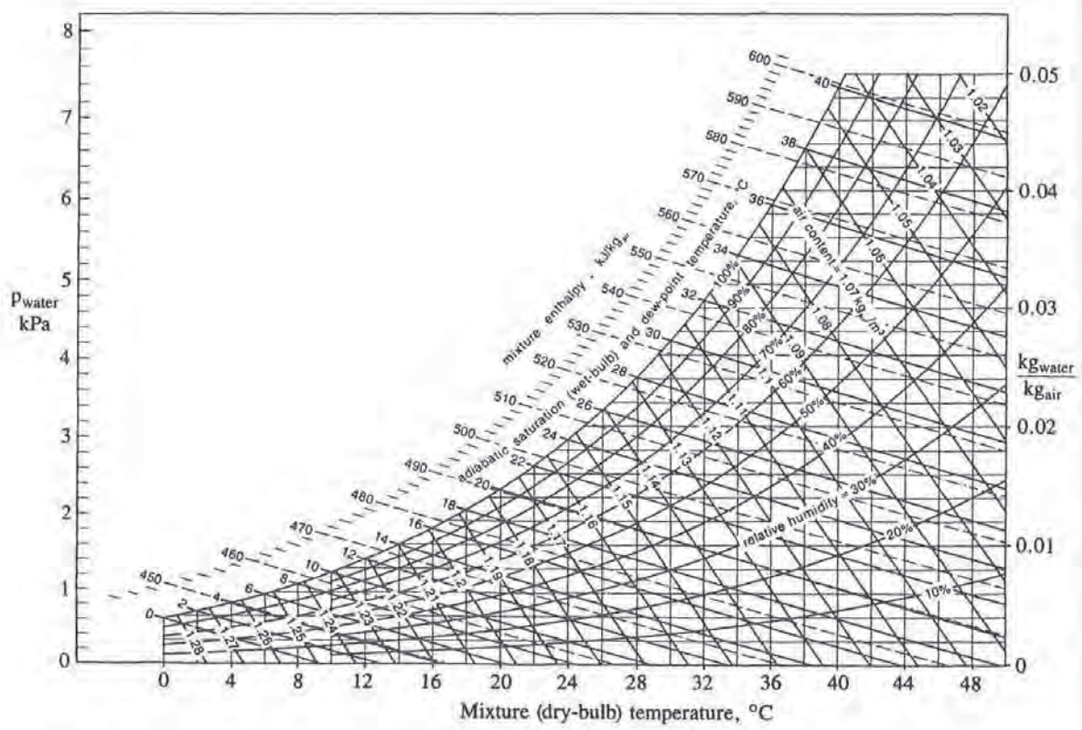


FIGURE 3-1
Psychrometric chart for air-water mixtures at 1 atmosphere. (*From Reynolds.*[4])

PETITIONER'S EXHIBIT 1002
US PATENT NO. 6,581,565
Page 1603

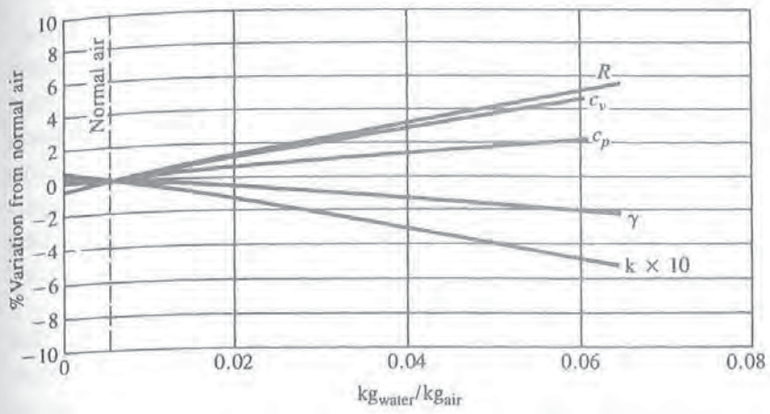
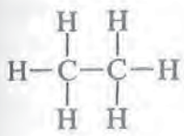


FIGURE 3-2
Effect of humidity on properties of air: R is the gas constant; c_v and c_p are specific heats at constant volume and pressure, respectively; $\gamma = c_p/c_v$; k is the thermal conductivity. (*From Taylor.*[5])

molecular structure is necessary in order to understand combustion mechanisms.[6] The different classes are as follows:

Alkyl Compounds

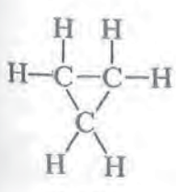
Paraffins
(alk*anes*)



C_nH_{2n+2}

Single-bonded open-chain saturated hydrocarbon molecules: i.e., no more hydrogen can be added. For the larger molecules straight-chain and branched-chain configurations exist. These are called normal (*n*-) and iso compounds, respectively. Examples: CH_4, methane; C_2H_6, ethane; C_3H_8, propane; C_8H_{18}, *n*-octane and isooctane. There are several "isooctanes," depending on the relative position of the branches. By isooctane is usually meant 2,2,4-trimethylpentane, indicating five carbon atoms in the straight chain (pentane) with three methyl (CH_3) branches located respectively at C-atoms 2, 2, and 4. Radicals deficient in one hydrogen take the name methyl, ethyl, propyl, etc.

Cycloparaffins
or *napthenes*
(*cyclanes*)

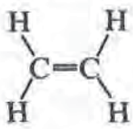


C_nH_{2n}

Single bond (no double bond) ring hydrocarbons. Unsaturated, since ring can be broken and additional hydrogen added. Examples: C_3H_6, cyclopropane (three C-atom ring); C_4H_8, cyclobutane (four C-atom ring); C_5H_{10}, cyclopentane (five C-atom ring).

PETITIONER'S EXHIBIT 1002
US PATENT NO. 6,581,565
Page 1604

Olefins
(alk*enes*)



C_nH_{2n}

Open-chain hydrocarbons containing a double bond; hence they are unsaturated. Examples are: C_2H_4, ethene (or ethylene); C_3H_6, propene (or propylene); C_4H_8, butene (or butylene); . . . . From butene upwards several structural isomers are possible depending on the location of the double bond in the basic carbon chain. Straight- and branched-chain structures exist. Diolefins contain two double bonds.

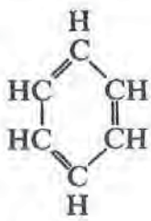
Acetylenes
(alk*ynes*)

H—C≡C—H

C_nH_{2n-2}

Open-chain unsaturated hydrocarbons containing one carbon-carbon triple bond. First member is acetylene, H—C≡C—H. Additional members of the alkyne series comprise open-chain molecules, similar to higher alkenes but with each double bond replaced by a triple bond.

Aromatics

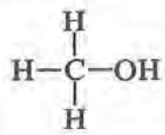


C_nH_{2n-6}

Building block for aromatic hydrocarbons is the benzene (C_6H_6) ring structure shown. This ring structure is very stable and accommodates additional $-CH_2$ groups in side chains and not by ring expansion. Examples: C_7H_8, toluene; C_8H_{10}, xylene (several structural arrangements); . . . . More complex aromatic hydrocarbons incorporate ethyl, propyl, and heavier alkyl side chains in a variety of structural arrangements.

Alcohols

Monohydric alcohols



$C_nH_{2n+1}OH$

In these organic compounds, one hydroxyl (—OH) group is substituted for one hydrogen atom. Thus methane becomes methyl alcohol, CH_3OH (also called methanol); ethane becomes ethyl alcohol, C_2H_5OH (ethanol); etc.

3.4 COMBUSTION STOICHIOMETRY

This section develops relations between the composition of the reactants (fuel and air) of a combustible mixture and the composition of the products. Since these relations depend only on the conservation of mass of each chemical element in the reactants, only the relative elemental composition of the fuel and the relative proportions of fuel and air are needed.

PETITIONER'S EXHIBIT 1002
US PATENT NO. 6,581,565
Page 1605

If sufficient oxygen is available, a hydrocarbon fuel can be completely oxidized. The carbon in the fuel is then converted to carbon dioxide CO_2 and the hydrogen to water H_2O. For example, consider the overall chemical equation for the complete combustion of one mole of propane C_3H_8:

$$C_3H_8 + aO_2 = bCO_2 + cH_2O \tag{3.3}$$

A carbon balance between the reactants and products gives $b = 3$. A hydrogen balance gives $2c = 8$, or $c = 4$. An oxygen balance gives $2b + c = 10 = 2a$, or $a = 5$. Thus Eq. (3.3) becomes

$$C_3H_8 + 5O_2 = 3CO_2 + 4H_2O \tag{3.4}$$

Note that Eq. (3.4) only relates the elemental composition of the reactant and product species; it does not indicate the process by which combustion proceeds, which is much more complex.

Air contains nitrogen, but when the products are at low temperatures the nitrogen is not significantly affected by the reaction. Consider the complete combustion of a general hydrocarbon fuel of average molecular composition C_aH_b with air. The overall complete combustion equation is

$$C_aH_b + \left(a + \frac{b}{4}\right)(O_2 + 3.773N_2) = aCO_2 + \frac{b}{2}H_2O + 3.773\left(a + \frac{b}{4}\right)N_2 \tag{3.5}$$

Note that only the *ratios* of the numbers in front of the symbol for each chemical species are defined by Eq. (3.5); i.e., only the relative proportions on a molar basis are obtained. Thus the fuel composition could have been written CH_y where $y = b/a$.

Equation (3.5) defines the *stoichiometric* (or chemically correct or theoretical) proportions of fuel and air; i.e., there is just enough oxygen for conversion of all the fuel into completely oxidized products. The stoichiometric air/fuel or fuel/air ratios (see Sec. 2.9) depend on fuel composition. From Eq. (3.5):

$$\left(\frac{A}{F}\right)_s = \left(\frac{F}{A}\right)_s^{-1} = \frac{(1 + y/4)(32 + 3.773 \times 28.16)}{12.011 + 1.008y}$$

$$= \frac{34.56(4 + y)}{12.011 + 1.008y} \tag{3.6}$$

The molecular weights of oxygen, atmospheric nitrogen, atomic carbon, and atomic hydrogen are, respectively, 32, 28.16, 12.011, and 1.008. $(A/F)_s$ depends only on y; Fig. 3-3 shows the variation in $(A/F)_s$ as y varies from 1 (e.g., benzene) to 4 (methane).

Example 3.1. A hydrocarbon fuel of composition 84.1 percent by mass C and 15.9 percent by mass H has a molecular weight of 114.15. Determine the number of moles of air required for stoichiometric combustion and the number of moles of products produced per mole of fuel. Calculate $(A/F)_s$, $(F/A)_s$, and the molecular weights of the reactants and the products.

PETITIONER'S EXHIBIT 1002
US PATENT NO. 6,581,565
Page 1606

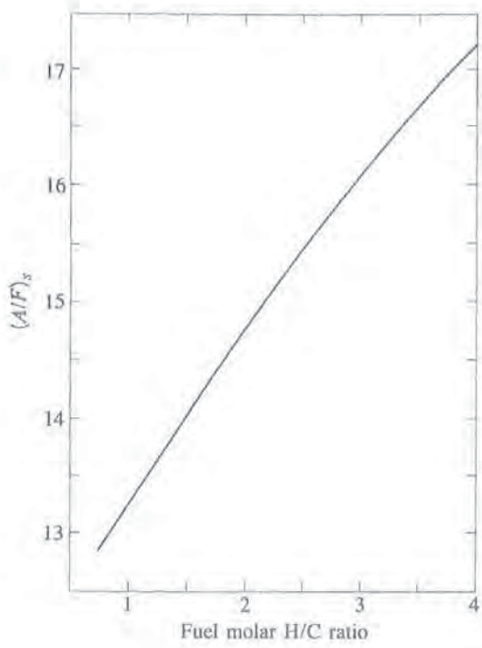


FIGURE 3-3
Stoichiometric air/fuel ratio for air–hydrocarbon fuel mixtures as a function of fuel molar H/C ratio.

Assume a fuel composition $C_a H_b$. The molecular weight relation gives

$$114.15 = 12.011a + 1.008b$$

The gravimetric analysis of the fuel gives

$$\frac{b}{a} = \frac{15.9/1.008}{84.1/12.011} = 2.25$$

Thus

$$a = 8 \qquad b = 18\dagger$$

The fuel is octane C_8H_{18}. Equation (3.5) then becomes

$$\underset{\text{Fuel}}{C_8H_{18}} + 12.5(\underset{\text{Air}}{O_2 + 3.773N_2}) = \underset{\text{Products}}{8CO_2 + 9H_2O + 47.16N_2}$$

In moles:

$$1 + 12.5(1 + 3.773) = 8 + 9 + 47.16$$

$$1 + 59.66 = 64.16$$

Relative mass:

$$114.15 + 59.66 \times 28.96 = 8 \times 44.01 + 9 \times 18.02 + 47.16 \times 28.16$$

$$114.5 + 1727.8 = 1842.3$$

† Note that for fuels which are mixtures of hydrocarbons, a and b need not be integers.

PETITIONER'S EXHIBIT 1002
US PATENT NO. 6,581,565
Page 1607

Per unit mass fuel:

$$1 \quad + \quad 15.14 \quad = 16.14$$

Thus for stoichiometric combustion, 1 mole of fuel requires 59.66 moles of air and produces 64.16 moles of products. The stoichiometric $(A/F)_s$ is 15.14 and $(F/A)_s$ is 0.0661.

The molecular weights of the reactants M_R and products M_P are

$$M_R = \frac{1}{n}\sum n_i M_i = \frac{1}{60.66}(1 \times 114.15 + 59.66 \times 28.96)$$

$$M_P = \frac{1}{n}\sum n_i M_i = \frac{1}{64.16}(8 \times 44.01 + 9 \times 18.02 + 47.16 \times 28.16)$$

or

$$M_R = 30.36 \qquad M_P = 28.71$$

Fuel-air mixtures with more than or less than the stoichiometric air requirement can be burned. With excess air or fuel-lean combustion, the extra air appears in the products in unchanged form. For example, the combustion of isooctane with 25 percent excess air, or 1.25 times the stoichiometric air requirement, gives

$$C_8H_{18} + 1.25 \times 12.5(O_2 + 3.773N_2) = 8CO_2 + 9H_2O + 3.13O_2 + 58.95N_2 \tag{3.7}$$

With less than the stoichiometric air requirement, i.e., with fuel-rich combustion, there is insufficient oxygen to oxidize fully the fuel C and H to CO_2 and H_2O. The products are a mixture of CO_2 and H_2O with carbon monoxide CO and hydrogen H_2 (as well as N_2). The product composition cannot be determined from an element balance alone and an additional assumption about the chemical composition of the product species must be made (see Secs. 4.2 and 4.9.2).

Because the composition of the combustion products is significantly different for fuel-lean and fuel-rich mixtures, and because the stoichiometric fuel/air ratio depends on fuel composition, the ratio of the actual fuel/air ratio to the stoichiometric ratio (or its inverse) is a more informative parameter for defining mixture composition. The *fuel/air equivalence ratio* ϕ,

$$\phi = \frac{(F/A)_{\text{actual}}}{(F/A)_s} \tag{3.8}$$

will be used throughout this text for this purpose. The inverse of ϕ, the *relative air/fuel ratio* λ,

$$\lambda = \phi^{-1} = \frac{(A/F)_{\text{actual}}}{(A/F)_s} \tag{3.9}$$

is also sometimes used.

PETITIONER'S EXHIBIT 1002
US PATENT NO. 6,581,565
Page 1608

For fuel-lean mixtures: $\phi < 1, \lambda > 1$
For stoichiometric mixtures: $\phi = \lambda = 1$
For fuel-rich mixtures: $\phi > 1, \lambda < 1$

When the fuel contains oxygen (e.g., with alcohols), the procedure for determining the overall combustion equation is the same except that fuel oxygen is included in the oxygen balance between reactants and products. For methyl alcohol (methanol), CH_3OH, the stoichiometric combustion equation is

$$CH_3OH + 1.5(O_2 + 3.773N_2) = CO_2 + 2H_2O + 5.66N_2 \tag{3.10}$$

and $(A/F)_s = 6.47$. For ethyl alcohol (ethanol), C_2H_5OH, the stoichiometric combustion equation is

$$C_2H_5OH + 3(O_2 + 3.773N_2) = 2CO_2 + 3H_2O + 11.32N_2 \tag{3.11}$$

and $(A/F)_s = 9.00$.

If there are significant amounts of sulfur in the fuel, the appropriate oxidation product for determining the stoichiometric air and fuel proportions is sulfur dioxide, SO_2.

For hydrogen fuel, the stoichiometric equation is

$$H_2 + \tfrac{1}{2}(O_2 + 3.773N_2) = H_2O + 1.887N_2 \tag{3.12}$$

and the stoichiometric (A/F) ratio is 34.3.

Note that the composition of the products of combustion in Eqs. (3.7) and (3.10) to (3.12) may not occur in practice. At normal combustion temperatures significant dissociation of CO_2 and of H_2O occurs (see Sec. 3.7.1). Whether, at low temperatures, recombination brings the product composition to that indicated by these overall chemical equations depends on the rate of cooling of the product gases. More general relationships for the composition of unburned and burned gas mixtures are developed in Chap. 4.

The stoichiometric (A/F) and (F/A) ratios of common fuels and representative single hydrocarbon and other compounds are given in App. D along with other fuel data.

3.5 THE FIRST LAW OF THERMODYNAMICS AND COMBUSTION†

3.5.1 Energy and Enthalpy Balances

In a combustion process, fuel and oxidizer react to produce products of different composition. The actual path by which this transformation takes place is understood only for simple fuels such as hydrogen and methane. For fuels with more complicated structure, the details are not well defined. Nonetheless, the first law

† The approach used here follows that developed by Spalding and Cole.[7]

PETITIONER'S EXHIBIT 1002
US PATENT NO. 6,581,565
Page 1609

of thermodynamics can be used to relate the end states of mixtures undergoing a combustion process; its application does not require that the details of the process be known.

The first law of thermodynamics relates changes in internal energy (or enthalpy) to heat and work transfer interactions. In applying the first law to a system whose chemical composition changes, care must be exercised in relating the reference states at which zero internal energy or enthalpy for each species or groups of species are assigned. We are not free, when chemical reactions occur, to choose independently the zero internal energy or enthalpy reference states of chemical substances transformed into each other by reaction.

Consider a system of mass m which changes its composition from reactants to products by chemical reaction as indicated in Fig. 3-4. Applying the first law to the system between its initial and final states gives

$$Q_{R-P} - W_{R-P} = U_P - U_R \tag{3.13}$$

Heat transfer Q_{R-P} and work transfer W_{R-P} due to normal force displacements may occur across the system boundary. The standard thermodynamic sign convention for each energy transfer interaction—positive for heat transfer *to* the system and positive for work transfer *from* the system—is used.

We will consider a series of special processes: first, a *constant volume* process where the initial and final temperatures are the same, T'. Then Eq. (3.13) becomes

$$Q_{R-P} = U'_P - U'_R = (\Delta U)_{V,T'} \tag{3.14}$$

The internal energy of the system has changed by an amount $(\Delta U)_{V,T'}$ which can be measured or calculated. Combustion processes are exothermic [i.e., Q_{R-P} and $(\Delta U)_{V,T'}$ are negative]; therefore the system's internal energy decreases. If Eq. (3.14) is expressed per mole of fuel, then $(\Delta U)_{V,T'}$ is known as the increase in

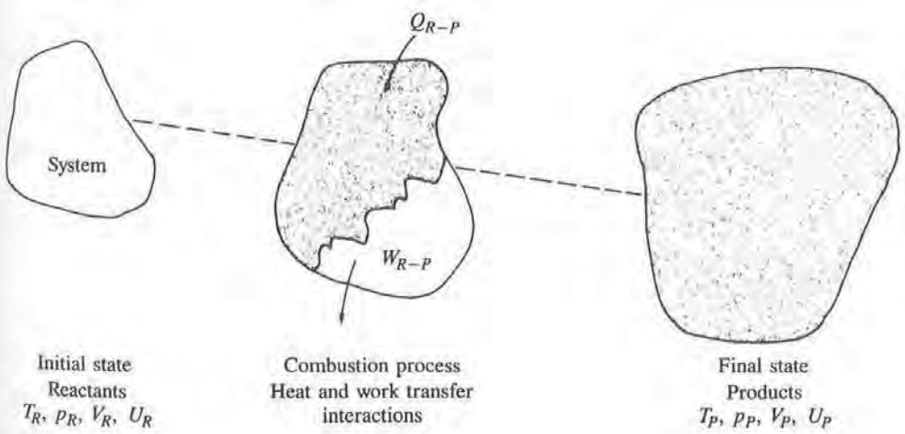


FIGURE 3-4
System changing from reactants to products for first law analysis.

PETITIONER'S EXHIBIT 1002
US PATENT NO. 6,581,565
Page 1610

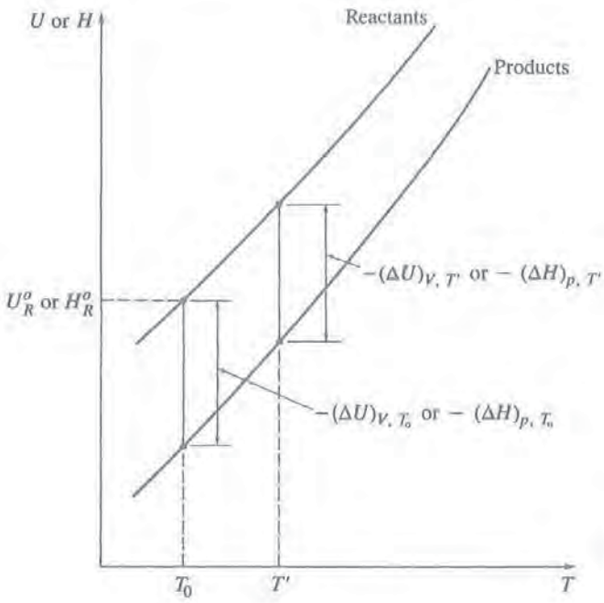


FIGURE 3-5
Schematic plot of internal energy (U) or enthalpy (H) of reactants and products as a function of temperature.

internal energy at constant volume, and $-(\Delta U)_{V,T'}$ is known as the *heat of reaction at constant volume* at temperature T'.

Next, consider a *constant pressure* process where the initial and final temperatures are the same, T'. For a constant pressure process

$$W_{R-P} = \int_R^P p\,dV = p(V_P - V_R) \tag{3.15}$$

so Eq. (3.13) becomes

$$Q_{R-P} - p(V'_P - V'_R) = U'_P - U'_R$$

or

$$\begin{aligned} Q_{R-P} &= (U'_P + pV'_P) - (U'_R + pV'_R) \\ &= H'_P - H'_R = (\Delta H)_{p,T'} \end{aligned} \tag{3.16}$$

The enthalpy of the system has changed by an amount $(\Delta H)_{p,T'}$, which can be measured or calculated. Again for combustion reactions, $(\Delta H)_{p,T'}$ is a negative quantity. If Eq. (3.16) is written per mole of fuel, $(\Delta H)_{p,T'}$ is called the increase in enthalpy at constant pressure and $-(\Delta H)_{p,T'}$ is called the *heat of reaction at constant pressure* at T'.

These processes can be displayed, respectively, on the internal energy or enthalpy versus temperature plot shown schematically in Fig. 3-5. If U (or H) for the reactants is arbitrarily assigned a value U_R° (or H_R°) at some reference temperature T_0, then the value of $(\Delta U)_{V,T_0}$[or $(\Delta H)_{p,T_0}$] fixes the relationship between $U(T)$ or $H(T)$, respectively, for the products and the reactants. Note that the slope of these lines (the specific heat at constant volume or pressure if the diagram is expressed per unit mass or per mole) increases with increasing tem-

PETITIONER'S EXHIBIT 1002
US PATENT NO. 6,581,565
Page 1611

perature; also, the magnitude of $(\Delta U)_{V,\,T'}$ [or $(\Delta H)_{p,\,T'}$] decreases with increasing temperature because c_v (or c_p) for the products is greater than for the reactants.

The difference between $(\Delta H)_{p,\,T'}$ and $(\Delta U)_{V,\,T'}$ is

$$(\Delta H)_{p,\,T'} - (\Delta U)_{V,\,T'} = p(V_P - V_R) \tag{3.17}$$

Only if the volumes of the products and reactants in the constant pressure process are the same are $(\Delta H)_{p,\,T'}$ and $(\Delta U)_{V,\,T'}$ equal. If all the reactant and product species are ideal gases, then the ideal gas law Eq. (3.1) gives

$$(\Delta H)_{p,\,T'} - (\Delta U)_{V,\,T'} = \bar{R}(n'_P - n'_R)T' \tag{3.18}$$

Note that any inert gases do not contribute to $(n'_P - n'_R)$.

With a hydrocarbon fuel, one of the products, H_2O, can be in the gaseous or liquid phase. The internal energy (or enthalpy) of the products in the constant volume (or constant pressure) processes described above in Fig. 3-5 will depend on the relative proportions of the water in the gaseous and liquid phases. The limiting cases of all vapor and all liquid are shown in Fig. 3-6*a* for a U-T plot. The internal energy differences between the curves is

$$|(\Delta U)_{V,\,T',\,\mathrm{H_2O\ liq}}| - |(\Delta U)_{V,\,T',\,\mathrm{H_2O\ vap}}| = m_{\mathrm{H_2O}}\, u'_{fg\ \mathrm{H_2O}} \tag{3.19}$$

where $m_{\mathrm{H_2O}}$ is the mass of water in the products and $u'_{fg\ \mathrm{H_2O}}$ is the internal energy of vaporization of water at the temperature and pressure of the products. Similar

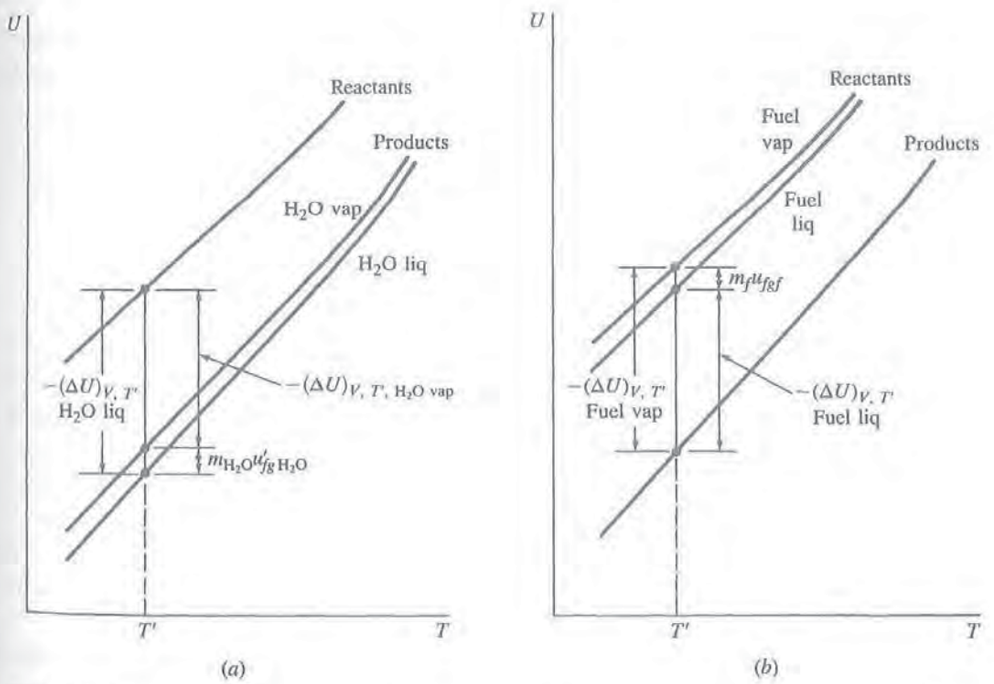


FIGURE 3-6
Schematic plots of internal energy of reactants and products as a function of temperature. (*a*) Effect of water in products as either vapor or liquid. (*b*) Effect of fuel in reactants as either vapor or liquid.

PETITIONER'S EXHIBIT 1002
US PATENT NO. 6,581,565
Page 1612

curves and relationships apply for enthalpy:

$$|(\Delta H)_{p,\,T',\,\mathrm{H_2O\ liq}}| - |(\Delta H)_{p,\,T',\,\mathrm{H_2O\ vap}}| = m_{\mathrm{H_2O}}\, h'_{fg\,\mathrm{H_2O}} \tag{3.20}$$

For some fuels, the reactants may contain the fuel as either liquid or vapor. The U-T (or H-T) line for the reactants with the fuel as liquid or as vapor will be different, as indicated in Fig. 3-6*b*. The vertical distance between the two reactant curves is $m_f u_{fgf}$ (or $m_f h_{fgf}$) where the subscript f denotes fuel.

3.5.2 Enthalpies of Formation

For fuels which are single hydrocarbon compounds, or where the precise fuel composition is known, the internal energies or enthalpies of the reactants and the products can be related through the enthalpies of formation of the reactants and products.

The *enthalpy of formation* $\Delta\tilde{h}_f^\circ$ of a chemical compound is the enthalpy increase associated with the reaction of forming one mole of the given compound from its elements, with each substance in its thermodynamic standard state at the given temperature.

The *standard state* is the state at one atmosphere pressure and the temperature under consideration. We will denote the standard state by the superscript °.

Since thermodynamic calculations are made as a difference between an initial and a final state, it is necessary to select a *datum state* to which all other thermodynamic states can be referred. While a number of datum states have been used in the literature, the most common datum is 298.15 K (25°C) and 1 atmosphere. We will use this datum throughout this text. Elements at their *reference state* are arbitrarily assigned zero enthalpy at the datum temperature. The reference state of each element is its stable standard state; e.g., for oxygen at 298.15 K, the reference state is O_2 gas.

Enthalpies of formation are tabulated as a function of temperature for all commonly occurring species. For inorganic compounds, the *JANAF Thermochemical Tables* are the primary reference source.[8] These tables include values of the molar specific heat at constant pressure, standard entropy, standard Gibbs free energy (called free energy in the tables), standard enthalpy, enthalpy of formation and Gibbs free energy of formation, and $\log_{10}$ equilibrium constant for the formation of each species from its elements. Some primary references for thermodynamic data on fuel compounds are Maxwell,[9] Rossini *et al.*,[10] and Stull *et al.*[11] Enthalpies of formation of species relevant to hydrocarbon fuel combustion are tabulated in Table 3.2. Selected values of thermodynamic properties of relevant species are tabulated in App. D.

For a given combustion reaction, the enthalpy of the products at the standard state relative to the enthalpy datum is then given by

$$H_P^\circ = \sum_{\text{products}} n_i \Delta\tilde{h}_{f,i}^\circ \tag{3.21a}$$

PETITIONER'S EXHIBIT 1002
US PATENT NO. 6,581,565
Page 1613

TABLE 3.2
Standard enthalpies of formation

Species	State†	$\Delta\tilde{h}_f^\circ$, MJ/kmol
O_2	Gas	0
N_2	Gas	0
H_2	Gas	0
C	Gas	0
CO_2	Gas	−393.52
H_2O	Gas	−241.83
H_2O	Liquid	−285.84
CO	Gas	−110.54
CH_4	Gas	−74.87
C_3H_8	Gas	−103.85
CH_3OH	Gas	−201.17
CH_3OH	Liquid	−238.58
C_8H_{18}	Gas	−208.45
C_8H_{18}	Liquid	−249.35

† At 298.15 K (25°C) and 1 atm.

and the enthalpy of the reactants is given by

$$H_R^\circ = \sum_{\text{reactants}} n_i \Delta\tilde{h}_{f,i}^\circ \tag{3.21b}$$

The enthalpy increase, $(\Delta H)_{p,\,T_0}$, is then obtained from the difference $(H_P^\circ - H_R^\circ)$. The internal energy increase can be obtained with Eq. (3.17).

Example 3.2. Calculate the enthalpy of the products and reactants, and the enthalpy increase and internal energy increase of the reaction, of a stoichiometric mixture of methane and oxygen at 298.15 K.

The stoichiometric reaction is

$$CH_4 + 2O_2 = CO_2 + 2H_2O$$

Thus, for H_2O gas, from Table 3.2 and Eq. (3.21*a*, *b*):

$$H_P^\circ = -393.52 + 2(-241.83) = -877.18 \text{ MJ/kmol } CH_4$$

For H_2O liquid:

$$H_P^\circ = -393.52 + 2(-285.84) = -965.20 \text{ MJ/kmol } CH_4$$

$$H_R^\circ = -74.87 \text{ MJ/kmol } CH_4$$

Hence for H_2O gas:

$$(\Delta H)_P^\circ = -877.18 + 74.87 = -802.31 \text{ MJ/kmol } CH_4$$

and for H_2O liquid:

$$(\Delta H)_P^\circ = -965.20 + 74.87 = -890.33 \text{ MJ/kmol } CH_4$$

PETITIONER'S EXHIBIT 1002
US PATENT NO. 6,581,565
Page 1614

Use Eq. (3.18) to find $(\Delta U)^\circ_V$. With H_2O gas, the number of moles of reactants and products are equal, so

$$(\Delta U)^\circ_V = (\Delta H)^\circ_p = -802.3 \text{ MJ/kmol } CH_4$$

For H_2O liquid:

$$(\Delta U)^\circ_V = -890.33 - 8.3143 \times 10^{-3}(1 - 3)298.15 \text{ MJ/kmol } CH_4$$

$$(\Delta U)^\circ_V = -885.4 \text{ MJ/kmol } CH_4$$

Note that the presence of nitrogen in the mixture or oxygen in excess of the stoichiometric amount would not change any of these calculations.

3.5.3 Heating Values

For fuels where the precise fuel composition is not known, the enthalpy of the reactants cannot be determined from the enthalpies of formation of the reactant species. The *heating value* of the fuel is then measured directly.

The heating value Q_{HV} or calorific value of a fuel is the magnitude of the heat of reaction at constant pressure or at constant volume at a standard temperature [usually 25°C (77°F)] for the complete combustion of unit mass of fuel. Thus

$$Q_{HV_p} = -(\Delta H)_{p, T_0} \tag{3.22a}$$

and

$$Q_{HV_V} = -(\Delta U)_{V, T_0} \tag{3.22b}$$

Complete combustion means that all carbon is converted to CO_2, all hydrogen is converted to H_2O, and any sulfur present is converted to SO_2. The heating value is usually expressed in joules per kilogram or joules per kilomole of fuel (British thermal units per pound-mass or British thermal units per pound-mole). It is therefore unnecessary to specify how much oxidant was mixed with the fuel, though this must exceed the stoichiometric requirement. It is immaterial whether the oxidant is air or oxygen.

For fuels containing hydrogen, we have shown that whether the H_2O in the products is in the liquid or gaseous phase affects the value of the heat of reaction. The term *higher heating value* Q_{HHV} (or gross heating value) is used when the H_2O formed is all condensed to the liquid phase; the term *lower heating value* Q_{LHV} (or net heating value) is used when the H_2O formed is all in the vapor phase. The two heating values at constant pressure are related by

$$Q_{HHV_p} = Q_{LHV_p} + \left(\frac{m_{H_2O}}{m_f}\right) h_{fg\,H_2O} \tag{3.23}$$

where (m_{H_2O}/m_f) is the ratio of mass of H_2O produced to mass of fuel burned. A similar expression with $u_{fg\,H_2O}$ replacing $h_{fg\,H_2O}$ applies for the higher and lower heating value at constant volume.

The heating value at constant pressure is the more commonly used; often the qualification "at constant pressure" is omitted. The difference between the heating values at constant pressure and constant volume is small.

PETITIONER'S EXHIBIT 1002
US PATENT NO. 6,581,565
Page 1615

Heating values† of fuels are measured in calorimeters. For gaseous fuels, it is most convenient and accurate to use a continuous-flow atmosphere pressure calorimeter. The entering fuel is saturated with water vapor and mixed with sufficient saturated air for complete combustion at the reference temperature. The mixture is burned in a burner and the combustion products cooled with water-cooled metal tube coils to close to the inlet temperature. The heat transferred to the cooling water is calculated from the measured water flow rate and water temperature rise. The heating value determined by this process is the higher heating value at constant pressure.

For liquid and solid fuels, it is more satisfactory to burn the fuel with oxygen under pressure at constant volume in a bomb calorimeter. A sample of the fuel is placed in the bomb calorimeter, which is a stainless-steel container immersed in cooling water at the standard temperature. Sufficient water is placed in the bomb to ensure that the water produced in the combustion process will condense. Oxygen at 30 atmospheres is admitted to the bomb. A length of firing cotton is suspended into the sample from an electrically heated wire filament to act as a source of ignition. When combustion is complete the temperature rise of the bomb and cooling water is measured. The heating value determined by this process is the higher heating value at constant volume.

The heating values of common fuels are tabulated with other fuel data in App. D. The following example illustrates how the enthalpy of a reactant mixture relative to the enthalpy datum we have defined can be determined from the measured heating value of the fuel.

Example 3.3. Liquid kerosene fuel of the lower heating value (determined in a bomb calorimeter) of 43.2 MJ/kg and average molar H/C ratio of 2 is mixed with the stoichiometric air requirement at 298.15 K. Calculate the enthalpy of the reactant mixture relative to the datum of zero enthalpy for C, O_2, N_2, and H_2 at 298.15 K.

The combustion equation per mole of C can be written

$$CH_2 + \tfrac{3}{2}(O_2 + 3.773N_2) = CO_2 + H_2O + 5.660N_2$$

or

$$14 \text{ kg fuel} + \left.\begin{matrix} 7.160 \text{ kmol} \\ 207.4 \text{ kg} \end{matrix}\right\} \text{air} \rightarrow \left.\begin{matrix} 7.66 \text{ kmol} \\ 221.4 \text{ kg} \end{matrix}\right\} \text{products}$$

where $M = 28.962$ for atmospheric air.

The heating value given is at constant volume, $-(\Delta U)^\circ_V$. $(\Delta H)^\circ_p$ is obtained from Eq. (3.18), noting that the fuel is in the liquid phase:

$$(\Delta H)^\circ_p = -43.2 + 8.3143 \times 10^{-3}\,(7.66 - 7.160) \times \frac{298.15}{14}$$

$$= -43.2 + 0.09 = -43.1 \text{ MJ/kg fuel}$$

† Standard methods for measuring heating values are defined by the American Society for Testing Materials.

PETITIONER'S EXHIBIT 1002
US PATENT NO. 6,581,565
Page 1616

The enthalpy of the products per kilogram of mixture is found from the enthalpies of formation (with H_2O vapor):

$$h_P = \frac{1(-393.52) + 1(-241.83)}{221.4}$$

$$= 2.87 \text{ MJ/kg}$$

The enthalpy of the reactants per kilogram of mixture is then

$$h_R = h_P - (\Delta h)_p^\circ = 2.87 + \frac{43.1 \times 14}{221.4} = 5.59 \text{ MJ/kg}$$

3.5.4 Adiabatic Combustion Processes

We now use the relationships developed above to examine two other special processes important in engine analysis: constant-volume and constant-pressure adiabatic combustion. For an adiabatic constant-volume process, Eq. (3.13) becomes

$$U_P - U_R = 0 \tag{3.24}$$

when U_P and U_R are evaluated relative to the same datum (e.g., the enthalpies of C, O_2, N_2, and H_2 are zero at 298.15 K, the datum used throughout this text).

Frequently, however, the tables or graphs of internal energy or enthalpy for species and reactant or product mixtures which are available give internal energies or enthalpies relative to the species or mixture value at some reference temperature T_0, i.e., $U(T) - U(T_0)$ or $H(T) - H(T_0)$ are tabulated. Since

$$U_P(T_0) - U_R(T_0) = (\Delta U)_{V, T_0}$$

it follows from Eq. (3.24) that

$$[U_P(T) - U_P(T_0)] - [U_R(T) - U_R(T_0)] = -(\Delta U)_{V, T_0} \tag{3.25}$$

relates the product and reactant states. Figure 3-7 illustrates the adiabatic constant-volume combustion process on a U-T diagram. Given the initial state of the reactants (T_R, V) we can determine the final state of the products (T_P, V).

For an adiabatic constant-pressure combustion process, Eq. (3.13) gives

$$H_P - H_R = 0$$

which combines with Eq. (3.16) to give

$$[H_P(T) - H_P(T_0)] - [H_R(T) - H_R(T_0)] = -(\Delta H)_{p, T_0} \tag{3.26}$$

Figure 3-7 illustrates this process also. Given the initial reactant state (T_R, p) we can determine the final product state (T_P, p).

Note that while in Figs. 3-5, 3-6, and 3-7 we have shown U and H for the reactants and products to be functions of T only, in practice for the products at high temperature U and H will be functions of p and T. The analysis presented here is general; however, to determine the final state of the products in an adia-

PETITIONER'S EXHIBIT 1002
US PATENT NO. 6,581,565
Page 1617

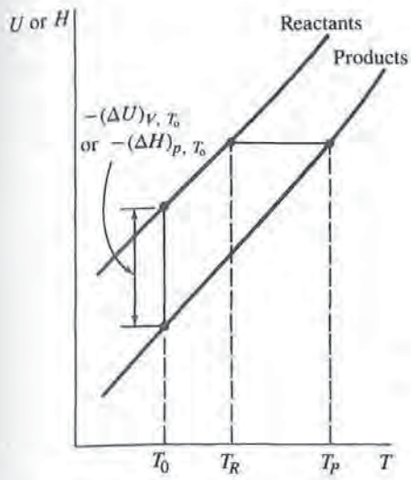


FIGURE 3-7
Adiabatic constant-volume combustion process on U-T diagram or adiabatic constant-pressure combustion process on H-T diagram.

batic combustion process, the constant-volume or constant-pressure constraint must also be used explicitly.

The final temperature of the products in an adiabatic combustion process is called the *adiabatic flame temperature*. Examples of typical adiabatic flame temperatures are shown later in Fig. 3-11.

3.5.5 Combustion Efficiency of an Internal Combustion Engine

In practice, the exhaust gas of an internal combustion engine contains incomplete combustion products (e.g., CO, H_2, unburned hydrocarbons, soot) as well as complete combustion products (CO_2 and H_2O) (see Sec. 4.9). Under lean operating conditions the amounts of incomplete combustion products are small. Under fuel-rich operating conditions these amounts become more substantial since there is insufficient oxygen to complete combustion. Because a fraction of the fuel's chemical energy is not fully released inside the engine during the combustion process, it is useful to define a *combustion efficiency*. The engine can be analyzed as an open system which exchanges heat and work with its surrounding environment (the atmosphere). Reactants (fuel and air) flow into the system; products (exhaust gases) flow out. Consider a mass m which passes through the control volume surrounding the engine shown in Fig. 3-8; the *net chemical energy release* due to combustion within the engine is given by

$$[H_R(T_A) - H_P(T_A)] = m\left(\sum_{i,\text{ reactants}} n_i \Delta\tilde{h}^\circ_{f,i} - \sum_{i,\text{ products}} n_i \Delta\tilde{h}^\circ_{f,i}\right)$$

Enthalpy is the appropriate property since $p_R = p_P = p_{\text{atm}}$. n_i is the number of moles of species i in the reactants or products per unit mass of working fluid and $\Delta\tilde{h}^\circ_{f,i}$ is the standard enthalpy of formation of species i at ambient temperature T_A.

The amount of fuel energy *supplied* to the control volume around the engine which can be released by combustion is $m_f Q_{\text{HV}}$. Hence, the *combustion*

PETITIONER'S EXHIBIT 1002
US PATENT NO. 6,581,565
Page 1618

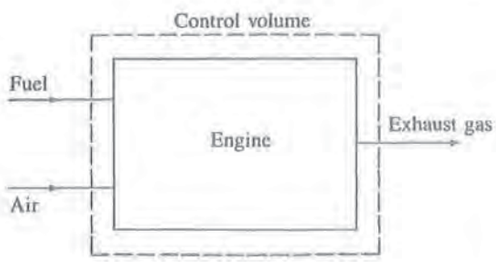


FIGURE 3-8
Control volume surrounding engine.

efficiency—the fraction of the fuel energy supplied which is released in the combustion process—is given by[12]

$$\eta_c = \frac{H_R(T_A) - H_P(T_A)}{m_f Q_{HV}} \tag{3.27}$$

Note that m and m_f could be replaced by the average mass flow rates $\dot{m}$ and $\dot{m}_f$.

Figure 3-9 shows how combustion efficiency varies with the fuel/air equivalence ratio for internal combustion engines. For spark-ignition engines, for lean equivalence ratios, the combustion efficiency is usually in the range 95 to 98 percent. For mixtures richer than stoichiometric, lack of oxygen prevents complete combustion of the fuel carbon and hydrogen, and the combustion efficiency steadily decreases as the mixture becomes richer. Combustion efficiency is little affected by other engine operating and design variables, provided the engine com-

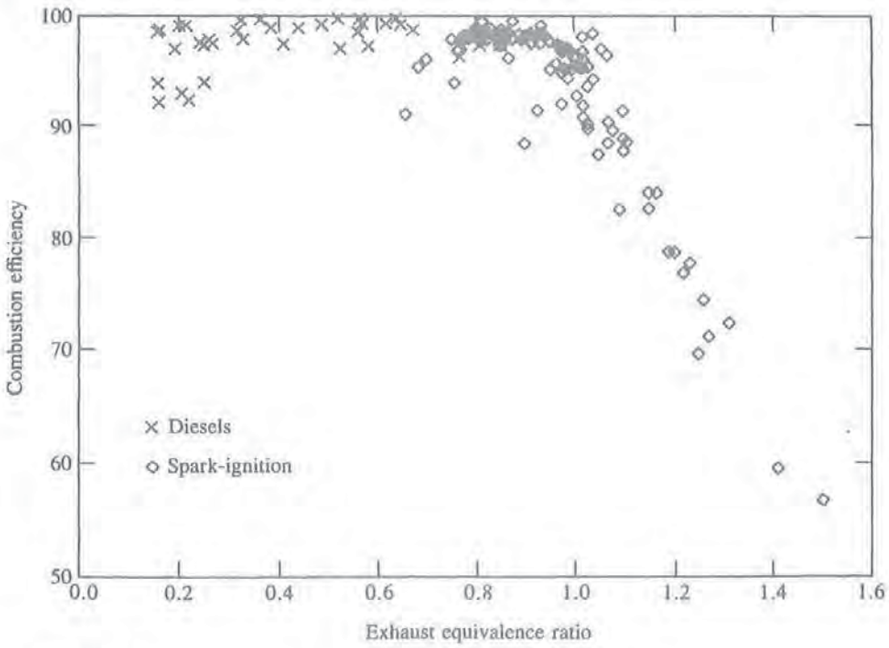


FIGURE 3-9
Variation of engine combustion efficiency with fuel/air equivalence ratio.

PETITIONER'S EXHIBIT 1002
US PATENT NO. 6,581,565
Page 1619

bustion process remains stable. For diesel engines, which always operate lean, the combustion efficiency is normally higher—about 98 percent. Details of exhaust gas composition, on which these combustion efficiencies are based, can be found in Sec. 4.9.

3.6 THE SECOND LAW OF THERMODYNAMICS APPLIED TO COMBUSTION

3.6.1 Entropy

In App. B, it is shown how the entropy of a mixture of ideal gases of known composition can be calculated. The discussion earlier relating enthalpies (or internal energies) of reactant and product mixtures applies to entropy also. The standard state entropies of chemical species are tabulated in the JANAF tables relative to zero entropy at 0 K. If the entropies of the elements at a datum temperature are arbitrarily set equal to zero, then the values of the entropy of a reactant mixture of given composition and of the resulting product mixture of given composition are both determined.

3.6.2 Maximum Work from an Internal Combustion Engine and Efficiency

An internal combustion engine can be analyzed as an open system which exchanges heat and work with its surrounding environment (the atmosphere). Reactants (fuel and air) flow into the system; products (exhaust gases) flow out. By applying the second law of thermodynamics to a control volume surrounding the engine, as illustrated in Fig. 3-8, we can derive an expression for the maximum useful work that the engine can deliver.

Consider a mass m of fluid as it passes through the control volume surrounding the engine. The first law gives

$$\Delta Q - \Delta W_U = \Delta H$$

where ΔW_U is the useful work transfer (i.e., non-$p\,dV$ work) to the environment and $\Delta H = H_P - H_R$. Since the heat transfer ΔQ occurs only with the atmosphere at temperature T_A, from the second law

$$\frac{\Delta Q}{T_A} \leq \Delta S$$

These equations combine to give

$$\Delta W_U \leq -(\Delta H - T_A \Delta S) = -\Delta B$$

where B is the steady-flow availability function, $H - T_A S$.[13] Usually $p_R = p_A$ and $T_R = T_A$. The maximum work will be obtained when $p_P = p_A$ and $T_P = T_A$.

PETITIONER'S EXHIBIT 1002
US PATENT NO. 6,581,565
Page 1620

TABLE 3.3
Enthalpies and free energies of combustion reactions

Reaction†	$\Delta\tilde{h}^\circ_{298}$, MJ/kmol	$\Delta\tilde{g}^\circ_{298}$, MJ/kmol
$C + O_2 \rightarrow CO_2$	−393.52	−394.40
$H_2 + \frac{1}{2}O_2 \rightarrow H_2O$	−240.91	−232.78
$CH_4 + 2O_2 \rightarrow CO_2 + 2H_2O$	−802.30	−800.76
$CH_4O(l) + \frac{3}{2}O_2 \rightarrow CO_2 + 2H_2O$	−638.59	−685.35
$C_3H_8(g) + 5O_2 \rightarrow 3CO_2 + 4H_2O$	−2044.0	−2074.1
$C_6H_6(l) + \frac{15}{2}O_2 \rightarrow 6CO_2 + 3H_2O$	−3135.2	−3175.1
$C_8H_{18}(l) + \frac{25}{2}O_2 \rightarrow 8CO_2 + 9H_2O$	−5074.6	−5219.9

† H_2O (gas) in products.

Under these conditions,

$$\Delta W_U \leq -[(H - TS)_{P_{T_A,\,p_A}} - (H - TS)_{R_{T_A,\,p_A}}] = -(\Delta G)_{T_A, p_A}$$

or
$$\Delta W_{U\,\max} = -(\Delta G)_{T_A,\,p_A} \tag{3.28}$$

G is the Gibbs free energy, $H - TS$, and $(\Delta G)_{T_A,\,p_A}$ is the Gibbs free energy increase in the reaction of the fuel-air mixture to products at atmospheric temperature and pressure. $-(\Delta G)_{T_A,\,p_A}$ will be a maximum when combustion is complete.

A fundamental measure of the effectiveness of any practical internal combustion engine is the ratio of the actual work delivered compared with this maximum work. This ratio will be called the *availability conversion efficiency* η_a:

$$\eta_a = \frac{\Delta W}{\Delta W_{U\,\max}} = -\frac{\Delta W}{(\Delta G)_{T_A,\,p_A}} \tag{3.29}$$

The property *availability* is the maximum useful work transfer that can be obtained from a system atmosphere (or control-volume atmosphere) combination at a given state. This efficiency therefore defines the fraction of the availability of the unburned fuel and air which, passing through the engine and interacting only with the atmosphere, is actually converted to useful work. Availability analysis of engine operation is proving valuable in identifying where the significant irreversibilities or losses in availability occur. This topic is discussed more fully in Sec. 5.7.

$(\Delta G)_{T_A,\,p_A}$, or $(\Delta g)_{T_A,\,p_A}$, is not an easy quantity to evaluate for practical fuels; it is the heating value, $-(\Delta h)_{T_A}$, which is usually measured. Values of $(\Delta g)^\circ_{298}$ and $(\Delta h)^\circ_{298}$ for selected fuel combustion reactions are given in Table 3.3. For the pure hydrocarbons they are closely comparable because at 298 K, $\Delta\tilde{s}^\circ \ll \Delta\tilde{h}^\circ/T$. For hydrogen and methanol the differences are larger, however. Because for practical fuels $-(\Delta h)^\circ_{298}$ is measured directly as the heating value of the fuel, it is standard practice to use the following definition of efficiency:

$$\eta_f = \frac{W_c}{m_f Q_{\mathrm{HV}}} \tag{3.30}$$

PETITIONER'S EXHIBIT 1002
US PATENT NO. 6,581,565
Page 1621

which was defined as the *fuel conversion efficiency* in Sec. 2.8. Note that sometimes the higher heating value is used in Eq. (3.30) and sometimes the lower heating value. Whichever value is used should be explicitly stated. The normal practice in internal combustion engine analysis is to use the lower heating value at constant pressure, since the engine overall is a steady flow device and the water in the exhaust is always in vapor form. We will use Q_{LHV_p} in Eq. (3.30) throughout this text. The fuel conversion efficiency is the most commonly used definition of engine efficiency because it uses an easily measured quantity, the heating value, to define the usable fuel energy supplied to the engine. For hydrocarbon fuels, since $\Delta\tilde{h}^\circ \approx \Delta\tilde{g}^\circ$, the fuel conversion efficiency and the availability conversion efficiency are closely comparable in value.

In practice, not all the fuel energy supplied to the engine is released by the combustion process since combustion is incomplete: the combustion efficiency [Eq. (3.27)] is less than unity. It is sometimes useful to separate out the effects of incomplete combustion by defining an efficiency which relates the actual work per cycle to the amount of fuel chemical energy released in the combustion process. We will call this the *thermal conversion efficiency* η_t:

$$\eta_t = \frac{W_c}{H_R(T_A) - H_P(T_A)} = -\frac{W_c}{(\Delta H)_{T_A}} = \frac{W_c}{\eta_c m_f Q_{\mathrm{HV}}} \tag{3.31}$$

Obviously the fuel conversion, thermal conversion, and combustion efficiencies are related by

$$\eta_f = \eta_c \eta_t \tag{3.32}$$

It is important to understand that there is a fundamental difference between availability conversion efficiency as defined by Eq. (3.29) [and the fuel conversion efficiency for internal combustion engines, Eq. (3.30), which closely approximates it] and the efficiency of a thermodynamic heat engine. The second law limit to the availability conversion efficiency is unity. For a thermodynamic heat engine (which experiences heat-transfer interactions with at least two heat reservoirs) the efficiency is limited to a value substantially less than unity by the temperatures of the heat reservoirs available.[13]

3.7 CHEMICALLY REACTING GAS MIXTURES

The working fluids in engines are mixtures of gases. Depending on the problem under consideration and the portion of the engine cycle in which it occurs chemical reactions may: (1) be so slow that they have a negligible effect on mixture composition (the mixture composition is essentially "frozen"); (2) be so rapid that the mixture state changes and the composition remains in chemical equilibrium; (3) be one of the rate-controlling processes that determine how the composition of the mixture changes with time.

PETITIONER'S EXHIBIT 1002
US PATENT NO. 6,581,565
Page 1622

3.7.1 Chemical Equilibrium

It is a good approximation for performance estimates in engines to regard the burned gases produced by the combustion of fuel and air as in chemical equilibrium.† By this we mean that the chemical reactions, by which individual species in the burned gases react together, produce and remove each species at equal rates. No net change in species composition results.

For example, if the temperature of a mass of carbon dioxide gas in a vessel is increased sufficiently, some of the CO_2 molecules *dissociate* into CO and O_2 molecules. If the mixture of CO_2, CO, and O_2 is in equilibrium, then CO_2 molecules are dissociating into CO and O_2 at the same rate as CO and O_2 molecules are *recombining* in the proportions required to satisfy the equation

$$CO + \tfrac{1}{2}O_2 = CO_2$$

In combustion products of hydrocarbon fuels, the major species present at low temperatures are N_2, H_2O, CO_2, and O_2 or CO and H_2. At higher temperatures (greater than about 2200 K), these major species dissociate and react to form additional species in significant amounts. For example, the adiabatic combustion of a stoichiometric mixture of a typical hydrocarbon fuel with air produces products with species mole fractions of: $N_2 \sim 0.7$; H_2O, $CO_2 \sim 0.1$; CO, OH, O_2, NO, $H_2 \sim 0.01$; H, O ~ 0.001; and other species in lesser amounts.

The second law of thermodynamics defines the criterion for chemical equilibrium as follows. Consider a system of chemically reacting substances undergoing a constant-pressure, constant-temperature process. In the absence of shear work (and electrical work, gravity, motion, capillarity), the first law gives

$$\delta Q = dH$$

The second law gives

$$\delta Q \leq T\, dS$$

Combining these gives

$$dH - T\, dS \leq 0$$

Since we are considering constant-temperature processes, this equation holds for finite changes:

$$\Delta H - T\, \Delta S = \Delta G \leq 0$$

Thus, reactions can only occur (at constant pressure and temperature) if G $(= H - TS)$ for the products is less than G for the reactants. Hence at equilibrium

$$(\Delta G)_{p,\,T} = 0 \tag{3.33}$$

† This assumption is not valid late in the expansion stroke and during the exhaust process (see Sec. 4.9). Nor does it take account of pollutant formation processes (see Chap. 11).

PETITIONER'S EXHIBIT 1002
US PATENT NO. 6,581,565
Page 1623

Consider a reactive mixture of ideal gases. The reactant species M_a, M_b, etc., and product species M_l, M_m, etc., are related by the general reaction whose stoichiometry is given by

$$\nu_a M_a + \nu_b M_b + \cdots = \nu_l M_l + \nu_m M_m + \cdots \tag{3.34a}$$

This can be written as

$$\sum_i \nu_i M_i = 0 \tag{3.34b}$$

where the ν_i are the stoichiometric coefficients and by convention are positive for the product species and negative for the reactant species.

Let an amount δn_a of M_a react with δn_b of M_b, etc., and produce δn_l of M_l, δn_m of M_m, etc. These amounts are in proportion:

$$\delta n_i = \nu_i \delta n \tag{3.35}$$

The change in Gibbs free energy of a mixture of ideal gases, at constant pressure and temperature, as the composition changes is given by

$$(\Delta G)_{p,\,T} = \sum_i \tilde{\mu}_i \delta n_i \tag{3.36}$$

where δn_i is the change in number of moles of species i and $\tilde{\mu}$ is the *chemical potential*. The chemical potential, an intensive property, is defined as

$$\tilde{\mu}_i = \left(\frac{\partial G}{\partial n_i}\right)_{p,\,T,\,n_j(j\neq i)} \tag{3.37}$$

It is equal in magnitude to the specific Gibbs free energy at a given temperature and pressure. For an ideal gas, it follows from Eqs. (B.13), (B.15) and (3.37) that

$$\tilde{\mu}_i = \tilde{\mu}_i^\circ(T) + \tilde{R}T \ln \frac{p_i}{p_0} \tag{3.38}$$

where $\tilde{\mu}_i^\circ$ equals $\tilde{g}_i^\circ$, the standard specific Gibbs free energy of formation. The standard state pressure p_0 is usually one atmosphere.

Substitution in Eq. (3.36) gives, at equilibrium,

$$\sum \left(\tilde{\mu}_i^\circ + \tilde{R}T \ln \frac{p_i}{p_0}\right)\delta n_i = 0$$

or

$$\sum \left(\tilde{\mu}_i^\circ + \tilde{R}T \ln \frac{p_i}{p_0}\right)\nu_i \delta n = 0$$

We can divide by δn and rearrange, to obtain

$$\sum \ln \left(\frac{p_i}{p_0}\right)^{\nu_i} = -\frac{(\sum \tilde{\mu}_i^\circ \nu_i)}{\tilde{R}T} = -\frac{\Delta G^\circ}{\tilde{R}T} = \ln K_p \tag{3.39}$$

K_p is the equilibrium constant at constant pressure:

$$K_p = \prod_i \left(\frac{p_i}{p_0}\right)^{\nu_i} \tag{3.40}$$

PETITIONER'S EXHIBIT 1002
US PATENT NO. 6,581,565
Page 1624

It is obtained from the Gibbs free energy of the reaction which can be calculated from the Gibbs free energy of formation of each species in the reaction, as indicated in Eq. (3.39) above. It is a function of temperature only.

In the JANAF tables,[8] to simplify the calculation of equilibrium constants, values of $\log_{10}(K_p)_i$, the equilibrium constants of formation of one mole of each species from their elements in their standard states, are tabulated against temperature. The equilibrium constant for a specific reaction is then obtained via the relation

$$\log_{10}(K_p)_{\text{reaction}} = \sum_i \nu_i \log_{10}(K_p)_i \tag{3.41}$$

With the JANAF table values of $(K_p)_i$, the pressures in Eqs. (3.40) and (3.41) must be in atmospheres.

The effect of pressure on the equilibrium composition can be deduced from Eq. (3.40). Substitution of the mole fractions $\tilde{x}_i$ and mixture pressure p gives

$$\prod_i \left(\frac{p_i}{p_0}\right)^{\nu_i} = \prod_i \left(\tilde{x}_i \frac{p}{p_0}\right)^{\nu_i} = \left(\frac{p}{p_0}\right)^{\sum_i \nu_i} \prod_i \tilde{x}_i^{\nu_i} = K_p$$

If $\sum_i \nu_i = 0$, changes in pressure have no effect on the composition. If $\sum_i \nu_i > 0$ (dissociation reactions), then the mole fractions of the dissociation products decrease as pressure increases. If $\sum_i \nu_i < 0$ (recombination reactions), the converse is true.

An equilibrium constant, K_c, based on concentrations (usually expressed in gram moles per cubic centimeter) is also used:

$$K_c = \prod_i [\mathrm{M}_i]^{\nu_i} \tag{3.42}$$

Equation (3.40) can be used to relate K_p and K_c:

$$K_p = K_c(\tilde{R}T)^{\sum_i \nu_i} \tag{3.43}$$

for $p_0 = 1$ atmosphere. For $\sum_i \nu_i = 0$, K_p and K_c are equal.

Example 3.4. A stoichiometric mixture of CO and O_2 in a closed vessel, initially at 1 atm and 300 K, is exploded. Calculate the composition of the products of combustion at 2500 K and the gas pressure.

The combustion equation is

$$\mathrm{CO} + \tfrac{1}{2}\mathrm{O_2} = \mathrm{CO_2}$$

The JANAF tables give $\log_{10} K_p$ (equilibrium constants of formation from the elements in their standard state) at 2500 K of CO_2, CO, and O_2 as 8.280, 6.840, and 0, respectively. Thus, the equilibrium constant for the CO combustion reaction above is, from Eq. (3.41),

$$\log_{10} K_p = 8.280 - 6.840 = 1.440$$

which gives $K_p = 27.5$.

PETITIONER'S EXHIBIT 1002
US PATENT NO. 6,581,565
Page 1625

If the degree of dissociation in the products is α (i.e., a fraction α of the CO_2 formed by complete combustion is dissociated), the product composition is

$$CO_2, (1-\alpha)\ ; \qquad CO, \alpha; \qquad O_2, \frac{\alpha}{2}$$

For this mixture, the number of moles of reactants n_R is $\frac{3}{2}$; the number of moles of products n_P is $(1 + \alpha/2)$.

The ideal gas law gives

$$p_R V = n_R \tilde{R} T_R \qquad p_P V = n_P \tilde{R} T_P$$

Thus

$$\frac{p_P}{n_P} = \frac{1}{1.5} \times \frac{2500}{300} = 5.555 \text{ atm/mol}$$

The equilibrium relation [Eq. (3.40)] gives

$$\frac{1-\alpha}{\alpha(\alpha/2)^{1/2}} \left(\frac{n_P}{p_P}\right)^{1/2} = 27.5$$

which can be solved to give $\alpha = 0.074$.

The composition of the products in mole fractions is, therefore,

$$x_{CO_2} = \frac{1-\alpha}{n_P} = 0.893$$

$$x_{CO} = \frac{\alpha}{n_P} = 0.071$$

$$x_{O_2} = \frac{\alpha/2}{n_P} = 0.037$$

The pressure of the product mixture is

$$p = 5.555 n_p = 5.76 \text{ atm}$$

Example 3.5. In fuel-rich combustion product mixtures, equilibrium between the species CO_2, H_2O, CO, and H_2 is often assumed to determine the burned gas composition. For $\phi = 1.2$, for C_8H_{18}–air combustion products, determine the mole fractions of the product species at 1700 K.

The reaction relating these species (often called the water gas reaction) is

$$CO_2 + H_2 = CO + H_2O$$

From the JANAF tables, $\log_{10} K_p$ of formation for these species at 1700 K are: CO_2, 12.180; H_2, 0; CO, 8.011; $H_2O(g)$, 4.699. The equilibrium constant for the above reaction is, from Eq. (3.41),

$$\log_{10} K_p = 8.011 + 4.699 - 12.180 = 0.530$$

from which $K_p = 3.388$.

The combustion reaction for C_8H_{18}–air with $\phi = 1.2$ can be written

$$C_8H_{18} + \frac{12.5}{1.2}(O_2 + 3.773N_2) \rightarrow aCO_2 + bH_2O + cCO + dH_2 + 39.30N_2$$

PETITIONER'S EXHIBIT 1002
US PATENT NO. 6,581,565
Page 1626

A carbon balance gives: $a + c = 8$

A hydrogen balance gives: $2b + 2d = 18$

An oxygen balance gives: $2a + b + c = 20.83$

The equilibrium relation gives $(bc)/(ad) = 3.388$ (since the equilibrated reaction has the same number of moles as there are reactants or products, the moles of each species can be substituted for the partial pressures).

These four equations can be solved to obtain

$$c^2 - 19.3c + 47.3 = 0$$

which gives $c = 2.89$, $a = 5.12$, $b = 7.72$, and $d = 1.29$. The total number of moles of products is

$$a + b + c + d + 39.3 = 56.3$$

and the mole fractions of the species in the burned gas mixture are

CO_2, 0.0908; H_2O, 0.137; CO, 0.051; H_2, 0.023; N_2, 0.698

Our development of the equilibrium relationship for one reaction has placed no restrictions on the occurrence of simultaneous equilibria. Consider a mixture of N reacting gases in equilibrium. If there are C chemical elements, conservation of elements will provide C equations which relate the concentrations of these N species. Any set of $(N - C)$ chemical reactions, each in equilibrium, which includes each species at least once will then provide the additional equations required to determine the concentration of each species in the mixture. Unfortunately, this complete set of equations is a coupled set of C linear and $(N - C)$ nonlinear equations which is difficult to solve for cases where $(N - C) > 2$. For complex systems such as this, the following approach to equilibrium composition calculations is now more widely used.

Standardized computer methods for the calculation of complex chemical equilibrium compositions have been developed. A generally available and well-documented example is the NASA program of this type.[14] The approach taken is to minimize explicitly the Gibbs free energy of the reacting mixture (at constant temperature and pressure) subject to the constraints of element mass conservation. The basic equations for the NASA program are the following.

If the stoichiometric coefficients a_{ij} are the number of kilomoles of element i per kilomole of species j, b_i^* is the number of kilomoles of element i per kilogram of mixture, and n_j is the number of kilomoles of species j per kilogram of mixture, element mass balance constraints are

$$\sum_{j=1}^{n} a_{ij} n_j - b_i^* = 0 \qquad \text{for } i = 1, 2, \ldots, l \tag{3.44}$$

The Gibbs free energy per kilogram of mixture is

$$g = \sum_{j=1}^{n} \tilde{\mu}_j n_j \tag{3.45}$$

PETITIONER'S EXHIBIT 1002
US PATENT NO. 6,581,565
Page 1627

For gases, the chemical potential $\tilde{\mu}_j$ is

$$\tilde{\mu}_j = \tilde{\mu}_j^\circ + \tilde{R}T \ln\left(\frac{n_j}{n}\right) + \tilde{R}T \ln p \tag{3.46}$$

where $\tilde{\mu}_j^\circ$ is the chemical potential in the standard state and p is the mixture pressure in atmospheres. Using the method of lagrangian multipliers, the term

$$G = g + \sum_{i=1}^{l} \lambda_i \sum_{j=1}^{n} (a_{ij} n_j - b_i^*)$$

is defined. The condition for equilibrium then becomes

$$\delta G = \sum_{j=1}^{n} \left(\mu_j + \sum_{i=1}^{l} \lambda_i a_{ij}\right)\delta n_j + \sum_{i=1}^{l} \sum_{j=1}^{n} (a_{ij} n_j - b_i^*)\delta\lambda_i = 0 \tag{3.47}$$

Treating the variations δn_j and $\delta\lambda_i$ as independent gives

$$\tilde{\mu}_j + \sum_{i=1}^{l} \lambda_i a_{ij} = 0 \qquad \text{for } j = 1, \ldots, n \tag{3.48}$$

and the original mass balance equation (3.44). Equations (3.44) and (3.48) permit the determination of equilibrium compositions for thermodynamic states specified by a temperature T and pressure p.

In the NASA program, the thermodynamic state may be specified by other pairs of state variables: enthalpy and pressure (useful for constant-pressure combustion processes); temperature and volume; internal energy and volume (useful for constant-volume combustion processes); entropy and pressure, and entropy and volume (useful for isentropic compressions and expansions). The equations required to obtain mixture composition are not all linear in the composition variables and an iteration procedure is generally required to obtain their solution. Once the composition is determined, additional relations, such as those in App. B which define the thermodynamic properties of gas mixtures, must then be used.

For each species, standard state enthalpies $\tilde{h}^\circ$ are obtained by combining standard enthalpies of formation at the datum temperature (298.15 K) $\Delta\tilde{h}_{f298}^\circ$ with sensible enthalpies $(\tilde{h}^\circ - \tilde{h}_{298}^\circ)$, i.e.,

$$\tilde{h}^\circ = \Delta\tilde{h}_{f298}^\circ + (\tilde{h}^\circ - \tilde{h}_{298}^\circ) \tag{3.49}$$

For the elements in their reference state, $\Delta\tilde{h}_{f298}^\circ$ is zero [the elements important in combustion are C (solid, graphite), $H_2(g)$, $O_2(g)$, $N_2(g)$].

For each species, the thermodynamic quantities specific heat, enthalpy, and entropy as functions of temperature are given in the form:

$$\frac{\tilde{c}_p^\circ}{\tilde{R}} = a_1 + a_2 T + a_3 T^2 + a_4 T^3 + a_5 T^4 \tag{3.50a}$$

$$\frac{\tilde{h}^\circ}{\tilde{R}T} = a_1 + \frac{a_2}{2} T + \frac{a_3}{3} T^2 + \frac{a_4}{4} T^3 + \frac{a_5}{5} T^4 + \frac{a_6}{T} \tag{3.50b}$$

PETITIONER'S EXHIBIT 1002
US PATENT NO. 6,581,565
Page 1628

$$\frac{\tilde{s}^\circ}{\tilde{R}} = a_1 \ln T + a_2 T + \frac{a_3}{2} T^2 + \frac{a_4}{3} T^3 + \frac{a_5}{4} T^4 + a_7 \qquad (3.50c)$$

The coefficients are obtained by least-squares matching with thermodynamic property data from the JANAF tables. Usually two sets of coefficients are included for two adjacent temperature intervals (in the NASA program these are 300 to 1000 K and 1000 to 5000 K) (see Sec. 4.7).

In some equilibrium programs, the species to be included in the mixture must be specified as an input to the calculation. In the NASA program, all allowable species are included in the calculation, though species may be specifically omitted from consideration.

For each reactant composition and pair of thermodynamic state variables, the program calculates and prints out the following:

1. *Thermodynamic mixture properties* (obtained from the equilibrium composition and the appropriate gas mixture rule; see App. B). p, T, ρ, h, s, M, $(\partial \ln V/\partial \ln p)_T$, $(\partial \ln V/\partial \ln T)_p$, c_p, γ_s, and a (sound speed)
2. *Equilibrium composition.* Mole fractions of each species (which are present in significant amounts), $\tilde{x}_i$

Figure 3-10 shows how the equilibrium composition of the products of combustion of isooctane-air mixtures at selected temperatures and 30 atm pressure varies with the equivalence ratio. At low temperatures, the products are N_2, CO_2, H_2O, and O_2 for lean mixtures and N_2, CO_2, H_2O, CO, and H_2 for rich mixtures. As temperature increases, the burned-gas mixture composition becomes much more complex with dissociation products such as OH, O, and H becoming significant.

Figure 3-11 shows adiabatic flame temperatures for typical engine conditions as a function of the equivalence ratio, obtained with the NASA program using the methodology of Sec. 3.5.4. The isooctane-air unburned mixture state was 700 K and 10 atm. Flame temperatures for adiabatic combustion at constant pressure (where p_R and H_R are specified) and at constant volume (where V_R and U_R are specified) are shown. Flame temperatures at constant volume are higher, because the final pressure is higher and dissociation is less. Maximum flame temperatures occur slightly rich of stoichiometric.

3.7.2 Chemical Reaction Rates

Whether a system is in chemical equilibrium depends on whether the time constants of the controlling chemical reactions are short compared with time scales over which the system conditions (temperature and pressure) change. Chemical processes in engines are often not in equilibrium. Important examples of nonequilibrium phenomena are the flame reaction zone where the fuel is oxidized, and the air-pollutant formation mechanisms. Such nonequilibrium processes are controlled by the rates at which the actual chemical reactions which convert

PETITIONER'S EXHIBIT 1002
US PATENT NO. 6,581,565
Page 1629

FIGURE 3-10
Mole fractions of equilibrium combustion products of isooctane-air mixtures as a function of fuel/air equivalence ratio at 30 atmospheres and (*a*) 1750 K; (*b*) 2250 K; and (*c*) 2750 K.

PETITIONER'S EXHIBIT 1002
US PATENT NO. 6,581,565
Page 1630

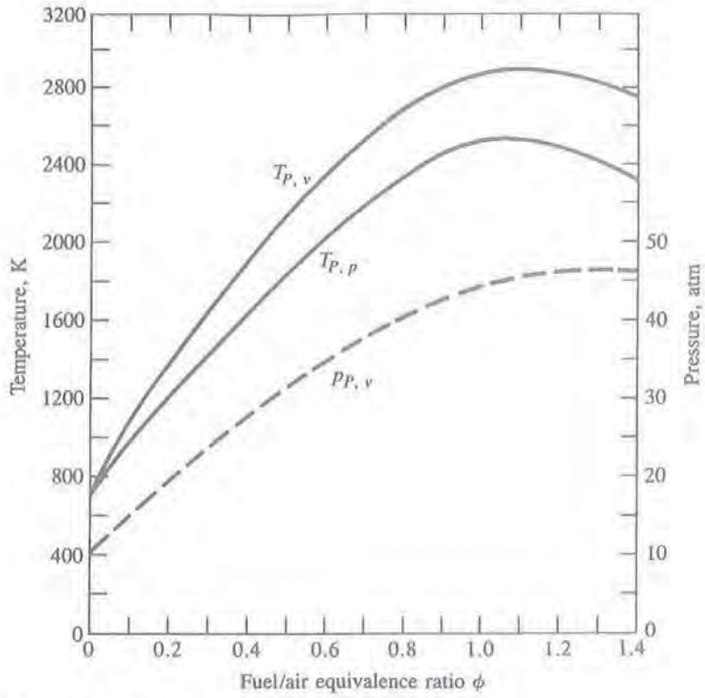


FIGURE 3-11
Equilibrium product temperatures for constant-volume ($T_{P,v}$) and constant-pressure ($T_{P,p}$) adiabatic combustion of isooctane-air mixture initially at 700 K and 10 atm, as a function of fuel/air equivalence ratio. Pressure ($p_{P,v}$) is equilibrium pressure for adiabatic constant-volume combustion.

reactants to products occur. The rates at which chemical reactions proceed depend on the concentration of the reactants, temperature, and whether any catalyst is present. This field is called chemical kinetics and some of its basic relations will now be reviewed.[2]

Most of the chemical reactions of interest in combustion are binary reactions, where two reactant molecules, M_a and M_b, with the capability of reacting together collide and form two product molecules, M_c and M_d; i.e.,

$$M_a + M_b = M_c + M_d \tag{3.51}$$

An important example of such a reaction is the rate-controlling step in the process by which the pollutant nitric oxide, NO, forms:

$$O + N_2 = NO + N$$

This is a second-order reaction since the stoichiometric coefficients of the reactants ν_a and ν_b are each unity and sum to 2. (The only first-order reactions are decomposition processes.) Third-order reactions are important in combustion, also. Examples are the recombination reactions by which radical species such as H, O, and OH combine during the final stage of the fuel oxidation process: e.g.,

$$H + H + M = H_2 + M^* \tag{3.52}$$

PETITIONER'S EXHIBIT 1002
US PATENT NO. 6,581,565
Page 1631

M is any molecule (such as N_2) which takes part in the collision and carries away the excess energy.

The law of mass action states that the rate at which product species are produced and the rate at which reactant species are removed is proportional to the product of the concentrations of reactant species, with the concentration of each species raised to the power of its stoichiometric coefficient ν_i. Thus, for reaction (3.51) above, the reaction rate R^+ in the forward (+) direction, reactants to products, is given by

$$R^+ = -\frac{d[M_a]^+}{dt} = \frac{d[M_c]^+}{dt} = k^+[M_a][M_b] \tag{3.53}$$

If the reaction can also proceed in the reverse (−) direction, then the backward rate R^- is given by

$$R^- = -\frac{d[M_c]^-}{dt} = \frac{d[M_a]^-}{dt} = k^-[M_c][M_d] \tag{3.54}$$

k^+ and k^- are the rate constants in the forward and reverse directions for this reaction. The *net rate* of production of products or removal of reactants is, therefore,

$$\begin{aligned} R^+ - R^- &= \frac{d[M_c]^+}{dt} + \frac{d[M_c]^-}{dt} = -\frac{d[M_a]^+}{dt} - \frac{d[M_a]^-}{dt} \\ &= k^+[M_a][M_b] - k^-[M_c][M_d] \end{aligned} \tag{3.55}$$

These results can be stated more generally as follows. Any reaction can be written as

$$\sum_{i=1}^{n} \nu_{R_i} M_{R_i} = \sum_{i=1}^{m} \nu_{P_i} M_{P_i} \tag{3.56}$$

where ν_i is the stoichiometric coefficient of species M_i, subscripts R and P denote reactants and products, respectively, and there are n reactant species and m product species. The forward reaction rate R^+ and the reverse reaction rate R^- are given by

$$\begin{aligned} R^+ &= k^+ \prod_{i=1}^{n} [M_{R_i}]^{\nu_{Ri}} \\ R^- &= k^- \prod_{i=1}^{m} [M_{P_i}]^{\nu_{Pi}} \end{aligned} \tag{3.57}$$

The net rate of removal of reactant species M_{R_i} is

$$-\frac{d[M_{R_i}]}{dt} = \nu_{R_i}(R^+ - R^-) \tag{3.58a}$$

PETITIONER'S EXHIBIT 1002
US PATENT NO. 6,581,565
Page 1632

and the net rate of production of product species M_{P_i} is

$$\frac{d[M_{P_i}]}{dt} = \nu_{P_i}(R^+ - R^-) \tag{3.58b}$$

The rate constants, k, usually follow the Arrhenius form:

$$k = A \exp\left(-\frac{E_A}{RT}\right) \tag{3.59}$$

where A is called the frequency or preexponential factor and may be a (moderate) function of temperature; E_A is the activation energy. The Boltzmann factor $\exp(-E_A/RT)$ defines the fraction of all collisions that have an energy greater than E_A—i.e., sufficient energy to make the reaction take place. The functional dependence of k on T and the constants in the Arrhenius form, Eq. (3.59), if that is appropriate, are determined experimentally.

At equilibrium, the forward and reverse reaction rates are equal. Then, from Eq. (3.55), with $R^+ - R^- = 0$:

$$\frac{k^+}{k^-} = \frac{[M_c][M_d]}{[M_a][M_b]} = K_c$$

where K_c is the equilibrium constant based on concentrations defined by Eq. (3.42). It can be related to K_p, the equilibrium constant based on partial pressures, by Eq. (3.43).

The chemical reaction mechanisms of importance in combustion are much more complex than the above illustrations of rate-controlled processes. Such mechanisms usually involve both parallel and sequential interdependent reactions. The methodology reviewed above still holds; however, one must sum algebraically the forward and reverse rates of all the reactions which produce (or remove) a species of interest. In such complex mechanisms it is often useful to assume that (some of) the reactive intermediate species or radicals are in *steady state*. That is, these radicals react so quickly once they are formed that their concentrations do not rise but are maintained in steady state with the species with which they react. The net rate at which their concentration changes with time is set equal to zero.

PROBLEMS

3.1. Isooctane is supplied to a four-cylinder spark-ignition engine at 2 g/s. Calculate the air flow rate for stoichiometric combustion. If the engine is operating at 1500 rev/min, estimate the mass of fuel and air entering each cylinder per cycle. The engine displaced volume is 2.4 liters. What is the volumetric efficiency?

3.2. Calculate the exhaust gas composition of a butane-fueled spark-ignition engine operating with equivalence ratio of 0.9. Assume the fuel is fully burned within the cylinder. Butane is C_4H_{10}.

PETITIONER'S EXHIBIT 1002
US PATENT NO. 6,581,565
Page 1633

3.3. The molar composition of dry exhaust gas of a propane-fueled SI engine is given below (water was removed before the measurement). Calculate the equivalence ratio.

$$CO_2 = 10.8\%, \quad O_2 = 4.5\%, \quad CO = 0\%, \quad H_2 = 0\%$$

3.4. Evaluate and compare the lower heating values per unit mass of stoichiometric mixture and per unit volume of stoichiometric mixture (at standard atmospheric conditions) for methane, isooctane, methyl alcohol, and hydrogen. Assume the fuel is fully vaporized.

3.5. The measured engine fuel flow rate is 0.4 g/s, air flow rate is 5.6 g/s, and exhaust gas composition (measured dry) is $CO_2 = 13.0\%$, $CO = 2.8\%$ with O_2 essentially zero. Unburned hydrocarbon emissions can be neglected. Compare the equivalence ratio calculated from the fuel and air flow with the equivalence ratio calculated from exhaust gas composition. The fuel is gasoline with a H/C ratio of 1.87. Assume a H_2 concentration equal to one-third the CO concentration.

3.6. The brake fuel conversion efficiency of an engine is 0.3. The mechanical efficiency is 0.8. The combustion efficiency is 0.94. The heat losses to the coolant and oil are 60 kW. The fuel chemical energy entering the engine per unit time, $\dot{m}_f Q_{HV}$, is 190 kW. What percentage of this energy becomes (*a*) brake work; (*b*) friction work; (*c*) heat losses; (*d*) exhaust chemical energy; (*e*) exhaust sensible energy.

3.7. An upper estimate can be made of the amount of NO formed in an engine from considering the equilibrium of the reaction $N_2 + O_2 = 2NO$. Calculate the NO concentration at equilibrium at 2500 K and 30 atm. $\log_{10} K_p = -1.2$ for this reaction at 2500 K. Assume N/O ratio in the combustion products is 15. N_2, O_2, and NO are the only species present.

3.8. Carbon monoxide reacts with air at 1 atm and 1000 K in an exhaust gas reactor. The mole fractions of the exhaust gas-air mixture flowing into the reactor are CO, 3%; O_2, 7%; N_2, 74%; CO_2, 6%; H_2O, 10%.

(*a*) Calculate the concentration of CO and O_2 in gram moles per cm^3 in the entering mixture.

(*b*) The rate of reaction is given by

$$d[CO]/dt = -4.3 \times 10^{11} \times [CO][O_2]^{0.25} \exp\,[-E/(RT)]$$

[ ] denotes concentration in gram moles per cm^3, $E/R = 20{,}000$ K. Calculate the initial reaction rate of CO, $d[CO]/dt$: time is in seconds.

(*c*) The equilibrium constant K_p for the reaction $CO + \frac{1}{2}O_2 = CO_2$ at 1000 K is 10^{10}. Find the equilibrium CO concentration.

(*d*) Determine the time to reach this equilibrium concentration of CO using the initial reaction rate. (The actual time will be longer but this calculation indicates approximately the time required.)

3.9. The exhaust gases of a hydrogen-fueled engine contain 22.3 percent H_2O, 7.44 percent O_2, and 70.2 percent N_2. At what equivalence ratio is it operating?

3.10. Gas is sampled at 1 atmosphere pressure from the exhaust manifold of an internal combustion engine and analyzed. The mole fractions of species in the exhaust are:

$$H_2O, 0.0468; \quad CO_2, 0.0585; \quad O_2, 0.123; \quad N_2, 0.772$$

Other species such as CO and unburned hydrocarbons can be neglected.

(*a*) The fuel is a synthetic fuel derived from coal containing only carbon and hydrogen. What is the ratio of hydrogen atoms to carbon atoms in the fuel?

PETITIONER'S EXHIBIT 1002
US PATENT NO. 6,581,565
Page 1634

(*b*) Calculate the fuel/air equivalence ratio at which this engine is operating.
(*c*) Is the internal combustion engine a conventional spark-ignition or a diesel engine? Explain.
(*d*) The engine has a displaced volume of 2 liters. Estimate approximately the percentage by which the fuel flow rate would be increased if this engine were operated at its maximum load at this same speed (2000 rev/min). Explain briefly what limits the equivalence ratio at maximum load.

3.11. The following are approximate values of the relative molecular mass (molecular weights): oxygen O_2, 32; nitrogen N_2, 28; hydrogen H_2, 2; carbon C, 12. Determine the stoichiometric fuel/air and air/fuel ratios on a mass basis, and the lower heating value per unit mass of stoichiometric mixture for the following fuels:

Methane (CH_4), isooctane (C_8H_{18}), benzene (C_6H_6), hydrogen (H_2), methyl alcohol (CH_3OH)

Heating values for these fuels are given in App. D.

3.12. Liquid petroleum gas (LPG) is used to fuel spark-ignition engines. A typical sample of the fuel consists of

70 percent by volume propane C_3H_8
5 percent by volume butane C_4H_{10}
25 percent by volume propene C_3H_6

The *higher heating values* of the fuels are: propane, 50.38 MJ/kg; butane, 49.56 MJ/kg; propylene (propene), 48.95 MJ/kg.
(*a*) Work out the overall combustion reaction for stoichiometric combustion of 1 mole of LPG with air, and the stoichiometric F/A and A/F.
(*b*) What are the higher and lower heating values for combustion of this fuel with excess air, per unit mass of LPG?

3.13. A spark-ignition engine is operated on isooctane fuel (C_8H_{18}). The exhaust gases are cooled, dried to remove water, and then analyzed for CO_2, CO, H_2, O_2. Using the overall combustion reaction for a range of equivalence ratios from 0.5 to 1.5, calculate the mole fractions of CO_2, CO, H_2, and O_2 in the dry exhaust gas, and plot the results as a function of equivalence ratio. Assume:
(*a*) that all the fuel is burnt inside the engine (almost true) and that the ratio of moles CO to moles H_2 in the exhaust is 3 : 1, and
(*b*) that there is no hydrogen in the exhaust for lean mixtures.
For high-power engine operation the air/fuel ratio is 14 : 1. What is the exhaust gas composition, in mole fractions, *before* the water is removed?

REFERENCES

1. Fristrom, R. M., and Westenberg, A. A.: *Flame Structure*, McGraw-Hill, 1965.
2. Glassman, I.: *Combustion*, Academic Press, 1977.
3. Kaye, G. W. C., and Laby, T. H.: *Tables of Physical and Chemical Constants*, Longmans, London, 1973.
4. Reynolds, W. C.: *Thermodynamic Properties in SI*, Department of Mechanical Engineering, Stanford University, 1979.
5. Taylor, C. F.: *The Internal Combustion Engine in Theory and Practice*, vol. 1, MIT Press, Cambridge, Mass., 1960.

PETITIONER'S EXHIBIT 1002
US PATENT NO. 6,581,565
Page 1635

6. Goodger, E. M.: *Hydrocarbon Fuels*, Macmillan, London, 1975.
7. Spalding, D. B., and Cole, E. H.: *Engineering Thermodynamics*, 3d ed., Edward Arnold, 1973.
8. *JANAF Thermochemical Tables*, National Bureau of Standards Publication NSRDS-NBS37, 1971.
9. Maxwell, J. B.: *Data Book on Hydrocarbons*, Van Nostrand, New York, 1950.
10. Rossini, F. D., Pitzer, K. S., Arnelt, R. L., Braun, R. M., and Primentel, G. C.: *Selected Values of Physical and Thermodynamic Properties of Hydrocarbons and Related Compounds*, Carnegie Press, Pittsburgh, Pa., 1953.
11. Stull, D. R., Westrum, E. F., and Sinke, G. C.: *The Chemical Thermodynamics of Organic Compounds*, John Wiley, New York, 1969.
12. Matthews, R. D.: "Relationship of Brake Power to Various Energy Efficiencies and Other Engine Parameters: The Efficiency Rule," *Int. J. of Vehicle Design*, vol. 4, no. 5, pp. 491–500, 1983.
13. Keenan, J. H.: *Thermodynamics*, John Wiley, New York, 1941 (MIT Press, Cambridge, Mass., 1970).
14. Svehla, R. A., and McBride, B. J.: "Fortran IV Computer Program for Calculation of Thermodynamic and Transport Properties of Complex Chemical Systems," NASA Technical Note TN D-7056, NASA Lewis Research Center, 1973.

PETITIONER'S EXHIBIT 1002
US PATENT NO. 6,581,565
Page 1636

CHAPTER 4

PROPERTIES OF WORKING FLUIDS

4.1 INTRODUCTION

The study of engine operation through an analysis of the processes that occur inside the engine has a long and productive history. The earliest attempts at this analysis used the constant-volume and constant-pressure ideal cycles as approximations to real engine processes (see Chap. 5). With the development of high-speed digital computers, the simulation of engine processes has become much more sophisticated and accurate (see Chap. 14). All these engine simulations (from the simplest to the most complex) require models for the composition and properties of the working fluids inside the engine, as well as models for the individual processes—induction, compression, combustion, expansion, and exhaust—that make up the engine operating cycle. This chapter deals with models for the working fluid composition, and thermodynamic and transport properties.

The composition of the working fluid, which changes during the engine operating cycle, is indicated in Table 4.1. The unburned mixture for a spark-ignition engine during intake and compression consists of air, fuel, and previously burned gases. It is, therefore, a mixture of N_2, O_2, CO_2, H_2O, CO, and H_2 for fuel-rich mixtures, and fuel (usually vapor). The composition of the unburned mixture does not change significantly during intake and compression. It is suffi-

PETITIONER'S EXHIBIT 1002
US PATENT NO. 6,581,565
Page 1637

TABLE 4.1
Working fluid constituents

Process	Spark-ignition engine	Compression-ignition engine
Intake	Air Fuel† Recycled exhaust‡ Residual gas§	Air Recycled exhaust‡ Residual gas§
Compression	Air Fuel vapor Recycled exhaust Residual gas	Air Recycled exhaust Residual gas
Expansion	Combustion products (mixture of N_2, H_2O, CO_2, CO, H_2, O_2, NO, OH, O, H, ...)	Combustion products (mixture of N_2, H_2O, CO_2, CO, H_2, O_2, NO, OH, O, H, ...)
Exhaust	Combustion products [mainly N_2, CO_2, H_2O, and either O_2 ($\phi < 1$) or CO and H_2 ($\phi > 1$)]	Combustion products (mainly N_2, CO_2, H_2O, and O_2)

† Liquid and vapor in the intake; mainly vapor within the cylinder.
‡ Sometimes used to control NO_x emissions (see Secs. 11.2, 15.3.2, and 15.5.1).
§ Within the cylinder.

ciently accurate to assume the composition is *frozen*. For the compression-ignition engine, the unburned mixture prior to injection contains no fuel; it consists of air and previously burned gas.

The combustion products or burned mixture gases, during the combustion process and much of the expansion process, are close to *thermodynamic equilibrium*. The composition of such mixtures has already been discussed (Sec. 3.7.1). As these combustion products cool, recombination occurs as indicated in Fig. 3-10. Towards the end of the expansion process, the gas composition departs from the equilibrium composition; recombination can no longer occur fast enough to maintain the reacting mixture in equilibrium. During the exhaust process, reactions are sufficiently slow so that for calculating thermodynamic properties the composition can be regarded as *frozen*.

The models used for predicting the thermodynamic properties of unburned and burned mixtures can be grouped into the five categories listed in Table 4.2. The first category is only useful for illustrative purposes since the specific heats of unburned and burned mixtures are significantly different. While the specific heats of the working fluids increase with increasing temperature in the range of interest, a constant-specific-heat model can be matched to the thermodynamic data over a limited temperature range. This approach provides a simple *analytic* model which can be useful when moderate accuracy of prediction will suffice. The appropriateness of frozen and equilibrium assumptions has already been discussed above. Approximations to thermodynamic equilibrium calculations are useful because of

PETITIONER'S EXHIBIT 1002
US PATENT NO. 6,581,565
Page 1638

TABLE 4.2
Categories of models for thermodynamic properties

	Unburned mixture	Burned mixture
1.	Single ideal gas throughout operating cycle with c_v (and hence c_p) constant	
2.	Ideal gas; $c_{v,u}$ constant	Ideal gas; $c_{v,b}$ constant
3.	Frozen mixture of ideal gases; $c_{v,i}(T)$	Frozen mixture of ideal gases; $c_{v,i}(T)$
4.	Frozen mixture of ideal gases; $c_{v,i}(T)$	Approximations fitted to equilibrium thermodynamic properties
5.	Frozen mixture of ideal gases; $c_{v,i}(T)$	Mixture of reacting ideal gases in thermodynamic equilibrium

Note: Subscripts i, u, and b denote species i in the gas mixture, the unburned mixture, and burned mixture properties, respectively.

the savings in computational time, relative to full equilibrium calculations, which can result from their use.

Values of thermodynamic properties of unburned and burned mixtures relevant to engine calculations are available from charts, tables, and algebraic relationships developed to match tabulated data. A selection of this material is included in this chapter and App. D. The references indicate additional sources.

4.2 UNBURNED MIXTURE COMPOSITION

The mass of charge trapped in the cylinder (m_c) is the inducted mass per cycle (m_i), plus the residual mass (m_r) left over from the previous cycle. The residual fraction (x_r) is

$$x_r = \frac{m_r}{m_c} \tag{4.1}$$

Typical residual fractions in spark-ignition engines range from 20 percent at light load to 7 percent at full load. In diesels, the residual fraction is smaller (a few percent) due to the higher compression ratio, and in naturally aspirated engines is approximately constant since the intake is unthrottled. If the inducted mixture is fuel and air (or air only), then the *burned gas fraction* (x_b) in the unburned mixture during compression equals the residual fraction.

In some engines, a fraction of the engine exhaust gases is recycled to the intake to dilute the fresh mixture for control of NO_x emissions (see Sec. 11.2). If

PETITIONER'S EXHIBIT 1002
US PATENT NO. 6,581,565
Page 1639

the percent of exhaust gas recycled (%EGR) is defined as the percent of the total intake mixture which is recycled exhaust,†

$$\text{EGR}(\%) = \left(\frac{m_{\text{EGR}}}{m_i}\right) \times 100 \tag{4.2}$$

where m_{EGR} is the mass of exhaust gas recycled, then the burned gas fraction in the fresh mixture is

$$x_b = \frac{m_{\text{EGR}} + m_r}{m_c} = \left(\frac{\text{EGR}}{100}\right)(1 - x_r) + x_r \tag{4.3}$$

Up to about 30 percent of the exhaust can be recycled; the burned gas fraction during compression can, therefore, approach 30 to 40 percent.

The composition of the burned gas fraction in the unburned mixture can be calculated as follows. The combustion equation for a hydrocarbon fuel of average molar H/C ratio y [e.g., Eq. (3.5)] can be written per mole O_2 as

$$\varepsilon\phi C + 2(1-\varepsilon)\phi H_2 + O_2 + \psi N_2 \rightarrow n_{CO_2}CO_2 + n_{H_2O}H_2O + n_{CO}CO + n_{H_2}H_2 + n_{O_2}O_2 + n_{N_2}N_2 \tag{4.4}$$

where ψ = the molar N/O ratio (3.773 for air)

$$\varepsilon = \frac{4}{4 + y}$$

y = the molar H/C ratio of the fuel
ϕ = fuel/air equivalence ratio
n_i = moles of species i per mole O_2 reactant

The n_i are determined using the following assumptions:

1. For lean and stoichiometric mixtures ($\phi \leq 1$) CO and H_2 can be neglected.
2. For rich and stoichiometric mixtures ($\phi \geq 1$) O_2 can be neglected.
3. For rich mixtures, either (*a*) the water gas reaction

$$CO_2 + H_2 = CO + H_2O$$

---

† An alternative definition of percent EGR is also used based on the ratio of EGR to fresh mixture (fuel and air):

$$\text{EGR}^*(\%) = \left(\frac{m_{\text{EGR}}}{m_a + m_f}\right) \times 100$$

The two definitions are related by

$$\frac{\text{EGR}^*}{100} = \frac{\text{EGR}}{100 - \text{EGR}} \quad \text{and} \quad \frac{\text{EGR}}{100} = \frac{\text{EGR}^*}{100 + \text{EGR}^*}$$

PETITIONER'S EXHIBIT 1002
US PATENT NO. 6,581,565
Page 1640

can be assumed to be in equilibrium with the equilibrium constant $K(T)$:

$$K(T) = \frac{n_{H_2O} n_{CO}}{n_{CO_2} n_{H_2}}$$

where $K(T)$ can be determined from a curve fit to JANAF table data:[8]

$$\ln K(T) = 2.743 - \frac{1.761 \times 10^3}{T} - \frac{1.611 \times 10^6}{T^2} + \frac{0.2803 \times 10^9}{T^3} \qquad (4.5)$$

where T is in K, or (*b*) K can be assumed constant over the normal engine operating range. A value of 3.5 is often assumed (see Sec. 4.9), which corresponds to evaluating the equilibrium constant at 1740 K.

The n_i obtained from an element balance and the above assumptions are shown in Table 4.3. The value of c is obtained by solving the quadratic:

$$(K-1)c^2 - c\{K[2(\phi - 1) + \varepsilon\phi] + 2(1 - \varepsilon\phi)\} + 2K\varepsilon\phi(\phi - 1) = 0 \qquad (4.6)$$

The mole fractions are given by

$$\tilde{x}_i = \frac{n_i}{n_b}$$

where $n_b = \sum_i n_i$ is given in the bottom line of Table 4.3.

While Eq. (4.4) is for a fuel containing C and H only, it can readily be modified for alcohols or alcohol-hydrocarbon blends. For a fuel of molar composition $CH_y O_z$, the reactant mixture

$$CH_y O_z + \frac{1}{\phi}\left(1 + \frac{y}{4} - \frac{z}{2}\right)(O_2 + \psi N_2)$$

can be rearranged per mole of O_2 reactant as

$$\zeta\phi\varepsilon C + 2\zeta\phi(1 - \varepsilon)H_2 + O_2 + \left(1 - \frac{\varepsilon z}{2}\right)\zeta\psi N_2 \qquad (4.7a)$$

TABLE 4.3
Burned gas composition under 1700 K

	n_i, moles/mole O_2 reactant	
Species	$\phi \le 1$	$\phi > 1$†
CO_2	$\varepsilon\phi$	$\varepsilon\phi - c$
H_2O	$2(1 - \varepsilon)\phi$	$2(1 - \varepsilon\phi) + c$
CO	0	c
H_2	0	$2(\phi - 1) - c$
O_2	$1 - \phi$	0
N_2	ψ	ψ
Sum: n_b	$(1 - \varepsilon)\phi + 1 + \psi$	$(2 - \varepsilon)\phi + \psi$

† c defined by Eq. (4.6).

PETITIONER'S EXHIBIT 1002
US PATENT NO. 6,581,565
Page 1641

where

$$\zeta = \frac{2}{2 - \varepsilon z(1 - \phi)} \tag{4.7b}$$

If we write

$$\phi^* = \zeta\phi \qquad \text{and} \qquad \psi^* = \left(1 - \frac{\varepsilon z}{2}\right)\zeta\psi \tag{4.7c}$$

the reactant expression (4.7*a*) becomes

$$\phi^*\varepsilon C + 2\phi^*(1 - \varepsilon)H_2 + O_2 + \psi^* N_2$$

which is identical in form to the reactant expression for a hydrocarbon fuel (4.4). Thus Table 4.3 can still be used to give the composition of the burned gas residual fraction in the unburned mixture, except that ϕ^* replaces ϕ and ψ^* replaces ψ in the expressions for n_i.

Now consider the unburned mixture. The number of moles of fuel per mole O_2 in the mixture depends on the molecular weight of the fuel, M_f. If the average molecular formula of the fuel is $(CH_y)_\alpha$ then

$$M_f = \alpha(12 + y)$$

The fresh fuel-air mixture (not yet diluted with EGR or residual),

$$\varepsilon\phi C + 2(1 - \varepsilon)\phi H_2 + O_2 + \psi N_2$$

then becomes

$$\frac{4}{M_f}(1 + 2\varepsilon)\phi(CH_y)_\alpha + O_2 + \psi N_2$$

The unburned mixture (fuel, air, and a burned gas fraction), per mole O_2 in the mixture, can be written:

$$(1 - x_b)\left[\frac{4}{M_f}(1 + 2\varepsilon)\phi(CH_y)_\alpha + O_2 + \psi N_2\right] + x_b(n_{CO_2} + n_{H_2O} + n_{CO} + n_{H_2} + n_{O_2} + n_{N_2})$$

The number of moles of each species in the unburned mixture, per mole O_2, is summarized in Table 4.4. The mole fractions of each species are obtained by dividing by the total number of moles of unburned mixture n_u,

$$n_u = (1 - x_b)\left[\frac{4(1 + 2\varepsilon)\phi}{M_f} + 1 + \psi\right] + x_b n_b \tag{4.8}$$

where n_b is given in Table 4.3.

The molecular weights of the (low-temperature) burned and unburned

PETITIONER'S EXHIBIT 1002
US PATENT NO. 6,581,565
Page 1642

TABLE 4.4
Unburned mixture composition

	n_i, moles/mole O_2 reactant	
Species	$\phi \leq 1$	$\phi > 1$
Fuel	$4(1 - x_b)(1 + 2\varepsilon)\phi/M_f$	
O_2	$1 - x_b\phi$	$1 - x_b$
N_2	ψ	ψ
CO_2	$x_b\varepsilon\phi$	$x_b(\varepsilon\phi - c)$
H_2O	$2x_b(1 - \varepsilon)\phi$	$x_b[2(1 - \varepsilon\phi) + c]$
CO	0	$x_b c$
H_2	0	$x_b[2(\phi - 1) - c]$
Sum†	n_u	n_u

† Given by Eq. (4.8).

mixture can now be determined. The mass of mixture (burned or unburned) per mole O_2 in the mixture, m_{RP}, is given by

$$m_{RP} = 32 + 4\phi(1 + 2\varepsilon) + 28.16\psi \tag{4.9}$$

The molecular weight of the burned mixture, M_b, is therefore

$$M_b = \frac{m_{RP}}{n_b} \tag{4.10}$$

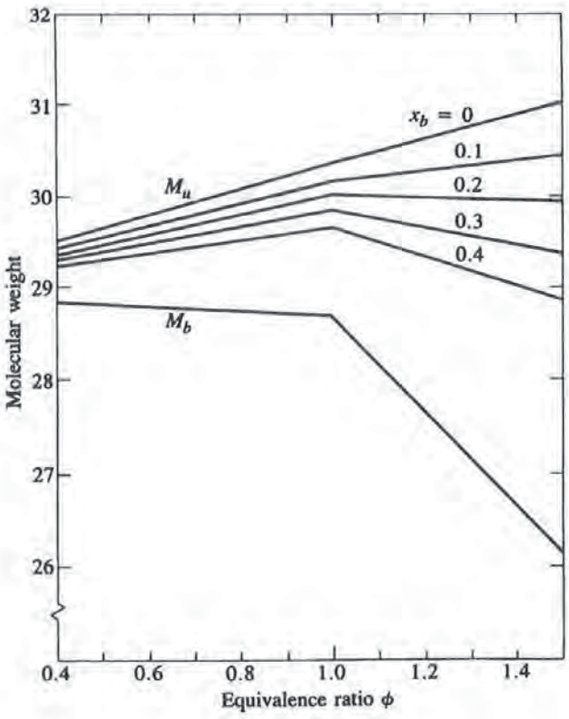


FIGURE 4-1
Molecular weight of unburned and low-temperature burned isooctane-air mixtures as a function of fuel/air equivalence ratio and burned gas fraction.

PETITIONER'S EXHIBIT 1002
US PATENT NO. 6,581,565
Page 1643

TABLE 4.5
Factors for relating properties on molar and mass basis

Quantity, per mole O_2 in the mixture	General equation‡		Equation for C_8H_{18}-air mixtures
Moles of burned mixture n_b	$n_b = (1-\varepsilon)\phi + 1 + \psi,$ $n_b = (2-\varepsilon)\phi + \psi,$	$\phi \le 1$ $\phi > 1$	$n_b = 0.36\phi + 4.773$ $n_b = 1.36\phi + 3.773$
Moles of unburned mixture n_u	$(1-x_b)\left[\frac{4(1+2\varepsilon)\phi}{M_f} + 1 + \psi\right] + x_b n_b$	$\begin{cases}\phi \le 1\\ \phi > 1\end{cases}$	$n_u = 0.08\phi + 4.773 + 0.28x_b\phi$ $n_u = 0.08\phi + 4.773 + x_b(1.28\phi - 1)$
Mass of mixture† (burned or unburned)	$m_{RP} = 32 + 4\phi(1+2\varepsilon) + 28.16\psi$		$138.2 + 9.12\phi$
Mass of air†	$32 + 28.16\psi$		138.2

† Units: kg/kmol or lbm/lb · mol.

‡ For hydrocarbon fuels, ψ for air = 3.773; for fuels containing oxygen, ϕ^* and ψ^* given by Eq. (4.7c) are substituted for ϕ and ψ, respectively.

The molecular weight of the unburned mixture, M_u, is

$$M_u = \frac{m_{RP}}{n_u} \tag{4.11}$$

Figure 4-1 gives M_u and M_b for a range of ϕ and x_b for air, isooctane, burned gas mixtures.

Frequently, thermodynamic properties of unburned and burned mixtures are expressed per unit mass of *air* in the *original* mixture (for burned mixture this is the mixture before combustion). To obtain properties in these units, we need the mass of original air, per mole O_2 in the mixture, which is

$$(32 + 28.16\ \psi)$$

with units of kilograms per kilomole or pound-mass per pound-mole.

Table 4.5 summarizes the factors needed to relate properties expressed on a molar and a mass basis.

4.3 GAS PROPERTY RELATIONSHIPS

The individual species in the unburned and burned gas mixtures can with sufficient accuracy be modeled as ideal gases. Ideal gas relationships are reviewed in App. B. The most important relationships for property determination for engine calculations are summarized below.

PETITIONER'S EXHIBIT 1002
US PATENT NO. 6,581,565
Page 1644

Since internal energy and enthalpy are functions of temperature only, the specific heats at constant volume and constant pressure are given by

$$c_v = \left(\frac{\partial u}{\partial T}\right)_v = \frac{du}{dT} = c_v(T) \tag{4.12a}$$

$$c_p = \left(\frac{\partial h}{\partial T}\right)_p = \frac{dh}{dT} = c_p(T) \tag{4.12b}$$

and

$$u - u_0 = \int_{T_0}^{T} c_v\, dT \tag{4.13a}$$

$$h - h_0 = \int_{T_0}^{T} c_p\, dT \tag{4.13b}$$

The entropy $s(T, v)$ or $s(T, p)$ is given by

$$s - s_0 = \int_{T_0}^{T} c_v \frac{dT}{T} + R \ln \frac{v}{v_0} \tag{4.14a}$$

$$s - s_0 = \int_{T_0}^{T} c_p \frac{dT}{T} - R \ln \frac{p}{p_0} \tag{4.14b}$$

The integrals in Eqs. (4.14*a*, *b*) are functions of temperature only, and are useful in evaluating entropy changes and in following isentropic processes. If we define

$$\Psi(T) = \int_{T_0}^{T} c_v(T) \frac{dT}{T} \tag{4.15a}$$

and

$$\Phi(T) = \int_{T_0}^{T} c_p(T) \frac{dT}{T} \tag{4.15b}$$

then

$$s - s_0 = \Psi + R \ln \left(\frac{v}{v_0}\right) \tag{4.16a}$$

$$s - s_0 = \Phi - R \ln \left(\frac{p}{p_0}\right) \tag{4.16b}$$

Thus, for example, the entropy change between states (T_1, p_1) and (T_2, p_2) is

$$s_2 - s_1 = \Phi_2 - \Phi_1 - R \ln \left(\frac{p_2}{p_1}\right) \tag{4.17}$$

For an isentropic process,

$$\ln \left(\frac{p_2}{p_1}\right) = \frac{\Phi_2 - \Phi_1}{R} \tag{4.18}$$

PETITIONER'S EXHIBIT 1002
US PATENT NO. 6,581,565
Page 1645

In these equations, the units of u and h can be on a per unit mass or molar basis [i.e., joules per kilogram (British thermal units per pound-mass) or joules per kilomole (British thermal units per pound-mole)]; similarly, s, c_v, c_p, R, Ψ, and Φ can be in joules per kilogram-kelvin (British thermal units per pound-mass-degree Rankine) or joules per kilomole-kelvin (British thermal units per pound-mole-degree Rankine).

For gas mixtures, once the composition is known, mixture properties are determined either on a mass or molar basis from

$$u = \sum x_i u_i \qquad \tilde{u} = \sum \tilde{x}_i \tilde{u}_i \tag{4.19a}$$

$$h = \sum x_i h_i \qquad \tilde{h} = \sum \tilde{x}_i \tilde{h}_i \tag{4.19b}$$

$$s = \sum x_i s_i \qquad \tilde{s} = \sum \tilde{x}_i \tilde{s}_i \tag{4.19c}$$

and

$$c_v = \sum x_i c_{v,i} \qquad \tilde{c}_v = \sum \tilde{x}_i \tilde{c}_{v,i} \tag{4.20a}$$

$$c_p = \sum x_i c_{p,i} \qquad \tilde{c}_p = \sum \tilde{x}_i \tilde{c}_{p,i} \tag{4.20b}$$

4.4 A SIMPLE ANALYTIC IDEAL GAS MODEL

While the first category of model listed in Table 4.2 is too inaccurate for other than illustrative purposes, the second category—constant but different specific heats for the unburned and burned gas mixtures—can with careful choice of specific heat values be made much more precise. The advantages of a simple analytic model may be important for certain problems.

Figure 4-2 shows an internal energy versus temperature plot for a stoichiometric mixture. It is a quantitative version of Fig. 3-5. The unburned mixture line is for a burned gas fraction of 0.1. The fuel is isooctane. Data to construct such graphs can be obtained from charts or tables or computer programs (see Secs. 4.5 to 4.7). The units for u are kilojoules per kilogram of air in the original mixture (the units of the charts in Sec. 4.5). The datum is zero enthalpy for O_2, N_2, H_2, and C (solid) at 298 K. Note that the specific heats of the unburned and burned mixtures (the slopes of the lines in Fig. 4-2) are a function of temperature; at high temperatures, the internal energy of the burned mixture is a function of temperature and pressure.

However, the temperature range of interest for the unburned mixture in an SI engine is 400 to 900 K (700 to 1600°R); for the burned gas mixture, the extreme end states are approximately 2800 K, 35 atm (5000°R, 500 lb/in^2 abs) and 1200 K, 2 atm (2200°R, 30 lb/in^2 abs). Linear approximations to the unburned and burned mixture curves which minimize the error in u over the temperature (and pressure) ranges of interest are shown as dashed lines. The error in T for a given u is less than 50 K.

PETITIONER'S EXHIBIT 1002
US PATENT NO. 6,581,565
Page 1646

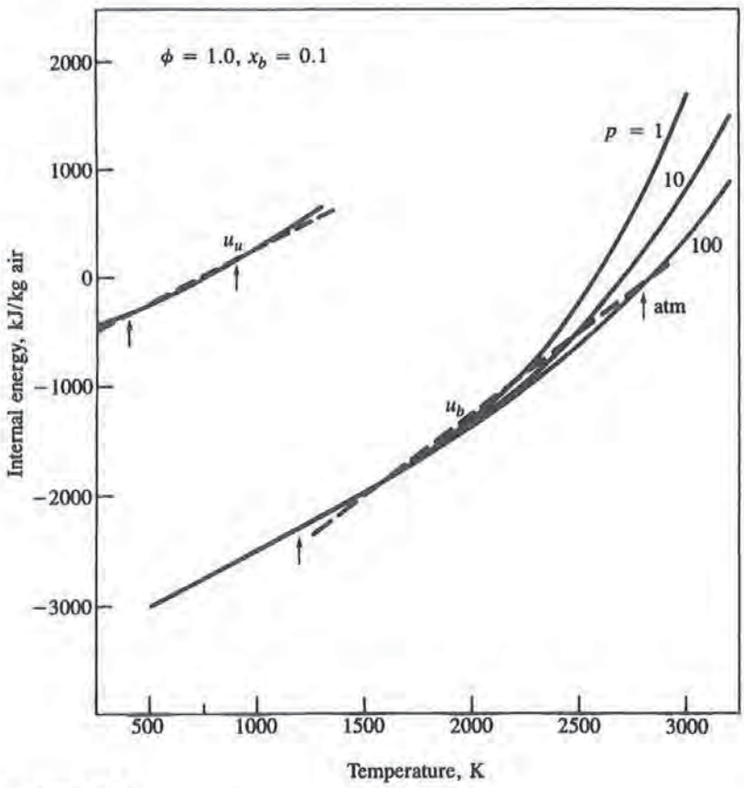


FIGURE 4-2
Internal energy versus temperature plot for stoichiometric unburned and burned gas mixtures: iso-octane fuel; unburned residual fraction 0.1.

The basis for this ideal gas model is

$$u_u = c_{v,u} T_u + h_{f,u} \qquad h_u = c_{p,u} T_u + h_{f,u} \tag{4.21a, b}$$

$$u_b = c_{v,b} T_b + h_{f,b} \qquad h_b = c_{p,b} T_b + h_{f,b} \tag{4.22a, b}$$

where $h_{f,u}$ and $h_{f,b}$ are the enthalpies of formation of unburned and burned gas mixture, respectively, at 0 K.

Then, for a constant-volume adiabatic combustion process,

$$u_u = u_b$$

or

$$c_{v,u} T_u + h_{f,u} = c_{v,b} T_b + h_{f,b}$$

If we solve for T_b and use the relations $(R_b/R_u) = (M_u/M_b)$ and $c_v/R = 1/(\gamma - 1)$, we obtain

$$T_b = (\gamma_b - 1)\left(\frac{M_b}{M_u}\right)\left(\frac{T_u}{\gamma_u - 1} + \frac{\Delta h_f}{R_u}\right) \tag{4.23}$$

where $\Delta h_f = h_{f,u} - h_{f,b}$.

For a constant-pressure adiabatic combustion process,

$$h_u = h_b$$

and it can similarly be shown that

$$T_b = \frac{\gamma_b - 1}{\gamma_b}\left(\frac{M_b}{M_u}\right)\left(\frac{\gamma_u}{\gamma_u - 1}\,T_u + \frac{\Delta h_f}{R_u}\right) \tag{4.24}$$

To use the model, suitable values of γ_u, γ_b, M_u, (M_b/M_u), and $\Delta h_f/R_u$ must be determined. Values for M_u and M_b can be obtained from Eqs. (4.10) and (4.11).† Values of γ_u, γ_b, and $\Delta h_f/R_u$ can be obtained from graphs such as Fig. 4-2 (see Example 4.1 below). Values for γ_u, γ_b, and $\Delta h_f/R_u$ are available in the literature (e.g., Refs. 1 and 2) for a range of ϕ and x_b. However, values used for computations should always be checked over the temperature range of interest, to ensure that the particular linear fit to $u(T)$ used is appropriate.

Example 4.1. Determine the values of γ_u, γ_b, and $\Delta h_f/R_u$ which correspond to the straight-line fits for $u_u(T)$ and $u_b(T)$ in Fig. 4-2.

Equations for the straight lines in Fig. 4-2 are

$$u_u \text{ (kJ/kg air)} = 0.96T(\text{K}) - 700$$

and

$$u_b \text{ (kJ/kg air)} = 1.5T(\text{K}) - 4250$$

From Table 4.5, for isooctane fuel with $\phi = 1.0$ and $x_b = 0.1$, the number of moles of unburned mixture per mole O_2 in the mixture is

$$n_u = 0.08 \times 1 + 4.773 + 0.28 \times 0.1 \times 1 = 4.881$$

The mass of air per mole O_2 in the mixture is 138.2. Thus, the number of moles of unburned mixture per unit mass of air in the original mixture is

$$\frac{4.881}{138.2} = 0.0353$$

The molar specific heat of the unburned mixture $\tilde{c}_{v,u}$ is therefore

$$\tilde{c}_{v,u} = \frac{0.96}{0.0353} = 27.2 \text{ kJ/kmol} \cdot \text{K}$$

Since $\tilde{R} = 8.314$ kJ/kmol · K,

$$\gamma_u = \frac{27.2 + 8.314}{27.2} = 1.31$$

The number of moles of burned mixture per mole O_2 is (from Table 4.5)

$$n_b = 0.36 \times 1 + 4.773 = 5.133$$

† The error in ignoring the effect of dissociation on M_b is small.

PETITIONER'S EXHIBIT 1002
US PATENT NO. 6,581,565
Page 1648

The number of moles of burned mixture per unit mass of air in the original mixture is

$$\frac{5.133}{138.2} = 0.0371$$

The molar specific heat $\tilde{c}_{v,b}$ is therefore

$$\tilde{c}_{v,b} = \frac{1.5}{0.0371} = 40.4 \text{ kJ/kmol} \cdot \text{K}$$

and γ_b is

$$\gamma_b = \frac{40.4 + 8.314}{40.4} = 1.21$$

To find $\Delta h_f/R_u$, R_u is given by

$$R_u = 8.314 \times 0.0353 = 0.293 \text{ kJ/kg air} \cdot \text{K}$$

and so

$$\frac{\Delta h_f}{R_u} = \frac{(-700) - (-4250)}{0.293} = 1.2 \times 10^4 \text{ K}$$

4.5 THERMODYNAMIC CHARTS

One method of presenting thermodynamic properties of unburned and burned gas mixtures for internal combustion engine calculations is on charts. Two sets of charts are in common use: those developed by Hottel *et al.*[3] and those developed by Newhall and Starkman.[4, 5] Both these sets of charts use U.S. units. We have developed a new set of charts in SI units, following the approach of Newhall and Starkman. Charts are no longer used extensively for engine cycle calculations; computer models for the thermodynamic properties of working fluids have replaced the charts. Nonetheless, charts are useful for illustrative purposes, and afford an easy and accurate method where a limited number of calculations are required. The charts presented below are for isooctane fuel, and the following equivalence ratios: $\phi = 0.4, 0.6, 0.8, 1.0, 1.2$.

4.5.1 Unburned Mixture Charts

The thermodynamic properties of each unburned fuel-air mixture are represented by two charts. The first chart is designed to relate the mixture temperature, pressure, and volume at the beginning and at the end of the compression process; the second gives the mixture internal energy and enthalpy as functions of temperature.

The following assumptions are made:

1. The compression process is reversible and adiabatic.

PETITIONER'S EXHIBIT 1002
US PATENT NO. 6,581,565
Page 1649

TABLE 4.6
Unburned mixture composition for charts

Equivalence ratio ϕ	(F/A)	Kilograms of mixture per kilogram of air	Moles of mixture per mole of O_2	Kilomole of mixture per kilogram of air	$n_u \bar{R}$,† J/kg air · K
0.4	0.0264	1.0264	$4.805 + 0.112x_b$	$0.0348 + 0.00081x_b$	289
0.6	0.0396	1.0396	$4.821 + 0.168x_b$	$0.0349 + 0.00122x_b$	290
0.8	0.0528	1.0528	$4.837 + 0.224x_b$	$0.0350 + 0.00162x_b$	291
1.0	0.0661	1.0661	$4.853 + 0.280x_b$	$0.0351 + 0.00203x_b$	292
1.2	0.0792	1.0792	$4.869 + 0.536x_b$	$0.0352 + 0.00388x_b$	292

† For $x_b = 0$. Error in neglecting x_b is usually small.

2. The fuel is in the vapor phase.
3. The mixture composition is homogeneous and frozen (no reactions between the fuel and air).
4. Each species in the mixture can be modeled as an ideal gas.
5. The burned gas fraction is zero.†

It proves convenient to assign zero internal energy or enthalpy to the unburned mixture at 298.15 K. Internal energy and enthalpies relative to this datum are called *sensible internal energy* u_s *or sensible enthalpy* h_s. By sensible we mean changes in u or h which result from changes in temperature alone, and we exclude changes due to chemical reaction or phase change.

Table 4.6 provides the basic composition data for the unburned mixture charts. Equations (4.13*a*, *b*) provide the basis for obtaining the $u_{s,u}(T)$ and $h_{s,u}(T)$ curves shown in Fig. 4-3.

Equations (4.15) and (4.16) provide the basis for following a reversible adiabatic (i.e., isentropic) compression process. Between end states 1 and 2, we obtain, per kilogram of air in the mixture,

$$\Psi(T_2) = \Psi(T_1) - n_u \bar{R} \ln\left(\frac{v_2}{v_1}\right) \tag{4.25a}$$

$$\Phi(T_2) = \Phi(T_1) + n_u \bar{R} \ln\left(\frac{p_2}{p_1}\right) \tag{4.25b}$$

where n_u is the number of moles of unburned mixture per kilogram of air. Values

† This assumption introduces negligible error into calculations of the compression process for mixtures with normal burned gas fractions, since the major constituent of the residual is N_2. The burned gas fraction must, however, be included when the unburned mixture properties are related to burned mixture properties in a combustion process.

PETITIONER'S EXHIBIT 1002
US PATENT NO. 6,581,565
Page 1650

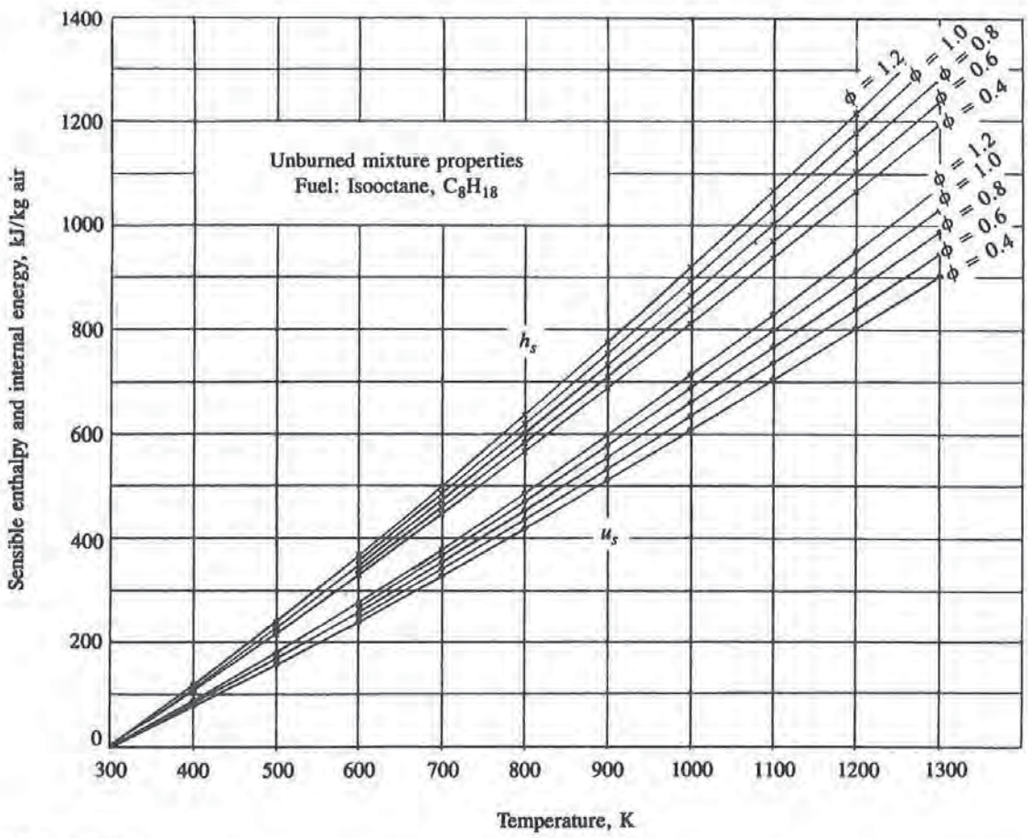


FIGURE 4-3
Sensible enthalpy and internal energy of unburned isooctane-air mixtures as function of temperature. Units: kJ/kg air in mixture.

of n_u and $n_u \tilde{R}$ are given in Table 4.6. $\Psi(T)$ and $\Phi(T)$ are given in Fig. 4-4. Note that v, p, and T are related by

$$p(\text{Pa})v(\text{m}^3/\text{kg air}) = n_u\tilde{R}(\text{J/kg air} \cdot \text{K})T(\text{K}) \tag{4.26}$$

Example 4.2. The compression process in an internal combustion engine can be modeled approximately as adiabatic and reversible (i.e., as an isentropic process). A spark-ignition engine with a compression ratio of 8 operates with a stochiometric fuel vapor–air mixture which is at 350 K and 1 atm at the start of the compression stroke. Find the temperature, pressure, and volume per unit mass of air at the end of the compression stroke. Calculate the compression stroke work.

Given $T_1 = 350$ K at the start of compression, find T_2 at the end of compression using the isentropic compression chart, Fig. 4-4, and Eq. (4.25*a*). For $T_1 = 350$ K, $\Psi_1 = 150$ J/kg air · K. From Eq. (4.25*a*),

$$\Psi_2(T_2) = \Psi_1(T_1) - n_u\tilde{R} \ln\left(\frac{v_2}{v_1}\right) = 150 - 292 \ln\left(\frac{1}{8}\right) = 757 \text{ J/kg air} \cdot \text{K}$$

PETITIONER'S EXHIBIT 1002
US PATENT NO. 6,581,565
Page 1651

Figure 4-4 then gives

$$T_2 = 682 \text{ K}$$

The ideal gas law [Eq. (4.26)] gives

$$v_1 = \frac{292 \times 350}{1 \times 1.013 \times 10^5} = 1.0 \text{ m}^3/\text{kg air}$$

and

$$p_2 = p_1\left(\frac{T_2}{T_1}\right)\left(\frac{v_1}{v_2}\right) = \frac{682}{350} \times 8 = 15.5 \text{ atm}$$

$$v_2 = \frac{1.0}{8} = 0.125 \text{ m}^3/\text{kg air}$$

Note that p_2 can also be obtained from Fig. 4-4 and Eq. (4.25*b*):

$$\ln\left(\frac{p_2}{p_1}\right) = \frac{\Phi_2 - \Phi_1}{n_u \tilde{R}} = \frac{980 - 180}{292} = 2.74$$

$$p_2 = 15.5 \text{ atm} = 1.57 \text{ MPa}$$

The compression stroke work, assuming the process is adiabatic and using the data in Fig. 4-3, is

$$-W_{1-2} = u_s(T_2) - u_s(T_1) = 350 - 40 = 310 \text{ kJ/kg air}$$

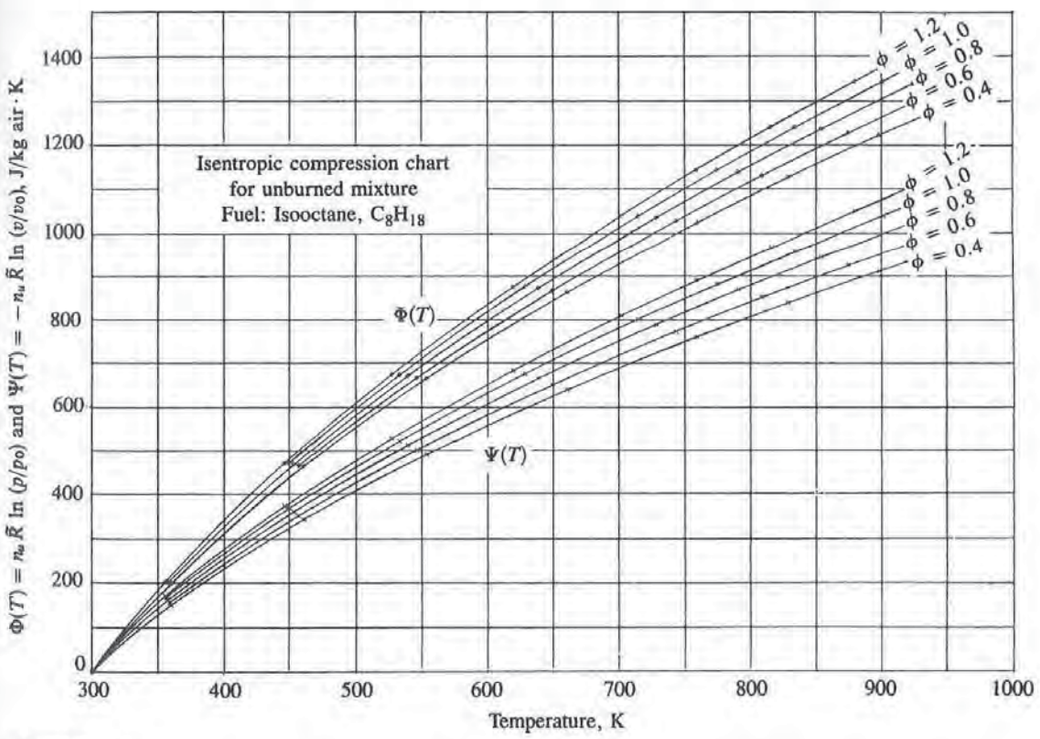


FIGURE 4-4
Isentropic compression functions, Φ and Ψ, as function of temperature for unburned isooctane-air mixtures. Units: J/kg air · K.

PETITIONER'S EXHIBIT 1002
US PATENT NO. 6,581,565
Page 1652

4.5.2 Burned Mixture Charts

The primary burned mixture charts are for the products of combustion at high temperatures, i.e., for the working fluid during the expansion process. The following assumptions are made:

1. Each species in the mixture can be modeled as an ideal gas.
2. The mixture is in thermodynamic equilibrium at temperatures above 1700 K; the mixture composition is frozen below 1700 K.
3. *Datum.* At the datum state of 298.15 K (25°C or 77°F) and 1 atm the chemical elements in their naturally occurring form (N_2, O_2, H_2 as diatomic gases and C as solid graphite) are assigned zero enthalpy and entropy.

The charts were prepared with the NASA equilibrium program described in Sec. 3.7.[9,10] The C/H/O/N ratio of the mixture is specified for each chart. The extensive properties (internal energy, enthalpy, entropy, and specific volume) are all expressed per unit mass of air in the original mixture; i.e., they correspond to the combustion of 1 kg of air with the appropriate mass of fuel. The mass basis for the unburned and burned mixture charts are the same.

Figures 4-5 to 4-9 are property charts for the high-temperature burned gas; each is a plot of internal energy versus entropy for a particular fuel and equivalence ratio. Lines of constant temperature, pressure, and specific volume are drawn on each chart. An illustration of the use of these charts follows.

Example 4.3. The expansion process in an internal combustion engine, following completion of combustion, can be modeled approximately as an adiabatic and reversible process (i.e., isentropic). Under full-load operation, the pressure in the cylinder of a spark-ignition engine at top-center immediately following combustion is 7100 kPa. Find the gas state at the end of the expansion stroke and the expansion stroke work. The compression ratio is 8, the mixture is stoichiometric, and the volume per unit mass of air at the start of expansion is 0.125 m^3/kg air.

Locate $p_1 = 7100$ kPa and $v_1 = 0.125$ m^3/kg air on the $\phi = 1.0$ burned gas chart (Fig. 4-8). This gives $T_1 = 2825$ K, $u_1 = -5$ kJ/kg air, and $s_1 = 9.33$ kJ/kg air · K. The gas expands at constant entropy to $v_2 = 8 \times v_1 = 1$ m^3/kg air. Following a constant entropy process from state 1 on Fig. 4-8 gives

$$T_2 = 1840 \text{ K}, \qquad p_2 = 570 \text{ kPa}, \qquad \text{and} \qquad u_2 = -1540 \text{ kJ/kg air}$$

The expansion stroke work, assuming the process is adiabatic, is

$$W_{1-2} = -(u_2 - u_1) = 1540 - 5 = 1535 \text{ kJ/kg air}$$

As the burned gases in an engine cylinder cool during the expansion process, the composition eventually "freezes"—becomes fixed in composition—because the chemical reactions become extremely slow. This is usually assumed to occur at about 1700 K (see Sec. 4.9). The equilibrium assumption is then no longer valid. For lean and stoichiometric mixtures this distinction is not important because the mole fractions of dissociated species below this temperature are

PETITIONER'S EXHIBIT 1002
US PATENT NO. 6,581,565
Page 1653

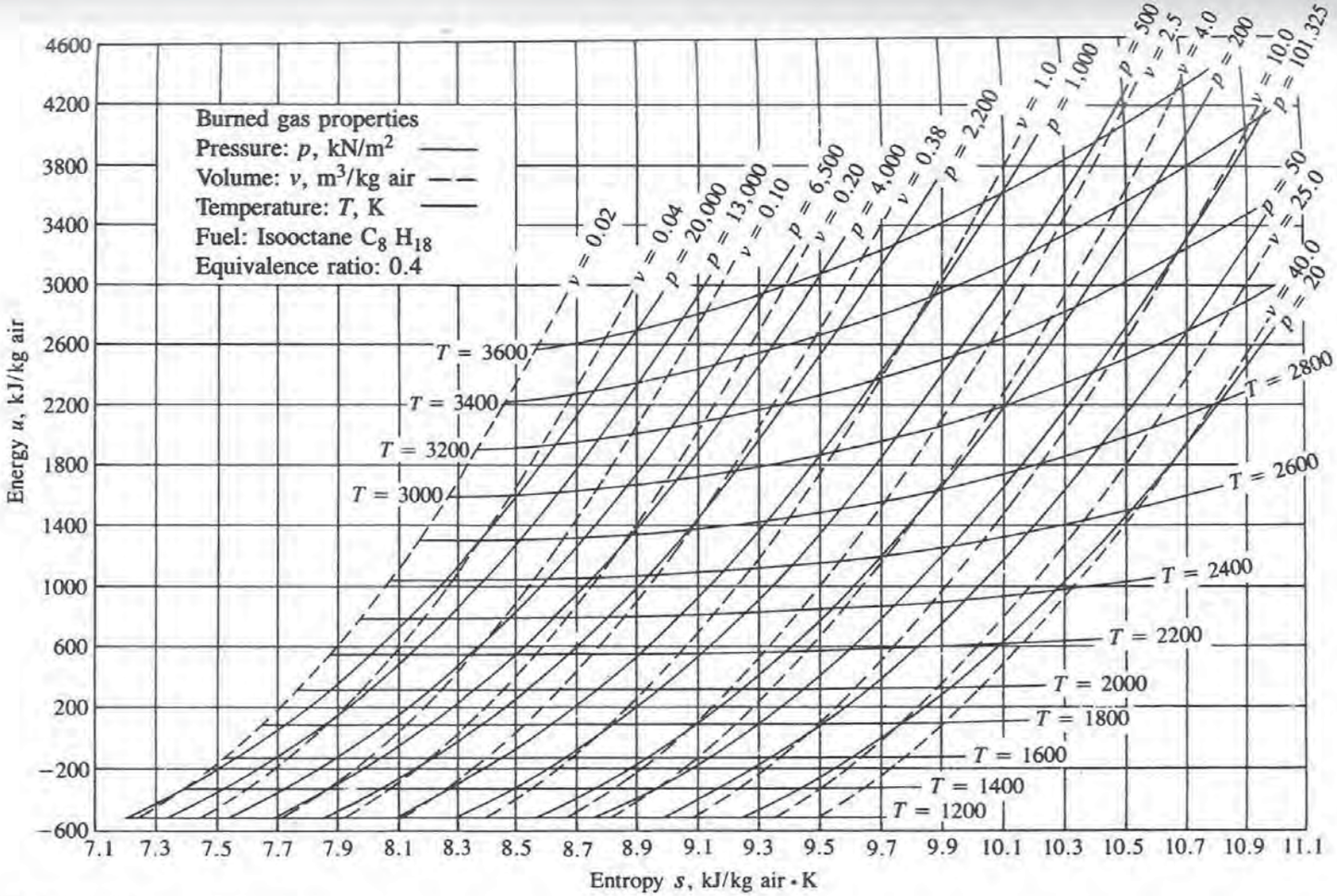


FIGURE 4-5
Internal energy versus entropy chart for equilibrium burned gas mixture, isooctane fuel; equivalence ratio 0.4.

PETITIONER'S EXHIBIT 1002
US PATENT NO. 6,581,565
Page 1654

FIGURE 4-6
Internal energy versus entropy chart for equilibrium burned gas mixture, isooctane fuel; equivalence ratio 0.6.

PETITIONER'S EXHIBIT 1002
US PATENT NO. 6,581,565
Page 1655

FIGURE 4-7
Internal energy versus entropy chart for equilibrium burned gas mixture, isooctane fuel; equivalence ratio 0.8.

PETITIONER'S EXHIBIT 1002
US PATENT NO. 6,581,565
Page 1656

FIGURE 4-8
Internal energy versus entropy chart for equilibrium burned gas mixture, isooctane fuel; equivalence ratio 1.0.

PETITIONER'S EXHIBIT 1002
US PATENT NO. 6,581,565
Page 1657

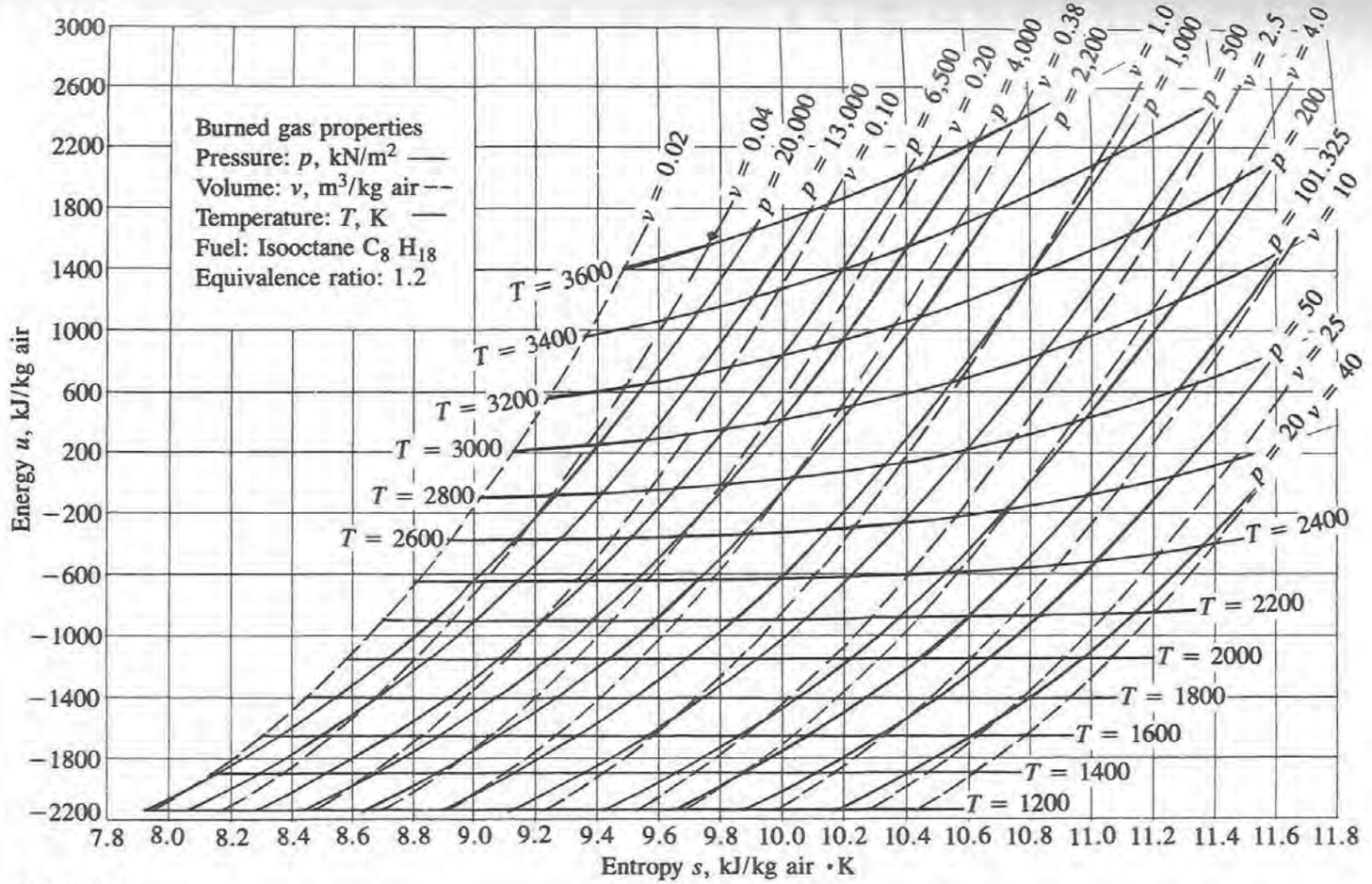


FIGURE 4-9
Internal energy versus entropy chart for equilibrium burned gas mixture, isooctane fuel; equivalence ratio 1.2.

PETITIONER'S EXHIBIT 1002
US PATENT NO. 6,581,565
Page 1658

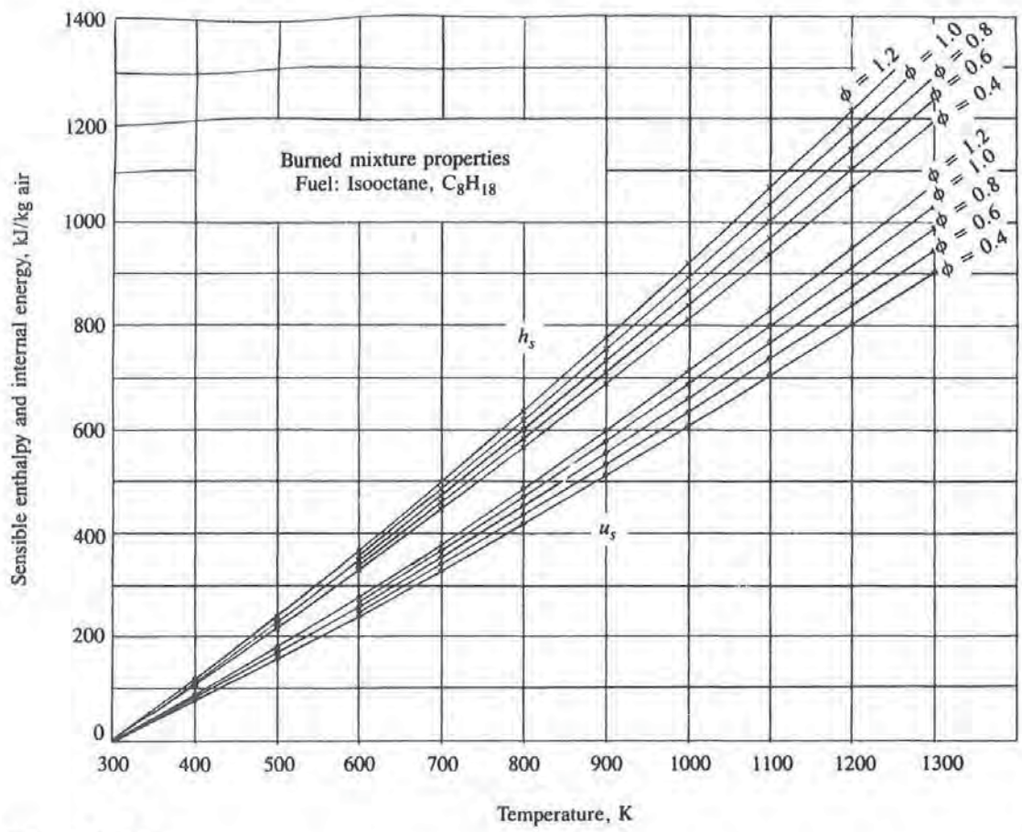


FIGURE 4-10
Sensible enthalpy and internal energy of low-temperature burned gases as function of temperature, isooctane fuel. Units: kJ/kg air in original mixture.

TABLE 4.7
Frozen burned gas composition: C_8H_{18}-air combustion

ϕ	CO_2	H_2O	CO	H_2	O_2	N_2	Sum	Units
0.4	0.0521	0.0586	—	—	0.122	0.767	1.000	mole fractions
	1.85	2.08	—	—	4.34	27.3	35.6	mol/kg air‡
0.6	0.0770	0.0866	—	—	0.0802	0.756	1.000	mole fractions
	2.78	3.13	—	—	2.89	27.3	36.1	mol/kg air‡
0.8	0.101	0.113	—	—	0.0395	0.746	1.000	mole fractions
	3.70	4.14	—	—	1.45	27.3	36.6	mol/kg air‡
1.0	0.125	0.140	—	—	—	0.735	1.000	mole fractions
	4.64	5.2	—	—	—	27.3	37.1	mol/kg air‡
1.2†	0.0905	0.138	0.0516	0.0224	—	0.698	1.000	mole fractions
	3.54	5.38	2.02	0.876	—	27.3	39.1	mol/kg air‡

† $K(T)$ in Eq. (4.6) evaluated at 1740 K; $K = 3.5$.
‡ Note mol/kg air; multiply by 10^{-3} for kmol/kg air.

small. For rich mixtures, a frozen composition must be selected and used because the mole fractions of CO_2, CO, H_2O, and H_2 would continue to change if equilibrium is assumed as the temperature decreases. Internal energy and enthalpy, per kilogram of air in the original mixture, of the frozen burned mixture are plotted against temperature in Fig. 4-10. The assumed frozen burned mixture compositions are listed in Table 4.7. These are sensible internal energies and enthalpies, given relative to their values at 298.15 K.

4.5.3 Relation between Unburned and Burned Mixture Charts

We now address the questions: Given unburned mixture at T_1, p_1, v_1, what is the state of the burned mixture following (1) constant-volume adiabatic combustion or (2) constant-pressure adiabatic combustion?

The datum for internal energy and enthalpy for the unburned mixture in Fig. 4-3 is different from the datum for internal energy and enthalpy for the burned mixture. For the unburned mixture, zero internal energy and enthalpy for the *mixture* at 298.15 K was assumed. For the burned mixture, zero enthalpy for the gaseous species O_2, N_2, and H_2, and C (solid graphite) at 298.15 K was assumed. These data can be related through the enthalpies of formation, from O_2, N_2, H_2, and C, of each species in the unburned mixture.

If $\Delta\tilde{h}^\circ_{f,i}$ is the enthalpy of formation of species i at 298.15 K, per kilomole, and $\Delta h^\circ_{f,u}$ is the enthalpy of formation of the unburned mixture at 298.15 K, per kilogram of air in the original mixture, then

$$\Delta h^\circ_{f,u} = \sum_i n_i \Delta\tilde{h}^\circ_{f,i} \tag{4.27}$$

where n_i is the number of kilomoles of species i per kilogram of air. The unburned mixture enthalpy h_u, with the same datum as the burned mixture enthalpy, is therefore given by the sum of the sensible enthalpy $h_{s,u}$ and $\Delta h^\circ_{f,u}$:

$$h_u = h_{s,u} + \Delta h^\circ_{f,u} \tag{4.28}$$

Similarly, the internal energy u_u is given by

$$u_u = u_{s,u} + \Delta u^\circ_{f,u} \tag{4.29}$$

$\Delta u^\circ_{f,u}$ can be obtained from

$$\Delta u^\circ_{f,u} = \sum_i n_i \Delta\tilde{u}^\circ_{f,i} \tag{4.30}$$

Alternately, Eq. (3.18) can be used to obtain $\Delta u^\circ_{f,u}$ from $\Delta h^\circ_{f,u}$:

$$\Delta u^\circ_{f,u} = \Delta h^\circ_{f,u} - (n_P - n_R)\tilde{R}T \tag{4.31}$$

Enthalpies and internal energies of formation of the relevant burned gas species and individual fuel compounds are given in Table 4.8 and App. D. Values of n_i are obtained from Tables 4.4 and 4.7. Following the procedure used in Example 4.4 below, expressions for $\Delta h^\circ_{f,u}$ and $\Delta u^\circ_{f,u}$ in kilojoules per kilogram of

PETITIONER'S EXHIBIT 1002
US PATENT NO. 6,581,565
Page 1660

TABLE 4.8
Standard enthalpies and internal energies of formation†

	$\Delta\tilde{h}^\circ_{f,i}$, MJ/kmol	$\Delta\tilde{u}^\circ_{f,i}$, MJ/kmol
CO_2	−393.5	−393.5
H_2O (gas)	−241.8	−240.6
CO	−110.5	−111.7
C_8H_{18} (gas)	−224.1	−204.3

† At 298.15 K. $\Delta\tilde{h}^\circ_{f,i}$ for O_2, N_2, and H_2 are zero by definition.
Sources: JANAF tables,[8] Rossini *et al.*[16]

air can be obtained. For the charts of Figs. 4-3 and 4-5 to 4-9, these expressions are:

$\phi = 0.4$:

$$\Delta h^\circ_{f,u} = -51.9 - 1181x_b \qquad \Delta u^\circ_{f,u} = -47.3 - 1183x_b$$

$\phi = 0.6$:

$$\Delta h^\circ_{f,u} = -77.8 - 1771x_b \qquad \Delta u^\circ_{f,u} = -70.9 - 1774x_b$$

$\phi = 0.8$:

$$\Delta h^\circ_{f,u} = -103.8 - 2361x_b \qquad \Delta u^\circ_{f,u} = -94.6 - 2365x_b \tag{4.32}$$

$\phi = 1.0$:

$$\Delta h^\circ_{f,u} = -129.7 - 2951x_b \qquad \Delta u^\circ_{f,u} = -118.2 - 2956x_b$$

$\phi = 1.2$:

$$\Delta h^\circ_{f,u} = -155.6 - 2759x_b \qquad \Delta u^\circ_{f,u} = -141.9 - 2769x_b$$

Example 4.4. Calculate $\Delta h^\circ_{f,u}$, the enthalpy of formation of the unburned mixture, and $\Delta u^\circ_{f,u}$, the internal energy of formation of the unburned mixture, for a C_8H_{18}-air mixture with $\phi = 1.0$ and burned gas fraction x_b.

Table 4.4 gives the moles of each species in the unburned mixture, per mole O_2 with $\phi = 1.0$, as

C_8H_{18}, $0.08(1 - x_b)$	CO_2, $0.64x_b$
O_2, $1 - x_b$	H_2O, $0.72x_b$
N_2, 3.773	CO and H_2, 0

Table 4.5 gives the mass of air per mole O_2 as 138.2 kg/kmol. Thus the number of kilomoles of each species per kilogram of air is

C_8H_{18}, $5.787 \times 10^{-4}\,(1 - x_b)$	CO_2, $4.629 \times 10^{-3}x_b$
O_2, $7.233 \times 10^{-3}\,(1 - x_b)$	H_2O, $5.208 \times 10^{-3}x_b$
N_2, 2.729×10^{-2}	CO and H_2, 0

PETITIONER'S EXHIBIT 1002
US PATENT NO. 6,581,565
Page 1661

With $\Delta\tilde{h}^\circ_{f,i}$ from Table 4.8, Eq. (4.27) gives

$$\Delta h^\circ_{f,u} = 5.787 \times 10^{-4} \times (-224.1 \times 10^6)(1 - x_b) + x_b[4.629 \times 10^{-3} \times (-393.5 \times 10^6) + 5.208 \times 10^{-3} \times (-241.8 \times 10^6)]$$

$$\Delta h^\circ_{f,u} = (-129.7 - 2951x_b) \times 10^3 \quad \text{J/kg air}$$

With $\Delta\tilde{u}^\circ_{f,i}$ from Table 4.8, Eq. (4.30) gives

$$\Delta u^\circ_{f,u} = 5.787 \times 10^{-4} \times (-204.3 \times 10^6)(1 - x_b) + x_b[4.629 \times 10^{-3} \times (-393.5 \times 10^6) + 5.208 \times 10^{-3} \times (-240.6 \times 10^6)]$$

$$\Delta u^\circ_{f,u} = (-118.2 - 2956x_b) \times 10^3 \quad \text{J/kg air}$$

Alternatively, we can determine $\Delta u^\circ_{f,u}$ from $\Delta h^\circ_{f,u}$ using Eq. (4.31). For this calculation, the "product" gas is the unburned mixture and the "reactant" gas is the mixture of elements from which the unburned mixture is formed. The number of gaseous moles in the unburned mixture n_P, per mole O_2 in the original mixture, is (from Table 4.5 for $\phi \leq 1$)

$$n_P = (1 - x_b)\left[4(1 + 2\varepsilon)\frac{\phi}{M_f} + 1 + \psi\right] + x_b[(1 - \varepsilon)\phi + 1 + \psi]$$

The elemental reactant mixture from which the unburned mixture is formed is, from Eq. (4.4),

$$\varepsilon\phi C + 2(1 - \varepsilon)\phi H_2 + O_2 + \psi N_2$$

Thus, n_R, the moles of *gaseous* elements, is

$$n_R = 2(1 - \varepsilon)\phi + 1 + \psi$$

For air, $\psi = 3.773$; for C_8H_{18} fuel, $\varepsilon = 0.64$ and $M_f = 114$. For $\phi = 1$,

$$n_P - n_R = -0.64 + 0.28x_b \quad \text{moles/mole } O_2$$

and

$$(n_P - n_R)\tilde{R}T = (-0.64 + 0.28x_b) \times 8.3143 \times 10^3 \times \frac{298.15}{138.2}$$

or

$$(n_P - n_R)\tilde{R}T = (-11.5 + 5.0x_b) \times 10^3 \quad \text{J/kg air}$$

Since

$$\Delta u^\circ_{f,u} = \Delta h^\circ_{f,u} - (n_P - n_R)\tilde{R}T$$

$$\Delta u^\circ_{f,u} = (-129.7 - 2951x_b) \times 10^3 - (-11.5 + 5.0x_b) \times 10^3$$

$$\Delta u^\circ_{f,u} = (-118.2 - 2956x_b) \times 10^3 \quad \text{J/kg air}$$

The combustion process links the unburned and burned mixture properties as follows:

For an adiabatic constant-volume combustion process,

$$u_b = u_u = u_{s,u} + \Delta u^\circ_{f,u} \tag{4.33}$$

and

$$v_b = v_u$$

PETITIONER'S EXHIBIT 1002
US PATENT NO. 6,581,565
Page 1662

Thus, given $u_{s,u}$ and v_u, the state of the burned mixture can be determined from the appropriate burned mixture chart.

For an adiabatic constant-pressure combustion process,

$$h_b = h_u = h_{s,u} + \Delta h^\circ_{f,u} \tag{4.34}$$

Since

$$u_b = h_b - pv_b$$

given $h_{s,u}$ and p, u_b and v_b must be found by trial and error along the specified constant-pressure line on the appropriate burned mixture chart.

Example 4.5. Calculate the temperature and pressure after constant-volume adiabatic combustion and constant-pressure adiabatic combustion of the unburned mixture (with $\phi = 1.0$ and $x_b = 0.08$) at the state corresponding to the end of the compression process examined in Example 4.2.

The state of the unburned mixture at the end of the compression process in Example 4.2 was

$$T_u = 682 \text{ K}, \qquad u_{s,u} = 350 \text{ kJ/kg air}, \qquad p_u = 1.57 \text{ MPa}, \qquad v_u = 0.125 \text{ m}^3\text{/kg air}$$

For an adiabatic *constant-volume* combustion process [Eq. (4.33)],

$$u_b = u_u = u_{s,u} + \Delta u^\circ_{f,u}$$

For $\phi = 1.0$, $\Delta u^\circ_{f,u}$ is given by Eq. (4.32) as

$$\Delta u^\circ_{f,u} = -118.2 - 2956x_b = -118.2 - 236.5 = -355 \text{ kJ/kg air}$$

Hence

$$u_b = 350 - 355 = -5 \text{ kJ/kg air}$$

Also

$$v_b = v_u = 0.125 \text{ m}^3\text{/kg air}$$

Locating (u_b, v_b) on the burned gas chart (Fig. 4-8) gives

$$T_b = 2825 \text{ K}, \qquad p_b = 7100 \text{ kPa}$$

For a *constant-pressure* combustion process [Eq. (4.34)],

$$h_b = h_u = h_{s,u} + \Delta h^\circ_{f,u}$$

For $\phi = 1.0$, $\Delta h^\circ_{f,u}$ is given by Eq. (4.32) as

$$\Delta h^\circ_{f,u} = -129.7 - 2951x_b = -129.7 - 236 = -366 \text{ kJ/kg air}$$

At $T_u = 682$ K, $h_{s,u} = 465$ kJ/kg air, so

$$h_b = 465 - 366 = 99 \text{ kJ/kg air}$$

Since $p_b = p_u = 1.57$ MPa, the internal energy u_b is given by

$$u_b = h_b - p_b v_b = 99 - 1.57 \times 10^3 v_b \qquad \text{kJ/kg air}$$

PETITIONER'S EXHIBIT 1002
US PATENT NO. 6,581,565
Page 1663

A trial-and-error solution for v_b and u_b along the $p = 1570$ kPa line on Fig. 4-8 gives

$$u_b = -655 \text{ kJ/kg air}, \qquad T_b = 2440 \text{ K}, \qquad v_b = 0.485 \text{ m}^3/\text{kg air}$$

(Use the ideal gas law to estimate p, T, or v more accurately.)

4.6 TABLES OF PROPERTIES AND COMPOSITION

Tables of thermodynamic properties of air are useful for analysis of motored engine operation, diesels and compressors. Keenan, Chao, and Kaye's *Gas Tables*[6] are the standard reference for the thermodynamic properties of air at low pressures (i.e., at pressures substantially below the critical pressure when the ideal gas law is accurate). These gas tables are in U.S. and SI units. A set of tables for air in SI units has been prepared by Reynolds[7] following the format of the Keenan *et al.* tables. A condensed table of thermodynamic properties of air, derived from Reynolds, is given in App. D. It contains:

h = enthalpy, kJ/kg
u = internal energy, kJ/kg
$\Psi = \int_0^T \left(\frac{c_v}{T}\right) dT$, kJ/kg · K
$\Phi = \int_0^T \left(\frac{c_p}{T}\right) dT$, kJ/kg · K
p_r = relative pressure
v_r = relative volume
c_p = specific heat at constant pressure, kJ/kg · K
c_v = specific heat at constant volume, kJ/kg · K
γ = ratio of specific heats

all as a function of T(K).

Φ is the standard state entropy at temperature T and 1 atm pressure, relative to the entropy at 0 K and 1 atm pressure. The entropy at pressures other than 1 atm is obtained using Eq. (4.14*b*).

The relative pressure p_r is defined by

$$\ln p_r = \frac{\Phi}{R} \tag{4.35}$$

and is a function of T only. Along a given isentropic, it follows from Eq. (4.18) that the ratio of actual pressures p_2 and p_1 corresponding to temperatures T_2 and T_1 is equal to the ratio of relative pressures, i.e.,

$$\left(\frac{p_2}{p_1}\right)_{s=\text{const}} = \left(\frac{p_{r2}}{p_{r1}}\right) \tag{4.36}$$

This affords a means of determining T_2, for an isentropic process, given T_1 and p_2/p_1 (see Example 4.6).

PETITIONER'S EXHIBIT 1002
US PATENT NO. 6,581,565
Page 1664

The relative volume v_r is defined by

$$v_r = \frac{RT}{p_r} \tag{4.37}$$

The units are selected so that v_r is in cubic meters per kilogram when T is in kelvins and p_r is in pascals. Along a given isentropic, the ratio of actual volumes V_2 and V_1 (for a fixed mass) at temperatures T_2 and T_1, from Eq. (4.37), is equal to the ratio of relative volumes

$$\left(\frac{V_2}{V_1}\right)_{s=\text{const}} = \left(\frac{v_{r2}}{v_{r1}}\right) \tag{4.38}$$

This affords a means of determining T_2 for an isentropic process, given T_1 and V_2/V_1 (see Example 4.6).

Tables giving the composition and thermodynamic properties of combustion products have been compiled. They are useful sources of property and species concentrations data in burned gas mixtures for a range of equivalence ratios, temperatures, and pressures. Summary information on four generally available sets of tables is given in Table 4.9. The most extensive set of tables of combustion product composition and thermodynamic properties is the AGARD set, *Properties of Air and Combustion Products with Kerosene and Hydrogen Fuels*, by Banes *et al.*[12] Note, however, that their enthalpy datum differs from the usual datum (enthalpy for O_2, N_2, H_2, and C is zero at 298.15 K). The elements in their reference state at 298.15 K were assigned arbitrary positive values for enthalpy to avoid negative enthalpies for the equilibrium burned gas mixture.

Example 4.6. In a diesel engine, the air conditions at the start of compression are $p_1 = 1$ atm and $T_1 = 325$ K. At the end of compression $p_2 = 60$ atm. Find the temperature T_2 and the compression ratio V_1/V_2.

Air tables (see App. D), at $T_1 = 325$ K, give

$$p_{r1} = 97.13 \qquad \text{and} \qquad v_{r1} = 960.6$$

Use Eq. (4.36),

$$\frac{p_{r2}}{p_{r1}} = \frac{p_2}{p_1} = 60$$

to give

$$p_{r2} = 5828$$

Tables then give

$$T_2 = 992 \text{ K} \qquad \text{and} \qquad v_{r2} = 48.92$$

The compression ratio is given by

$$\frac{V_1}{V_2} = \frac{v_{r1}}{v_{r2}} = \frac{960.6}{48.92} = 19.6$$

PETITIONER'S EXHIBIT 1002
US PATENT NO. 6,581,565
Page 1665

TABLE 4.9
Tables of properties of air and combustion products

Source	Properties P, composition C	Mixture	Units	ϕ range	T range	p range	Enthalpy datum
Keenan, Chao, and Kaye[6]	P	Air	U.S., SI		100–3600 K	Low	$h = 0$ at 0 K
		$(CH_2)_n$-air		0.25, 0.5, 1.0	100–2000 K	Low	$\tilde{h}_b = 0$ at 0 K
Reynolds[7]	P	Air	SI		200–1500 K	Low	
General Electric[11]	P and C	Air-$(CH_2)_n$	U.S.	0.25–4	600–5000°R	0.01–30 atm	h of C, H_2, N_2, O_2 zero at 0°R
AGARD[12]	P and C	Air	SI		100–6000 K	1–800 atm	Arbitrary, to keep $h_b > 0$
		$(CH_2)_n$-air		0.2–2			
		H_2-air		0.2–2			

PETITIONER'S EXHIBIT 1002
US PATENT NO. 6,581,565
Page 1666

4.7 COMPUTER ROUTINES FOR PROPERTY AND COMPOSITION CALCULATIONS

When large numbers of computations are being made or high accuracy is required, engine process calculations are carried out on a computer. Relationships which model the composition and/or thermodynamic properties of unburned and burned gas mixtures have been developed for computer use. These vary considerably in range of application and accuracy.

The most complete models are based on polynomial curve fits to the thermodynamic data for each species in the mixture and the assumptions that (1) the unburned mixture is frozen in composition and (2) the burned mixture is in equilibrium. The approach used as the basis for representing JANAF table thermodynamic data[8] in the NASA equilibrium program[9,10] (see Sec. 3.7) will be summarized here because it is consistent with the approach used throughout to calculate unburned and burned mixture properties.

For each species i in its standard state at temperature T(K), the specific heat $\tilde{c}_{p,i}$ is approximated by

$$\frac{\tilde{c}_{p,i}}{\tilde{R}} = a_{i1} + a_{i2}\,T + a_{i3}\,T^2 + a_{i4}\,T^3 + a_{i5}T^4 \tag{4.39}$$

The standard state enthalpy of species i is then given by

$$\frac{\tilde{h}_i}{\tilde{R}T} = a_{i1} + \frac{a_{i2}}{2}\,T + \frac{a_{i3}}{3}\,T^2 + \frac{a_{i4}}{4}\,T^3 + \frac{a_{i5}}{5}\,T^4 + \frac{a_{i6}}{T} \tag{4.40}$$

The standard state entropy of species i at temperature T(K) and pressure 1 atm, from Eq. (4.14), is then

$$\frac{\tilde{s}_i}{\tilde{R}} = a_{i1}\ln T + a_{i2}\,T + \frac{a_{i3}}{2}\,T^2 + \frac{a_{i4}}{3}\,T^3 + \frac{a_{i5}}{4}\,T^4 + a_{i7} \tag{4.41}$$

Values of the coefficients a_{ij} for CO_2, H_2O, CO, H_2, O_2, N_2, OH, NO, O, and H from the NASA program are given in Table 4.10. Two temperature ranges are given. The 300 to 1000 K range is appropriate for unburned mixture property calculations. The 1000 to 5000 K range is appropriate for burned mixture property calculations. Figure 4-11 gives values of c_p/R for the major species, CO_2, H_2O, O_2, N_2, H_2, and CO, as a function of temperature.

4.7.1 Unburned Mixtures

Polynomial functions for various fuels (in the vapor phase) have been fitted to the functional form:[13–15]

$$\tilde{c}_{p,f} = A_{f1} + A_{f2}\,t + A_{f3}\,t^2 + A_{f4}\,t^3 + \frac{A_{f5}}{t^2} \tag{4.42}$$

PETITIONER'S EXHIBIT 1002
US PATENT NO. 6,581,565
Page 1667

TABLE 4.10
Coefficients for species thermodynamic properties

Species	T range, K	a_{i1}	a_{i2}	a_{i3}	a_{i4}	a_{i5}	a_{i6}	a_{i7}
CO_2	1000–5000	0.44608(+1)	0.30982(−2)	−0.12393(−5)	0.22741(−9)	−0.15526(−13)	−0.48961(+5)	−0.98636(0)
	300–1000	0.24008(+1)	0.87351(−2)	−0.66071(−5)	0.20022(−8)	0.63274(−15)	−0.48378(+5)	0.96951(+1)
H_2O	1000–5000	0.27168(+1)	0.29451(−2)	−0.80224(−6)	0.10227(−9)	−0.48472(−14)	−0.29906(+5)	0.66306(+1)
	300–1000	0.40701(+1)	−0.11084(−2)	0.41521(−5)	−0.29637(−8)	0.80702(−12)	−0.30280(+5)	−0.32270(0)
CO	1000–5000	0.29841(+1)	0.14891(−2)	−0.57900(−6)	0.10365(−9)	−0.69354(−14)	−0.14245(+5)	0.63479(+1)
	300–1000	0.37101(+1)	−0.16191(−2)	0.36924(−5)	−0.20320(−8)	0.23953(−12)	−0.14356(+5)	0.29555(+1)
H_2	1000–5000	0.31002(+1)	0.51119(−3)	0.52644(−7)	−0.34910(−10)	0.36945(−14)	−0.87738(+3)	−0.19629(+1)
	300–1000	0.30574(+1)	0.26765(−2)	−0.58099(−5)	0.55210(−8)	−0.18123(−11)	−0.98890(+3)	−0.22997(+1)
O_2	1000–5000	0.36220(+1)	0.73618(−3)	−0.19652(−6)	0.36202(−10)	−0.28946(−14)	−0.12020(+4)	0.36151(+1)
	300–1000	0.36256(+1)	−0.18782(−2)	0.70555(−5)	−0.67635(−8)	0.21556(−11)	−0.10475(+4)	0.43053(+1)
N_2	1000–5000	0.28963(+1)	0.15155(−2)	−0.57235(−6)	0.99807(−10)	−0.65224(−14)	−0.90586(+3)	0.61615(+1)
	300–1000	0.36748(+1)	−0.12082(−2)	0.23240(−5)	−0.63218(−9)	−0.22577(−12)	−0.10612(+4)	0.23580(+1)
OH	1000–5000	0.29106(+1)	0.95932(−3)	−0.19442(−6)	0.13757(−10)	0.14225(−15)	0.39354(+4)	0.54423(+1)
NO	1000–5000	0.31890(+1)	0.13382(−2)	−0.52899(−6)	0.95919(−10)	−0.64848(−14)	0.98283(+4)	0.67458(+1)
O	1000–5000	0.25421(+1)	−0.27551(−4)	−0.31028(−8)	0.45511(−11)	−0.43681(−15)	0.29231(+5)	0.49203(+1)
H	1000–5000	0.25(+1)	0.0	0.0	0.0	0.0	0.25472(+5)	−0.46012(0)

Source: NASA Equilibrium Code.[9]

PETITIONER'S EXHIBIT 1002
US PATENT NO. 6,581,565
Page 1668

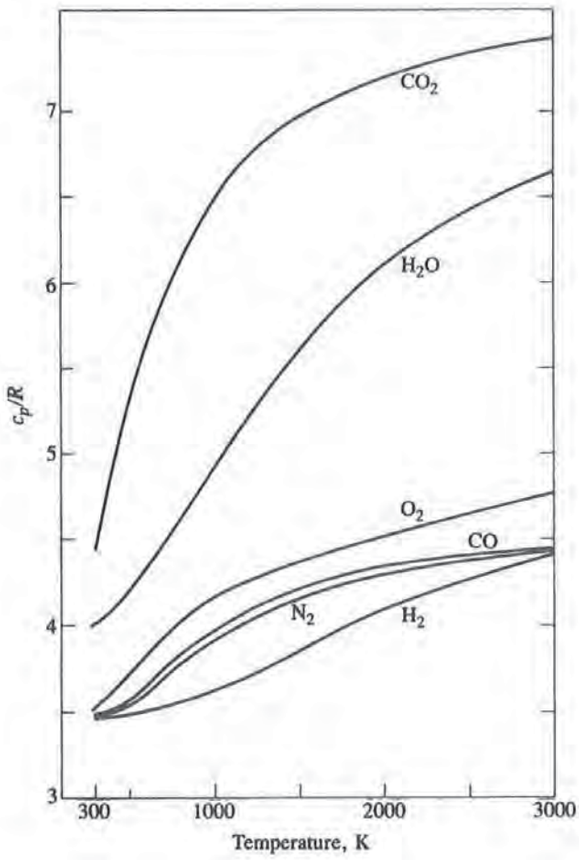


FIGURE 4-11
Specific heat at constant pressure, c_p/R, as function of temperature for species CO_2, H_2O, O_2, N_2, H_2, and CO. (*From JANAF tables.*[8])

$$\tilde{h}_f = A_{f1}\,t + A_{f2}\,\frac{t^2}{2} + A_{f3}\,\frac{t^3}{3} + A_{f4}\,\frac{t^4}{4} - \frac{A_{f5}}{t} + A_{f6} + A_{f8} \qquad (4.43)$$

where $t = T(\mathrm{K})/1000$. A_{f6} is the constant for the datum of zero enthalpy for C, H_2, O_2, and N_2 at 298.15 K. For a 0 K datum, A_{f8} is added to A_{f6}. For pure hydrocarbon compounds, the coefficients A_{fi} were found by fitting Eqs. (4.42) and (4.43) to data from Rossini *et al.*[16] Values for relevant pure fuels are given in Table 4.11. The units for $\tilde{c}_{p,f}$ are cal/gmol·K, and for $\tilde{h}_f$ are kcal/gmol.

Multicomponent fuel coefficients were determined as follows.[14] Chemical analysis of the fuel was performed to obtain the H/C ratio, average molecular weight, heating value, and the weight percent of aromatics, olefins, and total paraffins (including cycloparaffins). The fuel was then modeled as composed of a representative aromatic, olefin, and paraffin hydrocarbon. From atomic conservation of hydrogen and carbon and the chemical analysis results, component molar fractions and average carbon numbers can be determined. Table 4.11 gives values for the coefficients A_{f1} to A_{f8} for typical petroleum-based fuels. The units of the coefficients give $\tilde{c}_{p,f}$ and $\tilde{h}_f$ in cal/gmol·K and kcal/gmol, respectively, with $t = T(\mathrm{K})/1000$.

PETITIONER'S EXHIBIT 1002
US PATENT NO. 6,581,565
Page 1669

TABLE 4.11
Coefficients for polynomials [Eqs. (4.42) and (4.43)] for fuel enthalpy and specific heat

Fuel	Formula	Molecular weight	$(A/F)_s$	$(F/A)_s$	A_{f1}	A_{f2}	A_{f3}	A_{f4}	A_{f5}	A_{f6}	A_{f8}
Methane	CH_4	16.04	17.23	0.0580	−0.29149	26.327	−10.610	1.5656	0.16573	−18.331	4.3000
Propane	C_3H_8	44.10	15.67	0.0638	−1.4867	74.339	−39.065	8.0543	0.01219	−27.313	8.852
Hexane	C_6H_{14}	86.18	15.24	0.0656	−20.777	210.48	−164.125	52.832	0.56635	−39.836	15.611
Isooctane	C_8H_{18}	114.2	15.14	0.0661	−0.55313	181.62	−97.787	20.402	−0.03095	−60.751	20.232
Methanol	CH_3OH	32.04	6.47	0.1546	−2.7059	44.168	−27.501	7.2193	0.20299	−48.288	5.3375
Ethanol	C_2H_5OH	46.07	9.00	0.1111	6.990	39.741	−11.926	0	0	−60.214	7.6135
Gasoline	$C_{8.26}H_{15.5}$	114.8	14.64	0.0683	−24.078	256.63	−201.68	64.750	0.5808	−27.562	17.792
	$C_{7.76}H_{13.1}$	106.4	14.37	0.0696	−22.501	227.99	−177.26	56.048	0.4845	−17.578	15.235
Diesel	$C_{10.8}H_{18.7}$	148.6	14.4	0.0694	−9.1063	246.97	−143.74	32.329	0.0518	−50.128	23.514

Units of A_{fi} such that $\tilde{h}_f$ is in kcal/gmol and $\tilde{c}_{p,f}$ is in cal/gmol·K with $t = T(\text{K})/1000$.
A_{f6} gives enthalpy datum at 298.15 K; $(A_{f6} + A_{f8})$ gives enthalpy datum at 0 K.

PETITIONER'S EXHIBIT 1002
US PATENT NO. 6,581,565
Page 1670

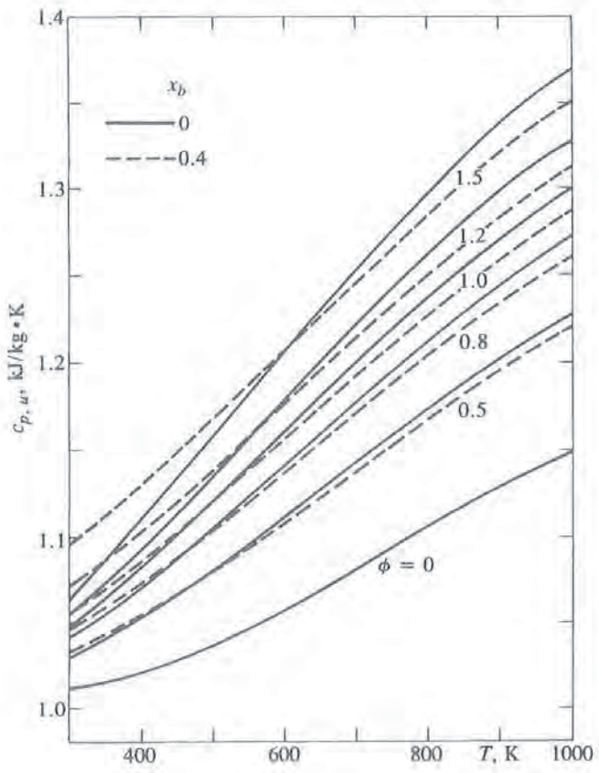


FIGURE 4-12
Specific heat at constant pressure of unburned gasoline, air, burned gas mixtures as function of temperature, equivalence ratio, and burned gas fraction. Units: kJ/kg mixture · K.

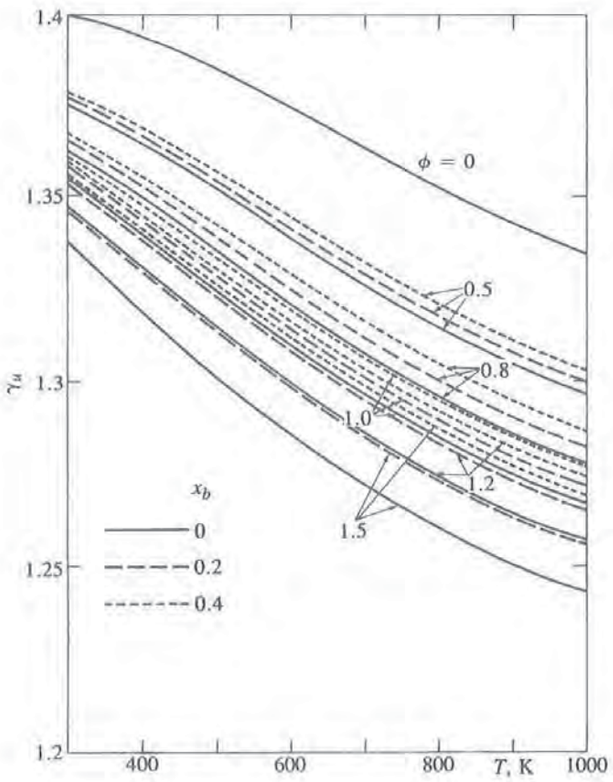


FIGURE 4-13
Ratio of specific heats, $\gamma_u = c_{p,u}/c_{v,u}$, of unburned gasoline, air, burned gas mixtures as function of temperature, equivalence ratio, and burned gas fraction.

PETITIONER'S EXHIBIT 1002
US PATENT NO. 6,581,565
Page 1671

The thermodynamic properties of the unburned mixture can now be obtained. With the moles of each species per mole O_2, n_i, determined from Table 4.4, and the mass of mixture per mole O_2, m_{RP}, determined from Table 4.5, the unburned mixture properties are given by

$$c_{p,u} = \frac{1}{m_{RP}} \sum_i n_i \tilde{c}_{p,i} \tag{4.44a}$$

$$h_u = \frac{1}{m_{RP}} \sum_i n_i \tilde{h}_i \tag{4.44b}$$

$$s_u = \frac{1}{m_{RP}} \left\{ \sum n_i \left[\tilde{s}_i^\circ - \tilde{R} \ln \left(\frac{n_i}{n_u} \right) \right] - n_u \tilde{R} \ln p \right\} \tag{4.44c}$$

where p is in atmospheres.

Figures 4-12 and 4-13, obtained with the above relations, show how $c_{p,u}$ and $\gamma_u (= c_{p,u}/c_{v,u})$ vary with temperature, equivalence ratio, and burned gas fraction, for a gasoline-air mixture.

4.7.2 Burned Mixtures

The most accurate approach for burned mixture property and composition calculations is to use a thermodynamic equilibrium program at temperatures above about 1700 K and a frozen composition below 1700 K. The properties of each species at high and low temperatures are given by polynomial functions such as Eqs. (4.39) to (4.41) and their coefficients in Table 4.10. The NASA equilibrium program (see Sec. 3.7) is readily available for this purpose and is well documented.[9, 10] The following are examples of its output.

Figure 3-10 showed species concentration data for burned gases as a function of equivalence ratio at 1750, 2250, and 2750 K, at 30 atm. Figure 4-14 shows the burned gas molecular weight M_b, and Figs. 4-15 and 4-16 give $c_{p,b}$ and γ_b as functions of equivalence ratio at 1750, 2250, and 2750 K, at 30 atm. Figures 4-17 and 4-18 show $c_{p,b}$ and γ_b as a function of temperature and pressure for selected equivalence ratios for mixtures lean and rich of stoichiometric.[17] For rich mixtures ($\phi > 1$), for $T > 2000$ K, $c_{p,b}$ and γ_b are equilibrium values. For 1200 K $\leq T \leq$ 2000 K, "frozen" composition data are shown where the gas composition is in equilibrium at the given T and p but is frozen as c_p and c_v are computed. Below about 1500 K, fixed composition data are shown corresponding to a value of 3.5 for the water-gas equilibrium constant which adequately describes exhaust gases (see Sec. 4.9).

Because the computational time involved in repeated use of a full equilibrium program can be substantial, simpler equilibrium programs and approximate fits to the equilibrium thermodynamic data have been developed. The approach usually used is to estimate the composition and/or properties of undissociated combustion products and then to use iterative procedures or corrections to account for the effects of dissociation.

PETITIONER'S EXHIBIT 1002
US PATENT NO. 6,581,565
Page 1672

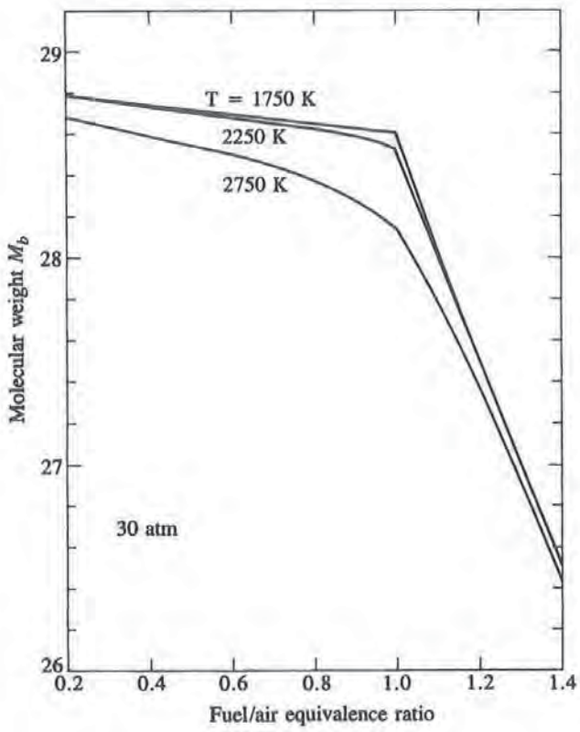


FIGURE 4-14
Molecular weight of equilibrium burned gases as a function of equivalence ratio at $T = 1750$, 2250, and 2750 K, and 30 atm. Fuel: isooctane.

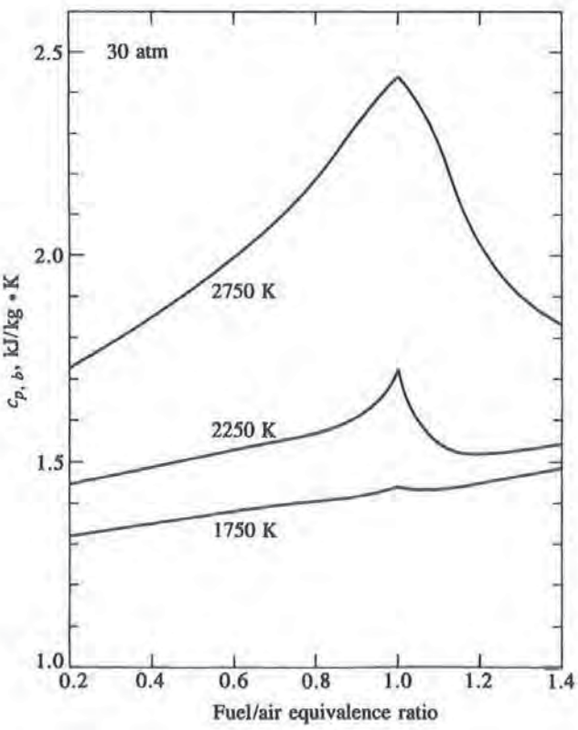


FIGURE 4-15
Specific heat at constant pressure of equilibrium burned gases as a function of equivalence ratio at $T = 1750$, 2250, and 2750 K, and 30 atm. Fuel: isooctane. Units: kJ/kg mixture · K.

PETITIONER'S EXHIBIT 1002
US PATENT NO. 6,581,565
Page 1673

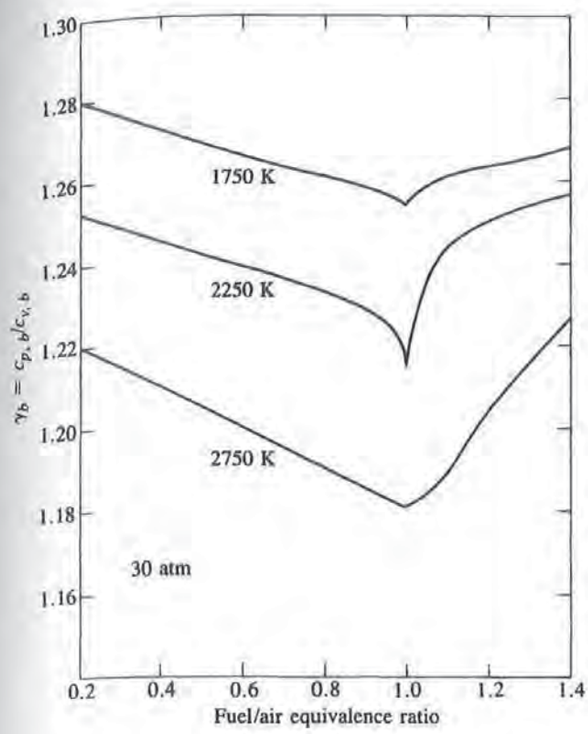
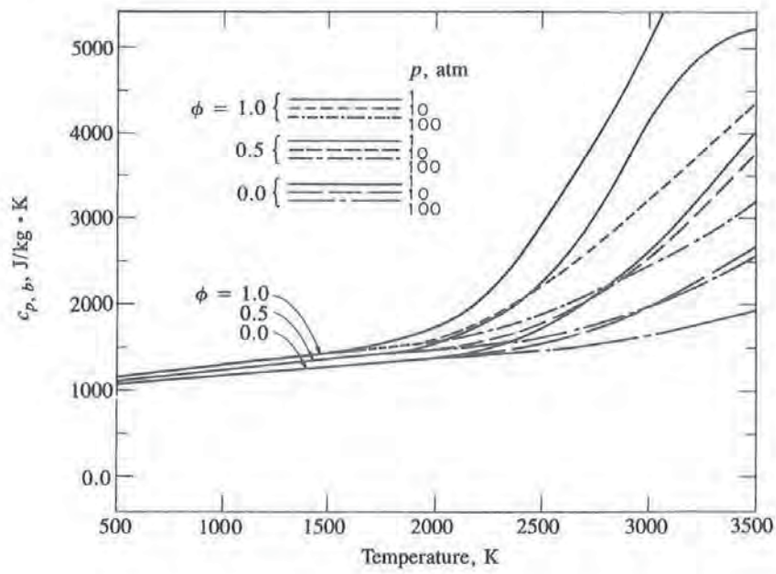


FIGURE 4-16
Ratio of specific heats, $\gamma_b = c_{p,b}/c_{v,b}$, for equilibrium burned gases as a function of equivalence ratio at $T = 1750$, 2250, and 2750 K, and 30 atm. Fuel: isooctane.

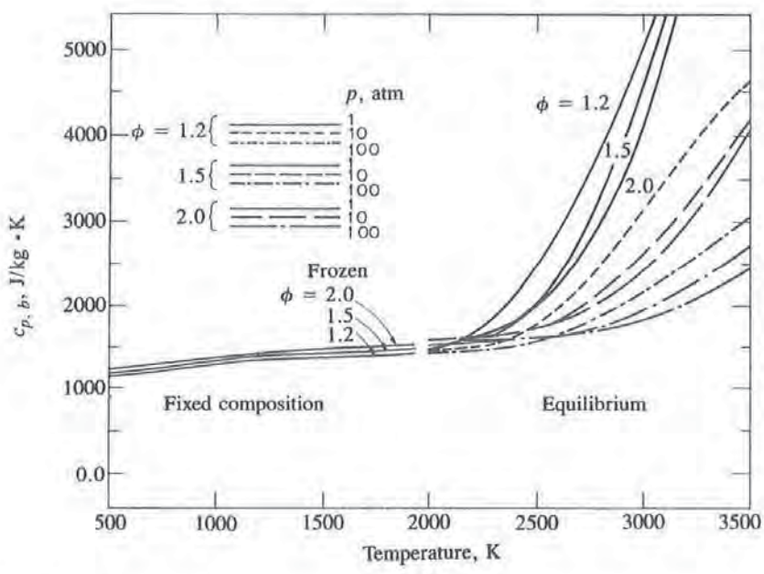
A computer program for calculating properties of equilibrium combustion products, designed specifically for use in internal combustion engine applications, has been developed by Olikara and Borman and is readily available.[18] The fuel composition ($C_nH_mO_lN_k$), fuel/air equivalence ratio, and product pressure and temperature are specified. The species included in the product mixture are: CO_2, H_2O, CO, H_2, O_2, N_2, Ar, NO, OH, O, H, and N. The element balance equations and equilibrium constants for seven nonredundant reactions provide the set of 11 equations required for solution of these species concentrations (see Sec. 3.7). The equilibrium constants are curve fitted from data in the JANAF tables.[8] The initial estimate of mole fractions to start the iteration procedure is the nondissociated composition. Once the mixture composition is determined, the thermodynamic properties and their derivatives with respect to temperature, pressure, and equivalence ratio are computed. This limited set of species has been found to be sufficiently accurate for engine burned gas calculations, and is much more rapid than the extensive NASA equilibrium program.[9, 10]

Several techniques for estimating the *thermodynamic properties* of high-temperature burned gases for engine applications have been developed. One commonly used approach is that developed by Krieger and Borman.[19] The internal energy and gas constant of undissociated combustion products were first described by polynomials in gas temperature. The second step was to limit the range of T and p to values found in internal combustion engines. Then the deviations between the equilibrium thermodynamic property data published by Newhall and Starkman[4, 5] and the calculated nondissociated values were fitted

PETITIONER'S EXHIBIT 1002
US PATENT NO. 6,581,565
Page 1674



(*a*)



(*b*)

FIGURE 4-17
Specific heat at constant pressure for equilibrium, frozen, and fixed composition burned gases as a function of temperature and pressure: (*a*) equivalence ratio $\phi \leq 1.0$; (*b*) equivalence ratio $\phi > 1$. Units: J/kg mixture · K. Fuel: C_nH_{2n}.

by an exponential function of T, p, and ϕ. For $\phi \leq 1$, a single set of equations resulted. For $\phi \geq 1$, sets of equations were developed, each set applying to a specific value of equivalence ratio (see Ref. 19). In general, the fit for internal energy is within $2\frac{1}{2}$ percent over the pressure and temperature range of interest, and the error over most of the range is less than 1 percent. For many applica-

PETITIONER'S EXHIBIT 1002
US PATENT NO. 6,581,565
Page 1675

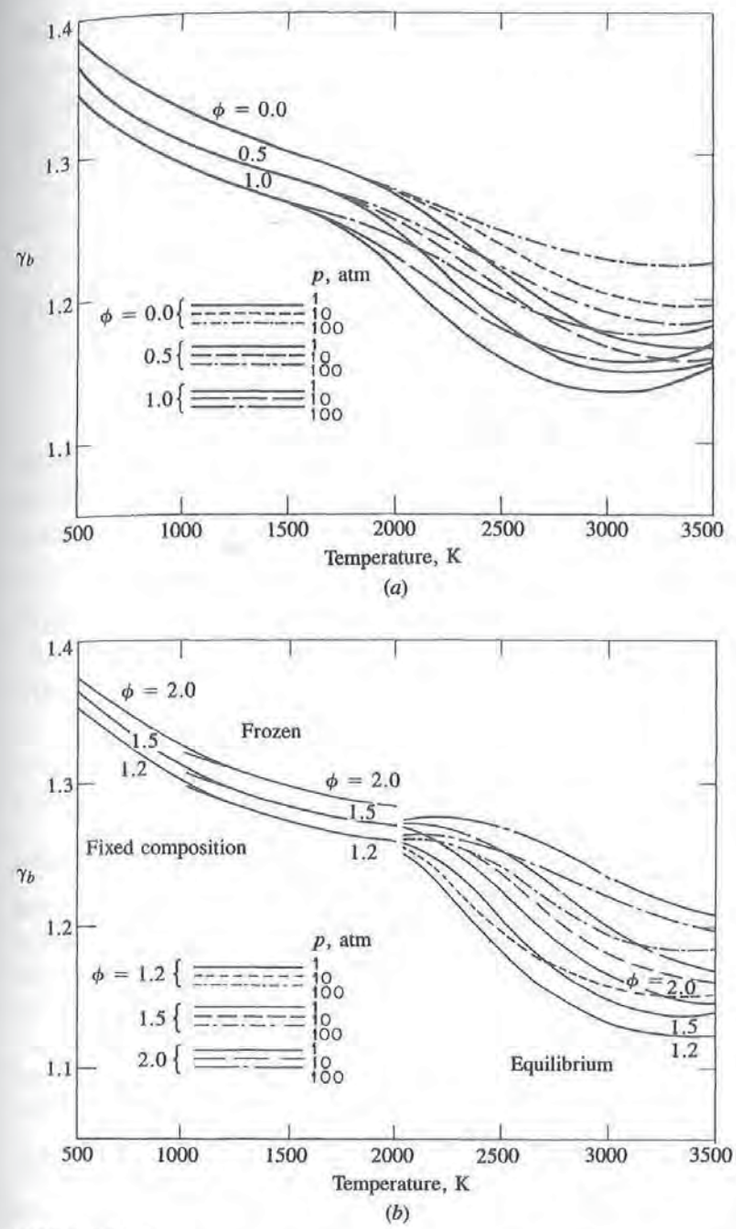


FIGURE 4-18
Ratio of specific heats, $\gamma_b = c_{p,b}/c_{v,b}$, for equilibrium, frozen, and fixed composition burned gases as a function of temperature and pressure: (*a*) equivalence ratio $\phi \leq 1.0$; (*b*) equivalence ratio $\phi > 1$. Fuel: C_nH_{2n}.

tions, the undissociated equations for thermodynamic properties are sufficiently accurate.

An alternative approach for property calculations, applicable to a wide range of hydrocarbon and alcohol fuels, is used extensively in the author's laboratory.[20] With this method, the products of combustion of hydrocarbon (or

PETITIONER'S EXHIBIT 1002
US PATENT NO. 6,581,565
Page 1676

alcohol)-air mixtures are divided into triatomic, diatomic, and monatomic molecules, M_3, M_2, and M_1, respectively. Then, if Y is the extra number of moles of diatomic molecules due to dissociation of triatomic molecules and U is the extra number of monatomic molecules due to dissociation of diatomic molecules, the combustion reaction can be written as

$$\varepsilon\phi C + 2(1-\varepsilon)\phi H_2 + O_2 + \psi N_2 \rightarrow$$
$$[(2-\varepsilon)\phi - 2Y]M_3 + [1 - \phi + 3Y - U + \psi]M_2 + 2UM_1 \qquad \text{for } \phi \leq 1 \qquad (4.45)$$
$$[(2-\varepsilon\phi)\phi - 2Y]M_3 + [2(\phi-1) + 3Y - U + \psi]M_2 + 2UM_1 \qquad \text{for } \phi > 1$$

The method is based upon a fitting of data obtained from sets of detailed chemical equilibrium calculations to this functional form. Two general dissociation reactions:

$$2M_3 = 3M_2 \qquad \text{and} \qquad M_2 = 2M_1$$

are then used with fitted equilibrium constants $K_1(T)$ and $K_2(T)$ to calculate the relative species concentrations. This approach has been developed to give equations for enthalpy which sum the translational, rotational, and vibrational contributions to the specific heat, and the enthalpy of formation:

$$m_{RP}h = \frac{R}{2}(8N_3 + 7N_2 + 5N_1)T + R(3N_3 + N_2)\frac{T_v}{\exp(T_v/T) - 1} + m_{RP}h_f \qquad (4.46)$$

where N_3, N_2, and N_1 are the number of moles of triatomic, diatomic, and monatomic molecules respectively per mole O_2 reactant, T_v is a fitted vibrational temperature, m_{RP} is the mass of products per mole O_2 reactant [Eq. (4.9)], and h_f is the average specific enthalpy of formation of the products.

The molecular weight is given by

$$M_b = \frac{m_{RP}}{1 + (1-\varepsilon)\phi + \psi + Y + U} \qquad \text{for } \phi \leq 1$$
$$\text{or} \qquad M_b = \frac{m_{RP}}{(2-\varepsilon)\phi + \psi + Y + U} \qquad \text{for } \phi > 1 \qquad (4.47)$$

U and Y are found using an approximate solution to the equations obtained by applying the fitted equilibrium constants to the dissociation reactions; h_f is obtained by fitting a correction to the undisssociated products enthalpy of formation. Equations are presented for the partial derivatives of enthalpy h and density ρ with respect to T, p, and ϕ.[20] These relationships have been tested for fuels with H/C ratios of 4 to 0.707, equivalence ratios 0.4 to 1.4, pressures 1 to 30 atm, and temperatures 1000 to 3000 K. The error for burned mixture temperatures relevant to engine calculations is always less than ± 10 K. The errors in density are less than ± 0.2 percent.

PETITIONER'S EXHIBIT 1002
US PATENT NO. 6,581,565
Page 1677

4.8 TRANSPORT PROPERTIES

The processes by which mass, momentum, and energy are transferred from one point in a system to another are called rate processes. In internal combustion engines, examples of such processes are evaporation of liquid fuel, fuel-air mixing, friction at a gas/solid interface, and heat transfer between gas and the walls of the engine combustion chamber. In engines, most of these processes are turbulent and are therefore strongly influenced by the properties of the fluid flow. However, turbulent rate processes are usually characterized by correlations between dimensionless numbers (e.g., Reynolds, Prandtl, Nusselt numbers, etc.), which contain the fluid's transport properties of viscosity, thermal conductivity, and diffusion coefficient as well as the flow properties.

The simplest approach for computing the transport properties is based on the application of kinetic theory to a gas composed of hard-sphere molecules. By analyzing the momentum flux in a plane Couette flow,† it can be shown (Chapman and Cowling, Ref. 21, p. 218) that the viscosity μ of a monatomic hard-sphere gas [where $\mu = \tau/(du/dx)$, τ being the shear stress and (du/dx) the velocity gradient] is given by

$$\mu = \frac{[5/(16\sqrt{\pi})](m\tilde{k}T)^{1/2}}{d^2} \tag{4.48}$$

where m is the mass of the gas molecule, d is the molecular diameter, and $\tilde{k}$ is Boltzmann's constant, 1.381×10^{-23} J/K.

For such a gas, the viscosity varies as $T^{1/2}$, but will not vary with gas pressure or density. Measurements of viscosity show it does only vary with temperature, but generally not proportionally to $T^{1/2}$. The measured temperature dependence can only be explained with more sophisticated models for the intermolecular potential energy than that of a hard sphere. Effectively, at higher temperatures, the higher average kinetic energy of a pair of colliding molecules requires that they approach closer to each other and experience a greater repulsive force to be deflected in the collision. As a result, the molecules appear to be smaller spheres as the temperature increases.

An expression for the thermal conductivity k of a monatomic hard-sphere gas [$k = \dot{q}/(dT/dx)$, where $\dot{q}$ is the heat flux per unit area and dT/dx is the temperature gradient] can be derived from an analysis of the thermal equivalent of plane Couette flow (Ref. 21, p. 235):

$$k = \frac{[75/(64\sqrt{\pi})](\tilde{k}^3 T/m)^{1/2}}{d^2} \tag{4.49}$$

† In Couette flow, the fluid is contained between two infinite plane parallel surfaces, one at rest and one moving with constant velocity. In the absence of pressure gradients, the fluid velocity varies linearly across the distance between the surfaces.

PETITIONER'S EXHIBIT 1002
US PATENT NO. 6,581,565
Page 1678

which has the same temperature dependence as μ. Equations (4.48) and (4.49) can be combined to give

$$k = \tfrac{5}{2}\mu c_v$$

since, for a monatomic gas, the specific heat at constant volume is $3\tilde{k}/(2m)$. This simple equality is in good agreement with measurements of μ and k for monatomic gases.

The above model does not take into account the vibrational and rotational energy exchange in collisions between polyatomic molecules which contribute to energy transport in gases of interest in engines. Experimental measurements of k and μ show that k is less than $\frac{5}{2}\mu c_v$ for such polyatomic gases, where c_v is the sum of the translational specific heat and the specific heat due to internal degrees of freedom. It was suggested by Eucken that transport of vibrational and rotational energy was slower than that of translational energy. He proposed an empirical expression

$$k = \frac{9\gamma - 5}{4}\mu c_v \tag{4.50}$$

or

$$\mathrm{Pr} = \frac{\mu c_p}{k} = \frac{4\gamma}{9\gamma - 5}$$

where Pr is the Prandtl number, which is in good agreement with experimental data.

A similar analysis of a binary diffusion process, where one gas diffuses through another, leads to an expression for the binary diffusion coefficient D_{ij}. D_{ij} is a transport property of the gas mixture composed of species i and j, defined by Fick's law of molecular diffusion which relates the fluxes of species i and j, Γ_{xi} and Γ_{xj}, in the x direction to the concentration gradients, dn_i/dx and dn_j/dx (n is the molecular number density):

$$\Gamma_{xi} = -D_{ij}\left(\frac{dn_i}{dx}\right) \qquad \Gamma_{xj} = -D_{ij}\left(\frac{dn_j}{dx}\right)$$

The binary diffusion coefficient for a mixture of hard-sphere molecules is (Ref. 21, p. 245)

$$D_{ij} = \frac{3}{16nd^2}\left(\frac{2\tilde{k}T}{\pi m_{ij}}\right)^{1/2} \tag{4.51}$$

where m_{ij} is the reduced mass $m_i m_j/(m_i + m_j)$.

A more rigorous treatment of gas transport properties, based on more realistic intermolecular potential energy models, can be found in Hirschfelder *et al.*,[22] who also present methods for computing the transport properties of mixtures of gases. The NASA computer program "Thermodynamic and Transport Properties of Complex Chemical Systems"[10] computes the viscosity, thermal conduc-

PETITIONER'S EXHIBIT 1002
US PATENT NO. 6,581,565
Page 1679

tivity, and Prandtl number in addition to the thermodynamic calculations described in Secs. 3.7 and 4.7 for high-temperature equilibrium and frozen gas composition mixtures. The procedures used in the NASA program to compute these transport properties are based on the techniques described in Hirschfelder *et al.*[22] The NASA program has been used to compute the transport properties of hydrocarbon-air combustion products.[17] These quantities are functions of temperature T, equivalence ratio ϕ, and (except for viscosity) pressure p. Approximate correlations were then fitted to the calculated data of viscosity and Prandtl number. The principal advantage of these correlations is computational speed. For Prandtl number ($\mu c_p/k$), it was found convenient to use γ, the specific heat ratio (c_p/c_v), as an independent variable. Values of γ and c_p then permit determination of the thermal conductivity.

The viscosity of hydrocarbon-air combustion products over the temperature range 500 up to 4000 K, for pressures from 1 up to 100 atm, for $\phi = 0$ up to $\phi = 4$ is shown in Fig. 4-19. The viscosity as a function of temperature of hydrocarbon-air combustion products differs little from that of air. Therefore, a power law based on air viscosity data was used to fit the data:

$$\mu_{\text{air}}(\text{kg/m} \cdot \text{s}) = 3.3 \times 10^{-7} \times T^{0.7} \tag{4.52}$$

where T is in kelvins. The viscosity of combustion products is almost indepen-

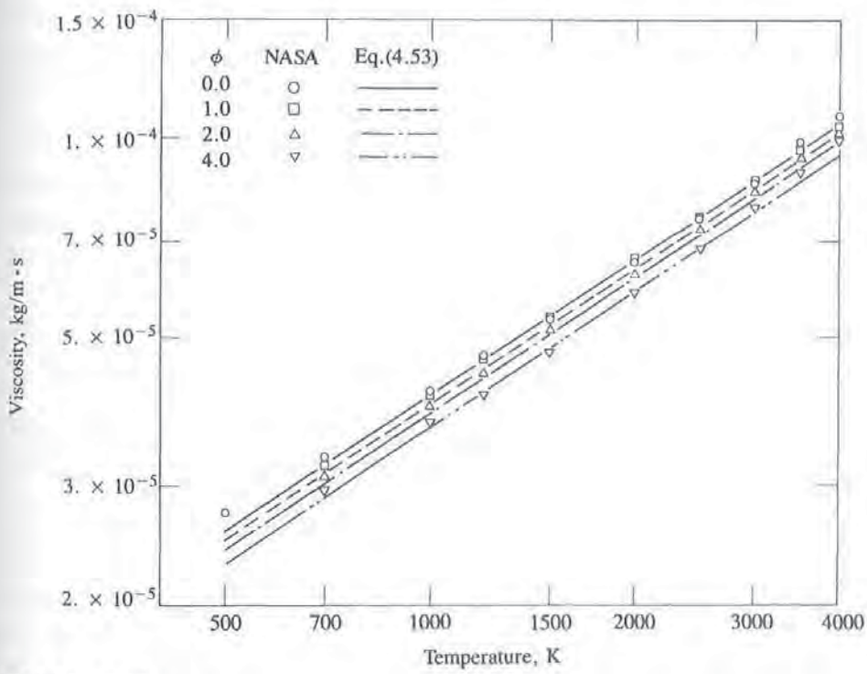


FIGURE 4-19
Viscosity, kg/m·s, of combustion products as a function of temperature and equivalence ratio. Equations shown are (4.52) and (4.53).

PETITIONER'S EXHIBIT 1002
US PATENT NO. 6,581,565
Page 1680

dent of pressure. This correlation was corrected to include the effect of the equivalence ratio ϕ on the viscosity of hydrocarbon-air combustion products:

$$\mu_{\text{prod}} = \frac{\mu_{\text{air}}}{1 + 0.027\phi} \tag{4.53}$$

Figure 4-19 shows that the viscosity predicted using Eqs. (4.52) and (4.53) is very close to the viscosity values calculated with the NASA program. There is less than 4 percent error.

The Prandtl number of hydrocarbon-air combustion products has also been correlated over the above ranges of temperatures, pressures, and equivalence ratios. Since the expression for Prandtl number of a monatomic hard-sphere molecule gas is a function of γ, a second-order polynomial of γ was used to curve-fit the calculated Prandtl number data. A good fit to the data for lean combustion product mixtures was the following:

$$\text{Pr} = 0.05 + 4.2(\gamma - 1) - 6.7(\gamma - 1)^2 \qquad \phi \leq 1 \tag{4.54}$$

The values of Pr predicted with Eq. (4.54) are within 5 percent of the equilibrium Pr values calculated with the NASA program. For rich mixtures the following equation is a good fit to the equilibrium values of Pr using equilibrium values of γ, for temperatures greater than 2000 K:

$$\text{Pr} = \frac{0.05 + 4.2(\gamma - 1) - 6.7(\gamma - 1)^2}{1 + 0.015 \times 10^{-6}(\phi T)^2} \qquad 1 < \phi \leq 4 \tag{4.55}$$

The predicted values of Pr in this case are also close to the calculated values of Pr, with less than 10 percent error. Equation (4.55) is also a reasonable fit to the frozen values† of Pr for rich mixtures, using frozen values of γ, for the temperature range 1200 to 2000 K. As there are no data for Pr of rich mixtures at low temperatures, we suggest that where a fixed composition for the mixture is appropriate (e.g., during the exhaust process in an internal combustion engine), Eq. (4.55) can also be used with fixed composition values of γ.

The Prandtl number can be obtained from the above relations if γ is known. The thermal conductivity can be obtained from the Prandtl number if values of μ and c_p are known. Values of γ_b and $c_{p,b}$ as functions of temperature, pressure, and equivalence ratio are given in Figs. 4-15 to 4-18.

Since the fundamental relations for viscosity and thermal conductivity are complicated, various approximate methods have been proposed for evaluating these transport properties for gas mixtures. A good approximation for the vis-

† In the NASA program, "frozen" means the gas composition is in equilibrium at the given T and p, but is frozen as c_p, c_v, and k are computed.

PETITIONER'S EXHIBIT 1002
US PATENT NO. 6,581,565
Page 1681

cosity of a multicomponent gas mixture is

$$\mu_{\text{mixt}} = \sum_{i=1}^{v} \frac{\tilde{x}_i^2}{\tilde{x}_i^2/\mu_i + 1.385 \sum_{j=1,\, j\neq 1}^{v} \tilde{x}_i \tilde{x}_j (\tilde{R}T/pM_i D_{ij})} \tag{4.56}$$

where $\tilde{x}_i$ and M_i are the mole fraction and molecular weight of the ith species, μ_i is the viscosity of the ith species, v is the number of species in the mixture, and D_{ij} is the binary diffusion coefficient for species i and j.[22]

4.9 EXHAUST GAS COMPOSITION

While the formulas for the products of combustion used in Sec. 3.4 are useful for determining unburned mixture stoichiometry, they do not correspond closely to the actual burned gas composition. At high temperatures (e.g., during combustion and the early part of the expansion stroke) the burned gas composition corresponds closely to the equilibrium composition at the local temperature, pressure, and equivalence ratio. During the expansion process, recombination reactions simplify the burned gas composition. However, late in the expansion stroke and during exhaust blowdown, the recombination reactions are unable to maintain the gases in chemical equilibrium and, in the exhaust process, the composition becomes frozen. In addition, not all the fuel which enters the engine is fully burned inside the cylinder; the combustion inefficiency even when excess air is present is a few percent (see Fig. 3-9). Also, the contents of each cylinder are not necessarily uniform in composition, and the amounts of fuel and air fed to each cylinder of a multicylinder engine are not exactly the same. For all these reasons, the composition of the engine exhaust gases cannot easily be calculated.

It is now routine to measure the composition of engine exhaust gases. This is done to determine engine emissions (e.g., CO, NO_x, unburned hydrocarbons, and particulates). It is also done to determine the relative proportions of fuel and air which enter the engine so that its operating equivalence ratio can be computed. In this section, typical engine exhaust gas composition will be reviewed, and techniques for calculating the equivalence ratio from exhaust gas composition will be given.

4.9.1 Species Concentration Data

Standard instrumentation for measuring the concentrations of the major exhaust gas species has been developed.[23] Normally a small fraction of the engine exhaust gas stream is drawn off into a sample line. Part of this sample is fed directly to the instrument used for unburned hydrocarbon analysis, a flame ionization detector (FID). The hydrocarbons present in the exhaust gas sample are burned in a small hydrogen-air flame, producing ions in an amount proportional to the number of carbon atoms burned. The FID is effectively a carbon atom counter. It is calibrated with sample gases containing known amounts of hydrocarbons. Unburned hydrocarbon concentrations are normally expressed as a mole fraction

PETITIONER'S EXHIBIT 1002
US PATENT NO. 6,581,565
Page 1682

or volume fraction in parts per million (ppm) as C_1. Sometimes results are expressed as ppm propane (C_3H_8) or ppm hexane (C_6H_{14}); to convert these to ppm C_1 multiply by 3 or 6, respectively. Older measurements of unburned hydrocarbons were often made with a nondispersive infrared (NDIR) analyzer, where the infrared absorption by the hydrocarbons in a sample cell was used to determine their concentration.[23] Values of HC concentrations in engine exhaust gases measured by an FID are about two times the equivalent values measured by an NDIR analyzer (on the same carbon number basis, e.g., C_1). NDIR-obtained concentrations are usually multiplied by 2 to obtain an estimate of actual HC concentrations. Substantial concentrations of oxygen in the exhaust gas affect the FID measurements. Analysis of *unburned* fuel-air mixtures should be done with special care.[23] To prevent condensation of hydrocarbons in the sample line (especially important in diesel exhaust gas), the sample line is often heated.

NDIR analyzers are used for CO_2 and CO concentration measurements. Infrared absorption in a sample cell containing exhaust gas is compared to absorption in a reference cell. The detector contains the gas being measured in two compartments separated by a diaphragm. Radiation not absorbed in the sample cell is absorbed by the gas in the detector on one side of the diaphragm. Radiation not absorbed in the reference cell is absorbed by the gas in the other half of the detector. Different amounts of absorption in the two halves of the detector result in a pressure difference being built up which is measured in terms of diaphragm distention. NDIR detectors are calibrated with sample gases of known composition. Since water vapor IR absorption overlaps CO_2 and CO absorption bands, the exhaust gas sample is dried with an ice bath and chemical dryer before it enters the NDIR instrument.

Oxygen concentrations are usually measured with paramagnetic analyzers. Oxides of nitrogen, either the amount of nitric oxide (NO) or total oxides of nitrogen ($NO + NO_2$, NO_x), are measured with a chemiluminescent analyzer. The NO in the exhaust gas sample stream is reacted with ozone in a flow reactor. The reaction produces electronically excited NO_2 molecules which emit radiation as they decay to the ground state. The amount of radiation is measured with a photomultiplier and is proportional to the amount of NO. The instrument can also convert any NO_2 in the sample stream to NO by decomposition in a heated stainless steel tube so that the total NO_x ($NO + NO_2$) concentration can be determined.[23] Gas chromatography can be used to determine all the inorganic species (N_2, CO_2, O_2, CO, H_2) or can be used to measure the individual hydrocarbon compounds in the total unburned hydrocarbon mixture. Particulate emissions are measured by filtering the particles from the exhaust gas stream onto a previously weighed filter, drying the filter plus particulate, and reweighing.

SPARK-IGNITION ENGINE DATA. Dry exhaust gas composition data, as a function of the fuel/air equivalence ratio, for several different multi- and single-cylinder automotive spark-ignition engines over a range of engine speeds and loads are shown in Fig. 4-20. The fuel compositions (gasolines and isooctane) had H/C ratios ranging from 2.0 to 2.25. Exhaust gas composition is substantially

PETITIONER'S EXHIBIT 1002
US PATENT NO. 6,581,565
Page 1683

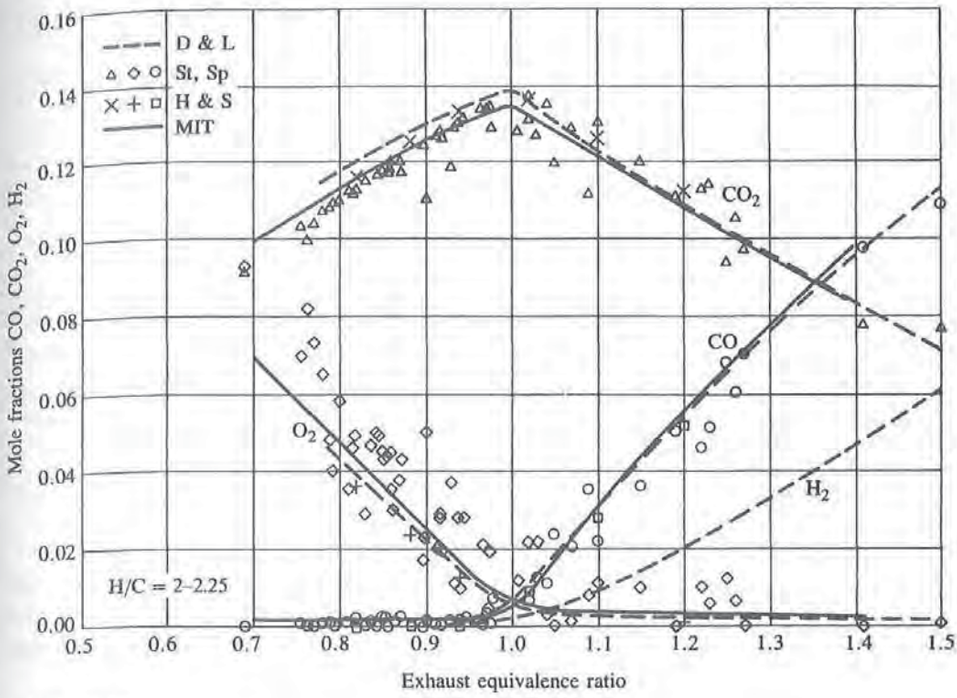


FIGURE 4-20
Spark-ignition engine exhaust gas composition data in mole fractions as a function of fuel/air equivalence ratio. Fuels: gasoline and isooctane, H/C 2 to 2.25. (*From D'Alleva and Lovell,*[24] *Stivender,*[25] *Harrington and Shishu,*[26] *Spindt,*[27] *and data from the author's laboratory at MIT.*)

different on the lean and the rich side of the stoichiometric air/fuel or fuel/air ratios; thus, the fuel/air equivalence ratio ϕ (or its inverse, the relative air/fuel ratio λ) is the appropriate correlating parameter. On the lean side of stoichiometric, as ϕ decreases, CO_2 concentrations fall, oxygen concentrations increase, and CO levels are low but not zero ($\sim$0.2 percent). On the rich side of stoichiometric, CO and H_2 concentrations rise steadily as ϕ increases and CO_2 concentrations fall. O_2 levels are low ($\sim$0.2 to 0.3 percent) but are not zero. At stoichiometric operation, there is typically half a percent O_2 and three-quarters of a percent CO.

Fuel composition has only a modest effect on the magnitude of the species concentrations shown. Measurements with a wide range of liquid fuels show that CO concentrations depend only on the equivalence ratio or relative fuel/air ratio (see Fig. 11-20).[26] A comparison of exhaust CO concentrations with gasoline, propane (C_3H_8), and natural gas (predominantly methane, CH_4) show that only with the high H/C ratio of methane, and then only for CO $\geq$ 4 percent, is fuel composition significant.[28] The values of CO_2 concentration at a given ϕ are slightly affected by the fuel H/C ratio. For example, for stoichiometric mixtures with 0.5 percent O_2 and 0.75 percent CO, as the H/C ratio decreases CO_2 concentrations increase from 13.7 percent for isooctane (H/C = 2.25), to 14.2 to 14.5 percent for typical gasolines (H/C in range 2–1.8), to 16 for toluene (H/C = 1.14).[29]

PETITIONER'S EXHIBIT 1002
US PATENT NO. 6,581,565
Page 1684

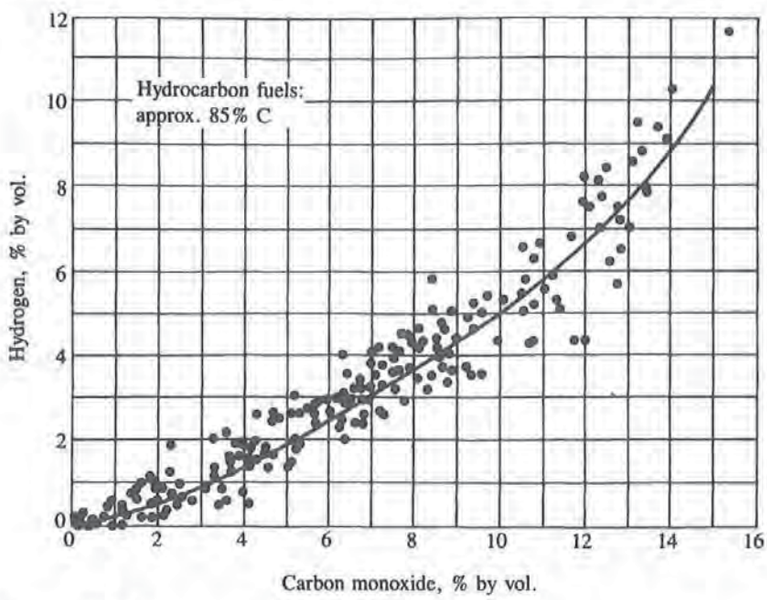


FIGURE 4-21
Hydrogen concentration in spark-ignition engine exhaust as a function of carbon monoxide concentration. Units: percent by volume.[30]

Unburned hydrocarbon exhaust concentrations vary substantially with engine design and operating conditions. Spark-ignition engine exhaust levels in a modern low-emission engine are typically of the order of 2000 ppm C_1 with liquid hydrocarbon fuels, and about half that level with natural gas and propane fuels.

Hydrogen concentrations in engine exhaust are not routinely measured. However, when the mixture is oxygen-deficient—fuel rich—hydrogen is present with CO as an incomplete combustion product. Figure 4-21 summarizes much of the available data on H_2 concentrations plotted as a function of CO.[30]

DIESEL EXHAUST DATA. Since diesels normally operate significantly lean of stoichiometric ($\phi \leq 0.8$) and the diesel combustion process is essentially complete (combustion inefficiency is ≤ 2 percent), their exhaust gas composition is straightforward. Figure 4-22 shows that O_2 and CO_2 concentrations vary linearly with the fuel/air equivalence ratio over the normal operating range. Diesel emissions of CO and unburned HC are low.

4.9.2 Equivalence Ratio Determination from Exhaust Gas Constituents

Exhaust gas composition depends on the relative proportions of fuel and air fed to the engine, fuel composition, and completeness of combustion. These relationships can be used to determine the operating fuel/air equivalence ratio of an engine from a knowledge of its exhaust gas composition. A general formula for

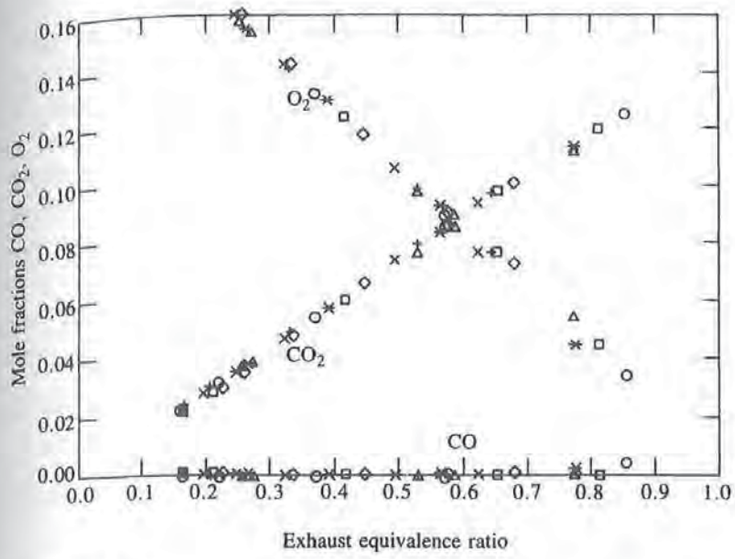


FIGURE 4-22
Exhaust gas composition from several diesel engines in mole fractions on a dry basis as a function of fuel/air equivalence ratio.[31]

the composition of fuel can be represented as $C_nH_mO_r$. For conventional petroleum-based fuels, oxygen will be absent; for fuels containing alcohols, oxygen will be present. The overall combustion reaction can be written as

$$\text{Fuel} + \text{oxidizer} \rightarrow \text{products}$$

The fuel is $C_nH_mO_r$; the oxidizer is air ($O_2 + 3.773N_2$). The products are CO_2, H_2O, CO, H_2, O_2, NO_x, N_2, unburned hydrocarbons (unburned fuel and products of partial fuel reaction), and soot particles (which are mainly solid carbon). The amount of solid carbon present is usually sufficiently small (≤ 0.5 percent of the fuel mass) for it to be omitted from the analysis. The overall combustion reaction can be written explicitly as

$$C_nH_mO_r + \frac{n_{O_2}}{\phi}(O_2 + 3.773N_2) = n_P(\tilde{x}_{C_aH_b}C_aH_b + \tilde{x}_{CO}CO + \tilde{x}_{CO_2}CO_2 + \tilde{x}_{O_2}O_2 + \tilde{x}_{N_2}N_2 + \tilde{x}_{NO}NO + \tilde{x}_{NO_2}NO_2 + \tilde{x}_{H_2O}H_2O + \tilde{x}_{H_2}H_2) \quad (4.57)$$

where ϕ is the measured equivalence ratio $[(F/A)_{\text{actual}}/(F/A)_{\text{stoichiometric}}]$, n_{O_2} is the number of O_2 molecules required for complete combustion ($n + m/4 - r/2$), n_P is the total number of moles of exhaust products, and $\tilde{x}_i$ is the mole fraction of the ith component.

There are several methods for using Eq. (4.57) to determine ϕ, the equivalence ratio, depending on the amount of information available. Normally CO_2, CO, O_2, NO_x concentrations as mole fractions and unburned hydrocarbon (as

PETITIONER'S EXHIBIT 1002
US PATENT NO. 6,581,565
Page 1686

mole fraction or ppm C_1, i.e., $\tilde{x}_{CH_{b/a}}$) are measured. The concentration of the inorganic gases are usually measured *dry* (i.e., with H_2O removed) or *partially dry*. Unburned hydrocarbons may be measured *wet* or *dry* or *partially dry*. NO_x is mainly nitric oxide (NO); its concentration is usually sufficiently low (<0.5 percent) for its effect on equivalence ratio determination to be negligibly small. Thus, in Eq. (4.57) there are seven unknowns which are: ϕ, $\tilde{x}_{H_2}$, $\tilde{x}_{H_2O}$, $\tilde{x}_{N_2}$, n_P, a, b. (There will be additional unknowns if the measurements listed above are incomplete.)

To solve for these unknowns we need seven additional equations. We can obtain five equations using an atomic balance for each element and the definition of mole fraction, as follows:

Carbon balance:

$$n = n_P(a\tilde{x}_{C_aH_b} + \tilde{x}_{CO} + \tilde{x}_{CO_2}) \tag{4.58}$$

Hydrogen balance:

$$m = n_P(b\tilde{x}_{C_aH_b} + 2\tilde{x}_{H_2O} + 2\tilde{x}_{H_2}) \tag{4.59}$$

Oxygen balance:

$$r + \frac{2n_{O_2}}{\phi} = n_P(\tilde{x}_{CO} + 2\tilde{x}_{CO_2} + \tilde{x}_{NO} + 2\tilde{x}_{O_2} + \tilde{x}_{H_2O}) \tag{4.60}$$

Nitrogen balance:

$$\frac{7.546n_{O_2}}{\phi} = n_P(2\tilde{x}_{N_2} + \tilde{x}_{NO}) \tag{4.61}$$

Mole fractions add up to 1:

$$\tilde{x}_{C_aH_b} + \tilde{x}_{CO} + \tilde{x}_{H_2} + \tilde{x}_{H_2O} + \tilde{x}_{N_2} + \tilde{x}_{NO} + \tilde{x}_{CO_2} + \tilde{x}_{O_2} = 1 \tag{4.62}$$

An additional assumption is made, based on available exhaust gas composition data, that CO_2, CO, H_2O, and H_2 concentrations are related by

$$\frac{\tilde{x}_{CO}\,\tilde{x}_{H_2O}}{\tilde{x}_{CO_2}\,\tilde{x}_{H_2}} = K \tag{4.63}$$

where K is a constant.† Values of 3.8[24, 25] and 3.5[27] are commonly used for K. The difference between these values has little effect on the computed magnitude of ϕ. To complete the analysis, various assumptions are made concerning the composition and relative importance of the unburned hydrocarbons. The most common approaches are summarized below.

† Equation (4.63) is often described as assuming a specific value for the water-gas reaction equilibrium constant. In fact K is an empirical constant determined from exhaust gas composition data.

PETITIONER'S EXHIBIT 1002
US PATENT NO. 6,581,565
Page 1687

OXYGEN BALANCE AIR/FUEL AND EQUIVALENCE RATIOS. For fuels comprised of carbon and hydrogen only, when all species are measured with the *same background moisture* (wet, dry, or partially dry), the following expression based on the ratio of measured and computed oxygen-containing species to measured carbon-containing species gives the air/fuel ratio. It has been assumed that the unburned hydrocarbons have the same C/H ratio as the fuel:[32]

$$\left(\frac{A}{F}\right) = 4.773 \left(\frac{M_{\text{air}}}{M_f}\right) \frac{(CO_2) + (CO)/2 + (H_2O)/2 + (NO)/2 + (NO_2) + (O_2)}{(HC) + (CO) + (CO_2)} \tag{4.64}$$

where ( ) are molar concentrations (all with the same background moisture) in percent, $M_{\text{air}} = 28.96$, $M_f = 12.01 + 1.008y$ where y is the H/C ratio of the fuel, (HC) is molar percent unburned hydrocarbons as C_1, and

$$(H_2O) = 0.5y \frac{(CO_2) + (CO)}{(CO)/[K(CO_2)] + 1} \tag{4.65}$$

Since nitrogen oxides collectively comprise less than 0.5 percent of the exhaust mixture, their concentrations can be omitted with negligible error.

The fuel/air equivalence ratio ϕ is obtained from the ratio of the stoichiometric air/fuel ratio [Eq. (3.6)] and Eq. (4.64) above.

CARBON BALANCE AIR/FUEL AND EQUIVALENCE RATIOS. When oxygen analysis is not available, for fuels comprised of carbon and hydrogen only, a carbon balance air/fuel ratio may be employed:[25, 32]

$$\frac{A}{F} = \frac{M_{\text{air}}}{M_f} \left[\frac{100 + (HC) - (CO)/2 + 3(H_2O)/2 - (H_2O)_a}{(HC) + (CO) + (CO_2)} - \frac{y}{2} \right] \tag{4.66}$$

The symbols are as defined above. (H_2O) is the molar percent water in the combustion products defined by Eq. (4.65) and $(H_2O)_a$ is the molar percent water vapor at the analyzers.

This carbon balance (A/F) is sensitive to moisture concentration at the analyzers. The use of ice bath exhaust sample chillers generally reduces the $(H_2O)_a$ term to less than 1 percent and little accuracy is then lost by neglecting it. For completely "wet" analysis (uncondensed), $(H_2O)_a = (H_2O)$, and Eq. (4.66) is accurate. For partially dry exhaust gas analysis, knowledge of the dew point of the mixture will provide the $(H_2O)_a$ term by reference to steam tables.

The fuel/air equivalence ratio ϕ is obtained from the ratio of the stoichiometric air/fuel ratio [Eq. (3.6)] and Eq. (4.66) above.

EQUIVALENCE RATIO BASED ON WET HC AND DRY INORGANIC GAS ANALYSIS. Engine exhaust gas composition is often determined by analyzing a fully dried sample stream for CO_2, CO, O_2, and NO_x, and a fully wet (uncondensed) stream with an FID for unburned hydrocarbons. Equations (4.64) and (4.66) are not applicable under these circumstances. The following equations

PETITIONER'S EXHIBIT 1002
US PATENT NO. 6,581,565
Page 1688

define the exhaust gas composition and equivalence ratio under these conditions. The notation $\tilde{x}_i$ denotes the wet mole fraction of species i and $\tilde{x}_i^*$ denotes the dry mole fraction of species i. Equations (4.57) to (4.62), with Eq. (4.63) to relate CO_2, CO, H_2O, and H_2 concentrations and the assumption that $b/a = m/n$, were used to derive these results. The equations apply for a fuel of composition $C_mH_nO_r$.

The fuel/air equivalence ratio is given by

$$\phi = \frac{2n_{O_2}}{n_P \tilde{x}_{H_2O} + n_P(1 - \tilde{x}_{H_2O})(\tilde{x}^*_{CO} + 2\tilde{x}^*_{CO_2} + 2\tilde{x}^*_{O_2} + \tilde{x}^*_{NO} + 2\tilde{x}^*_{NO_2}) - r} \tag{4.67}$$

where the wet and dry mole fractions are related by

$$\tilde{x}_i = (1 - \tilde{x}_{H_2O})\tilde{x}_i^*$$

and

$$\begin{aligned}
n_P &= \frac{n}{\tilde{x}_{CH_{b/a}} + (1 - \tilde{x}_{H_2O})(\tilde{x}^*_{CO} + \tilde{x}^*_{CO_2})} \\
\tilde{x}_{H_2O} &= \frac{m}{2n} \frac{\tilde{x}^*_{CO} + \tilde{x}^*_{CO_2}}{[1 + \tilde{x}^*_{CO}/(K\tilde{x}^*_{CO_2}) + (m/2n)(\tilde{x}^*_{CO} + \tilde{x}^*_{CO_2})]} \\
\tilde{x}_{H_2} &= \frac{\tilde{x}_{H_2O}\,\tilde{x}^*_{CO}}{K\tilde{x}^*_{CO_2}} \\
\tilde{x}_{N_2} &= \frac{3.773 n_{O_2}}{\phi n_P} - (1 - \tilde{x}_{H_2O})\frac{(\tilde{x}^*_{NO} + \tilde{x}^*_{NO_2})}{2}
\end{aligned} \tag{4.68}$$

Note that $\tilde{x}_{CH_{b/a}}$ is the measured (wet) HC concentration as a mole fraction C_1 (ppm $C_1 \times 10^{-6}$): $\tilde{x}_{CH_{b/a}} = a\tilde{x}_{C_aH_b}$. Figure 4-23 shows wet exhaust gas concentrations, based on the MIT measured dry concentrations of CO_2, CO, O_2 shown in Fig. 4-20, and wet HC concentration, as well as Eqs. (4.68).

For lean mixtures, varying the value of K between 1.5 and 5.5 had a negligible effect on the value of ϕ computed from Eq. (4.67). For stoichiometric mixtures, varying K from 2.5 to 4.5 varied the computed ϕ by 2 to 3 percent. For $\phi \approx 1.2$, varying K from 2.5 to 4.5 varied the computed ϕ by 3 to 4 percent. The error in ϕ involved in omitting NO_x is 0.2 percent for an NO_x level of 1000 ppm, increasing to 1 percent for an NO_x level of 5000 ppm. The sensitivity of the computed ϕ to errors in the measurements of CO_2, CO, and O_2 is modest within the normal range of ϕ used. A 2 percent error in CO_2 or CO or O_2 at $\phi \approx 1$ gives about a 0.1 percent error in computed ϕ. For leaner and richer mixtures, the error in ϕ increases for errors in measured CO_2 concentration, and CO ($\phi > 1$) and O_2 ($\phi < 1$) concentrations, but is still significantly less than the measurement error in fuel and air flow.

4.9.3 Effects of Fuel/Air Ratio Nonuniformity

Neither the masses of air inducted into the different cylinders of a multicylinder engine per cycle nor the masses of fuel which enter the different cylinders per

PETITIONER'S EXHIBIT 1002
US PATENT NO. 6,581,565
Page 1689

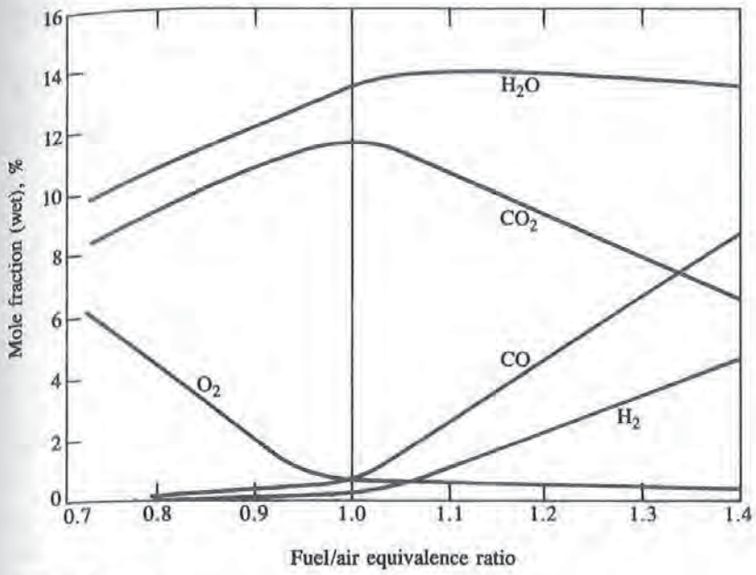


FIGURE 4-23
Wet exhaust gas species concentrations as a function of fuel/air equivalence ratio, based on the dry exhaust gas composition data in Fig. 4-20 and Eqs. (4.68).

cycle are exactly equal. In addition, mixing of fuel and air within each cylinder is not necessarily completely uniform. Thus the exhaust gas composition may correspond to a distribution in the fuel/air ratio in the unburned mixture about the mean value. For example, if the mean fuel/air ratio is stoichiometric, extra oxygen will be contributed by any cylinders operating lean of the average and extra carbon monoxide by any cylinders rich of the average, so that the exhaust gas will have higher levels of O_2 and CO (and a lower level of CO_2) relative to an engine operating with identical fuel/air ratios in each cylinder.

Eltinge has developed a method for defining this nonuniformity in the fuel/air ratio distribution for spark-ignition engines which operate close to stoichiometric.[29] A function $f(x)$ for the fuel/air ratio distribution ($x = F/A$) was assumed, with standard deviation S_x. For each value of x (i.e., F/A), complete utilization of the available oxygen was assumed (i.e., no exhaust HC) and the CO_2, H_2O, CO, H_2 concentrations were related by Eq. (4.63) (with $K = 3.5$). The concentrations of each species for each (F/A) were weighted by the distribution function $f(x)$ and summed to produce the average exhaust concentration. (A correction to allow for the presence of unburned HC in the exhaust was also developed.) Figure 4-24 shows one set of results, for a fuel H/C ratio of 1.8 (typical of gasoline), for a normal distribution in the fuel/air ratio. For each mean (F/A) and maldistribution parameter S_x (the standard deviation of the F/A distribution) the corresponding dry concentrations of CO_2, CO, and O_2 are shown. This type of information can be used to define the fuel-air mixture nonuniformities in spark-ignition engines operating relatively close to stoichiometric. For diesel engines the variations of major exhaust gas species concentrations with fuel/air equiva-

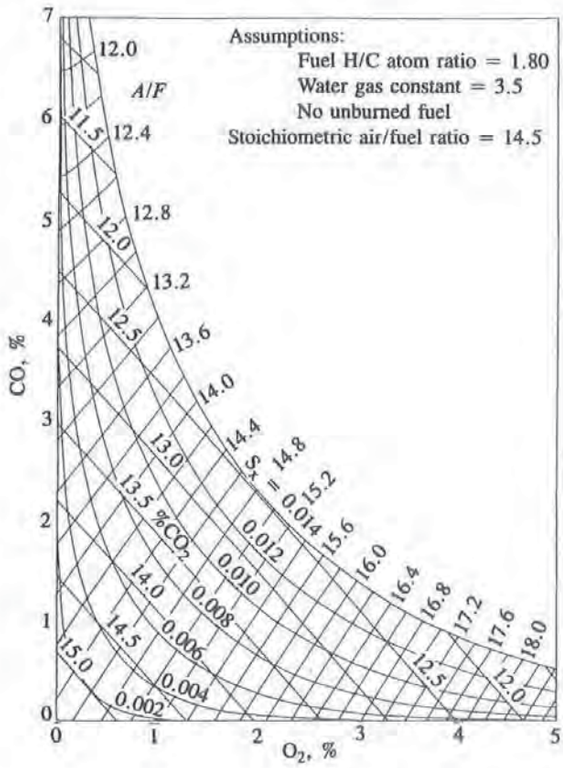


FIGURE 4-24
Computed relationship between dry exhaust gas composition (CO_2, CO, and O_2), air/fuel ratio, and maldistribution parameter S_x. Fuel: $(CH_{1.8})_n$. The correction to be added to the burned gas (F/A) which allows for the measured unburned hydrocarbon concentration is $4.7 \times 10^{-7} \times$ HC (ppm C_1) (*From Eltinge.*[29])

lence ratio are linear, so the effects of any nonuniformities are not apparent in this manner (see Fig. 4-22).

4.9.4 Combustion Inefficiency

Internal combustion engine exhaust contains combustible species: CO, H_2, unburned hydrocarbons, and particulates. When their concentrations are known, the combustion efficiency η_c given by Eq. (3.27) can be calculated. The chemical energy carried out of the engine in these combustibles represents the combustion inefficiency, $1 - \eta_c$:

$$1 - \eta_c = \frac{\sum_i x_i Q_{\mathrm{HV}_i}}{[\dot{m}_f/(\dot{m}_a + \dot{m}_f)]Q_{\mathrm{HV}_f}} \tag{4.69}$$

where the x_i are the mass fractions of CO, H_2, HC, and particulates, respectively, the Q_{HV_i} are the lower heating values of these species, and the subscripts f and a denote fuel and air. The heating values for CO (10.1 MJ/kg) and H_2(120 MJ/kg) are well defined. The composition of the unburned HC is not usually known. However, the heating values of hydrocarbons are closely comparable, so the fuel heating value (typically 42 to 44 MJ/kg) is used. The particulates (only present in diesels) are soot with some adsorbed hydrocarbons; usually the mass fraction is low enough for their contribution to be small, and a heating value for solid carbon (32.8 MJ/kg) can be used. Combustion efficiency data as a function of equivalence ratio have already been presented in Fig. 3-9.

PETITIONER'S EXHIBIT 1002
US PATENT NO. 6,581,565
Page 1691

PROBLEMS

4.1. (*a*) Calculate the low-temperature burned gas composition resulting from the combustion of 7 g/s air with 0.48 g/s ethane (C_2H_6). Assume K = 3.5 in Eq. (4.6).
(*b*) Calculate the low-temperature burned gas composition for the combustion of 7 g/s air with 0.48 g/s ethanol (C_2H_6O). Assume K = 3.5 in Eq. (4.6). (Note the large difference in burned gas composition due to this difference in fuel.)

4.2. To evaluate the accuracy of the simple analytic ideal gas model, use the results of Example 4.1 and Eqs. (4.23) (constant-volume adiabatic combustion) and (4.24) (constant-pressure adiabatic combustion) to calculate T_b for a stoichiometric isooctane-air mixture. Compare this result with that obtained using Figs. 4-3 and 4-8. Assume the following unburned mixture conditions: $T = 700$ K, $v = 0.125$ m^3/kg air, $p = 15$ atm, and $x_b = 0.1$.

4.3. (*a*) In Fig. 4-1, why does M_u decrease as x_b increases?
(*b*) In Fig. 4-14, why does M_b decrease as T increases?
(*c*) In Fig. 4-14, why does M_b decrease as ϕ increases?

4.4. Show how, for an ideal gas with fixed composition, the molecular weight M is related to the specific heats c_p and c_v, and $\tilde{R}$. Use Figs. 4-15 and 4-16 to calculate M_b for $T_b = 1750$, 2250, and 2750 K, and $\phi = 1.0$. Compare these results with values of M_b obtained from Fig. 4-14 and explain any differences.

4.5. EGR, exhaust gas recirculation, is often used to reduce NO_x by acting as a diluent in the intake mixture.
(*a*) For low-temperature isooctane-air combustion products at $\phi = 1.0$, determine the percentage of the burned gases' average specific heat at constant pressure which comes from each component in the burned gas mixture.
(*b*) Compare the specific heat at constant pressure of isooctane-air combustion products at $\phi = 1.0$ to that of air, both at 1750 K. This difference is one reason why EGR instead of leaner fuel-air mixture is used to control NO_x emissions.

4.6. Explain qualitatively the causes of the trends in the curves in Fig. 4-23 as ϕ is increased from 1.0 and decreased from 1.0.

4.7. Compare the O_2, CO_2, and CO data in Fig. 4-22 with the predictions of the elemental balance in Table 4.3. Explain any differences. Assume diesel fuel is a hydrocarbon with H/C ratio of 2.

4.8. The following exhaust data were obtained from a four-stroke cycle spark-ignition engine. CO, CO_2, and NO_x molar concentrations are all measured fully dry; HC is measured fully wet as ppm C_1. Determine the fuel/air equivalence ratio ϕ for the following three sets of data. Make the following assumptions: (1) the constant K in Eq. (4.63) equals 3.5; (2) the fuel composition is $C_8H_{15.12}$; (3) the unburned hydrocarbon H/C ratio is the same as that of the fuel; and (4) NO_x is entirely NO.
(*a*) CO_2 14.0%, CO 0.64%, O_2 0.7%, NO_x 3600 ppm, HC 3200 ppm.
(*b*) CO_2 13.8%, CO 3.05%, O_2 0%, NO_x 1600 ppm, HC 3450 ppm.
(*c*) CO_2 12.5%, CO 0.16%, O_2 4.0%, NO_x 4600 ppm, HC 2100 ppm.

4.9. The exhaust from a spark-ignition engine has the following composition (in mole fractions):

$$CO_2 = 0.12;\ H_2O = 0.14;\ CO = 0.01;\ H_2 = 0.005;$$

$$N_2 = 0.7247;\ C_8H_{18} = 0.0003$$

The fuel is isooctane, C_8H_{18}; as shown above, a small fraction of the fuel escapes

PETITIONER'S EXHIBIT 1002
US PATENT NO. 6,581,565
Page 1692

from the cylinder unburned. The lower heating value of isooctane is 44.4 MJ/kg, of carbon monoxide is 10.1 MJ/kg, and of hydrogen is 120 MJ/kg. The atomic weights of the elements are: C = 12, O = 16, H = 1, N = 14.

(*a*) Calculate the combustion *in*efficiency in the engine; i.e., the percentage of the entering fuel enthalpy which is not fully released in the combustion process and leaves the engine in the exhaust gases (for this problem, the exhaust can be assumed to be at room temperature).

(*b*) What fraction of this inefficiency is due to the unburned fuel emissions?

4.10. A 2-liter displacement four-cylinder engine, operating at 2000 rev/min and 30 percent of its maximum power at that speed, has the following exhaust composition (in percent by volume or mole percent):

CO_2, 11%; H_2O, 11.5%; CO, 0.5%; H_2, 0%; O_2, 2%; unburned hydrocarbons (expressed as CH_2, i.e., with a molecular weight of 14), 0.5%; N_2, 74.5%

The fuel is $(CH_2)_n$ with a heating value of 44 MJ/kg. The atomic weights of the elements are C = 12, H = 1, O = 16, N = 14. The heating values of CO and HC are 10 and 44 MJ/kg, respectively.

(*a*) Is the engine a diesel or spark-ignition engine? Is there enough oxygen in the exhaust to burn the fuel completely? Briefly explain.

(*b*) Calculate the fraction of the input fuel energy ($m_f Q_{HV}$) which exits the engine unburned as (1) CO and (2) unburned HC.

(*c*) An inventor claims a combustion efficiency of 100 percent can be achieved. What percentage improvement in engine specific fuel consumption would result?

4.11. A gasoline engine operates steadily on a mixture of isooctane and air. The air and fuel enter the engine at 25°C. The fuel consumption is 3.0 g/s. The output of the engine is 50 kW. The temperature of the combustion products in the exhaust manifold is 660 K. At this temperature, an analysis of the combustion products yields the following values (on a dry volumetric basis):

CO_2, 11.4%; O_2, 1.6%; CO, 2.9%; N_2, 84.1%

(*a*) Find the composition in moles (number of moles per mole of isooctane) of the reactants and the reaction products.

(*b*) Determine the heat-transfer rate from the working fluid as the working fluid passes through the engine.

Constants for the calculations:

	Enthalpy of formation, kJ/kmol	Sensible enthalpy at 660 K, kJ/kmol
C_8H_{18}	−259280	—
CO_2	−393522	15823
CO	−110529	10789
H_2O	−241827	12710
O_2	—	11200
N_2	—	10749

4.12. A direct-injection four-stroke cycle diesel engine is used to provide power for pumping water. The engine operates at its maximum rated power at 2000 rev/min,

PETITIONER'S EXHIBIT 1002
US PATENT NO. 6,581,565
Page 1693

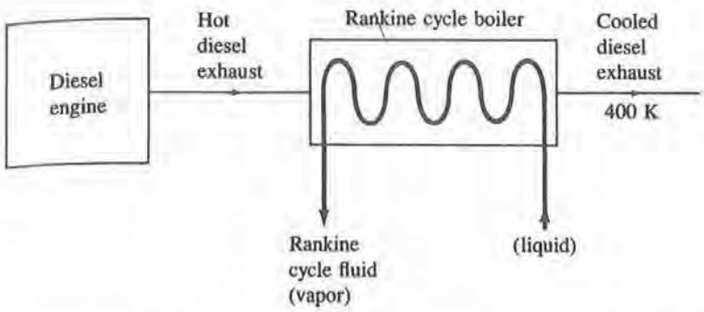


FIGURE P4-12

with an equivalence ratio of 0.8 and an air flow of 0.5 kg/s. The gross indicated fuel conversion efficiency is 45 percent, and the heat losses from the working fluid to the engine coolant and elsewhere within the engine are 280 kW. Diesel fuel has a heating value of 42 MJ/kg and stoichiometric fuel/air ratio of 0.067. Fuel and air enter the engine at ambient conditions. The mechanical efficiency of the diesel engine is 85 percent.

(*a*) Calculate the rated brake power of the engine, the average sensible enthalpy of the exhaust gases as they leave the engine, and the average exhaust gas temperature.

(*b*) Since the exhaust gas temperature is significantly above ambient, the advantages of using the diesel exhaust gas stream to heat the boiler of a Rankine cycle (see sketch) and generate additional power are to be explored. If the exhaust gases *leave* the Rankine-cycle system boiler at 400 K and 30 percent of the heat transferred from the exhaust gas stream in the boiler is converted to power at the Rankine-cycle power plant drive shaft, calculate the additional power obtained and the brake fuel conversion efficiency of the combined cycle system (diesel plus Rankine cycle).

4.13. A diesel engine has a compression ratio of 22 : 1. The conditions in the cylinder at the start of compression are $p = 101.3$ kPa and $T = 325$ K. Calculate the pressure and temperature at the end of compression, assuming the compression process is isentropic:

(*a*) Assume the cylinder contains an ideal gas with $\gamma = 1.4$ and $R = 287$ J/kg·K.

(*b*) Assume the cylinder contains air which may be regarded as a semiperfect gas (use the gas tables).

(*c*) Compare the work of compression in (*a*) and (*b*) above.

In practice, heat losses reduce the final compression temperature by 100 K. For a diesel engine operating at an equivalence ratio of 0.75 (full load):

(*d*) Calculate the ratio of heat loss during compression to the fuel energy added per cycle.

4.14. While the geometric compression ratio of an engine is V_{max}/V_{min}, the actual compression process starts somewhere between bottom-center and when the inlet valve closes, and it is conditions at time of spark (for an SI engine) or fuel injection (for a CI engine) that determine ignition. At low engine speed, compression starts about the time when the inlet valve closes. With this assumption, for the diesel engine of Prob. 4.13, calculate the air pressure and temperature at the start of injection. The inlet valve closes at 30° after BC; injection commences 15° before TC. Use the gas tables. Compare your answers with those of Prob. 4.13(*b*).

PETITIONER'S EXHIBIT 1002
US PATENT NO. 6,581,565
Page 1694

4.15. Use an equilibrium computer code (which calculates the composition and properties of chemically reacting gas mixtures in equilibrium) to calculate the data you need for the following graphs:

(*a*) Values of c_p, γ, molecular weight, and gas composition (mole fractions of N_2, CO_2, H_2O, CO, H_2, O_2, OH, O, H, and NO) as a function of the equivalence ratio ($\phi = 0.2$ to 1.4) for products of combustion of isooctane (C_8H_{18}) with air at $p = 40$ atm and $T = 2500$ K. Put all species concentrations on the same graph. Use a log scale for the composition axis.

(*b*) Unburned mixture consisting of isooctane vapor and air at 700 K and 20 atm is burned first at constant pressure and then at constant volume.

(1) Calculate the enthalpy and internal energy of isooctane vapor at 700 K in cal/gmol; also calculate the volume per unit mass of mixture (cm^3/g) for $\phi = 0.2, 0.4, 0.6, 0.8, 1.0, 1.2, 1.4$.

(2) Use these data and the equilibrium program to calculate the temperature attained after combustion at constant pressure, and temperature and pressure attained after combustion at constant volume. Plot these temperatures and pressures against the equivalence ratio ϕ.

Thermodynamic data for isooctane vapor

T, K	$\tilde{c}_p$, cal/mol·K	$\tilde{h} - \tilde{h}_{298}$, kcal/mol	$\Delta\tilde{h}_f^\circ$, kcal/mol
298	45.14	0.00	−53.57
700	85.66	27.02	−62.79

4.16. A heavy wall bomb with a volume of 1000 cm^3 contains a mixture of isooctane with the stoichiometric air requirement at $p = 101.3$ kPa and $T = 25°C$. The mixture is then ignited with a spark. Find the pressure and temperature of the equilibrium combustion products just after combustion is complete (i.e., before heat losses to the wall are significant). Assume the burned gases are uniform.

4.17. A gas engine, running on a gaseous mixture of butane, C_4H_{10}, and air has the following conditions in the cylinder prior to constant-volume adiabatic combustion: pressure, 6.48×10^5 N/m^2; temperature, 600 K. The charge composition is air plus 50 percent of the stoichiometric quantity of butane fuel. Calculate the pressure and temperature at the end of combustion using the data given below.

For air	T, K	$\tilde{u}$, J/gmol
	298	6,161
	600	12,596
For butane	T, K	$\tilde{u}$, J/gmol
	298	−77
	600	38,424

PETITIONER'S EXHIBIT 1002
US PATENT NO. 6,581,565
Page 1695

Internal energy of combustion of butane at 298 K is $\Delta\tilde{u} = -2.659$ MJ/gmol. Extract from gas tables for products of combustion for 50 percent stoichiometric fuel:

T, K	$\tilde{u}$, J/gmol
298	6,293
2075	54,227
2080	54,380

REFERENCES

1. Komiyama, K., and Heywood, J. B.: "Predicting NO_x Emissions and the Effects of Exhaust Gas Recirculation in Spark-Ignition Engines," SAE paper 730475, *SAE Trans.*, vol. 82, 1973.
2. Danieli, G., Ferguson, C., Heywood, J., and Keck, J. "Predicting the Emissions and Performance Characteristics of a Wankel Engine," SAE paper 740186, *SAE Trans.*, vol. 83, 1974.
3. Hottel, H. C., Williams, G. C., and Satterfield, C. N.: *Thermodynamic Charts for Combustion Processes*, John Wiley, 1949. See also charts in C. F. Taylor, *The Internal Combustion Engine in Theory and Practice*, vol. 1, MIT Press, 1960.
4. Newhall, H. K., and Starkman, E. S.: "Thermodynamic Properties of Octane and Air for Engine Performance Calculations," in *Digital Calculations of Engine Cycles, Progress in Technology*, vol. TP-7, pp. 38–48, SAE, 1964.
5. Starkman, E. S., and Newhall, H. K.: "Thermodynamic Properties of Methane and Air, and Propane and Air for Engine Performance Calculations," SAE paper 670466, *SAE Trans.*, vol. 76, 1967.
6. Keenan, J. H., Chao, J., and Kaye, J.: *Gas Tables*, 2d ed., John Wiley, 1983.
7. Reynolds, W. C.: *Thermodynamic Properties in SI; Graphs, Tables, and Computational Equations for Forty Substances*, Department of Mechanical Engineering, Stanford University, 1979.
8. *JANAF Thermochemical Tables*, 2d ed., NSRDS-NB537, U.S. National Bureau of Standards, June 1971.
9. Gordon, S., and McBride, B. J.: "Computer Program for the Calculation of Complex Chemical Equilibrium Composition, Rocket Performance, Incident and Reflected Shocks, and Chapman-Jouguet Detonations," NASA publication SP-273, 1971 (NTIS number N71-37775).
10. Svehla, R. A., and McBride, B. J.: "Fortran IV Computer Program for Calculation of Thermodynamic and Transport Properties of Complex Chemical Systems," NASA technical note TND-7056, 1973 (NTIS number N73-15954).
11. Fremont, H. A., *et al.*: *Properties of Combustion Gases*, General Electric Company, Cincinnati, Ohio, 1955.
12. Banes, B., McIntyre, R. W., and Sims, J. A.: *Properties of Air and Combustion Products with Kerosene and Hydrogen Fuels*, vols. I–XIII, Propulsion and Energetics Panel, Advisory Group for Aerospace Research and Development (AGARD), NATO, published by Bristol Siddeley Engines Ltd., Filton, Bristol, England, 1967.
13. Hires, S. D., Ekchian, A., Heywood, J. B., Tabaczynski, R. J., and Wall, J. C.: "Performance and NO_x Emissions Modelling of a Jet Ignition Prechamber Stratified Charge Engine," SAE paper 760161, *SAE Trans.*, vol. 85, 1976.
14. LoRusso, J. A.: "Combustion and Emissions Characteristics of Methanol, Methanol-Water, and Gasoline-Methanol Blends in a Spark Ignition Engine," S. M. Thesis, Department of Mechanical Engineering, MIT, May 1976.
15. By, A., Kempinski, B., and Rife, J. M.: "Knock in Spark-Ignition Engines," SAE paper 810147, 1981.

PETITIONER'S EXHIBIT 1002
US PATENT NO. 6,581,565
Page 1696

16. Rossini, F. D., Pitzer, K. S., Arnett, R. L., Braun, R. M., and Primentel, G. C.: *Selected Values of Physical and Thermodynamic Properties of Hydrocarbons and Related Compounds*, Carnegie Press, Pittsburgh, Pa., 1953.
17. Mansouri, S. H., and Heywood, J. B.: "Correlation for the Viscosity and Prandtl Number of Hydrocarbon-Air Combustion Products," *Combust. Sci. Technology*, vol. 23, pp. 251–256, 1980.
18. Olikara, C., and Borman, G. L.: "A Computer Program for Calculating Properties of Equilibrium Combustion Products with Some Applications to I.C. Engines," SAE paper 750468, 1975.
19. Krieger, R. B., and Borman, G. L.: "The Computation of Apparent Heat Release for Internal Combustion Engines," in *Proc. Diesel Gas Power*, ASME paper 66-WA/DGP-4, 1966.
20. Martin, M. K., and Heywood, J. B.: "Approximate Relationships for the Thermodynamic Properties of Hydrocarbon-Air Combustion Products," *Combust. Sci. Technology*, vol. 15, pp. 1–10, 1977.
21. Chapman, S., and Cowling, T. G.: *The Mathematical Theory of Non-Uniform Gases*, Cambridge University Press, Cambridge, 1955.
22. Hirschfelder, J. O., Curtiss, C. F., and Bird, R. B.: *Molecular Theory of Gases and Liquids*, John Wiley, 1954.
23. Patterson, D. J., and Henein, N. A.: *Emissions from Combustion Engines and Their Control*, Ann Arbor Science Publishers, 1972.
24. D'Alleva, B. A., and Lovell, W. G.: "Relation of Exhaust Gas Composition to Air-Fuel Ratio," *SAE J.*, vol. 38, no. 3, pp. 90–96, March 1936.
25. Stivender, D. L.: "Development of a Fuel-Based Mass Emission Measurement Procedure," SAE paper 710604, 1971.
26. Harrington, J. A., and Shishu, R. C.: "A Single-Cylinder Engine Study of the Effects of Fuel Type, Fuel Stoichiometry and Hydrogen-to-Carbon Ratio on CO, NO, and HC Exhaust Emissions," SAE paper 730476, 1973.
27. Spindt, R. S., "Air-Fuel Ratios from Exhaust Gas Analysis," SAE paper 650507, *SAE Trans.*, vol. 74, 1965.
28. Fleming, R. D., and Eccleston, D. B.: "The Effect of Fuel Composition, Equivalence Ratio, and Mixture Temperature on Exhaust Emissions," SAE paper 710012, 1971.
29. Eltinge, L.: "Fuel-Air Ratio and Distribution from Exhaust Gas Composition," SAE paper 680114, *SAE Trans.*, vol. 77, 1968.
30. Leonard, L. S.: "Fuel Distribution by Exhaust Gas Analysis," SAE paper 379A, 1961.
31. Bishop, R. P.: "Combustion Efficiency in Internal Combustion Engines," B.S. Thesis, Department of Mechanical Engineering, MIT, February 1985.
32. The Engine Test Code Subcommittee of the General Technical Committee, *General Motors Automotive Engine Test Code for Four Cycle Spark Ignition Engines*, 6th ed., 1975.

PETITIONER'S EXHIBIT 1002
US PATENT NO. 6,581,565
Page 1697

CHAPTER 5

IDEAL MODELS OF ENGINE CYCLES

5.1 INTRODUCTION

The operating cycle of an internal combustion engine can be broken down into a sequence of separate processes: intake, compression, combustion, expansion, and exhaust. With models for each of these processes, a simulation of a complete engine cycle can be built up which can be analysed to provide information on engine performance. Models of individual engine processes at various levels of approximation have been developed. In this chapter we consider the simplest set of models which provide useful insights into the performance and efficiency of engines. The cycles analysed are commonly called the constant-volume, constant-pressure, and limited-pressure cycles; each title describes the approximation made for the engine combustion process.† The description of more accurate simulations of engine processes is deferred until Chap. 14.

For each engine cycle, a choice of models for working fluid thermodynamic properties must be made. These models have been reviewed in Chap. 4. Ideal

† These cycles are also referred to by the titles Otto cycle, Diesel cycle, and dual cycle, respectively, for historical reasons. The more descriptive titles used above are preferred because they avoid the often-made assumption that the SI or Otto engine is best approximated by the constant-volume cycle, and the CI or diesel engine is best approximated by the constant-pressure cycle. These assumptions are not necessarily correct.

PETITIONER'S EXHIBIT 1002
US PATENT NO. 6,581,565
Page 1698

engine cycle models combined with a simple ideal gas model (specific heats constant throughout the engine cycle—model 1 in Table 4.2) provide analytic results and are useful for illustrative purposes; we will call these cycles *ideal gas standard cycles*. Ideal engine cycles combined with more realistic models of working fluid properties (a frozen mixture of ideal gases for the unburned mixture and an equilibrium mixture for the burned mixture—model 5 in Table 4.2) are called *fuel-air cycles* and provide more quantitative information on engine operation.

An internal combustion engine is not a heat engine in the thermodynamic definition of the term. It is not a closed system. The working fluid does not execute a thermodynamic cycle. The temperature changes which occur around minimum and maximum cylinder volumes are not primarily a result of heat-transfer interactions. An engine can best be analyzed as an open system which exchanges heat and work with its surrounding environment (the atmosphere). Reactants (fuel and air) flow into the system; products (exhaust gases) flow out. (An overall second law analysis of the engine from this point of view has already been presented in Sec. 3.6.) Thus, the cycles discussed in this chapter are not thermodynamic cycles. Rather, each is a consecutive sequence of processes through which we can follow the state of the working fluid as the engine executes a complete operating cycle.

5.2 IDEAL MODELS OF ENGINE PROCESSES

The sequence of processes which make up a typical SI and CI engine operating cycle has been described in Sec. 1.3. To illustrate these processes, cylinder pressure (p) and volume (V) data from a throttled four-stroke cycle SI engine are plotted as a p-V diagram in Fig. 5-1. The cycle can be divided into compression,

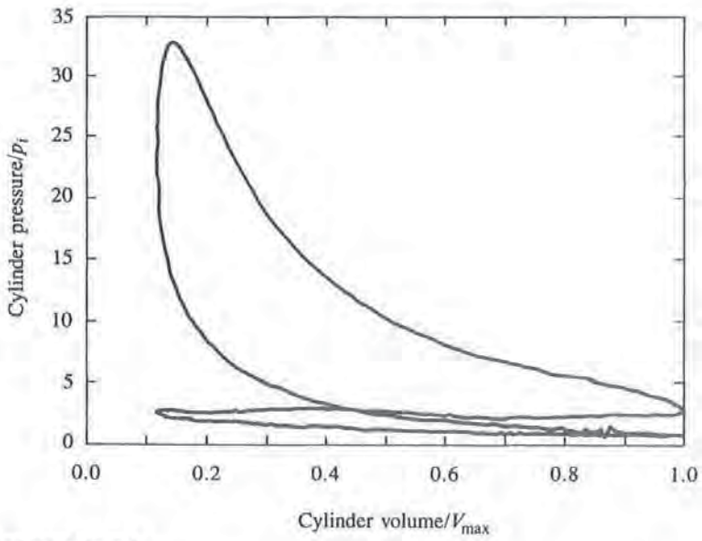


FIGURE 5-1
Pressure-volume diagram of firing spark-ignition engine. $r_c = 8.4$, 3500 rev/min, $p_i = 0.4$ atm, $p_e = 1$ atm, $\text{imep}_n = 2.9$ atm.

PETITIONER'S EXHIBIT 1002
US PATENT NO. 6,581,565
Page 1699

TABLE 5.1
Ideal models of engine processes

Process	Assumptions
Compression (1-2)	1. Adiabatic and reversible (hence isentropic)
Combustion (2-3)	1. Adiabatic 2. Combustion occurs at (*a*) Constant volume (*b*) Constant pressure (*c*) Part at constant volume and part at constant pressure (called limited pressure) 3. Combustion is complete ($\eta_c = 1$)
Expansion (3-4)	1. Adiabatic and reversible (hence isentropic)
Exhaust (4-5-6) and intake (6-7-1)	1. Adiabatic 2. Valve events occur at top- and bottom-center 3. No change in cylinder volume as pressure differences across open valves drop to zero 4. Inlet and exhaust pressures constant 5. Velocity effects negligible

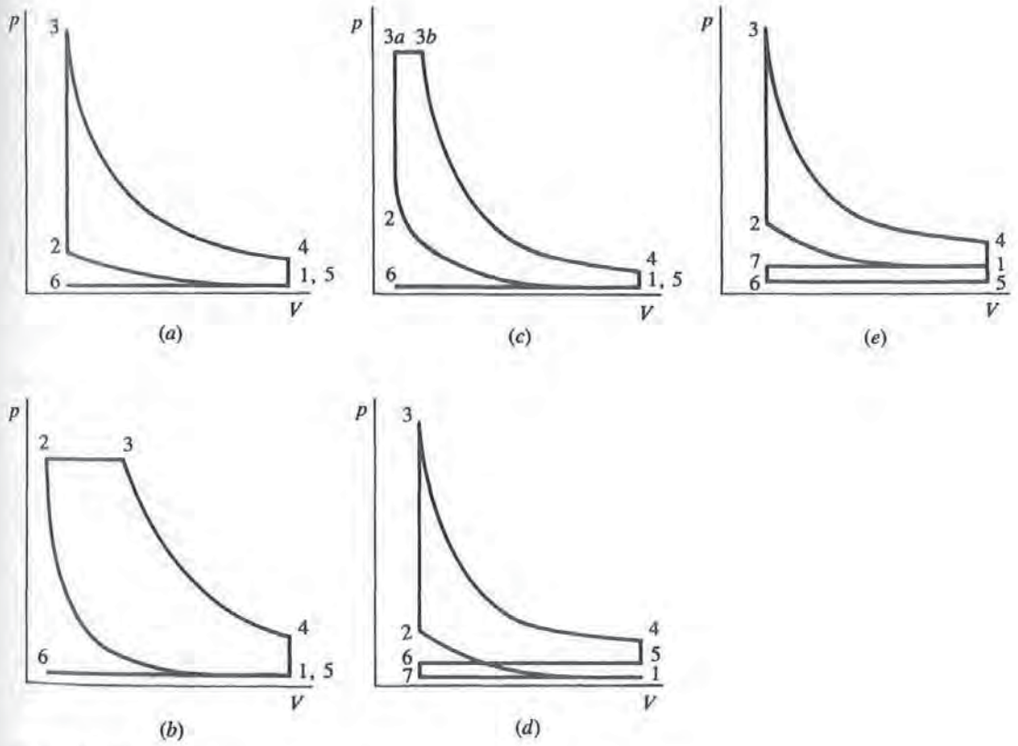


FIGURE 5-2
Pressure-volume diagrams of ideal cycles. Unthrottled operation: (*a*) constant-volume combustion; (*b*) constant-pressure combustion; (*c*) limited-pressure combustion. (*d*) Throttled constant-volume cycle; (*e*) supercharged constant-volume cycle.

PETITIONER'S EXHIBIT 1002
US PATENT NO. 6,581,565
Page 1700

combustion, expansion, exhaust, and intake processes. Sets of assumptions which simplify each of these processes to a form convenient for analysis are given in Table 5.1.

Pressure-volume diagrams for the constant-volume, constant-pressure, and limited-pressure cycles for unthrottled engine operation are illustrated in Fig. 5-2*a* to *c*. Throttled engine operation ($p_i < p_e$) and supercharged engine operation ($p_i > p_e$) are shown in Fig. 5-2*d* and *e*. In each cycle 1-2 is the compression process, 2-3 is the combustion process, 3-4 (or 2-4 in the constant-pressure cycle) is the expansion process, 4-5-6 is the exhaust process, and 6-7-1 is the intake process.

The most critical assumption in determining how useful these ideal cycles are as indicators of engine performance is the form assumed for the combustion process. The real engine combustion process occupies a finite crank angle period (between about 20 and 70 crank angle degrees), and the spark or fuel-injection timing may be retarded from its optimum advance to closer to TC. The constant-volume cycle is the limiting case of infinitely fast combustion at TC; the constant-pressure cycle would correspond to slow and late combustion; the limited-pressure cycle lies in between.

5.3 THERMODYNAMIC RELATIONS FOR ENGINE PROCESSES

The overall engine operating parameters of greatest interest which can be determined from a thermodynamic analysis of the engine operating cycle are:

The indicated fuel conversion efficiency $\eta_{f,i}$:

$$\eta_{f,i} = \frac{W_{c,i}}{m_f Q_{\text{LHV}}} \tag{5.1}$$

(which, since the combustion efficiency is unity, is equal to the indicated thermal conversion efficiency $\eta_{t,i}$; see Sec. 3.6.2)

The indicated mean effective pressure (imep):

$$\text{imep} = \frac{W_{c,i}}{V_d} = \frac{m_f Q_{\text{LHV}} \eta_{f,i}}{V_d} \tag{5.2}$$

$W_{c,i}$, the indicated work per cycle, is the sum of the compression stroke work and the expansion stroke work:

$$W_{c,i} = W_C + W_E \tag{5.3}$$

Using the notation of Fig. 5-2 to define the endpoints of each engine process, the following relationships are obtained by applying the first and second laws of thermodynamics to the cylinder contents:

PETITIONER'S EXHIBIT 1002
US PATENT NO. 6,581,565
Page 1701

Compression stroke:

$$\frac{v_1}{v_2} = r_c \tag{5.4}$$

Since the process is adiabatic and reversible

$$s_2 = s_1 \tag{5.5}$$

The compression work is

$$W_C = U_1 - U_2 = m(u_1 - u_2) \tag{5.6}$$

Combustion process:
For the constant-volume cycle,

$$v_3 = v_2 \qquad u_3 - u_2 = 0 \tag{5.7a, b}$$

For the constant-pressure cycle,

$$p_3 = p_2 \qquad h_3 - h_2 = 0 \tag{5.7c, d}$$

For the limited-pressure cycle,

$$v_{3a} = v_2 \qquad p_{3b} = p_{3a} \tag{5.7e, f}$$

and

$$u_{3a} - u_2 = 0 \qquad h_{3b} - h_{3a} = 0 \tag{5.7g, h}$$

Expansion stroke:
For the constant-volume cycle,

$$\frac{v_4}{v_3} = r_c \qquad s_4 = s_3 \tag{5.8a, b}$$

and the expansion work is

$$W_E = U_3 - U_4 = m(u_3 - u_4) \tag{5.9}$$

For the constant-pressure cycle,

$$p_3 = p_2 \qquad \frac{v_4}{v_2} = r_c \qquad s_4 = s_3 \tag{5.10a, b, c}$$

and the expansion work is

$$\begin{aligned} W_E &= U_3 - U_4 + p_2(V_3 - V_2) \\ &= m[(u_3 - u_4) + p_2(v_3 - v_2)] \\ &= m[(h_3 - h_4) + p_4 v_4 - p_2 v_2] \end{aligned} \tag{5.11}$$

PETITIONER'S EXHIBIT 1002
US PATENT NO. 6,581,565
Page 1702

For the limited-pressure cycle,

$$v_4/v_{3a} = r_c \qquad p_{3b} = p_{3a} \qquad s_4 = s_{3b} \tag{5.12a, b, c}$$

and the expansion work is

$$\begin{aligned} W_E &= U_{3b} - U_4 + p_3(V_{3b} - V_{3a}) \\ &= m[(u_{3b} - u_4) + p_3(v_{3b} - v_{3a})] \\ &= m[(h_{3b} - h_4) + p_4 v_4 - p_3 v_{3a}] \end{aligned} \tag{5.13}$$

The indicated fuel conversion efficiency is found by substitution into Eqs. (5.3) and (5.1):

For the constant-volume cycle:

$$\eta_{f,i} = \frac{m[(u_3 - u_4) - (u_2 - u_1)]}{m_f Q_{\text{LHV}}} \tag{5.14}$$

For the constant-pressure cycle:

$$\eta_{f,i} = \frac{m[(h_3 - h_4) - (u_2 - u_1) + p_4 v_4 - p_2 v_2]}{m_f Q_{\text{LHV}}} \tag{5.15}$$

For the limited-pressure cycle:

$$\eta_{f,i} = \frac{m[(h_{3b} - h_4) - (u_2 - u_1) + p_4 v_4 - p_3 v_{3a}]}{m_f Q_{\text{LHV}}} \tag{5.16}$$

The state of the mixture at point 1 in the cycle depends on the intake mixture properties and the residual gas properties at the end of the exhaust stroke.

When the exhaust valve opens at point 4, the cylinder pressure is above the exhaust manifold pressure and a *blowdown* process occurs. In the ideal exhaust process model, this blowdown occurs with the piston stationary at BC. During this blowdown process, the gas which remains inside the cylinder expands isentropically. The gases escaping from the cylinder undergo an unrestrained expansion or throttling process which is irreversible. It is assumed that the kinetic energy acquired by each gas element as it is accelerated through the exhaust valve is dissipated in a turbulent mixing process in the exhaust port into internal energy and flow work. Since it is also assumed that no heat transfer occurs, the enthalpy of each element of gas after it leaves the cylinder remains constant.

These processes are illustrated on an h-s diagram in Fig. 5-3. The gas remaining in the cylinder expands isentropically along the line 4-5. The first element of gas which leaves the cylinder at point 4 enters the exhaust manifold at state a on the pressure $= p_e$ line. An element that leaves the cylinder at an intermediate state b on the expansion line 4-5 would enter the exhaust manifold at state c. At the end of the blowdown process the gas in the cylinder and the last

PETITIONER'S EXHIBIT 1002
US PATENT NO. 6,581,565
Page 1703

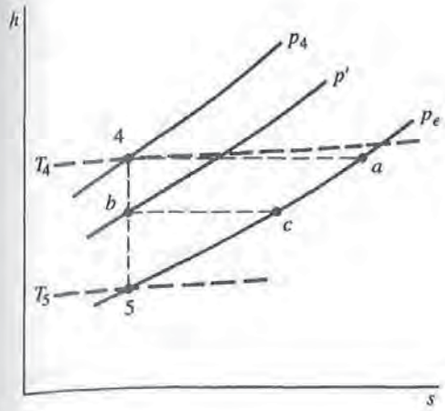


FIGURE 5-3
Enthalpy-entropy diagram of gas state during exhaust process. See text for explanation.

gas to leave have the same state—5. There is, therefore, a gradient in temperature within the exhausted gas. The temperature of the first element exhausted, T_a, is slightly less than T_4; the temperature of the last element exhausted is T_5.

A displacement of gas out of the cylinder follows the blowdown process as the piston moves from BC to TC. If heat-transfer and kinetic energy dissipation effects are neglected, no change in thermodynamic state of the gas occurs. In this *displacement* process, the mass of gas within the cylinder at the end of the blowdown process is further decreased by the ratio V_5/V_6.

The mass of residual gas m_r in the cylinder at point 6 in the cycle is obtained by first determining the state of the gas (T_5, v_5) at the end of the blowdown process following an isentropic expansion from p_4 to p_e and then by reducing the cylinder volume to the clearance volume V_6. The residual mass fraction is thus given by

$$\frac{m_r}{m} = x_r = \frac{v_4/v_5}{r_c} = \frac{v_2}{v_5} \tag{5.17}$$

The average state of the exhausted gas can be determined by considering the open system defined by the piston face, cylinder walls, and cylinder head, shown in Fig. 5-4. Applying the first law of thermodynamics for an open system gives

$$U_6 - U_4 = p_e(V_4 - V_6) - H_e \tag{5.18a}$$

where H_e is the enthalpy of the mass of gas exhausted from the cylinder. The average specific exhaust enthalpy is, therefore,

$$\bar{h}_e = \frac{m_4 u_4 - m_6 u_6 + p_e V_d}{m_4 - m_6} \tag{5.18b}$$

which, with $p = p_e$, defines the average exhausted-gas state.

The mixture temperature at the end of the intake stroke and at the start of the compression stroke (point 1 in Fig. 5-2) can now be determined, again using

PETITIONER'S EXHIBIT 1002
US PATENT NO. 6,581,565
Page 1704

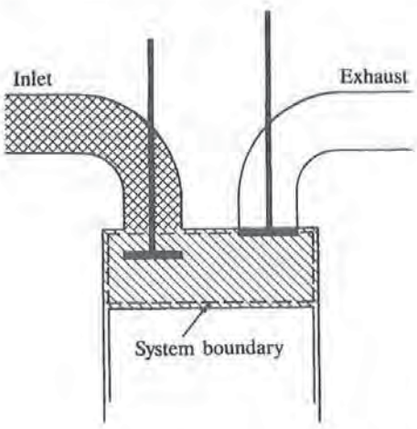


FIGURE 5-4
Definition of system boundary for thermodynamic analysis of ideal cycle processes.

the open system in Fig. 5-4. Application of the first law between points 6 and 1 gives

$$U_1 - U_6 = -p_i(V_1 - V_6) + (m_1 - m_6)h_i \tag{5.19a}$$

or

$$m_1u_1 - m_6u_6 = -p_i(V_1 - V_6) + (m_1 - m_6)h_i \tag{5.19b}$$

or

$$m_1h_1 = m_6h_6 + (m_1 - m_6)h_i + V_2(p_i - p_e) \tag{5.19c}$$

where h_i is the specific enthalpy of the inlet mixture and $p_1 = p_i$.

Note that when $p_i < p_e$, part of the residual gas in the cylinder at the end of the exhaust stroke will flow into the intake system when the intake valve opens. This flow will cease when the cylinder pressure equals p_i. However, provided no heat transfer occurs, this backflow will not affect Eqs. (5.19) above, since the flow of residual through the intake valve is a constant enthalpy process.

In many engines, the closing of the exhaust valve and the opening of the intake valve overlap. Flow of exhausted gases from the exhaust system through the cylinder into the intake system can then occur. Equations (5.18) and (5.19) would have to be modified to account for valve overlap.

In the four-stroke engine cycle, work is done on the piston during the intake and the exhaust processes. The work done by the cylinder gases on the piston during exhaust is

$$W_e = p_e(V_2 - V_1) \tag{5.20}$$

The work done by the cylinder gases on the piston during intake is

$$W_i = p_i(V_1 - V_2) \tag{5.21}$$

The net work to the piston over the exhaust and intake strokes, the *pumping work*, is

$$W_p = (p_i - p_e)(V_1 - V_2) \tag{5.22}$$

which, for the cylinder gas system, is negative for $p_i < p_e$ and positive for $p_i > p_e$.

PETITIONER'S EXHIBIT 1002
US PATENT NO. 6,581,565
Page 1705

The pumping mean effective pressure (pmep) is usually defined as a positive quantity. Thus:

For $p_i < p_e$: $$\text{pmep} = p_e - p_i \tag{5.23a}$$

For $p_i > p_e$: $$\text{pmep} = p_i - p_e \tag{5.23b}$$

The net and gross indicated mean effective pressures are related by

$$\text{imep}_n = \text{imep}_g - (p_e - p_i) \tag{5.24}$$

The net indicated fuel conversion efficiency is related to the gross indicated fuel conversion efficiency by

$$\eta_{f,\text{in}} = \eta_{f,\text{ig}}\left(1 - \frac{p_e - p_i}{\text{imep}_g}\right) \tag{5.25}$$

5.4 CYCLE ANALYSIS WITH IDEAL GAS WORKING FLUID WITH c_v AND c_p CONSTANT

If the working fluid in these ideal cycles is assumed to be an ideal gas, with c_v and c_p constant throughout the engine operating cycle, the equations developed in the previous section which describe engine performance and efficiency can be further simplified. We will use the notation of Fig. 5-2.

5.4.1 Constant-Volume Cycle

The compression work (Eq. 5.6) becomes

$$W_C = mc_v(T_1 - T_2) \tag{5.26}$$

The expansion work (Eq. 5.9) becomes

$$W_E = mc_v(T_3 - T_4) \tag{5.27}$$

The denominator in Eq. (5.14), $m_f Q_{\text{LHV}}$, can be related to the temperature rise during combustion. For the working fluid model under consideration, the $U(T)$ lines for the reactants and products on a U-T diagram such as Fig. 3-5 are parallel and have equal slopes, of magnitude c_v. Hence, for a constant-volume adiabatic combustion process

$$mc_v(T_3 - T_2) = m_f Q_{\text{LHV}} \tag{5.28}\dagger$$

† Note that if insufficient air is available for complete combustion of the fuel, Eq. (5.28) must be modified. The right-hand side of the equation should then be $\eta_c m_f Q_{\text{LHV}}$, where η_c is the combustion efficiency given by Eq. (3.27).

PETITIONER'S EXHIBIT 1002
US PATENT NO. 6,581,565
Page 1706

Note that the heating values at constant volume and constant pressure are the same for this working fluid. For convenience we will define

$$Q^* = \frac{m_f Q_{\text{LHV}}}{m} \tag{5.29}$$

Q^* is the specific internal energy (and enthalpy) decrease, during isothermal combustion, per unit mass of working fluid.

The relation for indicated fuel conversion efficiency (Eq. 5.14) becomes

$$\eta_{f,i} = \frac{(T_3 - T_4) - (T_2 - T_1)}{T_3 - T_2} = 1 - \frac{T_4 - T_1}{T_3 - T_2} \tag{5.30}$$

Since 1-2 and 3-4 are isentropic processes between the same volumes, V_1 and V_2,

$$\frac{T_2}{T_1} = \left(\frac{V_1}{V_2}\right)^{\gamma-1} = r_c^{\gamma-1} = \left(\frac{V_4}{V_3}\right)^{\gamma-1} = \frac{T_3}{T_4}$$

where $\gamma = c_p/c_v$. Hence:

$$\frac{T_4}{T_1} = \frac{T_3}{T_2}$$

and Eq. (5.30) can be rearranged as

$$\eta_{f,i} = 1 - \frac{1}{r_c^{\gamma-1}} \tag{5.31}$$

Values of $\eta_{f,i}$ for different values of γ are shown in Fig. 5-5. The indicated fuel conversion efficiency increases with increasing compression ratio and decreases as γ decreases.

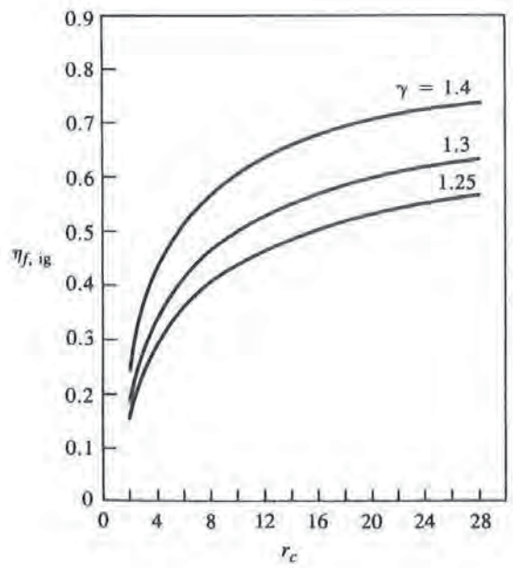


FIGURE 5-5
Ideal gas constant-volume cycle fuel conversion efficiency as a function of compression ratio; $\gamma = c_p/c_v$.

PETITIONER'S EXHIBIT 1002
US PATENT NO. 6,581,565
Page 1707

The indicated mean effective pressure, using Eqs. (5.2) and (5.31), becomes

$$\frac{\text{imep}}{p_1} = \left(\frac{Q^*}{c_v T_1}\right)\left(\frac{1}{\gamma - 1}\right)\left(\frac{r_c}{r_c - 1}\right)\left(1 - \frac{1}{r_c^{\gamma-1}}\right) \tag{5.32}$$

The dimensionless numbers r_c, γ, and $Q^*/(c_v T_1)$ are sufficient to describe the characteristics of the constant-volume ideal gas standard cycle, relative to its initial conditions p_1, T_1.

It is useful to compare the imep—a measure of the effectiveness with which the displaced volume of the engine is used to produce work—and the maximum pressure in the cycle, p_3. The ratio p_3/p_1 can be determined from the ideal gas law applied at points 2 and 3, and the relation

$$\frac{T_3}{T_2} = 1 + \frac{Q^*}{c_v T_1 r_c^{\gamma-1}} \tag{5.33}$$

obtained from Eq. (5.28). Equations (5.32) and (5.33) then give

$$\frac{\text{imep}}{p_3} = \frac{1}{(\gamma - 1)r_c^{\gamma}}\left(\frac{r_c}{r_c - 1}\right)\frac{1 - 1/r_c^{\gamma-1}}{c_v T_1/Q^* + 1/r_c^{\gamma-1}} \tag{5.34}$$

A high value of imep/p_3 is desirable. Engine weight will increase with increasing p_3 to withstand the increasing stresses in components.

The indicated fuel conversion efficiency and the ratios imep/p_1 and imep/p_3 for this ideal cycle model do not depend on whether the cycle is throttled or supercharged. However, the relationships between the working fluid properties at points 1 and 6 do depend on the degree of throttling or supercharging. For throttled engine operation, the residual gas mass fraction x_r can be determined as follows. From Eq. (5.17), since state 5 corresponds to an isentropic expansion from state 4 to $p = p_e$, x_r is given by

$$x_r = \frac{(p_e/p_4)^{1/\gamma}}{r_c} = \frac{(p_e/p_i)^{1/\gamma}(p_1/p_4)^{1/\gamma}}{r_c}$$

Since

$$\frac{p_1}{p_4} = \frac{p_1}{p_2}\frac{p_2}{p_3}\frac{p_3}{p_4} = \frac{1}{r_c^{\gamma}}\frac{T_2}{T_3}r_c^{\gamma} = \left(1 + \frac{Q^*}{c_v T_1 r_c^{\gamma-1}}\right)^{-1}$$

it follows that

$$x_r = \frac{1}{r_c}\frac{(p_e/p_i)^{1/\gamma}}{[1 + Q^*/(c_v T_1 r_c^{\gamma-1})]^{1/\gamma}} \tag{5.35}$$

The residual mass fraction increases as p_i decreases below p_e, decreases as r_c increases, and decreases as $Q^*/(c_v T_1)$ increases.

Through a similar analysis, the temperature of the residual gas T_6 can be determined:

$$\frac{T_6}{T_1} = \left(\frac{p_e}{p_i}\right)^{(\gamma-1)/\gamma}\left(1 + \frac{Q^*}{c_v T_1 r_c^{\gamma-1}}\right)^{1/\gamma} \tag{5.36}$$

PETITIONER'S EXHIBIT 1002
US PATENT NO. 6,581,565
Page 1708

The mixture temperature at point 1 in the cycle can be related to the inlet mixture temperature, T_i, with Eq. (5.19). For a working fluid with c_v and c_p constant, this equation becomes

$$c_p T_1 = x_r c_p T_6 + (1 - x_r) c_p T_i - \frac{R T_1}{r_c}\left(\frac{p_e}{p_i} - 1\right) \tag{5.37}$$

Use of Eqs. (5.36) and (5.37) leads to the relation

$$\frac{T_1}{T_i} = \frac{1 - x_r}{1 - 1/(\gamma r_c)[p_e/p_i + (\gamma - 1)]} \tag{5.38}$$

Extensive results for the constant-volume cycle with $\gamma = 1.4$ can be found in Taylor.[1]

5.4.2 Limited- and Constant-Pressure Cycles

The constant-pressure cycle is a limited-pressure cycle with $p_3 = p_2$. For the limited-pressure cycle, the compression work remains

$$W_C = m c_v (T_1 - T_2) \tag{5.39}$$

The expansion work, from Eq. (5.13), becomes

$$W_E = m[c_v(T_{3b} - T_4) + p_3(v_{3b} - v_{3a})] \tag{5.40}$$

For the combustion process, Eqs. (5.7*g*, *h*) give

$$m_{f\,2-3a} Q_{\text{LHV}} = m c_v (T_{3a} - T_2) \tag{5.41a}$$

$$m_{f\,3a-3b} Q_{\text{LHV}} = m c_p (T_{3b} - T_{3a}) \tag{5.41b}$$

or

$$m_f Q_{\text{LHV}} = m[c_v(T_{3a} - T_2) + c_p(T_{3b} - T_{3a})] \tag{5.41c}$$

for a working fluid with c_v and c_p constant throughout the cycle.

Combining Eqs. (5.1), (5.3), and (5.39) to (5.41) and simplifying gives

$$\eta_{f,i} = 1 - \frac{T_4 - T_1}{(T_{3a} - T_2) + \gamma(T_{3b} - T_{3a})}$$

Use of the isentropic relationships for the working fluid along 1-2 and 3*b*-4, with the substitutions

$$\alpha = \frac{p_3}{p_2} \qquad \beta = \frac{V_{3b}}{V_{3a}} \tag{5.42a, b}$$

leads to the result

$$\eta_{f,i} = 1 - \frac{1}{r_c^{\gamma-1}}\left[\frac{\alpha\beta^\gamma - 1}{\alpha\gamma(\beta - 1) + \alpha - 1}\right] \tag{5.43}$$

For $\beta = 1$ this result becomes the constant-volume cycle efficiency (Eq. 5.31). For $\alpha = 1$, this result gives the constant-pressure cycle efficiency as a special case.

PETITIONER'S EXHIBIT 1002
US PATENT NO. 6,581,565
Page 1709

The mean effective pressure is related to p_1 and p_3 via

$$\frac{\text{imep}}{p_1} = \frac{Q^*}{c_v T_1(\gamma - 1)}\left(\frac{r_c}{r_c - 1}\right)\eta_{f,i} \tag{5.44}$$

$$\frac{\text{imep}}{p_3} = \frac{1}{\alpha r_c^{\gamma}}\left(\frac{Q^*}{c_v T_1}\right)\left(\frac{1}{\gamma - 1}\right)\left(\frac{r_c}{r_c - 1}\right)\eta_{f,i} \tag{5.45}$$

5.4.3 Cycle Comparison

The above expressions are most useful if values for γ and $Q^*/(c_v T_1)$ are chosen to match real working fluid properties. Figure 5-5 has already shown the sensitivity of $\eta_{f,i}$ for the constant-volume cycle to the value of γ chosen. In Sec. 4.4, average values of γ_u and γ_b were determined which match real working fluid properties over the compression and expansion strokes, respectively. Values for a stoichiometric mixture appropriate to an SI engine are $\gamma_u \approx 1.3$, $\gamma_b \approx 1.2$. However, analysis of pressure-volume data for real engine cycles indicates that pV^n, where $n \approx 1.3$, is a good fit to the expansion stroke p-V data.[2] Heat transfer from the burned gases increases the exponent above the value corresponding to γ_b. A value of $\gamma = 1.3$ for the entire cycle is thus a reasonable compromise.

Q^*, defined by Eq. (5.29), is the enthalpy decrease during isothermal combustion per unit mass of working fluid. Hence

$$Q^* = \left(\frac{m_f}{m_a}\right)Q_{\text{LHV}}\left(\frac{m_a}{m}\right) \tag{5.46}$$

A simple approximation for (m_a/m) is $(r_c - 1)/r_c$; i.e., fresh air fills the displaced volume and the residual gas fills the clearance volume at the same density. Then, for isooctane fuel, for a stoichiometric mixture, Q^* is given by 2.92×10^6 $(r_c - 1)/r_c$ J/kg air. For $\gamma = 1.3$ and an average molecular weight $M = 29.3$, $c_v =$ 946 J/kg·K. For $T_1 = 333$ K, $Q^*/(c_v T_1)$ becomes 9.3 $(r_c - 1)/r_c$. For this value of $Q^*/(c_v T_1)$ all cycles would be burning a stoichiometric mixture with an appropriate residual gas fraction.

Pressure-volume diagrams for the three ideal cycles for the same compression ratio and unburned mixture composition are shown in Fig. 5-6. For each cycle, $\gamma = 1.3$, $r_c = 12$, $Q^*/(c_v T_1) = 9.3(r_c - 1)/r_c = 8.525$. Overall performance characteristics for each of these cycles are summarized in Table 5.2. The constant-volume cycle has the highest efficiency, the constant-pressure cycle the lowest efficiency. This can be seen from Eq. (5.43) where the term in square brackets is equal to unity for the constant-volume cycle and greater than unity for the limited- and constant-pressure cycles. The imep values are proportional to $\eta_{f,i}$ since the mass of fuel burned per cycle is the same in all three cases.

As the peak pressure p_3 is decreased, the ratio of imep to p_3 increases. This ratio is important because imep is a measure of the useful pressure on the piston, and the maximum pressure chiefly affects the strength required of the engine structure.

PETITIONER'S EXHIBIT 1002
US PATENT NO. 6,581,565
Page 1710

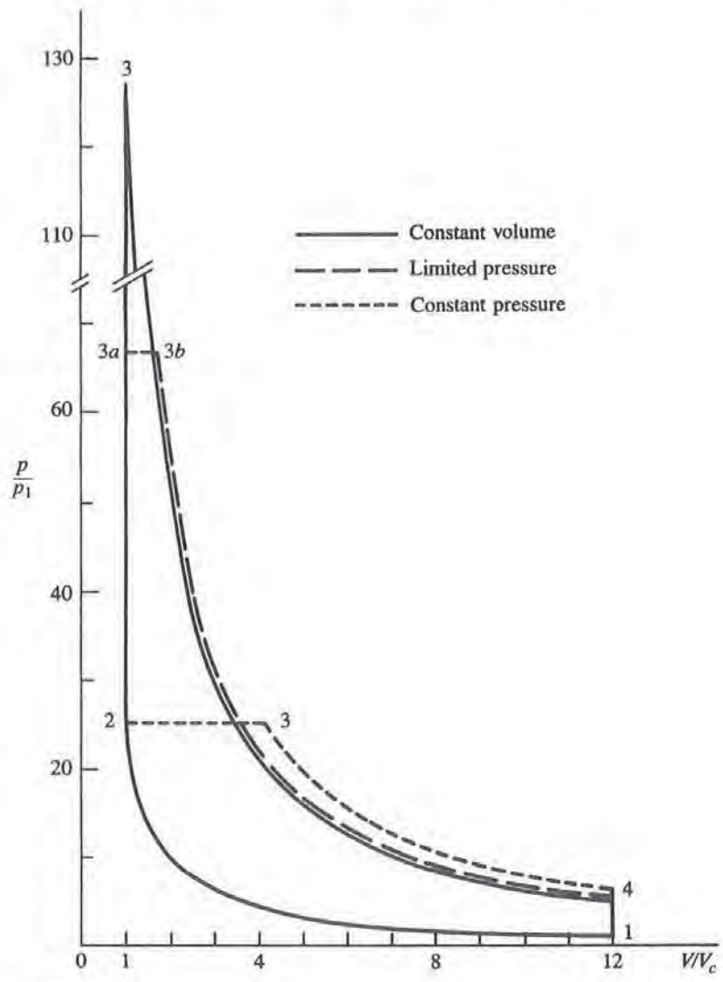


FIGURE 5-6
Pressure-volume diagrams for constant-volume, limited-pressure, and constant-pressure ideal gas standard cycles. $r_c = 12, \gamma = 1.3, Q^*/(c_v T_1) = 9.3(r_c - 1)/r_c = 8.525, p_{3a}/p_1 = 67$.

TABLE 5.2
Comparison of ideal cycle results

	$\eta_{f,i}$	$\frac{\text{imep}}{p_1}$	$\frac{\text{imep}}{p_3}$	$\frac{p_{max}}{p_1}$
Constant volume	0.525	16.3	0.128	128
Limited pressure	0.500	15.5	0.231	67
Constant pressure	0.380	11.8	0.466	25.3

$\gamma = 1.3; r_c = 12; Q^*/(c_v T_1) = 8.525$.

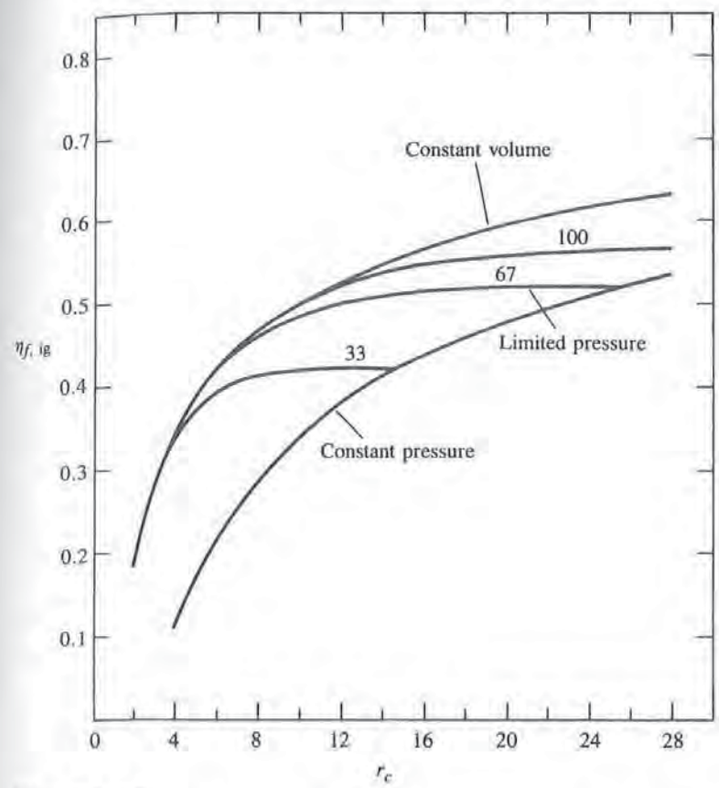


FIGURE 5-7
Fuel conversion efficiency as a function of compression ratio, for constant-volume, constant-pressure, and limited-pressure ideal gas cycles. $\gamma = 1.3$, $Q^*/(c_v T_1) = 9.3(r_c - 1)/r_c$. For limited-pressure cycle, $p_3/p_1 = 33, 67, 100$.

A more extensive comparison of the three cycles is given in Figs. 5-7 and 5-8, over a range of compression ratios. For all cases $\gamma = 1.3$ and $Q^*/(c_v T_1) = 9.3(r_c - 1)/r_c$. At any given r_c, the constant-volume cycle has the highest efficiency and lowest imep$/p_3$. For a given maximum pressure p_3, the constant-pressure cycle has the highest efficiency (and the highest compression ratio). For the limited-pressure cycle, at constant p_3/p_1, there is little improvement in efficiency and imep above a compression ratio of about 8 to 10 as r_c is increased.

Example 5.1 shows how ideal cycle equations relate residual and intake conditions with the gas state at point 1 in the cycle. An iterative procedure is required if intake conditions are specified.

Example 5.1. For $\gamma = 1.3$, compression ratio $r_c = 6$, and a stoichiometric mixture with intake temperature 300 K, find the residual gas fraction, residual gas temperature, and mixture temperature at point 1 in the constant-volume cycle for $p_e/p_i = 1$ (unthrottled operation) and 2 (throttled operation).

PETITIONER'S EXHIBIT 1002
US PATENT NO. 6,581,565
Page 1712

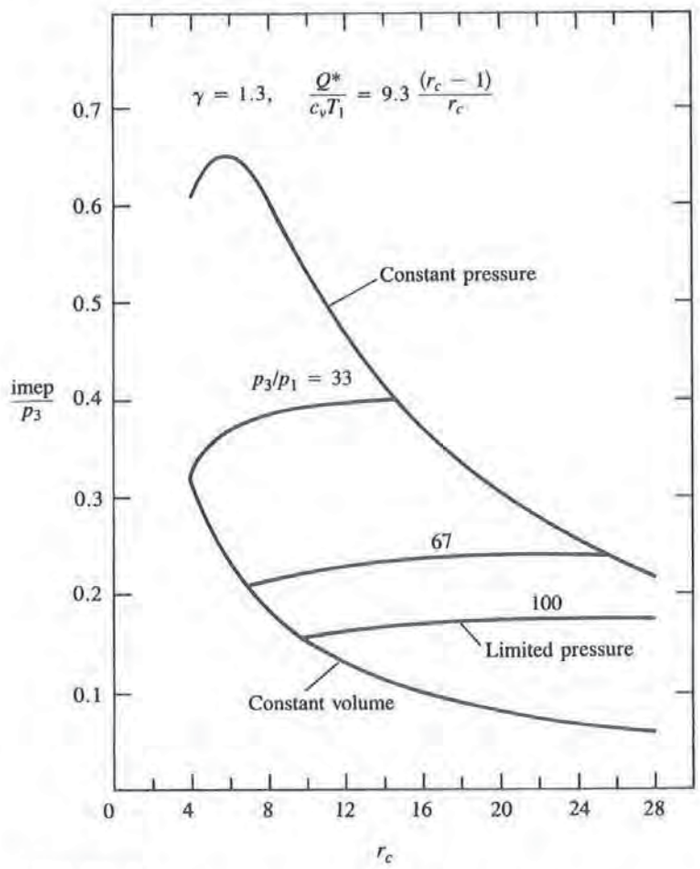


FIGURE 5-8
Indicated mean effective pressure (imep) divided by maximum cycle pressure (p_3) as a function of compression ratio for constant-volume, constant-pressure, and limited-pressure cycles. Details same as Fig. 5-7.

For a stoichiometric mixture, for isooctane,

$$Q^* = \frac{m_f}{m} Q_{\text{LHV}} = \left(\frac{m_f}{m_i}\right)\left(\frac{m_i}{m}\right) Q_{\text{LHV}} = \frac{44.38}{16.14}(1 - x_r) = 2.75(1 - x_r) \qquad \text{MJ/kg}$$

For $\gamma = 1.3$, $c_v = 946$ J/kg · K and

$$\frac{Q^*}{c_v T_1} = \frac{2.75 \times 10^6}{946 T_1}(1 - x_r) = \frac{2910}{T_1}(1 - x_r) \qquad (a)$$

Equations (5.35), (5.36), and (5.38), for $r_c = 6$ and $\gamma = 1.3$, become

$$x_r = \frac{1}{6} \frac{(p_e/p_i)^{0.769}}{[1 + Q^*/(c_v T_1 \times 6^{0.3})]^{0.769}} \qquad (b)$$

$$\frac{T_r}{T_1} = \left(\frac{p_e}{p_i}\right)^{0.23}\left(1 + \frac{Q^*}{c_v T_1 \times 6^{0.3}}\right)^{0.769} \qquad (c)$$

PETITIONER'S EXHIBIT 1002
US PATENT NO. 6,581,565
Page 1713

$$\frac{T_1}{300} = \frac{1 - x_r}{1 - [1/(1.3 \times 6)](p_e/p_i + 0.3)} \qquad (d)$$

A trial-and-error solution of Eqs. (*a*) to (*d*) is required. It is easiest to estimate x_r, solve for T_1 from (*d*), evaluate $Q^*/(c_v T_1)$ from (*a*), and check the value of x_r assumed with that given by (*b*).

For $(p_e/p_i) = 1$ (unthrottled operation) the following solution is obtained:

$$x_r = 0.044, \qquad T_1 = 344 \text{ K}, \qquad \frac{Q^*}{c_v T_1} = 8.1, \qquad T_r = 1316 \text{ K}$$

For $(p_e/p_i) = 2$ the following solution is obtained:

$$x_r = 0.082, \qquad T_1 = 391 \text{ K}, \qquad \frac{Q^*}{c_v T_1} = 6.8, \qquad T_r = 1580 \text{ K}$$

5.5 FUEL-AIR CYCLE ANALYSIS

A more accurate representation of the properties of the working fluid inside the engine cylinder is to treat the unburned mixture as frozen in composition and the burned gas mixture as in equilibrium. Values for thermodynamic properties for these working fluid models can be obtained with the charts for unburned and burned gas mixtures described in Sec. 4.5, or the computer codes summarized in Sec. 4.7. When these working fluid models are combined with the ideal engine process models in Table 5.1, the resulting cycles are called fuel-air cycles.[1] The sequence of processes and assumptions are (with the notation of Fig. 5-2):

1-2 Reversible adiabatic compression of a mixture of air, fuel vapor, and residual gas without change in chemical composition.

2-3 Complete combustion (at constant volume or limited pressure or constant pressure), without heat loss, to burned gases in chemical equilibrium.

3-4 Reversible adiabatic expansion of the burned gases which remain in chemical equilibrium.

4-5-6 Ideal adiabatic exhaust blowdown and displacement processes with the burned gases fixed in chemical composition.

6-7-1 Ideal intake process with adiabatic mixing between residual gas and fresh mixture, both of which are fixed in chemical composition.

The basic equations for each of these processes have already been presented in Sec. 5.3. The use of the charts for a complete engine cycle calculation will now be illustrated.

PETITIONER'S EXHIBIT 1002
US PATENT NO. 6,581,565
Page 1714

5.5.1 SI Engine Cycle Simulation

The mixture conditions at point 1 must be known or must be estimated. The following approximate relationships can be used for this purpose:[3]

$$x_r = \left\{1 + \frac{T_r}{T_i}\left[r_c\left(\frac{p_i}{p_e}\right) - \left(\frac{p_i}{p_e}\right)^{(\gamma-1)/\gamma}\right]\right\}^{-1} \tag{5.47}$$

$$T_1 = T_r r_c x_r\left(\frac{p_i}{p_e}\right) \tag{5.48}$$

where $T_r = 1400$ K and $(\gamma - 1)/\gamma = 0.24$ are appropriate average values to use for initial estimates.

Given the equivalence ratio ϕ and initial conditions T_1 (K), $p_1 = p_i$ (Pa), and v_1 (m^3/kg air), the state at point 2 at the end of compression through a volume ratio $v_1/v_2 = r_c$ is obtained from Eq. (4.25*a*) and the isentropic compression chart (Fig. 4-4). The compression work W_C (J/kg air) is found from Eq. (5.6) with the internal energy change determined from the unburned mixture chart (Fig. 4-3).

The use of charts to relate the state of the burned mixture to the state of the unburned mixture prior to combustion, for adiabatic constant-volume and constant-pressure combustion, has already been illustrated in Sec. 4.5.3.

For the *constant-volume cycle*,

$$u_3 = u_{s2} + \Delta u^\circ_{f,u} \qquad \text{J/kg air} \tag{5.49}$$

where u_{s2} is the sensible internal energy of the unburned mixture at T_2 from Fig. 4-3 and $\Delta u^\circ_{f,u}$ is the internal energy of formation of the unburned mixture [given by Eq. (4.32)]. Since $v_3 = v_2$, the burned gas state at point 3 can be located on the appropriate burned gas chart (Figs. 4-5 to 4-9).

For the *constant-pressure cycle*,

$$h_3 = h_{s2} + \Delta h^\circ_{f,u} \qquad \text{J/kg air} \tag{5.50}$$

Since $p_3 = p_2$, the burned gas state at point 3 can be located (by iteration) on the high-temperature burned gas charts, as illustrated by Example 4.5.

For the *limited-pressure cycle*, application of the first law to the mixture between states 2 and 3*b* gives

$$h_{3b} = u_{3b} + p_3 v_{3b} = u_2 + p_3 v_2 = u_{s2} + \Delta u^\circ_{f,u} + p_3 v_2 \qquad \text{J/kg air} \tag{5.51}$$

Since p_3 for a limited-pressure cycle is given, point 3*b* can be located on the appropriate burned gas chart.

The expansion process 3-4 follows an isentropic line from v_3 to v_4 ($v_4 = v_1$) on the burned mixture charts. Equation (5.9) [or (5.11) or (5.13)] now gives the expansion work W_E. The state of the residual gas at points 5 and 6 in the cycle is obtained by continuing this isentropic expansion from state 4 to $p = p_e$. The residual gas temperature can be read from the equilibrium burned gas chart; the residual gas fraction is obtained from Eq. (5.17). If values of T_r and x_r were assumed at the start of the cycle calculation to determine T_1, the assumed values

PETITIONER'S EXHIBIT 1002
US PATENT NO. 6,581,565
Page 1715

can be checked against the calculated values and an additional cycle computation carried out with the new calculated values if required. The convergence is rapid.

The indicated fuel conversion efficiency is obtained from Eq. (5.1). The indicated mean effective pressure is obtained from Eq. (5.2). The volumetric efficiency (see Sec. 2.10) for a four-stroke cycle engine is given by

$$\eta_v = \frac{r_c(1 - x_r)}{v_1 \rho_{a,i}(r_c - 1)} \tag{5.52}$$

where $\rho_{a,i}$ is the inlet air density (in kilograms per cubic meter) and v_1 is the chart mixture specific volume (in cubic meters per kilogram of air in the original mixture).

Example 5.2. Calculate the performance characteristics of the constant-volume fuel-air cycle defined by the initial conditions of Examples 4.2, 4.3, and 4.5. The compression ratio is 8; the fuel is isooctane and the mixture is stoichiometric; the pressure and temperature inside the cylinder at the start of compression are 1 atm and 350 K, respectively. Use the notation of Fig. 5-2*a* to define the states at the beginning and end of each process.

Example 4.2 analyzed the compression process:

$$T_1 = 350 \text{ K}, \quad p_1 = 101.3 \text{ kPa}, \quad v_1 = 1 \text{ m}^3/\text{kg air}, \quad u_{s1} = 40 \text{ kJ/kg air}$$

$$T_2 = 682 \text{ K}, \quad p_2 = 1.57 \text{ MPa}, \quad v_2 = 0.125 \text{ m}^3/\text{kg air}, \quad u_{s2} = 350 \text{ kJ/kg air}$$

$$W_{1\text{-}2} = W_C = -310 \text{ kJ/kg air}$$

Example 4.5 analyzed the constant-volume adiabatic combustion process (it was assumed that the residual gas fraction was 0.08):

$$u_{b3} = u_{u2} = u_{s,u2} + \Delta u^\circ_{f,u} = -5 \text{ kJ/kg air}, \quad s_3 = 9.33 \text{ kJ/kg air} \cdot \text{K}$$

$$v_3 = v_2 = 0.125 \text{ m}^3/\text{kg air}, \quad T_3 = 2825 \text{ K}, \quad p_3 = 7100 \text{ kPa}$$

Example 4.3 analyzed the expansion process, from these conditions after combustion at TC, to the volume v_4 at BC of 1 m^3/kg air:

$$T_4 = 1840 \text{ K}, \quad p_4 = 570 \text{ kPa}, \quad u_4 = -1540 \text{ kJ/kg air}$$

$$W_{3\text{-}4} = W_E = 1535 \text{ kJ/kg air}$$

To check the assumed residual gas fraction, the constant entropy expansion process on the chart in Fig. 4-8 is continued from state 4 to the exhaust pressure p_5 of 1 atm = 101.3 kPa. This gives $v_5 = 4.0$ m^3/kg air and $T_5 = 1320$ K. The residual fraction from Eq. (5.17) is

$$x_r = \frac{v_2}{v_5} = \frac{0.125}{4.0} = 0.031$$

which is significantly different from the assumed value of 0.08. The combustion and expansion calculations are now repeated with the new residual fraction of 0.031 (the compression process will not be changed significantly and the initial temperature is

PETITIONER'S EXHIBIT 1002
US PATENT NO. 6,581,565
Page 1716

assumed fixed):

$$u_{b3} = 350 - 118.2 - 2956 \times 0.031 = 140 \text{ kJ/kg air}$$

With $v_3 = 0.125$ m^3/kg air, Fig. 4-8 gives

$$p_3 = 7270 \text{ kPa}, \qquad T_3 = 2890 \text{ K}$$

Expand at constant entropy to $v_4 = 1$ m^3/kg air:

$$p_4 = 595 \text{ kPa}, \qquad T_4 = 1920 \text{ K}, \qquad u_4 = -1457 \text{ kJ/kg air}$$

$$W_{3\text{-}4} = W_E = 1597 \text{ kJ/kg air}$$

Continue expansion at constant entropy to the exhaust pressure, $p_5 = 1$ atm:

$$v_5 = 4 \text{ m}^3\text{/kg air}, \qquad T_5 = 1360 \text{ K}$$

Equation (5.17) now gives the residual fraction

$$x_r = \frac{v_2}{v_5} = \frac{0.125}{4} = 0.031$$

which agrees with the value assumed for the second iteration.

The fuel conversion efficiency can now be calculated:

$$\eta_{f,i} = \frac{W_E + W_C}{m_f Q_{\text{LHV}}}$$

where $m_f = \text{kg fuel/kg air at state 1} = \left(\frac{F}{A}\right)(1 - x_r)$

Thus

$$\eta_{f,i} = \frac{1597 - 310}{0.0661 \times (1 - 0.031) \times 44.4 \times 10^3} = 0.45$$

The indicated mean effective pressure is

$$\text{imep} = \frac{W_E + W_C}{V_d} = \frac{1597 - 310}{1 - 0.125} = 1470 \text{ kPa}$$

or

$$\frac{\text{imep}}{p_1} = 14.6$$

5.5.2 CI Engine Cycle Simulation

With a diesel engine fuel-air cycle calculation, additional factors must be taken into account. The mixture during compression is air plus a small amount of residual gas. At point 2 liquid fuel is injected into the hot compressed air at temperature T_2; as the fuel vaporizes and heats up, the air is cooled. For a constant-volume mixing process which is adiabatic overall, the mixture internal energy is unchanged, i.e.:

$$m_f[u_{fg} + c_{v,f}(T_{2'} - T_0)] + m_a c_{v,a}(T_{2'} - T_2) = 0 \qquad (5.53)$$

PETITIONER'S EXHIBIT 1002
US PATENT NO. 6,581,565
Page 1717

where m_f is the mass of fuel injected, u_{fg} is the latent heat of vaporization of the fuel, $c_{v,f}$ is the specific heat at constant volume of the fuel vapor, $T_{2'}$ is the mixture temperature (assumed uniform) after vaporization and mixing is complete, m_a is the mass of air used, and $c_{v,a}$ is the specific heat at constant volume of air. Substitution of typical values for fuel and air properties gives $(T_2 - T_{2'}) \approx 70$ K at full load. Localized cooling in a real engine will be greater.

The limited-pressure cycle is a better approximation to the diesel engine than the constant-pressure or constant-volume cycles.

Note that because nonuniformities in the fuel/air ratio exist during and after combustion in the CI engine, the burned gas charts which assume uniform composition will not be as accurate an approximation to working fluid properties as they are for SI engines.

5.5.3 Results of Cycle Calculations

Extensive results of constant-volume fuel-air cycle calculations are available.[1, 3, 4] Efficiency is little affected by variables other than the compression ratio r_c and equivalence ratio ϕ. Figures 5-9 and 5-10 show the effect of variations in these two parameters on indicated fuel conversion efficiency and mean effective pressure. From the available results, the following conclusions can be drawn:

1. The effect of increasing the compression ratio on efficiency at a constant equivalence ratio is similar to that demonstrated by the constant γ constant-volume cycle analysis (provided the appropriate value of γ is used; see Fig. 5-19).
2. As the equivalence ratio is decreased below unity (i.e., the fuel-air mixture is made progressively leaner than stoichiometric), the efficiency increases. This occurs because the burned gas temperatures after combustion decrease, decreasing the burned gas specific heats and thereby increasing the effective value of γ over the expansion stroke. The efficiency increases because, for a given volume-expansion ratio, the burned gases expand through a larger temperature ratio prior to exhaust; therefore, per unit mass of fuel, the expansion stroke work is increased.
3. As the equivalence ratio increases above unity (i.e., the mixture is made progressively richer than stoichiometric), the efficiency decreases because lack of sufficient air for complete oxidation of the fuel more than offsets the effect of decreasing burned gas temperatures which decrease the mixture's specific heats.
4. The mean effective pressure, from Eq. (5.2), is proportional to the product $\phi\eta_{f,i}$. This exhibits a maximum between $\phi \approx 1.0$ and $\phi \approx 1.1$, i.e., slightly rich of stoichiometric. For ϕ less than the value corresponding to this maximum, the decreasing fuel mass per unit displaced volume more than offsets the increasing fuel conversion efficiency. For ϕ greater than this value, the decreasing fuel conversion efficiency (due to decreasing combustion efficiency) more than offsets the increasing fuel mass.

PETITIONER'S EXHIBIT 1002
US PATENT NO. 6,581,565
Page 1718

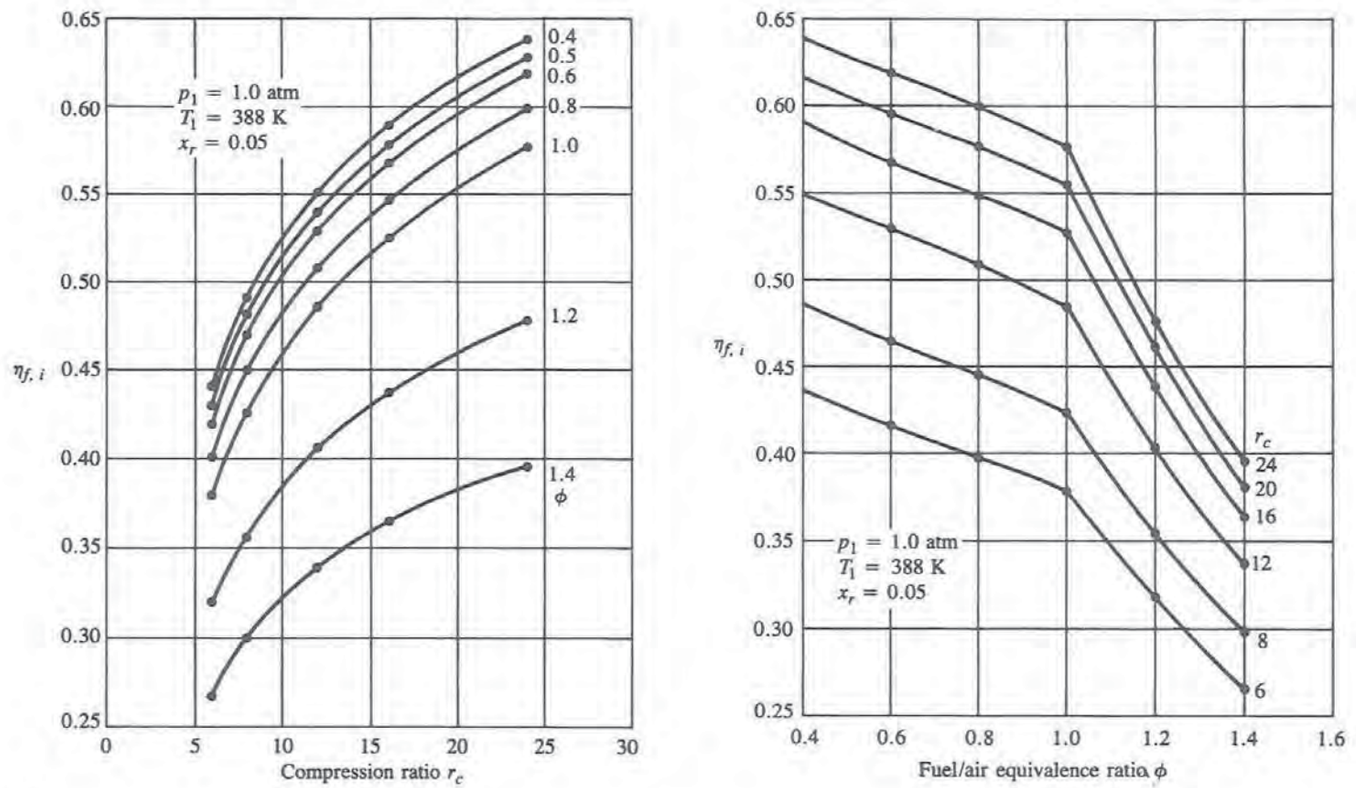


FIGURE 5-9
Fuel-air cycle results for indicated fuel conversion efficiency as a function of compression ratio and equivalence ratio. Fuel: octene; $p_1 = 1$ atm, $T_1 = 388$ K, $x_r = 0.05$. (*From Edson and Taylor.*[4])

PETITIONER'S EXHIBIT 1002
US PATENT NO. 6,581,565
Page 1719

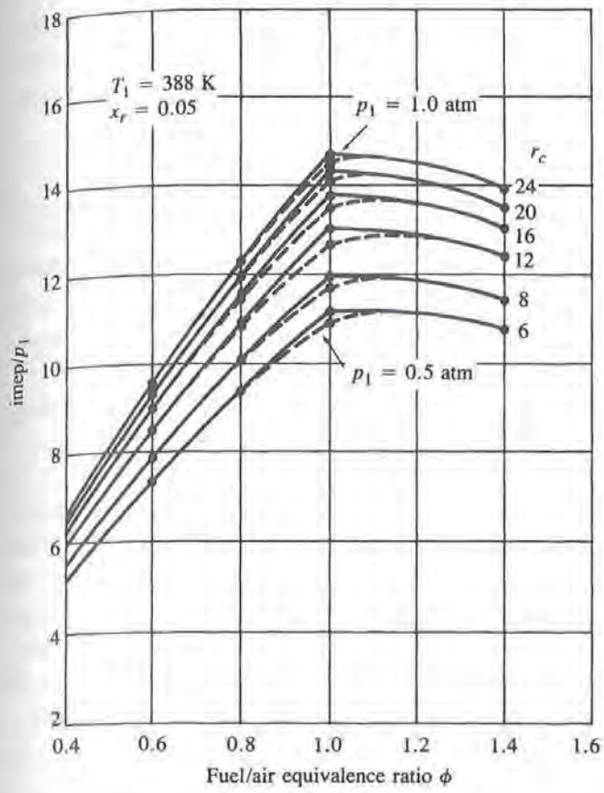


FIGURE 5-10
Fuel-air cycle results for indicated mean effective pressure as a function of equivalence ratio and compression ratio. Fuel: octene; $p_1 = 1$ atm, $T_1 = 388$ K, $x_r = 0.05$. (*From Edson and Taylor.*[4])

5. Variations in initial pressure, inlet temperature, residual gas fraction, and atmospheric moisture fraction have only a modest effect on the fuel conversion efficiency. The effects of variations in these variables on imep are more substantial, however, because imep depends directly on the initial charge density.
6. Comparison of results from limited-pressure and constant-volume fuel-air cycles[1] shows that placing a realistic limit on the maximum pressure reduces the advantages of increased compression ratio on both efficiency and imep.

5.6 OVEREXPANDED ENGINE CYCLES

The gas pressure within the cylinder of a conventional four-stroke engine at exhaust valve opening is greater than the exhaust pressure. The available energy of the cylinder gases at this point in the cycle is then dissipated in the exhaust blowdown process. Additional expansion within the engine cylinder would increase the indicated work per cycle, as shown in Fig. 5-11, where expansion continues beyond point 4′ (the conventional ideal cycle exhaust valve opening point) at $V_{4'} = r_c V_c$ to point 4 at $V_4 = r_e V_c$. The exhaust stroke in this overexpanded cycle is 4-5-6. The intake stroke is 6-1. The area 14′451 has been added

PETITIONER'S EXHIBIT 1002
US PATENT NO. 6,581,565
Page 1720

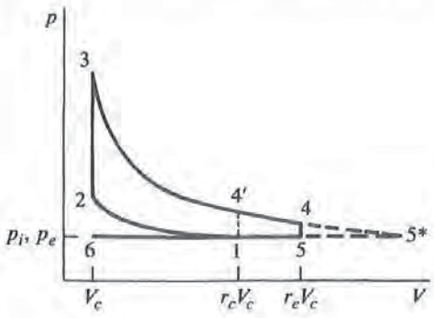


FIGURE 5-11
Pressure-volume diagram for overexpanded engine cycle (1234561) and Atkinson cycle (1235*61). r_c and r_e are volumetric compression and expansion ratios, respectively.

to the conventional cycle p-V diagram area, for the same fuel input, thereby increasing the engine's efficiency.

Complete expansion within the cylinder to exhaust pressure p_e (point 5*) is called the *Atkinson cycle*. Unthrottled operation is shown in Fig. 5-11; throttled operating cycles can also be generated. Many crank and valve mechanisms have been proposed to achieve this additional expansion. For example, it can be achieved in a conventional four-stroke cycle engine by suitable choice of exhaust valve opening and intake valve closing positions relative to BC. If the crank angle between exhaust valve opening and BC on the expansion stroke is less than the crank angle between BC and intake valve closing on the compression stroke, then the actual volumetric expansion ratio is greater than the actual volumetric compression ratio (these *actual* ratios are both less than the *nominal* compression ratio with normal valve timing).

The effect of overexpansion on efficiency can be estimated from an analysis of the ideal cycle shown in Fig. 5-11. An ideal gas working fluid with specific heats constant throughout the cycle will be assumed. The indicated work per cycle for the overexpanded cycle is

$$W_{c,i} = m[(u_3 - u_4) - (u_2 - u_1) - p_1(v_4 - v_1)] \tag{5.54}$$

The isentropic relations for 1-2 and 3-4 are

$$\frac{T_2}{T_1} = r_c^{\gamma-1} \qquad \frac{T_3}{T_4} = r_e^{\gamma-1}$$

With Eq. (5.33) to relate T_3 and T_2, the following expression for indicated fuel conversion efficiency can be derived from Eqs. (5.1), (5.29), and (5.54):

$$\eta_{f,i} = 1 - \frac{1}{(rr_c)^{\gamma-1}}\left\{1 + \frac{c_v T_1}{Q^*} r_c^{\gamma-1}[1 - \gamma r^{\gamma-1} + (\gamma - 1)r^{\gamma}]\right\} \tag{5.55}$$

where

$$r = \frac{r_e}{r_c}$$

Note that the efficiency given by Eq. (5.55) is a function of load (via Q^*), and is a

PETITIONER'S EXHIBIT 1002
US PATENT NO. 6,581,565
Page 1721

maximum at maximum load. This contrasts with the ideal constant-volume cycle efficiency [Eq. (5.31)], which is independent of load. The ratio r_e/r_c for complete expansion is given by

$$r^{\gamma} = 1 + \frac{Q^*}{c_v T_1 r_c^{\gamma - 1}} \tag{5.56}$$

The effect of overexpansion on fuel conversion efficiency is shown in Fig. 5-12 for $r_c = 4$, 8, and 16 with $\gamma = 1.3$. The ratio of overexpanded cycle efficiency to the standard cycle efficiency is plotted against r. The Atkinson cycle (complete expansion) values are indicated by the transition from a continuous line to a dashed line. Significant increases in efficiency can be achieved, especially at low compression ratios.

One major disadvantage of this cycle is that imep and power density decrease significantly because only part of the total displaced volume is filled with fresh charge. From Eqs. (5.2), (5.29), and the relations $V_d = V_1(r_e - 1)/r_c$ and

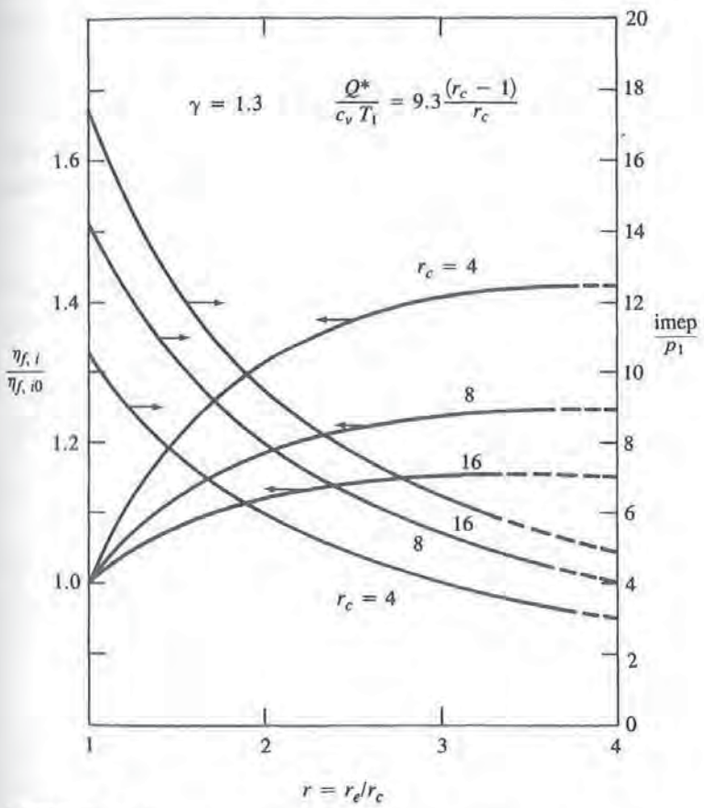


FIGURE 5-12
Indicated fuel conversion efficiency and mean effective pressure for overexpanded engine cycle as a function of r_e/r_c. Efficiencies given relative to $r_e = r_c$ value, $\eta_{f,i0}$. $\gamma = 1.3$, $Q^*/(c_v T_1) = 9.3(r_c - 1)/r_c$. Solid to dashed line transition marks the complete expansion point (Atkinson cycle).

PETITIONER'S EXHIBIT 1002
US PATENT NO. 6,581,565
Page 1722

$p_1 V_1 = mRT_1$ it follows that imep for the overexpanded cycle is given by

$$\frac{\text{imep}}{p_1} = \left(\frac{Q^*}{c_v T_1}\right)\left(\frac{1}{\gamma - 1}\right)\left(\frac{r_c}{r_e - 1}\right)\eta_{f,i} \tag{5.57}$$

Values of imep/p_1 are plotted in Fig. 5-12 as a function of $r(=r_e/r_c)$. The substantial decrease from the standard constant-volume cycle values at $r = 1$ is clear.

5.7 AVAILABILITY ANALYSIS OF ENGINE PROCESSES

5.7.1 Availability Relationships

Of interest in engine performance analysis is the amount of *useful work* that can be extracted from the gases within the cylinder at each point in the operating cycle. The problem is that of determining the maximum possible work output (or minimum work input) when a system (the charge within the cylinder) is taken from one specified state to another in the presence of a specified environment (the atmosphere). The first and second laws of thermodynamics together define this maximum or minimum work, which is best expressed in terms of the property of such a system-environment combination called *availability*[5] or sometimes *exergy*.[6, 7]

Consider the system-atmosphere combination shown in Fig. 5-13. In the absence of mass flow across the system boundary, as the system changes from state 1 to state 2, the first and second laws give

$$W_{1\text{-}2} = -(U_2 - U_1) + Q_{1\text{-}2}$$
$$Q_{1\text{-}2} \leq T_0(S_2 - S_1)$$

Combining these two equations gives the *total work* transfer:

$$W_{t,\,1\text{-}2} \leq -[(U_2 - U_1) - T_0(S_2 - S_1)] \tag{5.58}$$

The work done by the system against the atmosphere is not available for pro-

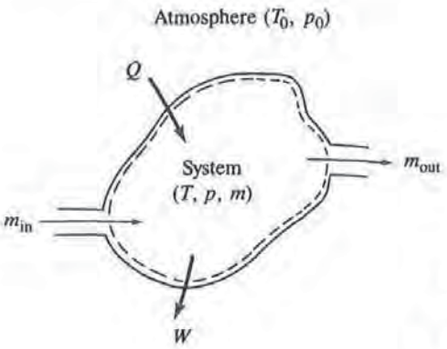


FIGURE 5-13
System-atmosphere configuration for availability analysis.

PETITIONER'S EXHIBIT 1002
US PATENT NO. 6,581,565
Page 1723

ductive use. It must, therefore, be subtracted from the total work to obtain the *useful work transfer*:

$$W_{U,1\text{-}2} \leq -[(U_2 - U_1) + p_0(V_2 - V_1) - T_0(S_2 - S_1)] \tag{5.59}$$

The *maximum* useful work will be obtained when the final state of the system is in thermal and mechanical equilibrium with the atmosphere.† The *availability* of this system which is in communication with the atmosphere

$$A = U + p_0 V - T_0 S \tag{5.60}$$

is thus the property of the system-atmosphere combination which defines its capacity for useful work. The useful work such a system-atmosphere combination can provide, as the system changes from state 1 to state 2, is less than or equal to the change in availability:

$$W_{U,\,1\text{-}2} \leq -(A_2 - A_1) \tag{5.61}$$

When mass flow across the system boundary occurs, the availability associated with this mass flow is

$$B = H - T_0 S \tag{5.62}$$

B is usually called the *steady-flow availability function.*

With these relations, an availability balance for the gas working-fluid system around the engine cycle can be carried out. For any process between specified end states which this system undergoes (interacting only with the atmosphere), the change in availability ΔA is given by

$$\Delta A = A_{\text{in}} - A_{\text{out}} - A_{\text{destroyed}} \tag{5.63}$$

The availability transfers in and out occur as a result of work transfers, heat transfers, and mass transfers across the system boundary. The availability transfer associated with a work transfer is equal to the work transfer. The availability transfer dA_Q associated with a heat transfer δQ occurring when the system temperature is T is given by

$$dA_Q = \delta Q\left(1 - \frac{T_0}{T}\right) \tag{5.64}$$

since both an energy and entropy transfer occurs across the system boundary. The availability transfer associated with a mass transfer is given by Eq. (5.62).

† The issue of chemical equilibrium with the atmosphere must also be considered. Attainment of chemical equilibrium with the environment requires the capacity to extract work from the partial pressure differences between the various species in the working fluid and the partial pressures of those same species in the environment. This would require such devices as ideal semipermeable membranes and efficient low input pressure, high pressure ratio, expansion devices (which are not generally available for mobile power plant systems). Inclusion of these additional steps to achieve full equilibrium beyond equality of temperature and pressure is inappropriate.[8]

PETITIONER'S EXHIBIT 1002
US PATENT NO. 6,581,565
Page 1724

Availability is destroyed by the irreversibilities that occur in any real process. The availability destroyed is given by

$$A_{\text{destroyed}} = T_0 \Delta S_{\text{irrev}} \tag{5.65}$$

where ΔS_{irrev} is the entropy increase associated with the irreversibilities occurring within the system boundary.[7, 8]

5.7.2 Entropy Changes in Ideal Cycles

The ideal models of engine processes examined earlier in this chapter provide useful illustrative examples for availability analysis. First, however, we will consider the variation in the entropy of the cylinder gases as they proceed through these ideal operating cycles.

For an adiabatic reversible compression process, the entropy is constant. For the combustion process in each of the ideal gas standard cycles, the entropy increase can be calculated from the relations of Eq. (4.14) (with constant specific heats):

$$s - s_0 = c_v \ln\left(\frac{T}{T_0}\right) + R \ln\left(\frac{v}{v_0}\right) = c_p \ln\left(\frac{T}{T_0}\right) - R \ln\left(\frac{p}{p_0}\right)$$

For the constant-volume cycle:

$$S_3 - S_2 = m(s_3 - s_2) = mc_v \ln\left(\frac{T_3}{T_2}\right) \tag{5.66a}$$

For the constant-pressure cycle:

$$S_3 - S_2 = m(s_3 - s_2) = mc_p \ln\left(\frac{T_3}{T_2}\right) \tag{5.66b}$$

For the limited-pressure cycle:

$$S_{3b} - S_2 = c_v \ln\left(\frac{T_{3a}}{T_2}\right) + c_p \ln\left(\frac{T_{3b}}{T_{3a}}\right) = c_v \ln \alpha + c_p \ln \beta \tag{5.66c}$$

with α and β defined by Eq. (5.42).

Since the expansion process, after combustion is complete, is adiabatic and reversible, there is no further change in entropy, 3 to 4 (or 3*b* to 4). Figure 5-14 shows the entropy changes that occur during each process of these three ideal engine operating cycles, calculated from the above equations, on a T-s diagram. The three cycles shown correspond to those of the p-V diagrams of Fig. 5-6 with $r_c = 12$, $\gamma = 1.3$, and $Q^*/(c_v T_1) = 8.525$. Since the combustion process was assumed to be adiabatic, the increase in entropy during combustion clearly demonstrates the irreversible nature of this process.

PETITIONER'S EXHIBIT 1002
US PATENT NO. 6,581,565
Page 1725

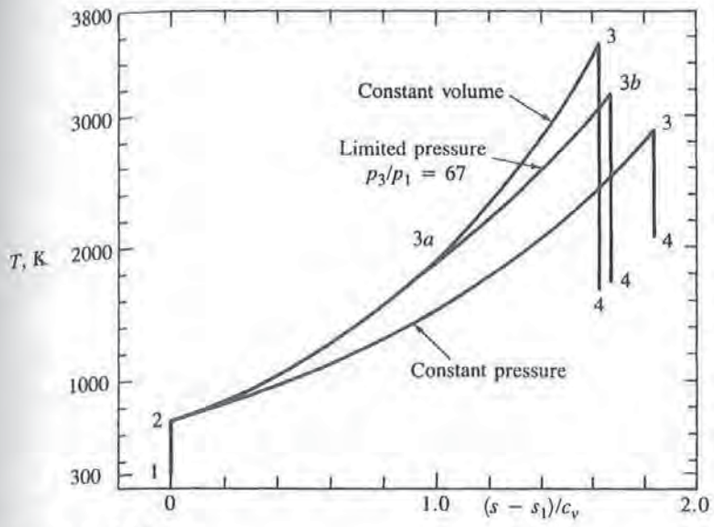


FIGURE 5-14
Temperature-entropy diagram for ideal gas constant-volume, constant-pressure, and limited-pressure cycles. Assumptions same as in Fig. 5-6.

5.7.3 Availability Analysis of Ideal Cycles

An availability analysis for each process in the ideal cycle illustrates the magnitude of the availability transfers and where the losses in availability occur.[9] In general, for the system of Fig. 5-4 in communication with an atmosphere at p_0, T_0 as indicated in Fig. 5-13, the change in availability between states i and j during the portion of the cycle when the valves are closed is given by

$$A_j - A_i = m(a_j - a_i) = m[(u_j - u_i) + p_0(v_j - v_i) - T_0(s_j - s_i)] \qquad (5.67)$$

The appropriate normalizing quantity for these changes in availability is the thermomechanical availability of the fuel supplied to the engine cylinder each cycle, $m_f(-\Delta g_{298})$† (see Sec. 3.6.2). However, it is more convenient to use $m_f(-\Delta h_{298})$‡ $= m_f Q_{\text{LHV}}$ as the normalizing quantity since it can be related to the temperature rise during combustion via Eq. (5.28). As shown in Table 3.3, these two quantities differ by only a few percent for common hydrocarbon fuels. Equation (5.67), with Eq. (5.29), then becomes

$$\frac{A_j - A_i}{m_f Q_{\text{LHV}}} = \frac{m(a_j - a_i)}{m_f Q_{\text{LHV}}} = \frac{a_j - a_i}{Q^*} \qquad (5.68)$$

† Δg_{298} is the Gibbs free energy change for the combustion reaction, per unit mass of fuel.
‡ Δh_{298} is the enthalpy change for the combustion reaction, again per unit mass of fuel.

PETITIONER'S EXHIBIT 1002
US PATENT NO. 6,581,565
Page 1726

The compression process is isentropic, so:

$$\frac{A_2 - A_1}{m_f Q_{LHV}} = \frac{a_2 - a_1}{Q^*} = \frac{(u_2 - u_1) + p_0(v_2 - v_1)}{Q^*}$$
$$= \frac{c_v T_1}{Q^*}\left[\left(\frac{T_2}{T_1} - 1\right) - (\gamma - 1)\left(1 - \frac{V_2}{V_1}\right)\right]$$
$$= \frac{c_v T_1}{Q^*}\left[(r_c^\gamma - 1) - (\gamma - 1)\left(1 - \frac{1}{r_c}\right)\right] \tag{5.69}$$

where we have assumed $p_0 = p_1$. The first term in the square brackets is the compression stroke work transfer. The second term is the work done by the atmosphere on the system, which is subtracted because it does not increase the *useful work* which the system-atmosphere combination can perform.

During combustion, for the constant-volume cycle, the volume and internal energy remain unchanged (Eqs. 5.7*a*, *b*). Thus

$$\frac{A_3 - A_2}{m_f Q_{LHV}} = \frac{a_3 - a_2}{Q^*} = -\frac{T_0(s_3 - s_2)}{Q^*}$$
$$= -\frac{c_v T_0}{Q^*}\ln\left(\frac{T_3}{T_2}\right) = -\frac{c_v T_0}{Q^*}\ln\left(1 + \frac{Q^*}{c_v T_1 r_c^{\gamma-1}}\right) \tag{5.70}$$

This loss in availability results from the increase in entropy associated with the irreversibilities of the combustion process. This lost or destroyed availability, as a fraction of the initial availability of the fuel-air mixture, decreases as the compression ratio increases (since T_2 increases as the compression ratio increases, T_3/T_2 decreases for fixed heat addition) and increases as Q^* decreases [e.g., when the mixture is made leaner; see Eq. (5.46)]. The changes in availability during combustion for the constant-pressure and limited-pressure cycles are more complex because there is a transfer of availability out of the system equal to the expansion work transfer which occurs.

For the constant-volume cycle expansion stroke:

$$\frac{A_4 - A_3}{m_f Q_{LHV}} = \frac{a_4 - a_3}{Q^*} = \frac{(u_4 - u_3) + p_0(v_4 - v_3)}{Q^*}$$
$$= \frac{c_v T_3}{Q^*}\left[\left(\frac{T_4}{T_3} - 1\right) + (\gamma - 1)\left(\frac{p_0}{p_3}\right)\left(\frac{V_4}{V_3} - 1\right)\right]$$
$$= -\left[\left(1 + \frac{c_v T_1 r_c^{\gamma-1}}{Q^*}\right)\left(1 - \frac{1}{r_c^{\gamma-1}}\right) - (\gamma - 1)\frac{c_v T_1}{Q^*}\left(\frac{r_c - 1}{r_c}\right)\right] \tag{5.71}$$

The availability of the exhaust gas at state 4 relative to its availability at (T_1, p_1) is given by

$$\frac{A_4 - A_1}{m_f Q_{LHV}} = \frac{c_v T_1}{Q^*}\left[\left(\frac{T_4}{T_1} - 1\right) - \frac{T_0}{T_1}\ln\left(\frac{T_4}{T_1}\right)\right] \tag{5.72}$$

PETITIONER'S EXHIBIT 1002
US PATENT NO. 6,581,565
Page 1727

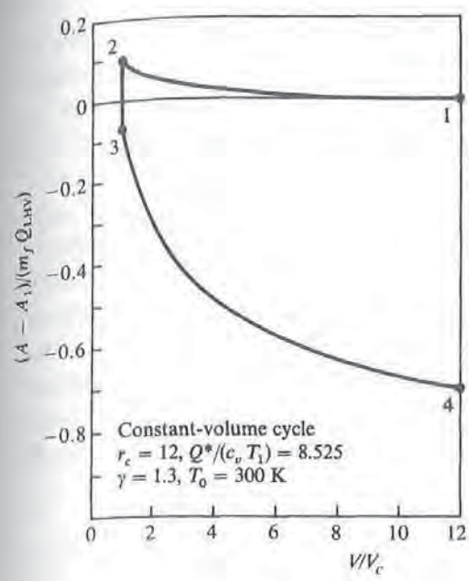


FIGURE 5-15
Availability of cylinder charge relative to availability at state 1 for constant-volume ideal gas cycle as a function of cylinder volume. Availability made dimensionless by $m_f Q_{LHV}$. Assumptions as in Fig. 5-6.

The availability of the gases inside the cylinder relative to their availability at (T_1, p_1) over the compression and expansion strokes of the constant-volume operating cycle example used in Figs. 5-6 and 5-14 is shown in Fig. 5-15. Equations (5.69) and (5.71), with T_2 and T_4 replaced by temperatures intermediate between T_1 and T_2 and T_3 and T_4, respectively, were used to compute the variations during compression and expansion. Table 5.3 summarizes the changes in availability during each process and the availability of the cylinder gases, at the beginning and end of each process, relative to the datum for the atmosphere

TABLE 5.3
Availability changes in constant-volume cycle

Process or state	$\frac{A_j - A_i}{m_f Q_{LHV}}$	$\frac{A_i}{m_f Q_{LHV}}$
1		1.0294
1-2	0.0976	
2		1.1270
2-3	−0.1710	
3		0.9560
3-4	−0.6237	
4		0.3323
Fuel conversion efficiency $\eta_{f,i}$	0.526	
Availability conversion efficiency $\eta_{a,i}$	0.511	

$r_c = 12$, $\gamma = 1.3$, $Q^*/(c_v T_1) = 8.525$, $T_0 = 300$ K, $T_1 = 333$ K.

PETITIONER'S EXHIBIT 1002
US PATENT NO. 6,581,565
Page 1728

(1 atm, 300 K). The availability at state 1 of the fuel, air, residual-gas mixture is $(1.0286 + 0.0008)m_f Q_{LHV}$. 1.0286 is the ratio $(-\Delta g^\circ_{298})/(-\Delta h^\circ_{298})$ for isooctane (see Table 3.3). The second number, 0.0008, allows for the difference between T_1 and T_0. Because both work-transfer processes in this ideal cycle case are reversible, the fuel conversion efficiency $\eta_{f,i}$ is given by $(A_3 - A_4)/(m_f Q_{LHV}) - (A_2 - A_1)/(m_f Q_{LHV})$. It is, of course, equal to the value obtained for $r_c = 12$ and $\gamma = 1.3$ from the formula for efficiency (Eq. 5.31), obtained previously. The availability conversion efficiency is $\eta_{f,i}/1.0286$. Note that it is the availability destroyed during combustion, plus the inability of this ideal constant-volume cycle to use the availability remaining in the gas at state 4, that decrease the availability conversion efficiency below unity. Both these loss mechanisms decrease in magnitude, relative to the fuel availability, as the compression ratio increases. This is the fundamental reason why engine indicated efficiency increases with an increasing compression ratio.

5.7.4 Effect of Equivalence Ratio

The fuel-air cycle with its more accurate models for working fluid properties can be used to examine the effect of variations in the fuel/air equivalence ratio on the availability conversion efficiency. Figure 5-16 shows the temperature attained and the entropy rise that occurs in constant-volume combustion of a fuel-air mixture of different equivalence ratios, following isentropic compression from ambient temperature and pressure through different volumetric compression ratios.[8] The entropy increase is the result of irreversibilities in the combustion process and mixing of complete combustion products with excess air. The significance of these combustion-related losses—the destruction of availability that occurs in this process—is shown in Fig. 5-17 where the availability after constant-volume combustion divided by the availability of the initial fuel-air mixture is shown as a function of equivalence ratio for compression ratios of 12 and 36.[8] The loss of

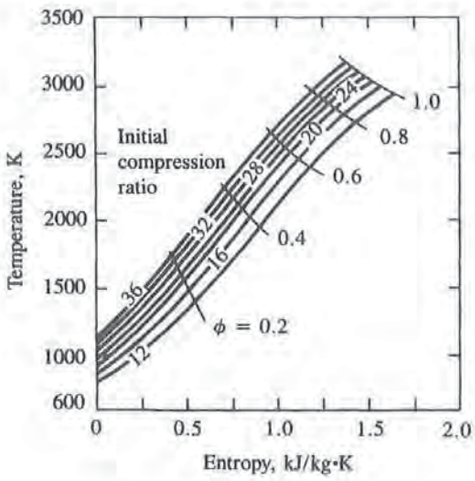


FIGURE 5-16
Temperature and entropy of combustion products after constant-volume combustion following isentropic compression from ambient conditions through specified compression ratio as a function of compression ratio and equivalence ratio. (*From Flynn et al.*[8])

PETITIONER'S EXHIBIT 1002
US PATENT NO. 6,581,565
Page 1729

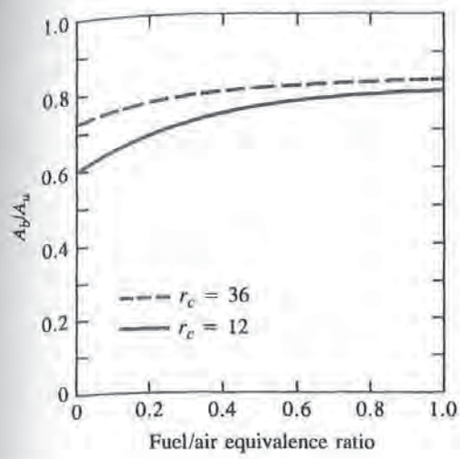


FIGURE 5-17
Availability of combustion products after constant-volume combustion relative to availability before combustion following isentropic compression from ambient through specified compression ratio as a function of equivalence ratio. (*From Flynn et al.*[8])

availability increases as the equivalence ratio decreases.† The combustion loss is a stronger function of the rise in temperature and pressure which occurs than of the change in the specific heat ratio that occurs.

Why then does engine efficiency increase with a decreasing equivalence ratio as shown in Fig. 5-9? The reason is that the expansion stroke work transfer, as a fraction of the fuel availability, increases as the equivalence ratio decreases; hence, the availability lost in the exhaust process, again expressed as a fraction of the fuel availability, decreases. The increase in the expansion stroke work as the equivalence ratio decreases more than offsets the increase in the availability lost during combustion; so the availability conversion efficiency (or the fuel conversion efficiency which closely approximates it) increases.

5.8 COMPARISON WITH REAL ENGINE CYCLES

To put these ideal models of engine processes in perspective, this chapter will conclude with a brief discussion of the additional effects which are important in real engine processes.

A comparison of a real engine p-V diagram over the compression and expansion strokes with an equivalent fuel-air cycle analysis is shown in Fig. 5-18.[4] The real engine and the fuel-air cycle have the same geometric compression ratio, fuel chemical composition and equivalence ratio, residual fraction and mixture density before compression. Midway through the compression stroke,

† This is consistent with the ideal gas standard cycle result (Eq. 5.70). As ϕ decreases, so does $Q^*/(c_v T_1)$. The factor which multiplies the natural logarithm (which increases) has a greater impact than the logarithmic term (which decreases).

PETITIONER'S EXHIBIT 1002
US PATENT NO. 6,581,565
Page 1730

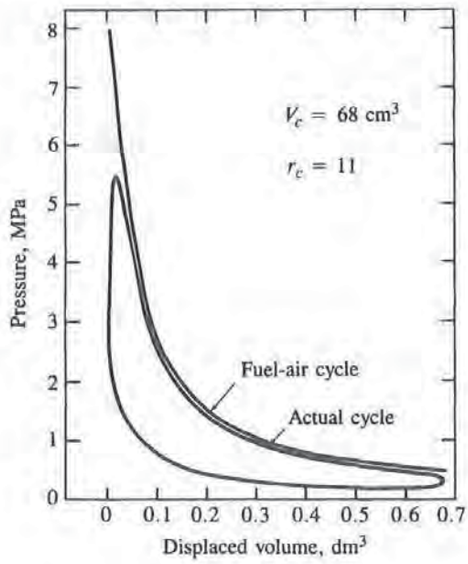


FIGURE 5-18
Pressure-volume diagram for actual spark-ignition engine compared with that for equivalent fuel-air cycle. $r_c = 11$. (*From Edson and Taylor.*[4])

the pressure in the fuel-air cycle has been made equal to the real cycle pressure.† The compression stroke pressures for the two cycles essentially coincide. Modest differences in pressure during intake and the early part of the compression process result from the pressure drop across the intake valve during the intake process and the closing of the intake valve 40 to 60° after BC in the real engine. The expansion stroke pressures for the engine fall below the fuel-air cycle pressures for the following reasons: (1) heat transfer from the burned gases to the walls; (2) finite time required to burn the charge; (3) exhaust blowdown loss due to opening the exhaust valve before BC; (4) gas flow into crevice regions and leakage past the piston rings; (5) incomplete combustion of the charge.

These differences, in decreasing order of importance, are described below. Together, they contribute to the enclosed area on the p-V diagram for a properly adjusted engine with optimum timing being about 80 percent of the enclosed area of an equivalent fuel-air cycle p-V diagram. The indicated fuel conversion or availability conversion efficiency of the actual engine is therefore about 0.8 times the efficiency calculated for the fuel-air cycle.[1] Use is often made of this ratio to estimate the performance of actual engines from fuel-air cycle results.

1. *Heat transfer.* Heat transfer from the unburned mixture to the cylinder walls has a negligible effect on the p-V line for the compression process. Heat transfer from the burned gases is much more important (see Chap. 12). Due to heat transfer during combustion, the pressure at the end of combustion in the real

† Note that in the fuel-air cycle with idealized valve timing, the compression process starts immediately after BC. In most engines, the charge compression starts later, close to the time that the inlet valve closes some 40 to 60° after BC. This matching process is approximate.

PETITIONER'S EXHIBIT 1002
US PATENT NO. 6,581,565
Page 1731

cycle will be lower. During expansion, heat transfer will cause the gas pressure in the real cycle to fall below an isentropic expansion line as the volume increases. A decrease in efficiency results from this heat loss.

2. *Finite combustion time.* In an SI engine with spark-timing adjusted for optimum efficiency, combustion typically starts 10 to 40 crank angle degrees before TC, is half complete at about 10° after TC, and is essentially complete 30 to 40° after TC. Peak pressure occurs at about 15° after TC (see Fig. 1-8). In a diesel engine, the burning process starts shortly before TC. The pressure rises rapidly to a peak some 5 to 10° after TC since the initial rate of burning is fast. However, the final stages of burning are much slower, and combustion continues until 40 to 50° after TC (see Fig. 1-15). Thus, the peak pressure in the engine is substantially below the fuel-air cycle peak pressure value, because combustion continues until well after TC, when the cylinder volume is much greater than the clearance volume. After peak pressure, expansion stroke pressures in the engine are higher than fuel-air cycle values in the absence of other loss mechanisms, because less work has been extracted from the cylinder gases. A comparison of the constant-volume and limited-pressure cycles in Fig. 5-6 demonstrates this point.

   For spark or fuel-injection timing which is retarded from the optimum for maximum efficiency, the peak pressure in the real cycle will be lower, and expansion stroke pressures after the peak pressure will be higher than in the optimum timing cycle.

3. *Exhaust blowdown loss.* In the real engine operating cycle, the exhaust valve is opened some 60° before BC to reduce the pressure during the first part of the exhaust stroke in four-stroke engines and to allow time for scavenging in two-stroke engines. The gas pressure at the end of the expansion stroke is therefore reduced below the isentropic line. A decrease in expansion-stroke work transfer results.

4. *Crevice effects and leakage.* As the cylinder pressure increases, gas flows into crevices such as the regions between the piston, piston rings, and cylinder wall. These crevice regions can comprise a few percent of the clearance volume. This flow reduces the mass in the volume above the piston crown, and this flow is cooled by heat transfer to the crevice walls. In premixed charge engines, some of this gas is unburned and some of it will not burn. Though much of this gas returns to the cylinder later in the expansion, a fraction, from behind and between the piston rings, flows into the crankcase. However, leakage in a well-designed and maintained engine is small (usually less than one percent of the charge). All these effects reduce the cylinder pressure during the latter stages of compression, during combustion, and during expansion below the value that would result if crevice and leakage effects were absent.

5. *Incomplete combustion.* Combustion of the cylinder charge is incomplete; the exhaust gases contain combustible species. For example, in spark-ignition engines the hydrocarbon emissions from a warmed-up engine (which come largely from the crevice regions) are 2 to 3 percent of the fuel mass under

PETITIONER'S EXHIBIT 1002
US PATENT NO. 6,581,565
Page 1732

normal operating conditions; carbon monoxide and hydrogen in the exhaust contain an additional 1 to 2 percent or more of the fuel energy, even with excess air present (see Sec. 4.9). Hence, the chemical energy of the fuel which is released in the actual engine is about 5 percent less than the chemical energy of the fuel inducted (the combustion efficiency, see Sec. 3.5.5, is about 95 percent). The fuel-air cycle pressures after combustion will be higher because complete combustion is assumed. In diesel engines, the combustion inefficiency is usually less, about 1 to 2 percent, so this effect is smaller.

SUMMARY. The effect of all these loss mechanisms on engine efficiency is best defined by an availability balance for the real engine cycle. A limited number of such calculations have been published (e.g., Refs. 8, 10, and 11). Table 5.4 shows the magnitude of the loss in availability (as a fraction of the initial availability) that occurs due to real cycle effects in a typical naturally aspirated diesel engine.[10] The combustion and exhaust losses are present in the ideal cycle models also (they are smaller, however[9]). The loss in availability due to heat losses, flow or aerodynamic losses, and mechanical friction are real engine effects.

Figure 5-19 shows standard and fuel-air cycle efficiencies as a function of the compression ratio compared with engine indicated efficiency data. The top three sets of engine data are for the best efficiency air/fuel ratio. Differences in the data are in part due to different fuels [(12) isooctane; (13) gasoline; (14) propane] which affect efficiency slightly through their different composition and heating values (see Table D.4). They also result from different combustion chamber shapes which affect the combustion rate and heat transfer. The trends in the data with increasing compression ratio and the $\phi = 0.8$ fuel-air cycle curve (which corresponds approximately to the actual air/fuel ratios used) are similar. The factor of 0.8 relating real engine and fuel-air cycle efficiencies holds roughly. At compression ratios above about 14, however, the data show that the indicated efficiency of actual engines is essentially constant. Increasing crevice and heat

TABLE 5.4
Availability losses in naturally aspirated diesel

Loss mechanism	Loss, fraction of fuel availability
Combustion	0.225
Exhaust	0.144
Heat transfer	0.135
Aerodynamic	0.047
Mechanical friction	0.048
Total losses	0.599
Availability conversion efficiency (brake)	0.401

Source: Traupel.[10]

PETITIONER'S EXHIBIT 1002
US PATENT NO. 6,581,565
Page 1733

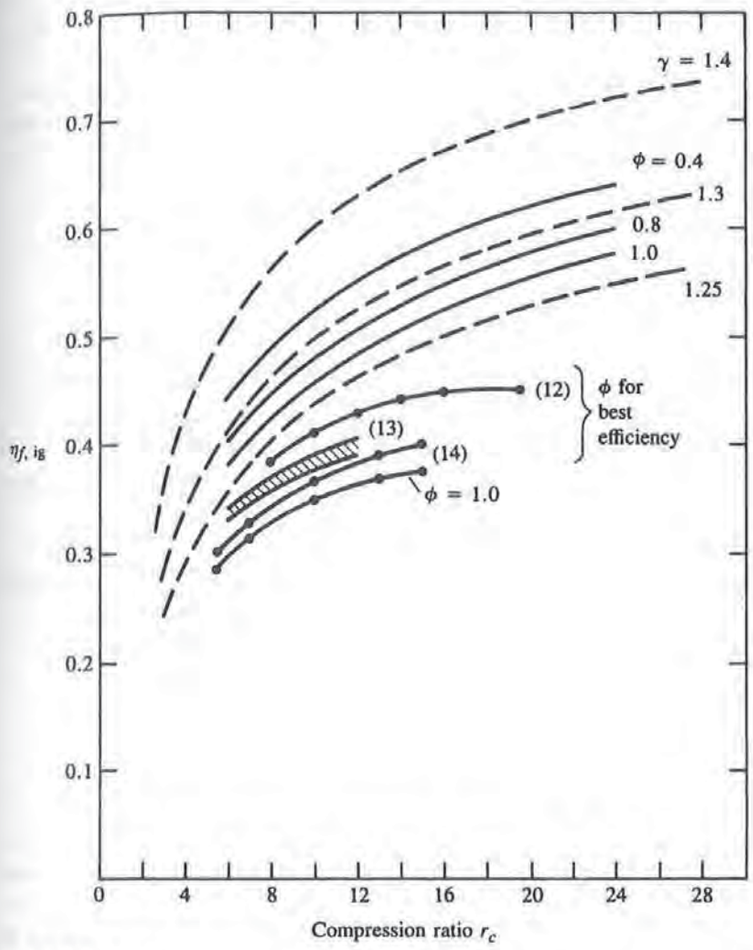


FIGURE 5-19
Indicated fuel conversion efficiency as a function of compression ratio for ideal gas constant-volume cycle (dashed lines, $\gamma = 1.25$, 1.3, 1.4) and fuel-air cycle (solid lines, $\phi = 0.4$, 0.8, 1.0). Also shown are available engine data for equivalence ratios given: best efficiency ϕ;[12–14] $\phi = 1$.[14]

losses offset the calculated ideal cycle efficiency increase as the compression ratio is raised above this value. The standard ideal gas cycle analysis results, with an appropriate choice for the value of γ (1.25 to 1.3), correspond closely to the fuel-air cycle analysis results.

The ideal cycle provides a convenient but crude approximation to the real engine operating cycle. It is useful for illustrating the thermodynamic aspects of engine operation. It can also provide approximate estimates of trends as major engine parameters change. The weakest link in these ideal cycles is the modeling of the combustion processes in SI and CI engines. None of the models examined in this chapter are sufficiently close to reality to provide accurate predictions of engine performance. More sophisticated models of the spark-ignition and diesel engine operating cycles have been developed and are the subject of Chap. 14.

PETITIONER'S EXHIBIT 1002
US PATENT NO. 6,581,565
Page 1734

PROBLEMS

5.1. Many diesel engines can be approximated by a limited-pressure cycle. In a limited-pressure cycle, a fraction of the fuel is burnt at constant volume and the remaining fuel is burnt at constant pressure. Use this cycle approximation with $\gamma = c_p/c_v = 1.3$ to analyze the following problem:

Inlet conditions:	$p_1 = 1.0$ bar, $T_1 = 289$ K
Compression ratio:	15 : 1
Heat added during combustion:	43,000 kJ/kg of fuel
Overall fuel/air ratio:	0.045 kg fuel/kg air

(*a*) Half of the fuel is burnt at constant volume, then half at constant pressure. Draw a p-V diagram and compute the fuel conversion efficiency of the cycle.

(*b*) Compare the efficiency and peak pressure of the cycle with the efficiency and peak pressure that would be obtained if all of the fuel were burnt at constant pressure or at constant volume.

5.2. It is desired to increase the output of a spark-ignition engine by either (1) raising the compression ratio from 8 to 10 or (2) increasing the inlet pressure from 1.0 atm to 1.5 atm. Using the constant-volume cycle as a model for engine operation, which procedure will give:

(*a*) The highest pressure of the cycle?

(*b*) The highest efficiency?

(*c*) The highest mep?

Assume $\gamma = 1.3$ and $(m_f Q_{HV})/(mc_v T_1) = 9.3(r_c - 1)/r_c$.

5.3. When a diesel engine, originally designed to be naturally aspirated, is turbocharged the fuel/air equivalence ratio ϕ at full load must be reduced to maintain the maximum cylinder pressure essentially constant. If the naturally aspirated engine was designed for $\phi = 0.75$ at full load, estimate the maximum permissible value of ϕ for the turbocharged engine at full load if the air pressure at the engine inlet is 1.6 atm. Assume that the engine can be modeled with the limited-pressure cycle, with half the injected fuel burned at constant volume and half at constant pressure. The compression ratio is 16. The fuel heating value is 42.5 MJ/kg fuel. Assume $\gamma = c_p/c_v = 1.35$, that the air temperature at the start of compression is 325 K, and $(F/A)_{stoich} = 0.0666$.

5.4. A spark-ignition engine is throttled when operating at part load (the inlet pressure is reduced) while the fuel/air ratio is held essentially constant. Part-load operation of the engine is modeled by the cycle shown in Fig. 5-2*d*; the inlet air is at pressure p_1, the exhaust pressure is atmospheric p_a, and the ambient temperature is T_a. Derive an expression for the *decrease* in net indicated fuel conversion efficiency due to throttling from the ideal constant-volume cycle efficiency and show that it is proportional to $(p_a/p_1 - 1)$. Assume mass fuel $\ll$ mass air.

5.5. (*a*) Use the ideal gas cycle with constant-volume combustion to describe the operation of an SI engine with a compression ratio of 9. Find the pressure and temperature at points 2, 3, 4, and 5 on Fig. 5-2a. Assume a pressure of 100 kPa and a temperature of 320 K at point 1. Assume $m_f/m = 0.06$, $c_v = 946$ J/kg·K, $\gamma = 1.3$. Q_{LHV} for gasoline is 44 MJ/kg.

(*b*) Find the indicated fuel conversion efficiency and imep for this engine under these operating conditions.

PETITIONER'S EXHIBIT 1002
US PATENT NO. 6,581,565
Page 1735

5.6. Use a limited-pressure cycle analysis to obtain a plot of indicated fuel conversion efficiency versus p_3/p_1 for a compression ratio of 15 with light diesel oil as fuel. Assume $m_f/m = 0.04$, $T_1 = 45°C$. Use $\gamma = 1.3$ and $c_v = 946$ J/kg·K.

5.7. Explain why constant-volume combustion gives a higher indicated fuel conversion efficiency than constant-pressure combustion for the same compression ratio.

5.8. Two engines are running at a bmep of 250 kPa. One is an SI engine with the throttle partially closed to maintain the correct load. The second engine is a naturally aspirated CI engine which requires no throttle. Mechanical friction mep for both engines is 100 kPa. If the intake manifold pressures for the SI and CI engines are 25 kPa and 100 kPa respectively, and both exhaust manifold pressures are 105 kPa, use an ideal cycle model to estimate and compare the *gross* imep of the two engines. You may neglect the pressure drop across the valves during the intake and exhaust processes.

5.9. (*a*) Plot net imep versus p_i for 20 kPa $< p_i <$ 100 kPa for a constant-volume cycle using the following conditions: $m_f/m = 0.06$, $T_1 = 40°C$, $c_v = 946$ J/kg·K, $\gamma = 1.3$, $r_c = 9.5$, $Q_{LHV} = 44$ MJ/kg fuel. Assume $p_e = 100$ kPa.

(*b*) What additional information is necessary to draw a similar plot for the engine's indicated torque, and indicated power?

5.10. (*a*) Draw a diagram similar to those in Fig. 5-2 for a supercharged cycle with constant-pressure combustion.

(*b*) Use the ideal gas cycle with constant-pressure combustion to model an engine with a compression ratio of 14 through such a supercharged cycle. Find the pressure and temperature at points corresponding to 2, 3, 4, and 5 in Fig. 5-2. Assume a pressure of 200 kPa and temperature of 325 K at point 1, and a pressure of 100 kPa at points 5 and 6. $m_f/m = 0.03$ and the fuel is a light diesel oil.

(*c*) Calculate the gross and net indicated fuel conversion efficiency and imep for this engine under these operating conditions.

5.11. Use the appropriate tables and charts to carry out a constant-pressure fuel-air cycle calculation for the supercharged engine described in Prob. 5.10. Assume the same initial conditions at point 1, with $\phi = 0.4$ and a residual gas fraction of 0.025. A single cycle calculation is sufficient.

(*a*) Determine the pressure and temperature at points 2, 3, 4, and 5. Calculate the compression stroke, expansion stroke, and pumping work per cycle per kg air.

(*b*) Find the gross and net indicated fuel conversion efficiency and imep.

(*c*) Compare the calculated residual gas fraction with the assumed value of 0.025.

5.12. One method proposed for reducing the pumping work in throttled spark-ignition engines is *early intake valve closing* (EIVC). The ideal cycle p-V diagram shown illustrates the concept. The EIVC cycle is 1-2-3-4-5-6-7-8-1 (the conventional throttled cycle is 1-2-3-4-5-6-7*-1). With EIVC, the inlet manifold is held at a pressure p_i (which is higher than the normal engine intake pressure, p_i^*), and the inlet valve is closed *during* the inlet stroke at 8. The trapped fresh charge and residual is then *expanded* to the normal cycle (lower) intake pressure, p_i^*. You can assume that both cycles have the same mass of gas in the cylinder, temperature, and pressure at state 1 of the cycle.

(*a*) On a sketch of the intake and exhaust process p-V diagram, shade in the area that corresponds to the difference between the pumping work of the EIVC cycle and that of the normal cycle.

(*b*) What value of p_i and V_{EIVC} will give the maximum reduction in pumping work for the EIVC cycle.

PETITIONER'S EXHIBIT 1002
US PATENT NO. 6,581,565
Page 1736

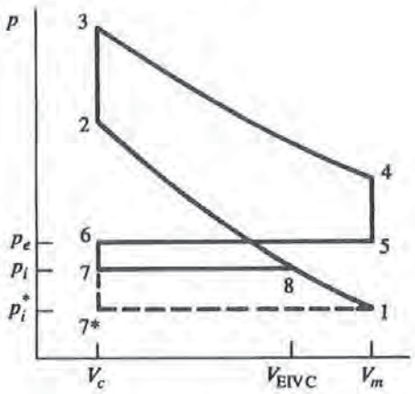


FIGURE P5-12

(*c*) Derive an expression for this maximum difference in pumping work between the normal cycle and the EIVC cycle in terms of p_e, p_i^*, V_c, and V_m. You can make the appropriate ideal cycle assumptions.

5.13. Calculate the following parameters for a constant-volume fuel-air cycle (Fig. 5-2*a*):

(*a*) The pressures and temperatures at states 1, 2, 3, 4, 5, and 6

(*b*) The indicated fuel conversion efficiency

(*c*) The imep

(*d*) The residual fraction

(*e*) The volumetric efficiency

Inlet pressure = 1 atm, exhaust pressure = 1 atm, inlet temperature = 300 K, compression ratio = 8 : 1, equivalence ratio = $\phi = 1$.

Calculate the above parameters (points *a*–*e*) using the SI units charts. Use 44.4 MJ/kg for heating value of the fuel. *Hint:* Start the calculations using the residual mass fraction 0.03 and the residual gas temperature 1370 K.

5.14. The cycle 1-2-3-4-5-6-1 is a conventional constant-volume fuel-air cycle with a compression ratio of 8. The fuel is isooctane, C_8H_{18}, with a lower heating value of 44.4 MJ/kg. The gas state at 1 is $T_1 = 300$ K, $p_1 = 1$ atmosphere with an equivalence ratio of 1.0 and zero residual fraction. The specific volume at state 1 is 0.9 m^3/kg air in the mixture. The temperature at the end of compression at state 2 is 600 K.

(*a*) Find the indicated fuel conversion efficiency and mean effective pressure of this fuel-air cycle model of a spark-ignition engine.

(*b*) The efficiency of the cycle can be increased by increasing the expansion ratio r_e while maintaining the same compression ratio r_c (cycle 1-2-3-4*A*-5*A*-6-1). (This

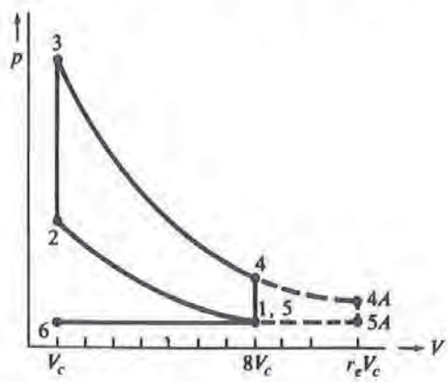


FIGURE P5-14

PETITIONER'S EXHIBIT 1002
US PATENT NO. 6,581,565
Page 1737

can be done with valve timing.) If the expansion ratio r_e is 12, while the compression ratio and other details of the cycle remain the same as in (*a*), what is the indicated efficiency and mean effective pressure (based on the new, larger, displaced volume) of this new engine cycle?

5.15. In spark-ignition engines, exhaust gas is recycled to the intake at part load to reduce the peak burned gas temperatures and lower emissions of nitrogen oxides.

(*a*) Calculate the reduction in burned gas temperature that occurs when, due to exhaust gas recycle, the burned gas fraction in the unburned gas mixture (x_b) inside the cylinder is increased from 10 percent (the normal residual fraction) to 30 percent. Assume combustion occurs at top-center, at constant volume, and is adiabatic. Conditions at the end of compression for both cases are: $T = 700$ K, $p = 1000$ kPa, $v = 0.2$ m^3/kg air in the original mixture; the equivalence ratio is 1.0. The fuel can be modeled as isooctane.

(*b*) The compression ratio is 8. The compression stroke work is 300 kJ/kg air in the original mixture. Find the indicated work per cycle for the compression and expansion strokes, per kilogram of air in the original mixture, for these two cases.

(*c*) Briefly explain how you would increase the work per cycle with 30 percent burned gas fraction in the unburned mixture to the value obtained with 10 percent burned gas fraction, with fixed engine geometry. (A qualitative answer, only, is required here.)

5.16. The following cycle has been proposed for improving the operation of a four-stroke cycle engine. Its aim is to expand the postcombustion cylinder gases to a lower pressure and temperature by extending the expansion stroke, and hence extract more work per cycle.

The cycle consists of: (1) an intake stroke; (2) a compression stroke, where the inlet valve remains open (and the cylinder pressure is constant) for the first portion of the stroke; (3) a combustion process, which occurs rapidly close to top-center; (4) an expansion stroke, where the exhaust valve remains closed until the end of the stroke; (5) an exhaust stroke, where the cylinder pressure blows down to the exhaust pressure rapidly and most of the remaining combustion products are expelled as the piston moves from the BC to the TC position. Thus, for this engine concept, the compression ratio r_c (ratio of cylinder volume at inlet valve closing to clearance volume) is less than the expansion ratio r_e (ratio of cylinder volume at exhaust valve opening to clearance volume).

(*a*) Sketch a p-V diagram for the cylinder gases for this cycle operating unthrottled.

(*b*) Using the charts in SI units developed for fuel-air cycle calculations, carry out an analysis of an appropriate ideal model for this cycle where the compression ratio r_c is 8 and the expansion ratio r_e is (1) 8; (2) 16. Assume the following:

Pressure in the cylinder at inlet valve close 1 atm
Mixture temperature at inlet valve close 300 K
Mixture equivalence ratio = 1.0
Fuel: isooctane C_8H_{18}
Lower heating value = 44.4 MJ/kg
Residual gas mass fraction at inlet valve close 0.05
Stoichiometric fuel/air ratio = 0.066

Calculate the indicated work per cycle per kg of air in the original mixture (the standard chart units) and the indicated mean effective pressure for these two expansion ratios. Base the mean effective pressure on the volume displaced by

PETITIONER'S EXHIBIT 1002
US PATENT NO. 6,581,565
Page 1738

the piston during the *expansion* stroke. Tabulate your answers. (*Note:* You are given the initial conditions for the cycle calculation; changing the value of r_e requires only modest changes in the cycle calculation.)

(*c*) Comment briefly on the effect of increasing the ratio r_e/r_c above 1.0 with this concept on engine efficiency and specific power (power per unit engine weight). Additional calculations are not required.

5.17. In a direct-injection stratified-charge (DISC) engine fuel is injected into the engine cylinder just before top-center (like a diesel); a spark discharge is then used to initiate the combustion process. A four-stroke cycle version of this engine has a displaced volume of 2.5 liters and a compression ratio of 12. At high load, the inlet pressure is boosted by a compressor to above atmospheric pressure. The compressor is geared directly to the engine drive shaft. The exhaust pressure is 1 atm. This DISC engine is to replace an equal displacement conventional naturally aspirated spark-ignition (SI) engine, which has a compression ratio of 8.

(*a*) Draw qualitative sketches of the appropriate constant-volume ideal cycle pressure-volume diagrams for the complete operating cycles for these two engines at maximum load.

(*b*) Use available fuel-air results to estimate how much the DISC engine inlet pressure must be boosted above atmospheric pressure by the compressor to provide the same maximum gross indicated power as the naturally aspirated SI engine. The SI engine operates with an equivalence ratio of 1.2; the DISC engine is limited by smoke emissions to a maximum equivalence ratio of 0.7.

(*c*) Under these conditions, will the brake powers of these engines be the same, given that the mechanical rubbing friction is the same? Briefly explain.

(*d*) At part load, the SI engine operates at an equivalence ratio of 1.0 and inlet pressure of 0.5 atm. At part load the DISC engine has negligible boost and operates with an inlet pressure of 1.0 atm. Use fuel-air cycle results to determine the equivalence ratio at which the DISC engine must be operated to provide the same net indicated mean effective pressure as the SI engine. What is the ratio of DISC engine net indicated fuel conversion efficiency to SI engine efficiency at these conditions?

5.18. The earliest successful reciprocating internal combustion engine was an engine developed by Lenoir in the 1860s. The operating cycle of this engine consisted of two strokes (i.e., one crankshaft revolution). During the first half of the first stroke, as the piston moves away from its top-center position, fuel-air mixture is drawn into the cylinder through the inlet valve. When half the total cylinder volume is filled with fresh mixture, the inlet valve is closed. The mixture is then ignited and burns rapidly. During the second half of the first stroke, power is delivered from the high-pressure burned gases to the piston. With the piston in its bottom-center position, the exhaust valve is opened. The second stroke, the exhaust stroke, completes the cycle as the piston returns to top-center.

(*a*) Sketch a cylinder pressure versus cylinder volume diagram for this engine.

(*b*) Using the charts in SI units developed for fuel-air cycle calculations, carry out a cycle analysis and determine the indicated fuel conversion efficiency and mean effective pressure for the Lenoir engine. Assume the following:

Inlet pressure = 1 atm
Inlet mixture temperature = 300 K
Mixture equivalence ratio = 1.0

PETITIONER'S EXHIBIT 1002
US PATENT NO. 6,581,565
Page 1739

Fuel: isooctane C_8H_{18}
Lower heating value = 44.4 MJ/kg
Clearance volume negligible

(*c*) Compare these values with typical values for the constant-volume fuel-air cycle. Explain (with thermodynamic arguments) why the two cycles have such different indicated mean effective pressures and efficiencies.
(*d*) Explain briefly why the real Lenoir engine would have a lower efficiency than the value you calculated in (*b*) (the actual *brake* fuel conversion efficiency of the engine was about 5 percent).

5.19. Estimate from fuel-air cycle results the indicated fuel conversion efficiency, the indicated mean effective pressure, and the maximum indicated power (in kilowatts) at wide-open throttle of these two four-stroke cycle spark-ignition engines:

A six-cylinder engine with a 9.2-cm bore, 9-cm stroke, compression ratio of 7, operated at an equivalence ratio of 0.8
A six-cylinder engine with an 8.3-cm bore, 8-cm stroke, compression ratio of 10, operated at an equivalence ratio of 1.1

Assume that actual indicated engine efficiency is 0.8 times the appropriate fuel-air cycle efficiency. The inlet manifold pressure is close to 1 atmosphere. The maximum permitted value of the mean piston speed is 15 m/s. Briefly summarize the reasons why:
(*a*) The efficiency of these two engines is approximately the same despite their different compression ratios.
(*b*) The maximum power of the smaller displacement engine is approximately the same as that of the larger displacement engine.

5.20. The constant-volume combustion fuel-air cycle model can be used to estimate the effect of changes in internal combustion engine design and operating variables on engine efficiency. The following table gives the major differences between a diesel and a spark-ignition engine both operating at half maximum power.

	Diesel engine	**Spark-ignition engine**
Compression ratio	16 : 1	9 : 1
Fuel/air equivalence ratio	0.4	1.0
Inlet manifold pressure	1 atm	0.5 atm

(*a*) Use the graphs of fuel-air cycle results (Figs. 5-9 and 5-10) to estimate the ratio of the diesel engine *brake* fuel conversion efficiency to the spark-ignition engine *brake* fuel conversion efficiency.
(*b*) Estimate what percentage of the higher diesel brake fuel conversion efficiency comes from:
(1) The higher diesel compression ratio
(2) The leaner diesel equivalence ratio
(3) The lack of intake throttling in the diesel compared with the spark-ignition engine

PETITIONER'S EXHIBIT 1002
US PATENT NO. 6,581,565
Page 1740

The values of fuel conversion efficiency and mean effective pressure given in the graphs are *gross* indicated values (i.e., values obtained from $\int p\,dV$ over the compression and expansion strokes only).

You may assume, if necessary, that for the real engines, the gross indicated efficiency and gross indicated mean effective pressure are 0.8 times the fuel-air cycle values. Also, the mechanical rubbing friction for each engine is 30 percent of the *net* indicated power or mep.

REFERENCES

1. Taylor, C. F.: *The Internal Combustion Engine in Theory and Practice*, vol. 1: *Thermodynamics, Fluid Flow, Performance*, 2d ed., chaps. 2 and 4, 1966.
2. Lancaster, D. R., Krieger, R. B., and Lienesch, J. H.: "Measurement and Analysis of Engine Pressure Data," SAE paper 750026, *SAE Trans.*, vol. 84, 1975.
3. Edson, M. H.: "The Influence of Compression Ratio and Dissociation on Ideal Otto Cycle Engine Thermal Efficiency," *Digital Calculations of Engine Cycles, SAE Prog. in Technology*, vol. 7, pp. 49–64, 1964.
4. Edson, M. H., and Taylor, C. F.: "The Limits of Engine Performance—Comparison of Actual and Theoretical Cycles," *Digital Calculations of Engine Cycles, SAE Prog. in Technology*, vol. 7, pp. 65–81, 1964.
5. Keenan, J. H.: *Thermodynamics*, John Wiley, New York, 1941; MIT Press, Cambridge, Mass., 1970.
6. Haywood, R. W.: "A Critical Review of the Theorems of Thermodynamic Availability, with Concise Formulations; Part 1. Availability," *J. Mech. Engng Sci.*, vol. 16, no. 3, pp. 160–173, 1974.
7. Haywood, R. W.: "A Critical Review of the Theorems of Thermodynamic Availability, with Concise Formulations; Part 2. Irreversibility," *J. Mech. Engng Sci.*, vol. 16, no. 4, pp. 258–267, 1974.
8. Flynn, R. F., Hoag, K. L., Kamel, M. M., and Primus, R. J.: "A New Perspective on Diesel Engine Evaluation Based on Second Law Analysis," SAE paper 840032, *SAE Trans.*, vol. 93, 1984.
9. Clarke, J. M.: "The Thermodynamic Cycle Requirements for Very High Rational Efficiencies," paper C53/76, Institution of Mechanical Engineers, *J. Mech. Engng Sci.*, 1974.
10. Traupel, W.: "Reciprocating Engine and Turbine in Internal Combustion Engineering," in *Proc. CIMAC Int. Congr. on Combustion Engines*, Zurich, pp. 39–54, 1957.
11. Clarke, J. M.: "Letter: Heavy Duty Diesel Fuel Economy," *Mech. Engng*, pp. 105–106, March 1983.
12. Caris, D. F., and Nelson, E. E.: "A New Look at High Compression Engines," *SAE Trans.*, vol. 67, pp. 112–124, 1959.
13. Kerley, R. V., and Thurston, K. W.: "The Indicated Performance of Otto-Cycle Engines," *SAE Trans.*, vol. 70, pp. 5–37, 1962.
14. Bolt, J. A., and Holkeboer, D. H.: "Lean Fuel-Air Mixtures for High-Compression Spark-Ignition Engines," *SAE Trans.*, vol. 70, p. 195, 1962.

PETITIONER'S EXHIBIT 1002
US PATENT NO. 6,581,565
Page 1741

CHAPTER 6

GAS EXCHANGE PROCESSES

This chapter deals with the fundamentals of the gas exchange processes—intake and exhaust in four-stroke cycle engines and scavenging in two-stroke cycle engines. The purpose of the exhaust and inlet processes or of the scavenging process is to remove the burned gases at the end of the power stroke and admit the fresh charge for the next cycle. Equation (2.38) shows that the indicated power of an internal combustion engine at a given speed is proportional to the mass flow rate of air. Thus, inducting the maximum air mass at wide-open throttle or full load and retaining that mass within the cylinder is the primary goal of the gas exchange processes. Engine gas exchange processes are characterized by overall parameters such as volumetric efficiency (for four-stroke cycles), and scavenging efficiency and trapping efficiency (for two-stroke cycles). These overall parameters depend on the design of engine subsystems such as manifolds, valves, and ports, as well as engine operating conditions. Thus, the flow through individual components in the engine intake and exhaust system has been extensively studied also. Supercharging and turbocharging are used to increase air flow through engines, and hence power density. Obviously, whether the engine is naturally aspirated or supercharged (or turbocharged) significantly affects the gas exchange processes. The above topics are the subject of this chapter.

For spark-ignition engines, the fresh charge is fuel, air, and (if used for emission control) recycled exhaust, so mixture preparation is also an important

PETITIONER'S EXHIBIT 1002
US PATENT NO. 6,581,565
Page 1742

goal of the intake process. Mixture preparation includes both achieving the appropriate mixture composition and achieving equal distribution of air, fuel, and recycled exhaust amongst the different cylinders. In diesels, only air (or air plus recycled exhaust) is inducted. Mixture preparation and manifold flow phenomena are discussed in Chap. 7. A third goal of the gas exchange processes is to set up the flow field within the engine cylinders that will give a fast-enough combustion process for satisfactory engine operation. In-cylinder flows are the subject of Chap. 8.

6.1 INLET AND EXHAUST PROCESSES IN THE FOUR-STROKE CYCLE

In a spark-ignition engine, the intake system typically consists of an air filter, a carburetor and throttle or fuel injector and throttle or throttle with individual fuel injectors in each intake port, and intake manifold. During the induction process, pressure losses occur as the mixture passes through or by each of these components. There is an additional pressure drop across the intake port and valve. The exhaust system typically consists of an exhaust manifold, exhaust pipe, often a catalytic converter for emission control, and a muffler or silencer. Figure 6-1 illustrates the intake and exhaust gas flow processes in a conventional spark-ignition engine. These flows are pulsating. However, many aspects of these flows can be analysed on a quasi-steady basis, and the pressures indicated in the intake system in Fig. 6-1*a* represent time-averaged values for a multicylinder engine.

The drop in pressure along the intake system depends on engine speed, the flow resistance of the elements in the system, the cross-sectional area through which the fresh charge moves, and the charge density. Figure 6-1*d* shows the inlet and exhaust valve lifts versus crank angle. The usual practice is to extend the valve open phases beyond the intake and exhaust strokes to improve emptying and charging of the cylinders and make the best use of the inertia of the gases in the intake and exhaust systems. The exhaust process usually begins 40 to 60° before BC. Until about BC the burned cylinder gases are discharged due to the pressure difference between the cylinder and the exhaust system. After BC, the cylinder is scavenged by the piston as it moves toward TC. The terms *blowdown* and *displacement* are used to denote these two phases of the exhaust process. Typically, the exhaust valve closes 15 to 30° after TC and the inlet valve opens 10 to 20° before TC. Both valves are open during an *overlap period*, and when $p_i/p_e < 1$, backflow of exhausted gas into the cylinder and of cylinder gases into the intake will usually occur. The advantage of valve overlap occurs at high engine speeds when the longer valve-open periods improve volumetric efficiency. As the piston moves past TC and the cylinder pressure falls below the intake pressure, gas flows from the intake into the cylinder. The intake valve remains open until 50 to 70° after BC so that fresh charge may continue to flow into the cylinder after BC.

In a diesel engine intake system, the carburetor or EFI system and the throttle plate are absent. Diesel engines are more frequently turbocharged. A

PETITIONER'S EXHIBIT 1002
US PATENT NO. 6,581,565
Page 1743

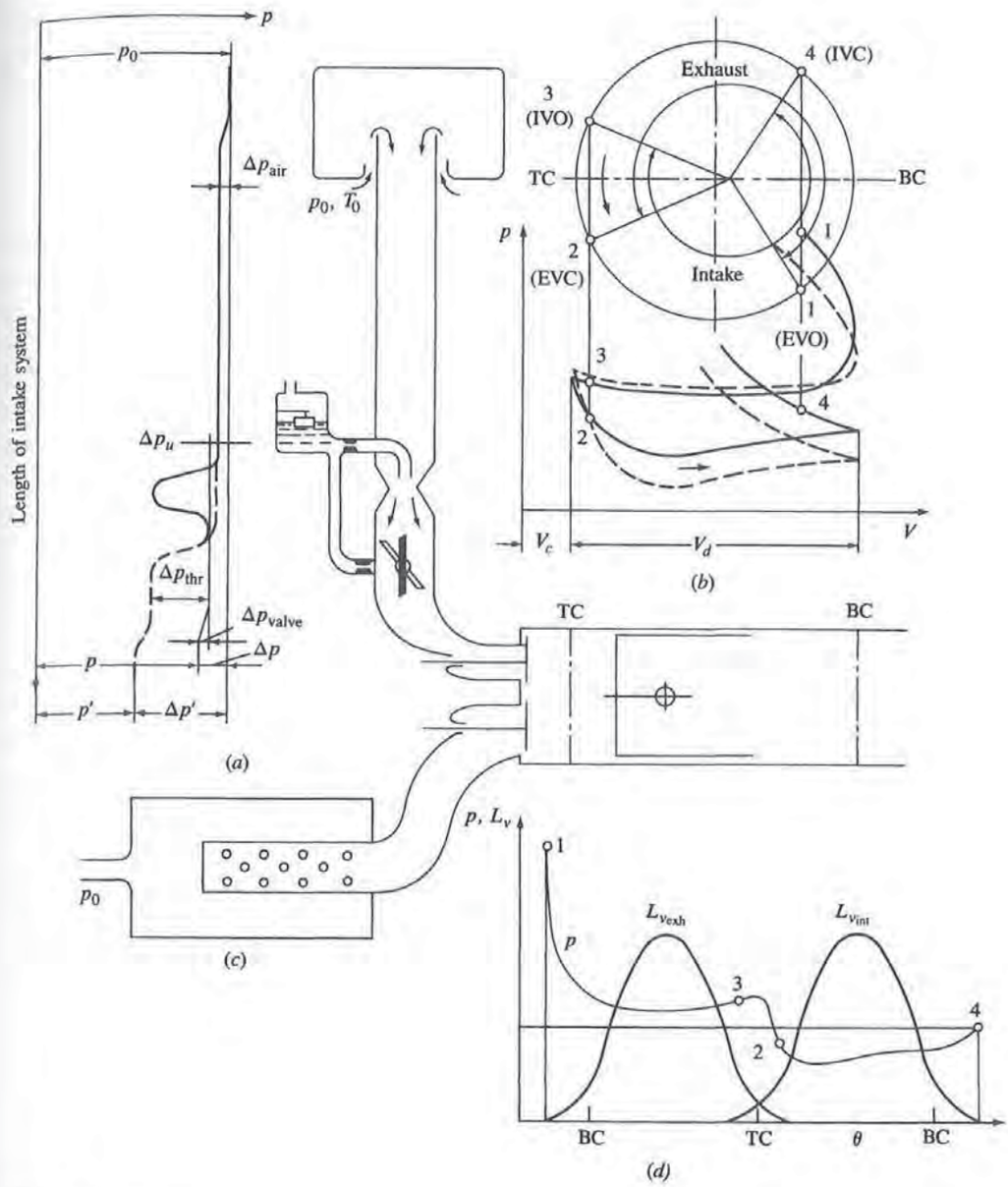


FIGURE 6-1
Intake and exhaust processes for four-stroke cycle spark-ignition engine: (*a*) intake system and average pressures within it; (*b*) valve timing and pressure-volume diagrams; (*c*) exhaust system; (*d*) cylinder pressure p and valve lift L_v versus crank angle θ. Solid lines are for wide-open throttle, dashed lines for part throttle; p_0, T_0, atmospheric conditions; Δp_{air} = pressure losses in air cleaner; Δp_u = intake losses upstream of throttle; Δp_{thr} = losses across throttle; Δp_{valve} = losses across the intake valve.[1]

PETITIONER'S EXHIBIT 1002
US PATENT NO. 6,581,565
Page 1744

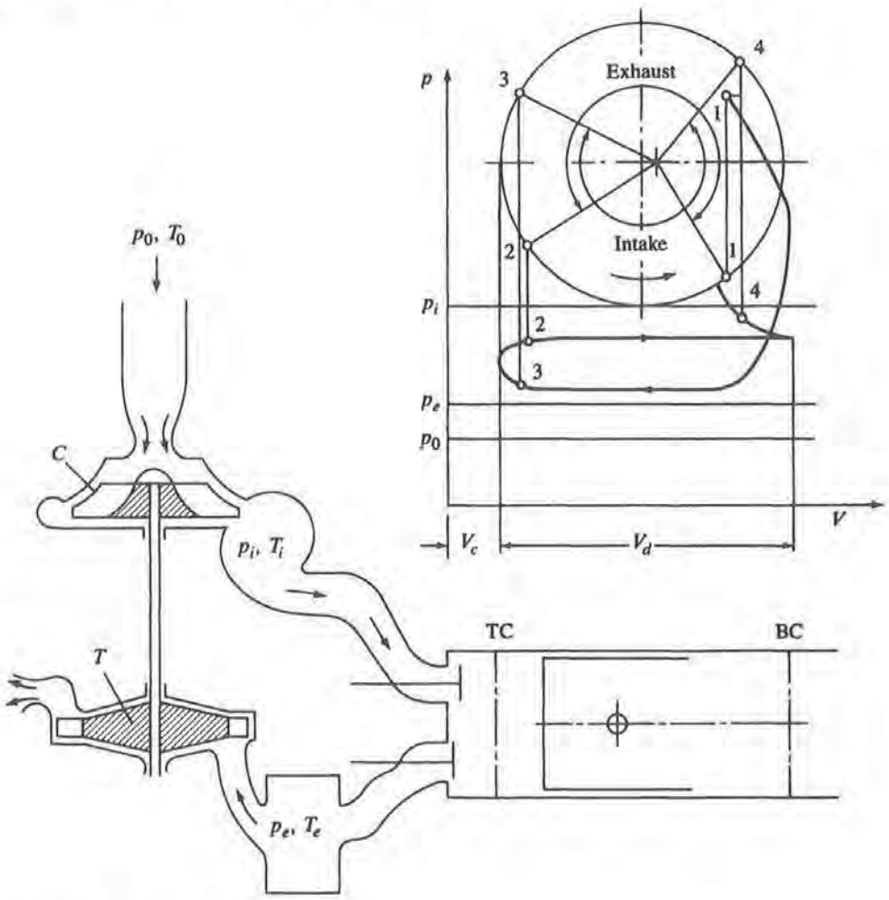


FIGURE 6-2
Intake and exhaust process for turbocharged four-stroke cycle engine. The turbocharger compressor C raises air pressure and temperature from ambient p_0, T_0 to p_i, T_i. Cylinder pressure during intake is less than p_i. During exhaust, the cylinder gases flow through the exhaust manifold to the turbocharger turbine T. Manifold pressure p_e may vary during the exhaust process and lies between cylinder pressure and ambient.[1]

similar set of diagrams illustrating the intake and exhaust processes for a turbocharged four-stroke diesel is shown in Fig. 6-2. When the exhaust valve opens, the burned cylinder gases are fed to a turbine which drives a compressor which compresses the air prior to entry to the cylinder.

Due to the time-varying valve open area and cylinder volume, gas inertia effects, and wave propagation in the intake and exhaust systems, the pressures in the intake, the cylinder, and the exhaust during these gas exchange processes vary in a complicated way. Analytical calculation of these processes is difficult (see Secs. 7.6.2 and 14.3 for a review of available methods). In practice, these processes are often treated empirically using overall parameters such as volumetric efficiency to define intake and exhaust system performance.

PETITIONER'S EXHIBIT 1002
US PATENT NO. 6,581,565
Page 1745

6.2 VOLUMETRIC EFFICIENCY

Volumetric efficiency is used as an overall measure of the effectiveness of a four-stroke cycle engine and its intake and exhaust systems as an air pumping device. It is defined [see Sec. 2.10, Eq. (2.27)] as

$$\eta_v = \frac{2\dot{m}_a}{\rho_{a,0} V_d N} \tag{6.1}$$

The air density $\rho_{a,0}$ can be evaluated at atmospheric conditions; η_v is then the overall volumetric efficiency. Or it can be evaluated at inlet manifold conditions; η_v then measures the pumping performance of the cylinder, inlet port, and valve alone. This discussion will cover unthrottled (wide-open throttle) engine operation only. It is the air flow under these conditions that constrains maximum engine power. Lesser air flows in SI engines are obtained by restricting the intake system flow area with the throttle valve.

Volumetric efficiency is affected by the following fuel, engine design, and engine operating variables:

1. Fuel type, fuel/air ratio, fraction of fuel vaporized in the intake system, and fuel heat of vaporization
2. Mixture temperature as influenced by heat transfer
3. Ratio of exhaust to inlet manifold pressures
4. Compression ratio
5. Engine speed
6. Intake and exhaust manifold and port design
7. Intake and exhaust valve geometry, size, lift, and timings

The effects of several of the above groups of variables are essentially quasi steady in nature; i.e., their impact is either independent of speed or can be described adequately in terms of mean engine speed. However, many of these variables have effects that depend on the unsteady flow and pressure wave phenomena that accompany the time-varying nature of the gas exchange processes.

6.2.1 Quasi-Static Effects

VOLUMETRIC EFFICIENCY OF AN IDEAL CYCLE. For the ideal cycles of Fig. 5-2*d* and *e*, an expression for volumetric efficiency can be derived which is a function of the following variables: intake mixture pressure p_i, temperature T_i, and fuel/air ratio (F/A); compression ratio r_c; exhaust pressure p_e; and molecular weight M and γ for the cycle working fluid. The overall volumetric efficiency is

$$\eta_v = \frac{m_a}{\rho_{a,0} V_d} = \frac{m(1 - x_r)}{\rho_{a,0}[1 + (F/A)]} \frac{r_c}{(r_c - 1)V_1}$$

PETITIONER'S EXHIBIT 1002
US PATENT NO. 6,581,565
Page 1746

where m is the mass in the cylinder at point 1 in the cycle. Since

$$p_i V_1 = m \frac{\tilde{R}}{M} T_1 \qquad \text{and} \qquad p_{a,0} = \rho_{a,0} \frac{\tilde{R}}{M_a} T_{a,0}$$

and Eq. (5.38) relates T_1 to T_i, the above expression for η_v can be written

$$\eta_v = \left(\frac{M}{M_a}\right)\left(\frac{p_i}{p_{a,0}}\right)\left(\frac{T_{a,0}}{T_i}\right)\frac{1}{[1+(F/A)]}\left\{\frac{r_c}{r_c-1} - \frac{1}{\gamma(r_c-1)}\left[\left(\frac{p_e}{p_i}\right)+(\gamma-1)\right]\right\} \tag{6.2}$$

For $(p_e/p_i) = 1$, the term in { } is unity.

EFFECT OF FUEL COMPOSITION, PHASE, AND FUEL/AIR RATIO. In a spark-ignition engine, the presence of gaseous fuel (and water vapor) in the intake system reduces the air partial pressure below the mixture pressure. For mixtures of air, water vapor, and gaseous or evaporated fuel we can write the intake manifold pressure as the sum of each component's partial pressure:

$$p_i = p_{a,i} + p_{f,i} + p_{w,i}$$

which with the ideal gas law gives

$$\frac{p_{a,i}}{p_i} = \left[1 + \left(\frac{\dot{m}_f}{\dot{m}_a}\right)\left(\frac{M_a}{M_f}\right) + \left(\frac{\dot{m}_w}{\dot{m}_a}\right)\left(\frac{M_a}{M_w}\right)\right]^{-1} \tag{6.3}$$

The water vapor correction is usually small (≤ 0.03). This ratio, $p_{a,i}/p_i$, for several common fuels as a function of $(\dot{m}_f/\dot{m}_a)$ is shown in Fig. 6-3. Note that $(\dot{m}_f/\dot{m}_a)$ only equals the engine operating fuel/air ratio if the fuel is fully vaporized.

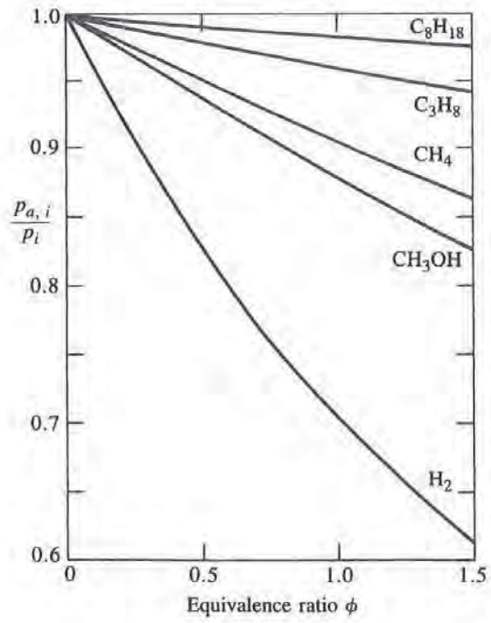


FIGURE 6-3
Effect of fuel (vapor) on inlet air partial pressure. Ratio of air inlet pressure $p_{a,i}$ to mixture inlet pressure p_i versus fuel/air equivalence ratio ϕ for isooctane vapor, propane, methane, methanol vapor, and hydrogen.

PETITIONER'S EXHIBIT 1002
US PATENT NO. 6,581,565
Page 1747

For conventional liquid fuels such as gasoline the effect of fuel vapor, and therefore fuel/air ratio, is small. For gaseous fuels and for methanol vapor, the volumetric efficiency is significantly reduced by the fuel vapor in the intake mixture.

FRACTION FUEL VAPORIZED, HEAT OF VAPORIZATION, AND HEAT TRANSFER. For a constant-pressure flow with liquid fuel evaporation and with heat transfer, the steady-flow energy equation is

$$[\dot{m}_a h_a + (1 - x_e)\dot{m}_f h_{f,L} + x_e \dot{m}_f h_{f,V}]_A = \dot{Q} + (\dot{m}_a h_a + \dot{m}_f h_{f,L})_B \qquad (6.4)$$

where x_e is the mass fraction evaporated and the subscripts denote: a, air properties; f, fuel properties; L, liquid; V, vapor; B before evaporation; A after evaporation. Approximating the change in enthalpy per unit mass of each component of the mixture by $c_p \Delta T$, and with $h_{f,V} - h_{f,L} = h_{f,LV}$ (the enthalpy of vaporization), Eq. (6-4) becomes

$$T_A - T_B = \frac{(\dot{Q}/\dot{m}_a) - x_e(F/A)h_{f,LV}}{c_{p,a} + (F/A)c_{f,L}} \qquad (6.5)$$

Since $c_{f,L} \approx 2c_{p,a}$ the last term in the denominator can often be neglected.

If no heat transfer to the inlet mixture occurs, the mixture temperature decreases as liquid fuel is vaporized. For complete evaporation of isooctane, with $\phi = 1.0$, $T_A - T_B = -19°C$. For methanol under the same conditions, $T_A - T_B$ would be $-128°C$. In practice heating occurs; also, the fuel is not necessarily fully evaporated prior to entry to the cylinder. Experimental data show that the decrease in air temperature that accompanies liquid fuel evaporation more than offsets the reduction in air partial pressure due to the increased amount of fuel vapor: for the same heating rate, volumetric efficiency with fuel vaporization is higher by a few percent.[2]

The ideal cycle equation for volumetric efficiency [Eq. (6.2)] shows that the effect of gas temperature variations, measured at entry to the cylinder, is through the factor $(T_{a,0}/T_i)$. Engine test data indicate that a square root dependence of volumetric efficiency on temperature ratio is closer to real engine behavior. The square root dependence is a standard assumption in engine test data reduction (see Sec. 2.12).

EFFECT OF INLET AND EXHAUST PRESSURE RATIO AND COMPRESSION RATIO. As the pressure ratio (p_e/p_i) and the compression ratio are varied, the fraction of the cylinder volume occupied by the residual gas *at the intake pressure* varies. As this volume increases so volumetric efficiency decreases. These effects on ideal-cycle volumetric efficiency are given by the $\{\ \}$ term in Eq. (6.2). For $\gamma = 1.3$ these effects are shown in Fig. 6-4.

PETITIONER'S EXHIBIT 1002
US PATENT NO. 6,581,565
Page 1748

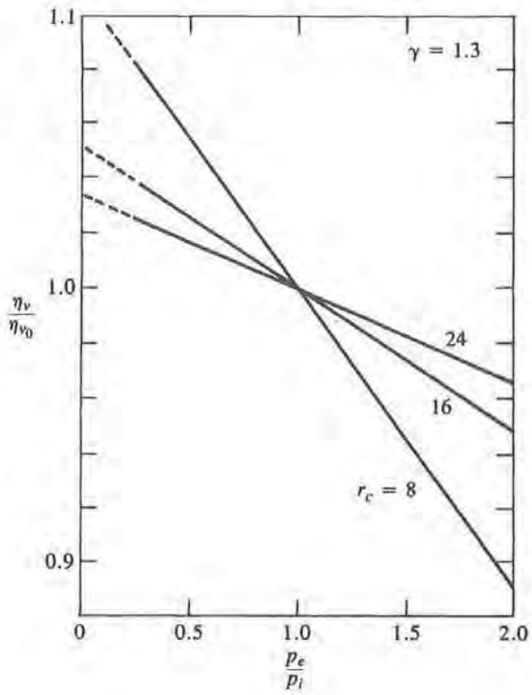


FIGURE 6-4
Effect of exhaust to inlet pressure ratio on ideal-cycle volumetric efficiency.

6.2.2 Combined Quasi-Static and Dynamic Effects

When gas flows unsteadily through a system of pipes, chambers, ports, and valves, both friction, pressure, and inertial forces are present. The relative importance of these forces depends on gas velocity and the size and shape of these passages and their junctions. Both quasi-steady and dynamic effects are usually significant. While the effects of changes in engine speed, and intake and exhaust manifold, port and valve design are interrelated, several separate phenomena which affect volumetric efficiency can be identified.

FRICTIONAL LOSSES. During the intake stroke, due to friction in each part of the intake system, the pressure in the cylinder p_c is less than the atmospheric pressure p_{atm} by an amount dependent on the square of the speed. This total pressure drop is the sum of the pressure loss in each component of the intake system: air filter, carburetor and throttle, manifold, inlet port, and inlet valve. Each loss is a few percent, with the port and valve contributing the largest drop. As a result, the pressure in the cylinder during the period in the intake process when the piston is moving at close to its maximum speed can be 10 to 20 percent lower than atmospheric. For each component in the intake (and the exhaust) system, Bernoulli's equation gives

$$\Delta p_j = \xi_j \rho v_j^2$$

where ξ_j is the resistance coefficient for that component which depends on its

PETITIONER'S EXHIBIT 1002
US PATENT NO. 6,581,565
Page 1749

geometric details and v_j is the local velocity. Assuming the flow is quasi-steady, v_j is related to the mean piston speed $\bar{S}_p$ by

$$v_j A_j = \bar{S}_p A_p$$

where A_j and A_p are the component minimum flow area and the piston area, respectively. Hence, the total quasi-steady pressure loss due to friction is

$$p_{\text{atm}} - p_c = \sum \Delta p_j = \sum \xi_j \rho v_j^2 = \rho \bar{S}_p^2 \sum \xi_j \left(\frac{A_p}{A_j}\right)^2 \tag{6.6}$$

Equation (6.6) indicates the importance of large component flow areas for reducing frictional losses, and the dependence of these losses on engine speed. Figure 6-5 shows an example of the pressure losses due to friction across the air cleaner, carburetor, throttle, and manifold plenum of a standard four-cylinder

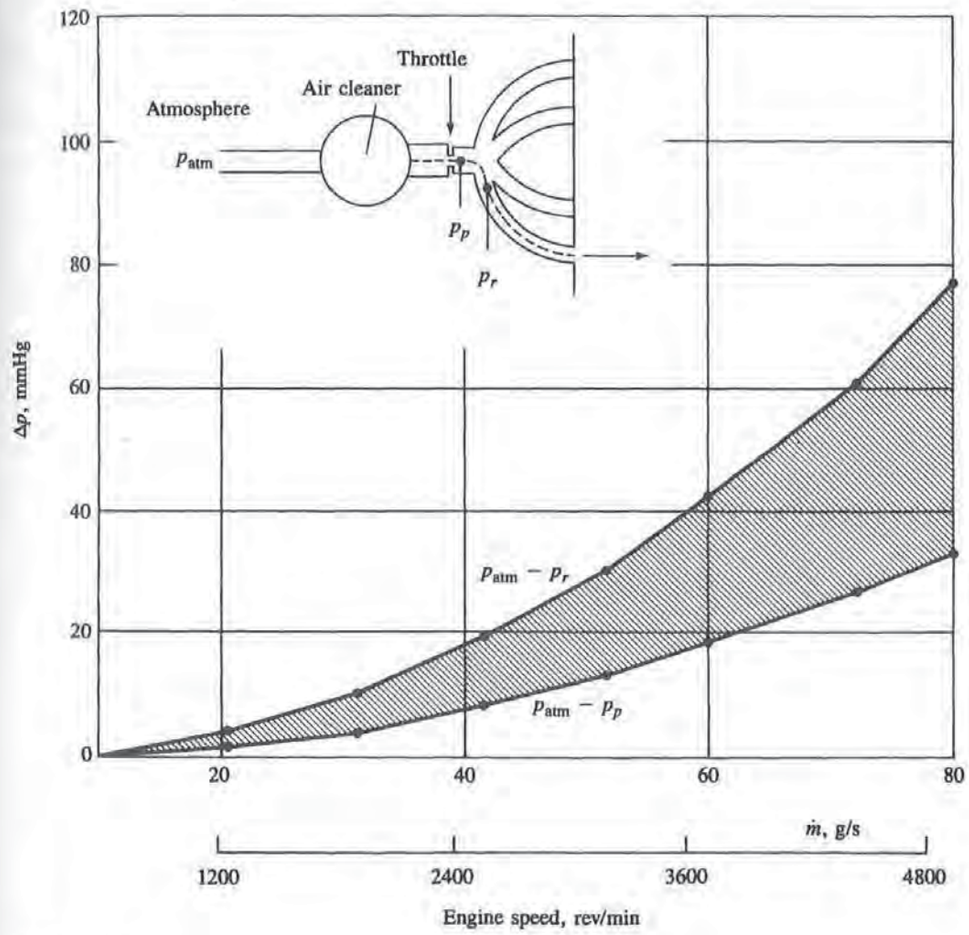


FIGURE 6-5
Pressure losses in the intake system of a four-stroke cycle spark-ignition engine determined under steady flow conditions.[3] Stroke = 89 mm. Bore = 84 mm.

PETITIONER'S EXHIBIT 1002
US PATENT NO. 6,581,565
Page 1750